SISSA - SCUOLA
INTERNAZIONALE
SUPERIORE
STUDI AVANZATI
TRIESTE
Strada Costiera 11

ISAS - INTERNATIONAL SCHOOL FOR ADVANCED STUDIES

ATTESTATO DI RICERCA

"DOCTOR PHILOSOPHIAE"

SEYFERT 1 GALAXIES

(OBSERVATIONAL PROPERTIES, INTERNAL REDDENING AND LUMINOSITY FUNCTION)

CANDIDATO:

CHENG FU-ZHEN

RELATORI:

PROF. L. DANESE

PROF. G. De ZOTTI

Anno Accademico 1983/84

TRIESTE

SEYFERT 1 GALAXIES

(OBSERVATIONAL PROPERTIES, INTERNAL REDDENING AND LUMINOSITY FUNCTION)

CANDIDATE:

CHENG FU-ZHEN

SUPERVISORS:

PROF. L. DANESE

PROF. G. De ZOTTI

A THESIS SUBMITTED FOR THE ATTAINMENT OF

THE DEGREE OF PHILOSOPHY DOCTOR AT THE

S.I.S.S.A. TRIESTE IN ITALY

OCTOBER 1984

CONTENT

CHAPTER I INTRODUCTION

1.1 Definition of Seyfert galaxies

In 1943 Carl K. Seyfert draw attention to the fact that "a very small proportion of extragalactic nebulae show spectra having many high-excitation emission lines located in the nuclei... Most of them are intermediate-type spirals with ill-defined amorphous arms, their most consistend characteristic being an exceedingly luminous stellar or semistellar nucleus which contains a relatively large percentage of the total light of the sestem." However, little attention was paid to this unusual class of objects, that we now call Seyfert galaxies, until the 1950s (Burbidge et al 1959; Woltjer 1959). The discuvery of QSOs which turned out to have optical spectra very similar to Seyfert nuclei (Burbidge et al 1963) gave a tremendous impotus to the study of these objects.

Let us now describe in some detail the general properties of Seyfert galaxies.

(1) Emission line spectra of Seyfert nuclei

The spectra of Seyfert galaxies may present high excitation lines, such as [O III], [Ne V], [Fe VII], [Fe X], etc(Seyfert 1943; Osterbrock 1977, 1981b). The emission lines, at least Balmer lines, have large [FWHM] ranging from 500 to 10^4km/s, if we express them in equivalent velocity. Khachikian and Weedman (1971, 1974) divided Seyfert galaxies into two subtypes, Sy 1 and Sy 2, in terms of the relative widths of forbidden and Balmer lines. The Sy 1 has broad Balmer lines but narrower forbidden lines. In Sy 2 galaxies the Balmer lines and the forbidden lines have similar widths. We shall discuss this classification in more detail in section 1.2.

(2) Size of Seyfert nuclei

There are few direct measurements of the actual sizes of Seyfert nuclei. The largest (NGC 1068) has emission lines arising over a region 8" in diameter (Walker 1968), i.e., about 850 pc (hereafter assuming H_o=50 km/s/Mpc), while the continuum source is unresolved. Using a 36-inch balloon-borne telescope, Schwarzchild (1973) was able to set an upper limit of 0.08",i.e. 0.8 pc, to the diameter of the continuum source in NGC 4151. VLBI results for 3C 120 show that the size of the com-

pact radio source is as small as 0.001", i.e., about 0.1 pc.

Many Seyfert nuclei are variable in brightness on time scales of days and years (Miller 1978, 1979; Peterson et al 1984). Light-travel-time arguments, $d \sim c\Delta t$, then imply that the size of the continuum source may be smaller than 10^{-3}pc.

(3) Brightness of Seyfert nuclei

Sandage (1973) has introduced a parameter called 'a' which is the ratio of luminosity of the compact nucleus or "miniquasar" to the luminosity of the underlying galaxy in the photometric V or B or U band. Veron (1979) considered the parameter 'a' as a classification standard. When 'a' is much larger than unity, the underlying galaxy is completely obliterated, the object looks star-like and is called a QSO; when 'a' is smaller than 0.1, the nucleus is not easily visible on photographs if the galaxy is not very near, so the galaxy looks normal. Therefore, we can say that if one would like to use the parameter 'a' to describe the characteristic of brightness of Seyfert nuclei, then Seyferts are the galaxies having 'a' $\geq$0.1

(4) Ultravielet excess of Seyfert galaxies

This is illustrated in the colour-colour diagram (Fig. 1). The crosses are the integrated colours of open clusters (Schmidt-Kaler 1967), which are collections of young stars. Seyfert galaxies show an UV excess even in comparison with such stars. This was the initial reason for attributing the continua to non-thermal sources. In addition, in Fig. 1 the segregation of Seyfert galaxies from the bright-nucleus galaxies (see Section 1.3) and diffuse galaxies is considerable, as mentioned above. These results are important because they mean that UBV photometry can provide a classification criterion.

Therefore, generally speaking, Seyfert galaxies are characterised by: (1) bright star-like nuclei which are surrounded by a faint envelope; (2) high-excitation and broad emission-line spectrum; (3) relatively UV excess, i,e., the positions in (U-B) versus (B-V) plot are above the black body line and close to Sandage's locus for QSOs (see Fig. 1). We wish to emphasize that it is impossible to distingnish Seyfert galaxies from QSOs on the basis of their emission line spectra and colours. We shall discuss this problem in Section 2.7.

1.2 Classification of Seyfert Galaxies

Because Seyfert galaxies are characterized by strong and broad emission lines, the nature of these lines was used as the classification criterion. On the basis of the relative widths of forbidden lines and Balmer lines, a simple division into classes 1 and 2 (Sy 1 and Sy 2) was made by Khachikian and Weedman (1971, 1974).

The Sy 1 galaxies, of which Mkn 1243 is very representative (Osterbrock 1984) (Fig 2), have broad Balmer lines but narrower forbidden lines. The Balmer lines in Sy 1 galaxies have usually FWHM 1000-5000 km/s or FWZI 4000-30000 km/s, and forbidden lines have FWHM 500 km/s. Widths $\sim$500 km/s are referred to as 'narrow', but we must keep in mind that they are 'broad' in comparison with the emission lines in non-active galactic nuclei.

In Sy 2 galaxies, of which Mkn 1157 (Fig 3) is very typical example , the Balmer lines and the forbidden lines have similar widths, typically FWHM between 500 and 1000 km/s. Sy 2 galaxies differ from other emission-line galaxies in which the Balmer lines generally do not exceed 200 km/s.

Recently, Feldman et al (1982) measured the widths of the [OIII] emission lines for 116 galactic nuclei. Galaxies observed include 53 Sy 1, 16 Sy 2, and 47 "star-burst" galaxies. The median FWHM for the [OIII] lines is 375 km/s for Sy 1, 510 km/s for Sy 2, and 160 km/s for star-burst nuclei. They suggested that an empirical criterion for dividing Seyfert galaxies from other emission line galaxies is a FWHM exceeding 250 km/s for the [OIII] lines. Their results for line widths are shown in histogram in Fig 4.

An useful secondary classification is the Balmer-line to forbidden-line intensity ratio, especially H_β / [OIII] λ 5007. The forbidden-lines are unusually strong in Sy 2 with an average H_β / [OIII] λ 5007 ratio of 0.1, whereas H_β and [OIII] λ 5007 typically have the same total flux for Sy 1 (Adams & Weedman 1975). For the narrow emission line galaxies, H_β is also comparable to [OIII] λ 5007 in most cases.

In addition, as mentioned previously (see Fig 1)

Sy 1, Sy 2 and NELGs can in most cases be distingnished on the basis of their UBV colours. In particular Sy 1's are bluer than Sy 2's.

A spectrophotometric survey of Seyfert galaxies was carried out by Osterbrock and Koski (1976) who showed that there is a continuous transition between Sy 1 and Sy 2, as it can be seen from Fig. 5. Mkn 509 is a typical Sy 1, and Mkn 176 is a typical Sy 2, whereas NGC 4151 and Mkn 6 = IC 450 have spectra intermediate between the Sy 1 and Sy 2 groups, and are thus classified as Sy 1.5. Osterbrock and Koski (1976) argued that the best way to describe the emission-line spectra of Fig. 5 is as various linear combinations of two basic components, one consisting of the broad Balmer emission line wings, the other of Sharp Balmer line cores and forbidden lines. Galaxies which have a relatively strong broad Balmer-line component are classified as Sy 1, while galaxies in which it is invisible are classified as Sy 2; the intermediate Sy 1.5 objects, such as NGC 4151 and Mkn 6, have relatively weak, but still visible, broad Balmer-line components.

Finer classifications introducing six or more sub-classes (Osterbrock 1977, 1981b; Shuder 1980) have been later partly abandoned. According to the latest classification (Osterbrock 1984) all objects with well marked composite line profiles are called Seyfert 1.5 galaxies. Objects with strong narrow components of H I emission lines and quite weak but easily visible broad components of H_α are called Sy 1.8 if they have weak but definitely present broad H_β components as well; if broad H_β cannot be detected with certainty by visual inspection, the objects are called Sy 1.9 (see Table 1 and Fig. 6, 7).

So far, of the known Seyfert galaxies, approximately 60% belong to the Sy 1, and 40% are Sy 2. A compilation of data on Seyfert galaxies known prior to October 1st, 1984 is presented in Table 2. This catalogue contains 416 objects, i.e. 40 more than the catalogue of Veron and Veron (1984).

The main sources of Seyfert galaxies are the Markarian lists; approximately 10% of Markarian galaxies turn out to be Seyfert galaxies (see Table 2). Additional Seyferts are found among Zwicky compact galaxies, Tololo galaxies and Arakelian galaxie. Most recently, X-ray surveys have proven to be a powerful tool to discover galaxies with active nuclei.

1.3 Relation to Other Classes of Galaxies

Let us now briefly outline the position of Seyferts in comparison to other classes of galaxies (see Fig. 8 taken from Sèrsic(1982), adapted from Ozernoy (1970)).

Ozernoy has proposed an ordering of the galaxies according to their degree of activity or excitation. He has taken as a starting point the observation that the difference between objects such as nucleus of our galaxy, a Seyfert nucleus or a QSO, lies only in the degree of intensity of liberation of internal energy.

An enlarged Hubble sequence (IG HII, Irr I, S, SO, E, C_1, and C_2) constitutes what Ozernoy calls the 'ground state' of galaxies. C_1 and C_2 are two additional hypothetical classes (Ozernoy 1970) which assimilate Zwicky's more massive and compact galaxies. IG HII are the so-called intergalactic HII regions observed by Sargent and Searle (1970). From the energetic point of view, the ground level coresponds to objects which emit very little or no non-thermal energy relative to their luminosity of thermal origin ($L_{NT} \ll L_T$).

On the other hand, Seyfert galaxies (SyG), strong radio galaxies (SRG), N galaxies (NG), and quasars (QSO) are considered the 'ceiling' of excitation activity ($L_{NT} \gg L_T$).

A seqence of moderate excitation $L_{NT} \approx L_T$ is formed by the Quasi-stellar galaxies (QSG), blue compacts (BCG), galaxies with nuclear emission (neG), giant HII regions (in some cases superposed to the stellar background of a SO galaxy (Irr II), and irregular galaxies of high surface brightness, possibly undergoing a burst of star formation (AIrrI).

The galaxies in the ground state ($L_{NT} \ll L_T$) are not connected genetically among themselves, and differ mainly by mass and angular momentum.

The vertical lines in Fig. 8 suggest, according to Ozernoy, probable directions for the excitation of galaxy nuclei. On the contrary, he holds that a transition in the horizontal sense (from QSO to SRG or viceversa, e.g.) is improbable.

Fig. 8 also shows Markarian UV galaxies (MkG). These galaxies with unusually strong UV continua (Markarian 1967) are important for us because approximately 10%

of MkG are Seyferts (Weedman 1977). Since 1967 B.E.Markarian and his colleagues have published 15 lists of galaxies with UV excess which contain 1500 objects (Markarian 1967, 1969a, 1969b; Markarin & Lipovetskii 1971, 1972, 1973, 1974, 1976a, 1976b; Markarian, Lipovetskii and Stepanyan 1977a, 1977b, 1979a, 1979b, 1979c, 1982). Mkn objects constitute a heterogeneous group which comprises a wide range of activity and concentration, as illustrated by Fig. 9 (van den Bergh 1975). MkG's were classified into two basic types (Merkarian 1967): (a) Type 's' galaxies which have sharpest and best defined images, and in which the source of the UV continuum is the bright nucleus of a galaxy; (b) Type 'd' galaxies which are diffuse and frequently have an UV continuum spread throughout the entire object. Intermediate classes also exist. A basically equivalent classification has been proposed by van der Bergh (1975) who has also divided Mkn galaxies into two classes, Haro galaxies and Morgan N-type glaxies. Haro galaxies, first described by Haro (1956), may be identified with Markarlian 'd' galaxies.

The concept of N galaxies has been introduced by Morgan (1958). A more specific definition was given by Mattews, Morgan and Schmidt (1964): " The 'N' galaxies — These are galaxies having brilliant, starlike nuclei containing most of the luminosity of the system. A faint, nebulous envelope of small visible extent is observed". A recent paper by Morgan & Dreiser (1983) shows us an excellent series of N galaxy drawings (see Fig. 10) which illustrate the continuous increase in contrast between nucleus and galaxy from relatively low-luminosity Seyfert galaxies like NGC 4151 to relatively high-luminosity quasars like 3C 48. Thereby N galaxies include a great variety of objects, such as Seyferts, BL Lac objects, QSOs, etc.

Markarlian 's' objects belong to N galaxies which may be further subdivided into Seyfert galaxies and BN (bright nucleus) galaxies (see Fig. 9). Most BN galaxies have narrow nuclear emission lines. In a U-B versus B-V co our plot (see Fig. 1) the BN galaxies are located close to the "blackbody" line while Seyfert galaxies have a large UV excess, that as suggested by Weedman (1973), is evidence of non-thermal continuum. Furthermore, as the observed luminosity is increasingly dominated by the nucleus, the colours of Seyfert glaxies approach $B-V \simeq +0.3$, $U-B \simeq -1$, i.e.

become similar to those of quasars (Sandage 1971). The possibility that these two types of objects are genetically related is strengthened by the similarity of their spectra (Khachikian & Weedman 1974).

The plan of the thesis is the following. The definition and the classification of Seyfert galaxies are given in Chapter I. We describe the observational properties of Sy 1 and possible interpretations in Chapter II. Chapter III concerns internal reddening of Sy 1 nuclei. Chpter IV deal with the problem of estimating the ratio of X-ray to optical luminosity of AGNs. Chaper V is devoted to calculating the optical luminosity function of Sy 1 nuclei. The main conclusions are summarised in Chapter VI.

CHAPTER II OBSERVATIONAL PROPERTIES OF SEYFERT 1 GALAXIES

2.1 Morphology

The morphology of Seyfert galaxies is very important for undersanding their structure and evolution. Early works by Vaucouleurs and de vacouleurs (1968), Morgan et al (1971) were limited to the "classical" Seyferts. An extensive morphological study on a sample of 80 Seyferts has been published by Adams (1977). Simkin et al (1980) have carried out a photographic survey of 30 Seyfert galaxies with $V_r < 5000$ km/s. An analysis of the structure and of the nuclear activity for 38 Sy 1's has been completed by Su and Simkin (1980).

Adams (1977) showed that the overwhelming majority of Seyfert galaxies display a disk structure; no preference for occurrence in normal or barred or transition-type galaxies is apparent. Taking into account that some objects in his sample have amorphous main bodies or are unresolved or barely resolved, he concluded that no more than 10% of Seyfert galaxies can be ellipticals. By contrast, 32.6% of a similar sample of "normal" galaxies are ellipticals (Humason et al 1956). But one must keep in mind that interference of the nucleus and the poor spatial resolution also limit our ability to classify the Seyfert galaxies in the Hubble system.

The lack of elliptical Seyferts is surprising in view of the strong spectroscopic similarity with QSOs: it is believed that at least the radio QSOs are associated with gaint elliptical galaxies (Sandage 1972, 1973). Various possible explanations have been proposed. Adams (1977) mentioned that selection effects in the discovery process (for both Seyferts and QSOs) may be so severe that the currently existing samples of the two classes of objects are not comparable. Alternatively it may be that the Seyfert nucleus is activated by infall of interstellar gas. Gas-poor galaxies, such as ellipticals, would then not become Seyferts; they may rather show a BL Lac type phenomenology.

Hutchings et al (1981), Wyckoff et al (1981) and Hutchings et al (1982) have investigated the morphology of the "fuzz" around more than 20 low redshift QSOs ($Z < 0.6$). They found that (1) quasars are the luminous nuclei of distant galaxies

whose average luminosity is $M_B = -21.5$, fainter than that of gaint ellipticals; (2) the morphology of many underlying galaxies is very similar to that of Sy 1's of similar luminosity and show features typical of spiral galaxies; (3) in the radio-loud QSOs the extent of the fuzz is larger and has a jetlike appearance; (4) the quasar nuclei are considerably more luminous relative to their host galaxies than other type of AGNs. Hutchings et al (1984) have extended this kind of analysis to 78 QSOs, divided into three groups: radio selected, optically selected and X-ray selected. The objects have redshifts $Z \lesssim 0.6$ and cover a luminosity range of $\sim$ 4 mag. Hutchings et al (1984) concluded that over 40% of the host galaxies show some spiral characteristics, the remainder having undetermined morphology, and that there is no positive evidence of ellipticals. Due to the limited resolution, about 1", it is impossible to give definite conclusions. However, as mentioned above, there are various indications that the morphology of galaxies underlying QSOs is not very different from that of Sy 1's.

Adams (1977) has suggested that the Sy 2's have spiral patterns less conspicuous than Sy 1's.

Adams (1977) also pointed out that more than 10% of Seyfert galaxies are in disturbed and/or interating systems. "Disturbed" galaxies are those showing gross structural peculiarities, such as jets or highly distorted main bodies. "Interacting" galaxies are those having one or more nearly companions of comparable size with some obvious evidence of interaction.

Khachikian et al (1982) reported that roughly 10% of UV bright galaxies show multiple nuclear structure and of these 10% have Seyfert characteristics. A noticeable example is the double Seyfert nucleus of Mkn 266 (Kollatschny & Fricke 1984). Such systems might be the result of merging, of tidal triggering of nuclear activity, or of disruptive processes inside the parent galaxies. Moreover, Adams (1977) noted a tendency for Seyfert galaxies to show annular structures. Due to observational limitations it is not possible to say whether these structures are actual "rings" or nearly circular spiral arms. The distinction is important because, in the former case, the rings would indicate a recent large-scale dynamical

perturbation, while in the latter case, the structure would presumably be part of a normal spiral pattern. Simkin et al (1980) offer a careful study of ring systems of nearby Seyfert galaxies, and concluded that: (1) 40% of Seyfert galaxies have outer rings; (2) 30% of Seyfert galaxies have both inner and outer rings. These percentages estimated are much higher than those applying to galaxies in the Second Reference Catalogue.

A most detailed morphological study has been carried out by Su and Simkin (1980). They found that most of the nearby, well resolved Seyfert galaxies in their sample exhibit disk patterns, and that Sy 1 have sharper ring and spiral patterns than Sy 2. They divided Sy 1 into five groups: S: both inner and outer spirals; RS: inner ring and outer spiral; RR: both inner and outer rings; DR: inner disk and outer ring; A: So or amorphous structure (Table 3). A strong correlation between morphological type and FWZI of H (Fig. 11) was discovered. Su and Simkin (1980) suggested that morphological structure is associated with nuclear activity, and that there is an evolutionary sequence from "S" to "A". According to their opinion at the 'S' end the gas starts to pour from the disk into the nucleus, and at the 'A' end the process is finished. The broader FWZI of the RR-A classes is associated with either an increased mass inthe nucleus or an increased rate of infall. These results and speculation are very interesting, although they are tentative.

A survey of critical objects with a large-aperture imaging space telescope is required. With such an instrument we could study a lot of distance Seyfert galaxies and more nearby QSOs, and get more conclusive results on morphology of Seyfert galaxies. Further theoretical explorations are of course important. For example, on the basis of the comparison of luminosity functions of Seyferts, QSOs, sprials and elliptical galaxies, Meurs (1982) suggested that: (1) the radio lud quasars may occur both in ellipticals and in spirals; (2) optically selected quasars may be related to Seyferts and spirals since most of the Seyferts are spirals. Of course, these two conclusions are rather tentative, but instructure for us.

2.2 Emission lines

Spectroscopic observations of Sy 1 galaxies give useful information about the line-emitting gas in these objects, and may enable us to deduce the gas distribution and dynamics, temperature, density, element abundance, etc., in the emission region. Sy 1's have a lot of emission lines, permitted lines, forbidden lines and semiforbidden lines. The permitted lines are broad and comprise strong hydrogen lines, in particular Balmer lines (Table 4, Fig. 12), He I, He II, Fe II (Table 5), C IV λ 1550 (Wu et al 1981; Fig. 13a), CO (Bieging et al. 1981), etc. The most frequently observed forbidden lines, which are narrower than permitted lines, are [O I], [O II], [O III], [N II], [S II], [Fe VII] (Table 5, Fig. 12), [Ne V] (Osterbrock 1977). [Fe X] λ 6374, with IP=234ev, and [Fe XI] λ 7892, with IP=262ev (Grandi 1978; Fig. 14), have been identified in several Sy 1 and Sy 2. The highest-ionization Sy 1 presently known, III Zw 77, shows these lines as well as [Fe XIV] λ 5303, with IP=361ev (Osterbrock 1981a). The semi-forbidden lines C III] λ 1909 and O IV] λ 1402 (Snijders et al 1980; Fig. 13) have also been detected in some Sy 1. For instance, NGC 4151 has a strong C III] emission line (Penston 1980; Boksenberg et al. 1980), with a FWZI 2000 km/s.

This section is devoted to emission line discussion, and includes five parts.

2.2.1 BLR and NLR

As mentioned in section 1.2, Osterbrock and Koski (1976) have emphasized that the broad Balmer-line wings provide a criterion for the distinction between Sy 1 and Sy 2. As already mentioned there are also intermediate Seyfert types whose H I profiles are composed of two parts, a narrow component(core)and a broad component (wings). The Balmer-line cores of Sy 1.5 have the same red-shift of, and profiles similar to, the forbidden lines. Balmer-lines core density relative to forbidden lines are also similar to those found in Sy 2's.

Woltjer (1959) has suggested that the great width of emission lines in the nuclei of Seyfert galaxies is due to a large velocity dispersion in the emitting gas. This interpretation of Doppler broadening received considerable support from observations by Walker (1968). He found that the nucleus of NGC 1068 is surrounded by a number of distinct clouds which have velocities of up to 600 km/s relative to the centre of the galaxy. Similar clouds having slightly lower velocities have been found by Ulrich (1973) within a few arc seconds of the nucleus of NGC 4151. Oke and Sargent (1968), Van den Bergh (1975) have suggested a model for Seyfert 1 nuclei (Fig 15) . The broad Balmer and other permitted line wings arise in fast moving (V ~ 3000 km /s) dense ($n_e \sim 10^8$ cm^{-3}) clouds, but the narrow permitted line cores and forbidden lines arise in more slowly moving (V~ 300 km/s) and less dense ($n_e \sim 10^5$cm^{-3}) clouds. Namely, there are broad-line region (BLR) and narrow-line region (NLR) in the Sy 1 nuclei. The density in BLR is sufficiently high to suppress the forbidden lines.

As mentioned in Section 1.1, the time scale of the variations in brightness sets limits to sizes of emitting regions. Data on the optical variability of Seyferts has been assembled by Cannon et al (1971), Lyutyi(1973), Penston et al (1974), Lyutyi and Pronik (1975), Mc Gimsey et al (1975), Scott et al (1976), Miller (1978, 1979a, 1979b). The optical continua of all Sy 1, like those of the QSOs, are variable. The time scale of the variations of optical continua is of the order of days; so that the sizes of continuum region are about 10^{-3}pc. On the other hand changesin the emission-line spectra of Sy 1 have been reported (Tohlin and Osterbrock 1976; Boksenberg and Netzer 1977; Cromwell and Weymann 1970; Phillips 1978; Schulz and Rafanelli 1981; Foltz et al 1981; Peterson et al 1982). In particular, Peterson et al (1982, 1984) have provided variability data of the emission-line spectra and optical continua of 31 Sy 1. They have indicated that some galaxies have Hβ profiles which show complicated structure (e.g., Mkn 279 and Akn 120), and this structure appears to change on time scales of a few months to a few years. This means that the sizes of BLRs in Syl are 10^{-1}pc to ~1pc.

The polarization data (as discuss in Section 2.2.5) further verify that there are two different regions, BLR and NLR, in Sy 1.

2.2.2 Physical conditions in BLR and NLR

As we know, the forbidden lines are suppressed by collisional de-excitation in BLR. This sets a lower limit to the electron density in this region, $N_e \gtrsim 10^8 cm^{-3}$. (Oke &Sargent 1968; Souffrin 1969; Osterbrock et al 1976). C III]λ 1909 appears as a strong broad line in some Sy 1. Since this line is collisionally de-excited at high densities (Osterbrock 1970), its presence indicates $N_e \lesssim 10^{10} cm^{-3}$ in that region.

In general, any measured intensity ratio involving two lines from two different upper levels of the same ion gives a single one-parameter relation between N_e and T. For instance, Seaton (1975) has derived the following relation for the [O III] intensity ratio:

$$\frac{I(\lambda 4959)+I(\lambda 5007)}{I(\lambda 4363)} \simeq 7.2 \left(\frac{1+0.0054\ X}{1+0.063X}\right) \exp\left(\frac{32970}{T}\right)$$

with $X=10^{-2} N_e \sqrt{T}$. For [S II] lines an analytic approximation to the intensity ratio is

$$\frac{I(6716)}{I(6731)} \simeq 1.50\left(\frac{1+1.38X}{1+5.29X}\right)$$

Therefore, if we measure the intensity ratios and we know Ne we can estimate T, and vice versa. Since the spectra of Seyfert galaxies show a wide range of ionization levels, undoubted there are also wide ranges in Ne and T. In the O^{2+} zone probably $Ne \approx 10^4 cm^{-3} - 10^6 cm^{-3}$, with $T \approx 10^4 - 2 \times 10^4 K$ (Boksenberg et al. 1975; Osterbrock et al. 1976; Osterbrock 1977). On the other hand, in the S^+ region $Ne \approx 10^3 cm^{-3}$. Penston et al. (1984) have studied the Fe^{9+} region in active galactic nuclei (AGN), and concluded that the radius of the Fe^{9+} zone in NGC 4151 lies between 1×10^{-4} and 0.5 pc, its density between 4×10^4 and $6 \times 10^{11} cm^{-3}$, and the broad lines of [Fe X] and [Fe XI] are produced in a region intermediate between the BLR and the NLR. It thus appears that the high ionization lines originate from the innermost parts of NLR (Grandi, 1978).

From the similarity of the narrow line spectrum of the Seyfert 1 galaxies with that of Cygnus A, whose element abundancy have been determined quite well, Osterbrock (1979) tentatively concluded that the element abundances of the NLR

of Sy 1 are more or less normal: H $\sim 10^4$, He $\sim 10^3$, N ~ 1, S ~ 0.3 and Fe ~ 0.1. Much less information is available on the abundance of the elements in BLR of Sy 1. Generally speaking, strong broad H I imply that H is the most abundant element. The measured intensity ratio of He I $\lambda 5876/H_\beta$ is 0.1-0.3 (Osterbrock 1979), and implies that their abundance ratio is order 0.1 by number.

Other important parameters are mass and radius. On the basis of observations of optical variability, we are able to estimate the size of the region where the variability occurs. However, NLR and BLR of many Sy 1 do not show variabilities. For this reason we have to use another method which based on recombination line theory, i.e., the volume, mass and radius are defined by the equations

$$L(H_\beta) = Ne\ Np\ \alpha_{H_\beta}\ h\nu_H\ V\ \epsilon$$

$$M = (Np\ m_p + N_{He}\ m_{He})\ V\ \epsilon$$

$$V = \frac{4}{3}\pi r^3$$

where ϵ is the 'filling factor', α_{H_β} is the recombination coefficient for emission of H_β, and to a good approximation $N_{He} = 0.1\ Np$ and $Ne = Np + 1.5\ N_{He}$. The most luminous nuclei of Sy 1 have $L(H_\beta) \approx 10^9\ L_\odot$ (Adams & Weedman 1975), thereby we get $M \approx 36\ M_\odot (10^9/Ne)$ and $r = 0.015\ \epsilon^{-1/3}\ (10^9/Ne)^{2/3}$ pc.

Now we can show crude physical parameters in BLR and NLR of Sy 1 as follows.

	BLR	NLR
Radius	0.1 - 1 pc	10^2 - 10^3 pc
Electron density	10^8 - 10^{11} cm^{-3}	10^3 - 10^6 cm^{-3}
Temperature	10^4 - 2×10^4K?	10^4 - 2×10^4K
Filling factor	10^{-2} - 10^{-3}	10^{-2} - 10^{-3}
Mass	$10^2\ M_\odot$	10^5 - $10^6\ M_\odot$
Velocity of clouds	10^3 - 10^4km/s	5×10^2 km/s
Relative abundance	H $\sim$ 1, He $\sim$ 0.1	H $\sim 10^4$, He $\sim 10^3$, N $\sim$ 1 O $\sim$ 4, Ne $\sim$ 1, S $\sim$ 0.3, Fe $\sim$ 0.1

In addition, a recent paper, "Detailed observations of NGC 4151 with IUE - III" (Ulrich et al 1984), has provided a lot of valuable information about BLR of NGC 4151. In terms of observations of the variability and width of the three strong ultraviolet emission lines, C IV, Mg II and C III], in the NGC 4151, Ulrich et al have found there is an evident stratification the BLR which is summarized as follows.

Stratification in BLR of NGC 4151

Subregion	Line observed	Velocity V (km/sec)	Size r (cm)	Physical conditions
BLR 1	C IV λ1550	14000	3×10^{16}	Ionized throughout
	He II λ1640?			$Ne \gtrsim 10^{10} cm^{-3}$?
	(no Mg II λ 2800,			Variable
	no C III λ1909)			
BLR 2	C IV λ1550	11000	6×10^{16}	Optically thick to
	Mg II λ 2800			Lyman continuum
	He I λ5876 *			$Ne \gtrsim 10^{10} cm^{-3}$
	(no C III] λ1909)			Variable
BLR 3	C IV λ1550 ?	4000	10^{18}	$Ne \leq 10^{10} cm^{-3}$
	Mg II λ 2800			Non-variable ?
	C III] λ 1909			More extended
	Balmer lines *			

* Boksenberg et al. (1975).

2.2.3. Photoionization

As mentioned above, [O III] (λ4959+λ5007)/(λ4363) intensity ratios indicate that in many Sy 1 the O^{+2} ion exists at $T \approx 10^4$ - 2×10^4K. This implies that the ionization is not of thermal origin because thermal ionization would require a temperature range $6.5 \times 10^4 K < T < 1.4 \times 10^6 K$ (Osterbrock 1979). By analogy with H II regions and planetary nebulae, it is natural to

imagine that the spectrum of Sy 1 nuclei is due to photoionization. But we have to note that no star or mixture of stars could give the wide range of ionizations, from [O I] and [S II] to [Ne V] and [Fe VII] even to [Fe X] and [Fe XI] observed in many Seyfert galaxies.

Williams and Weymann (1968) have proposed that ionization in Seyfert nuclei might be due to ultraviolet radiation emitted by the non-thermal continuum sources at their centres. Such photoionization model receives considerable support from many observational facts and theoretical analyses. Searle & Sargent (1968) indicated that the equivalent width of H_β emission in Seyfert nuclei and QSOs usually lies in the rather narrow range 20 Å $\leq$ EW(H_β) $\leq$ 100Å even if these objects cover three order of magnitude in absolute luminosity. This apparent coupling between H_β and continuum intensity is most easily understood if the ultraviolent part of the non-thermal spectrum ionizes the gas that produces the recombination line spectrum. On the other hand, the observed continuous spectrum can be decomposed into normal-galaxy and power law components which have the form $F_\nu \propto \nu^{-\alpha}$, with $\alpha \simeq 1.0 - 1.5$. The number of ionizing photons in such an extrapolated power-law spectrum is sufficient to balance the total number of recombinations observed through the H I lines (Osterbrock & Miller 1975; Davidson & Netzer 1979). Since the International Ultraviolet Explorer (IUE) was launched successfully on 26 January 1978, a number of AGNs which include several tens of Seyfert galaxies have been observed. As a general result the ultraviolet continuum is found to be dominated by a power law spectrum (Perola, 1983), thus reinforcing the view that photoionization models with power law continua apply to practically all types of AGNs with emission lines.

Wu et al (1983) have published UV observational data of 29 Seyfert galaxies among which there are 21 Sy 1, 5 Sy 1.5 and 3 Sy 2, and found that the observed fluxes of Ly_α, C IV λ1550, C III] λ 1909, and Mg II λ 2800 of Sy 1 and Sy 1.5 correlate well with the observed continuum flux at 1450 Å (Fig 16a,b), and that the correlations between the CIV luminosity and that at 1450 Å and the 2 - 10 kev band are good (Fig 17). They have concluded that these results support the hypo-

thesis that photoionization by the nonthermal continuum is the main source of heating for these AGNs. Other evidences are based on the observations of optical variability of Seyfert galaxies. In NGC 1068, 3516 and 4151 the H_α intensity fluctuated with a time-scale of 10 - 20 days, and the variability was correlated with that of the ultraviolet continuum except for a 1 - 2 months delay (Cherepashchuk & Lyutyi 1973). Peterson et al (1982, 1984) have reported the variability of 30 Sy 1, and found that changes in the H_β flux are correlated with changes in the optical continuum. Recent work (Ulrich 1984) has indicated that in NGC 4151 the C IV emission line intensity changes follow the continuum flux changes at 2500 A, but show a delay of at least 13 days. It is interesting that if photoionization has to account for the C^{+2} ions, the power law needs to be the dominant source of ionization at $\sim$260 A. More work is needed to verify this speculation.

As for the ionization level, [Ne V] and [Fe VII] are observed in many Sy 1 and Sy 1.5, but few Sy 2. According to the photoionization model, this suggests there may be a cut-off or turndown of the ionizing continuum in Sy 2 around 100 ev (Cohen 1981). The [Fe X] and [Fe XI] are also observed in a lot of Sy 1 and Sy 1.5. Their ionizing photons have X-ray energies. Indeed every Sy 1 or Sy 1.5 is an X-ray source, while the Sy 2 are weak X-ray emitters.

2.2.4 Line profiles

The profiles of the emission lines play an important role in studying the Seyfert galaxies and other active galactic nuclei. Various theoretical models of active galactic nuclei contain calculated profiles for comparison with observational data. There are a number of papers on this aspect (see Table 2). In particular, Osterbrock and Shuder (1982) have published observed profiles of H I, He I and HeII emission lines in 19 Sy 1. Of the 19 galaxies in this paper, 10 were found to have symmetric H_β line profiles, 6 galaxies were to have H_β line with redward asymme-

tries, and 3 galaxies were surprisingly found to have H_β lines with blueward asymmetries. They confirm the earlier report by Osterbrock (1977) that H_β is often wider than H_α, and H_γ wider than H_β (see Table 6). They think that these facts suggest that a combination of velocity fields, rather than a single field, may be part of the Seyfert phenomenon, with one type dominating in some galaxies, another type in others. However, the gas some times escapes from the nucleus and can spread through large volumes, having a kinetic energy 10^{56} ergs (Weedman 1977). The source of this energy is unknown and worth exploring.

Capriotti, Foltz and Byard (1979) explained the red asymmetry, assuming a radial outflow combined with absorption or extinction. But their interpretation cannot be generally true. Outflow or inflow combined with absorption or scattering can produce a red or blue asymmetric profile; rotation (Shields 1977) and electron scattering (Mathis 1970; Weymann 1970) can only produce symmetric profiles. Osterbrock and Shuder (1982) have examined the statistics of galaxies with symmetric profiles alone, for which rotation might be the main source of broadening, looking for a correlation between line width and apparent inclination. No correlation was found, in agreement with the previous results of Keel (1980) and Simkin et al. (1980). Thus, rotation around the rotation axis of the galaxy is apparently not the main broadening mechanism, even in the Sy 1 with symmetric line profiles. However, the rotation about a different axis cannot be ruled out in the Sy 1 with symmetric line profiles. Models incorporating outflow, inflow, roation about a different axis, and turbulence remain to be explored.

Heckman et al (1981) reported measurments of the profiles of the [O III]λ 5007 narrow emission lines in 36 Seyferts and radio galaxies among which there are 17 Sy 1 (see Table 7). Before then, there was comparatively little work on narrow line profiles (e.g., Glaspey et al 1976; Pelat and Alloin 1980). Heckman et al defined and tabulated an asymmetry index AI_{20} which describe the asymmetries of the spatially integrated [O III]λ5007 profiles (Table 7 and Fig 18),

$$AI_{20} = \frac{WL20 - WR20}{WL20 + WR20} = \frac{\Delta W20}{W20} \quad ,$$

where WL20 and WR20 are the half widths at the 20% intensity level to the left and right of the line center defined at the 80% intensity level.

By using of their data we plotted histogram of the asymmetry index (AI_{20}) for Sy 1 in their sample (Table 7 and Fig 19). This asymmetry shows blueshifts in 82.3% of [O III]λ5007 lines of their sample. The blueward asymmetries in the lines are accompanied by net blueshifts for the lines relative to the galaxy systematic velocities (Table 8).

Heckman et al suggest that blueward asymmetries in line profiles and their net blushifts have a common origin. An obvious explanation is that the redward wings of the line profiles are being preferentially attenuated. This situation would naturally occur if the emitting gas is mixed with dust and flowing radially with respect to the nucleus in NLR. Such a picture has been sketched previously by Grandi (1977) and Pelat et al (1980). Further, there is an excellent agreement between the degree of asymmetry in the [O III] lines, AI_{20}, and the H_α/H_β narrow emissi n-line intensity ratio, $AI_{20} \propto F(H_\alpha)/F(H_\beta)$. Moreover, for nuclei having a broad-line region, the degree of profile asymmetry, AI_{20} is inversely correlated with the [O II]λ3727/[O III]λ5007 and [O III]λ5007/[O I]λ6300 intensity ratios (Heckman et al. 1981). This suggests that the larger the asymmetries are, the larger is the amount of reddening by dust. Therefore, the above facts are powerful evidence that dust is playing an important role in determining the line profiles and the ionization structure of the NLR.

It is interesting that inspection of high resolution profiles of the [O III] λ5007 indicates that the profiles often have two component structures with a narrow "core" superposed on a broad, blueshifted "base" (Heckman et al 1981). This shows that the structure of NLR is also complicate.

The above observational results and statistical analyses are important checks on theoretical models, and provide a sound basis for further research. Perhaps the most widely adopted basic idea is that the observed high velocities result from radial, radiation-pressure driven flows (Blumenthal & Mathews 1975). Simpli-

fied spherically symmetric models of this type give forms of the line profiles in relatively good agreement with observations (Blumenthal & Mathews 1975; Capriottiet al 1980). However, they do not explain the lack of correlation of FWHM with luminosity. Osterbrock (1984) has plotted a schematic picture of BLR and NLR of Sy 1 (Fig 20). The tipped BLR is shown crosshatched; at its center is the photoionization source, probably an accretion disk aroud a black hole. The BLR is supposed to be optically thick to ionizing radiation along nearly all rays in its equatorial plane, but not at its poles, so that ionizing photons mostly escape only within a cone about this axis, which is also the axis along which radio plasma can escape. In a nearly "pure" Sy 1 the optical depth of the BLR is large and the cone shrinks to an angle of nearly 0°; in the opposite extreme the disk is optically thin in all directions, the object is nearly "pure" Sy 2, and the cone opens out to 90°. The NLR is composed of density condensations, each of which is mostly highly ionized on the face toward the photoionization source. Each condensation is optically thick, and is only slightly ionized on the side facing away from the source. The most distant condensations are not as highly ionized at their front faces as those nearer the source. The BLR has a similar structure, consisting of condensations also. This cylindrically symmetric wind picture is very suggestive, but highly schematic.

In summary, much work has been done to compare theoretical line profiles, generated under different aesuptions of the cloud kinematics and dynamics, with observed ones in order to deduce the nature of the motion and physical condition in BLR and NLR of Sy 1 (Blumenthal & Mathews 1975; Shields 1978; Davidson & Netzer 1979; Grandi & Phillips 1979; Capriotti et al 1980; Grandi 1980; Krolik et al 1981; Kwan & Carroll 1982; Krolik & Vrtilek 1984). However, many problems are still open.

2.2.5 Balmer decrement

The Balmer emission in most astrophysical plasmas, such as H II regions and planetary nebulae, arises from radiative ionization followed by recombination. Downward cascades within the newly recombined atoms produce emission lines whose intensity ratios can be calculated. For a nebula optically thick only in the Lyman lines (Menzel-Baker case B), the ratio of Balmer-line intensities (the Balmer decrement) is $H_\alpha : H_\beta : H_\gamma = 2.8 : 1.0 : 0.47$ for temperature near 10^4 K (Miller 1974). In Seyfert galaxies, the Balmer decrement is invariably steeper than this, but it turns out to be impossible to account for all observed decrements with any assumed amount of interstellar extinction (Fig. 21). In Fig. 21, the square marks the recombination decrement, and dashed line marks normal interstellar extinction path. The points roughly scatter about this line, but deviations from it are considerably large. It thus appears that the interpretation of this observational fact must take into account both the effect of reddening and deviations from the pure case B situation.

(1) Reddening effect. A substantial amount of reddening is needed to account for the observed decremtns. Of course, the absorbed energy has to be reradiated in the infrared band. Indeed, Seyfert nuclei are strong infrared sources (Rieke 1978; Lebofsky & Rieke 1979). Rieke (1978) found that the strength of the infrared excess (1-10 μm spectral slopes) is correlated with the strength of the reddening, as measured by the Balmer decrement. Ward et al. (1982) reporeted a correlation (Fig. 22) between Balmer decrement ($\log H_\alpha/H_\beta$) and (U-L) index (i.e. 0.36-3.5 μm). This investigation shows that a significant amount of reddening due to dust may be rpesent in Sy 1. On the other hand, if reddening of Sy 1 is due to dust, then a strong absorption dip at 2175 Å is expected in the UV spectrum of Sy 1's. Such a dip however is usually weak or absent (Malkan & Sargent 1982). There are two obvious possibilities: one is that other effects play an important role in determining the amplitude of Balmer decrements; another is that some special mechanism produces strong radiation around 2175 Å. As concerns a discussion of reddening effects we shall go into details in Chapter III.

(2) Non-reddening explanations. Netzer (1975) and Shields (1974) suggested that collisional excitation and self-absorption from the level n=2 are important under the high-density conditions of Seyfert nuclei. Their calculation show that, combined with interstellar extinction, they can put the Balmer decrement in the observed range of Fig. 21.

Lacy et al (1982) have reported nearly simultaneous IR, optical, and UV observations of hydrogen line emission from 18 Seyfert galaxies. Their main conclusions are as follows: (1) In many of the 18 observed Seyfert galaxies, P_α is stronger relative to the Balmer lines than is predicted by recombination calculations (Fig. 23), i.e., Seyfert galaxies tend to fall near the reddened case B line; (2) Reddening is the only mechanism which has been suggested that will enhance P_α relative to the Balmer lines by the amount observed in a significant number of the observed galaxies; (3) High densities and large optical depths are required in addition to reddening to explain the range of $P_\alpha/H_\alpha/H_\beta$ ratio. They also have indicated that several effects can alter the Ly_α/H_β ratio: reddening, collisional excitation of H_β and de-excitation of Ly_α, and large optical depths. Reddening by dust external to the galactic nuclei cannot by itself explain both the P_α/H_β and Ly_α/H_β ratios.

Additional evidence that dust is an important constituent of active nuclei follows from the analysis of polarization data.

The polarization of the optical continuum, first found in the nucleus of Sy 2, NGC 1068, by Walker (1966) and Dibay and Shakhovskoy (1966), was taken as evidence of synchrotron or other nonthermal emission (Visvanathan & Oke 1968). However, Jones and Stein (1975) pointed out that the dust cloud is also able to polarise the continuum. Angel et al. (1976) provided convincing evidences that: (1) the continuum radiation is circularly polarised; (2) the permitted lines of H I and probably also He II are polarized at nearly the same position angle and by the same amount as the neighbouring continuum. The forbidden lines are weakly polarized, at a position angle quite different from the continuum, indicating an origin outside the per-

mitted line region. In the last several years, the polairzation of about one hundred Seyfert galaxies was investigated (Martin et al. 1983). A large portion of the Seyfert galaxies observed are Sy 1, some of which were observed in great detail, for example, NGC 4151 (Thompson et al. 1979; Schmidt and Miller 1980), Mkn 231 and NGC 3516 (Thompson et al. 1980), IC 4329A and Mkn 376 (Martin 1982).

The polarization properties of Mkn 231 and NGC 3516 resemble those of NGC 1068 showing a strong wavelength dependence with the polarization increasing smoothly into the blue and the presence of polarized H_α emission (Thompson et al 1980). They suggested that the polarizaion of these objects is caused by an asymmetric dust envelope surrounding the nucleus, and pointed out that no polarization variability was detected with time-scales ranging from a few weeks to three years. The polarization of Mkn 376 and IC 4329A (Martin et al 1982) is also similar to NGC 1068. In particular, in the case of IC 4329A this fact together with the orientation of the electric vector along the dark dust line, suggests that the polarization is produced by aligned grains in the galactic disk.

However, the polarization data on NGC 4151 (Schmidt and Miller 1982) disclose that the narrow Balmer line cores and forbidden lines are polarized alike, but that the broad-line emission is unpolarized. The result confirm the distinction between a high-density, broad-line emission region and the lower-density, forbidden line emission region. The continuum polarization varies smoothly across the spectrum, but the angle is constant. Thompson et al (1979) pointed out that the continuum observations are consistent with electron scattering or a nonthermal mechanism if the polarization is diluted in the red by starlight; however, dust scattering in an asymmetrical cloud surrounding the nucleus cannot be ruled out. Schmidt & Miller (1982) suggested that a decline in degree of polarization in the near-UV results from dilution by unpolarized, blended, broad Balmer emission, and that elsewhere, the wavelength dependence is consistent with the presence of a uniformly polarized synchnotron component of shape $F_\nu \propto \nu^{-0.33}$.

Another important suggestion is that the large majority of Seyfert galaxies have little intrinsic optical polarization ($P < 0.2 - 0.5\%$) (Martin et al 1983).

When they use the correlation between P_{max} and E_{B-V} in our Galaxy,

$$P_{max} \approx \gamma 9 E_{B-V} \%\, mag^{-1}, \text{ where } \quad 1/3 \leq \gamma \leq 1,$$

the above degree of polarization shows a little of dust in the Seyfert galaxies. Their suggestion is not conclusive because the mechanism producing polarization is unclear for Sy 1 so far. However, this problem is worth exploring.

2.3 UV excess and IR excess

2.3.1 UV excess

Sy 1 nuclei have a smooth continuum which is largely nonstellar (Oke & Sargent 1968). From infrared to visual wavelengths the continuum spectra resemble a power law, $f \propto \nu^{\alpha}$ with a index, α, which ranges around -1 (Neugebauer et al 1979). In the blue and ultraviolet, however, the continuum becomes essentially flat, resuming its fall around 2500 Å and further steepening below 1200 Å. This excess of ultraviolet flux over the red power law has been referred to as the "3000 Å hump" (Richstone & Schmidt 1980) and is prominent in almost all quasar and Sy 1 spectra. The "hump" consistently appears in the rest wavelength ranges around 3000-4000 Å (Shields et al 1972; Phillips 1978). To measure the ultraviolet excess, Malkan & Sargent (1982) first substracted power laws from the spectra. They determined the power law slopes from the red and infrared data points (Fig. 24). All of the objects have a strong ultraviolet excess over the red power law. Fig. 25 shows the excess flux, i.e., observed minus power law. This ultraviolet excess always has a rapid rise from about 4000 to 3500 Å. At shorter wavelengths it falls gradually, and then steepens beyond 1400 Å. In at least for three objects in the sample , Mkn 79, Mkn 335 and Mkn 509, excess flux is present redward of 5000 Å.

This UV excess cannot be due to blended emission lines (Grandi & Phillips 1980; Neugebauer et al 1979). The most promising explanation, Balmer continuum emission, has been rejected because the observed ultraviolet excess is too strong and too flat (Grandi & Phillips 1980). Shields (1978) and Ulrich et al (1980) suggested that the ultraviolet excess is optically thick thermal emission, but they could not obtain satisfactory fits with blackbody temperatures from 10^4 to 2×10^4 K. Malkan and Sargent (1982) studied 7 Sy 1 and 1 QSO. They thought that UV excess from 4000 to 3500 Å is significantly contributes by Balmer continuum emission, and point out that several other observations support this point of view: (1) The excess flux at 3500 Å correlates well with the Balmer emission line fluxes(Yee 1980). No AGNs with very weak broad lines, such as NGC 1275 or a BI Lac object, has a "3000 Å hump"; (2) When the Balmer line fluxes vary, so does the

ultraviolet flux (Oke et al 1980); (3) De Bruyn (1980) found that the strong variability of the 3500 Å continuum is more closely linked to the Balmer lines higher than H_α ; (4) The continuum polarization of NGC 4151 drops rapidly at wavelengths less than 4000 Å (Schmidt & Miller 1980). Their explanation is that most of NGC 4151 near-ultraviolet flux is produced by the Balmer continuum, which, like the broad Balmer lines, is unpolarized.

However, when they fitted the spectra in detail with combinations of power-law and Balmer continuum emission, at least 4 Sy 1 had an additional component present from 5000 Å to the far-ultraviolet. It is probably not produced by photoionization, since its luminosity can exceed the total ionizing energy available in the power law. This component is well described by a blackbody at a single temperature, which ranges from 2×10^4 to 4×10^4 K (Malkan & Sargent 1982). So from visual to ultraviolet wavelengths the continuum spectra of Sy 1 seem to be produced by combination of power-law, recombination, and blackbody emission.

What produces this kind of blackbody emission ? Malkan & Sargent (1982) suggested that it is probably produced by accreting optically thick gas, perhaps in a disk. In order to compare observational spectra more accurately with the expected emission from optically thick accuretion disks, Malkan (1983) observed three high-redshift QSOs by using of the IUE to measure their spectra down to a rest wavelength of 800 Å which is much bluer than the maximum in the thermal component. He found that the UV excess flux actually has a broader spectral distribution than a single Planck function. To improve the fits, the Planck function was replaced with a thermal component containing a range of temperatures. The thermal emission was described by a physical model, i.e., an optically thick steady-state accretion around Schwaschild black holes or Kerr holes (Malkan 1983). The calculation indicated that the spectrum of a disk around a Schwarzschild hole looks very similar to that of a disk around a Kerr hole with two or three times the mass. These broader accretion-disk spectra fit the data singnificantly better than a single-temperature blackbody. Meanwhile Malkan (1983) said that three independent observations also support accretion disk model: (1) time scales of optical variability; (2) low

linear polarization; (3) weak Lyman jump. This is an attractive suggestion, even if the model is still very schematic.

2.3.2 IR excess

As described above, from infrared to visual wavelengths Sy 1 nuclei have power law continuum spectra which show that a substantial infrared excess (above the direct output of stars) is a universal or nearly universal characteristic of them. Rieke's (1978) survey for 53 Seyfert galaxies at 10.6 μm demostrated this conclusion further. The nature of the infrared continuua in Seyfert galaxies has been controversial. In general, the Sy 2 display a strong stellar component (Koski 1978), and an additional steeply rising component in the near-infra-red with a spectral shape characteristic of thermal emission by dust (Neugebauer et al. 1976; Rieke 1978). Unlike the Sy 2, Sy 1 are dominated in the visible by their nuclear emission. Although nonthermal infrared emission is believed to be present in Seyfert galaxies (Balzano & Weedman 1981), there is no conclusive evidence for nonthermal emission as the primary source of the infrared flux in any Seyfert galaxy. Such evidence would include short-term variability indication of a compact emission region, or a strong polarization characteristic of synchrotron radiations, as describe below.

Variability is observed at infrared wavelengths, but on time scales longer than in the optical or X-ray (Martin et al 1976; Dower et al 1980), and of sufficient duration to be compatible with the heating or cooling of dust and the sebsequent changes in thermal reemission (Lebofsky & Rieke 1980).

Three recent observational works have confirmed that the infrared emission is extended and not dominated by a bright central source in at least several Sy 1 galaxies. (1) Smith et al (1983) have observed the far-infrared flux from Sy 1, NGC 4051, at 130 μm and 170 μm with the 90 cm telescope on board the NASA Kuiper Airborne Observatory. Their detector system used a seven-channel array consisting of a central detector surrounded by six others in a close-packed configuration. The center-to-center separation between neighboring channals was 56". This instrument has made them to get observational data which show that the strong far-

infrared emission arises from an extended region. This result considerably strengthen s arguments that favor local sources of radiation, in particular thermal emission from dust heated by star formation. According to observational data they have estimated the ratio $F_\mu(93\mu m)/F(CO)$ for NGC 4051, and indicated that the estimated value agrees with that found in galactic H II region and NGC 1068. They concluded that dust is responsible for the majority of the luminosity, and that star formation is a likely source of this energy since the emission extends outside the nucleus, and since the spectral character and gas/dust ratio resemble that seen in galactic star formation region and the Sy 2, NGC 1068. (2) Cutri et al (1984) have reported the spatial extent of the $3.3\mu m$ emission feature in Sy 1.5, NGC 7469, by use of multiaperture observations. Nearly 80% of $4.7 \times 10^7 L_\odot$ that is emitted in the $3.3\mu m$ feature within 730 pc from the central source is found to arise in a region betwen 240 and 730 pc from the central source; This implies the presence of dust in this region with a temperature of $\geq 300K$. Their estimates have shown that neither the distant central continuum source nor the radiation from the BLR and NLR clouds is capable of heating grains with normal emissivities outside the nucleus to such high temperatures, and that dust heating must therefore occur in situ and is most likely due to radiation from young, hot stars in circumnuclear H II regions. (3) Bregman & Wittborn (1984) have obtained an $8-13\mu m$ spectrum of a Sy 1, Mkn 231. Comparison of their data with previously published data indicates that the infrared emission is extended and not dominated by a bright nucleus. On the basis of spectroscopic analysis they have suggested that dust in Mkn 231 is composed of crystalling silicates which condensed at higher temperatures, e.g. about 300K, than typical silicates in our Galaxy.

Infrared polarimetry has been obtained for two Sy 1, NGC 4151 and Mkn 231 (Kemp et al. 1977): only small polarizations ($P < 1\%$) were detected. Rudy et al (1982) presented polarimetry at $2.3\mu m$ of 8 Sy 1, seven of which had not been observed previously. There was no evidence of strongly polarized nonthrmal emission in any of the galaxies observed ($P > 1\%$).

Rieke (1978) suggested that if dust is present in the nuclear sources, it might

be expected to redden the source in the visible and to contribute to the infrared flux. hence we may expect a loose correlation between reddening, $\langle A \rangle$ estimated from the Balmer decrement, and infrared properties represented by the infrared spectral index α from 1 to 10 μm. A correlation is indeed found (Fig. 26). In Fig. 26 infrared excess is proportional to reddening. This implies that the infrared excess is due to thermal re-emission by dust, since reddening is due to dust.

In addition, there is some evidence that Sy 1 with relatively strong forbidden lines tend to have steep infrared continua (Rieke 1978). This means that the more gas that there is in the forbidden line region, the more dust there is.

On the other hand, Roche et al. (1984) have looked for the presence of dust emission features in the infrared. However, the 8 - 13 μm spectra of 4 Sy 1 and 6 Sy 2 which they observed show no evidence for dust emission features with the exception of the Sy 2, NGC 7582, which does show the narrow dust emission features at 8.65 and 11.25 μm. Two of the other Sy 2, NGC 1068 and 5506, have minima near 10 μm, attributed to absorption by cold silicate dust. The remainder have smooth featureless spectra well fit by power law.

In summary, at least in those Sy 1 with steep infrared spectra (relatively negative α) and extended infrared emission thermal re-radiation by dust is an important part of the infrared luminosity. However, for those Sy 1 with flat infrared spectra, the mechanism of infrared radiation is unclear. If nonthermal radiation, for example synchrotron radiation, is the main component, then infrared radiation is produced in optical continuum source.

Variability and polarization observations of infrared radiation are strongly required to udnerstand the radiation mechanisms. Perhaps power law, stellar radiation and thermal emission by dust can be put together in different mixture to explain the infrared spectra of Sy 1.

2.4. Radio structure

2.4.1. General properties

Seyfert galaxies are not generally strong radio sources (Kellermann 1972; 1984). The radio luminosity of Seyfert galaxies is typically 10^{39-41} ergs/s (de Bruyn & Wilson 1976) which, although greater than that of a normal spiral, is orders of magnitude weaker than that of most radio galaxies. Furthermore, the luminosity of a Seyfert nucleus in the radio band represents only a small fraction of its total luminosity which is dominated by infrared, X-ray radiation (10^{43-46} ergs/s). In general, Sy 1 have a radio luminosity less than that of most Sy 2 (de Bruyn & Wilson 1978; Sramek & Tovmassion 1975). A recent observation showed that for a given nonthermal optical luminosity, Sy 2 are 40 to 100 times more efficient than Sy 1 in generating radio emission (Ulvestad & Wilson 1984). The radio emission is associated with the nucleus of the galaxies and has a steep, nonthermal spectrum ($-0.5 > \alpha > -1.0$), a power at λ 21 cm $\approx 10^{21-22}$ WHz^{-1} sterad^{-1}. The size of the radio source is generally of the order several hundreds of parsecs to a few kiloparsecs, comparable in scale to the forbidden line region (de Bruyn & Wilson 1978). Double radio sources outside the optical nuceli are not found. The radio sources in Sy 1 may be physically smaller, on average, than those in Sy 2 (Wilson 1982). Correlations appear to exist between the [O III] 5007 and the continuum luminosity at λ 21 cm (Fig. 27), and between continuum luminosity at 10 m and λ 21cm (Fig. 28) (de Bruyn & Wilson 1978). These correlations are constant with the correlation between infrared radiation and forbidden line flux (Rieke, 1978).

To explain the correlation between radio and forbidden line flux, Wilson and Willis (1980) suggested that the relativistic particles and magnetic fields responsible for the radio emission may be in pressure equilibrium with the thermal gas responsible for the forbidden emission lines. The situation resembles the case found in the Crab Nebula where cosmic rays and a magnetic field of strength $\sim 10^{-4}$ gauss are in rough balance with the line emitting filaments ($T_e \sim 10^4$K, $N_e \sim 10^3$ cm^{-3}). This explanation implies that the mechanism of radio radiation is basically synchrotron (see Section 2.4.2).

However, the radio-infrared relation is harder to understand since the infrared radiation in most Sy 1 with flat infrared spectra appears to originate from much smaller regions than the radio emission. There are two kinds of explanations. First, the radio-infrared relation may simply follow from the radio-forbidden line relation coupled with the forbidden line-infrared correlation. Second, de Bruyn and Wilson suggested that if the relativistic electrons do not stream away from the infrared/optical continuum source at relativistic velocities they must be accelerated at distance in excess of a few parsecs from it. Perhaps such acceleration could be ascribed to the high velocity gas responsible for the forbidden emission lines via the often invoked plasma turbulence. The relation between the radio and infrared powers would then arise if the amplitude of these turbulent motions are somehow correlated with the infrared continuum power. Maybe the line emitting gases are accelerated by the optical/infrared radiation field. This suggestion seems to be strengthened by the relation between the continuum luminosity at λ 21 cm and the absolute magnitude in the U band for Sy 1 (Fig. 29). Of course, more observation data at different frequencies for Sy 1 are needed, to test correlations and the suggested interpretations.

2.4.2 Radio structure

Early studies of radio structure for a few bright Seyferts which are in the New General Catalog were carried out by Wade (1968), van der Kruit (1971) and Lequeux (1971), and showed that Seyfert nuclei emit moderate radio powers, stronger however than those of normal spirals. Subsequently, several Seyfert galaxies were detected in radio surveys of Markarian galaxies (Sramek & Tovmassin 1975; Sulentic 1976). Many more Seyfert galaxies were found to be radio emitters in an extensive survey of this kind of galaxy in λ 21 cm continuum radiation (1415 and 1412 MHz) (de Bruyn & Wilson 1976; Meurs & Wilson 1981; Wilson & Meurs 1982). Two excellent reviews of radio properties of Seyfert galaxies already exist (de Bruyn & Wilson 1978); Wilson 1982); In particular, observations of the sample of Markarian Seyferts with the VIA offer the possibility of exploring the central region of Seyferts in considerable detail (Wilson 1982; Ulvestad & Wilson 1984).

79 Seyfert galaxies in the first 9 Markarian lists have been studied (Ulvestad & Wilson 1984). 29 of the objects have 21cm flux densities about 10 mJy; they comprise a radio flux limited sample that has been mapped at the VLA. 18 galaxies were detected at Westerbork, but have flux densities less than 10 mJy at 21 cm. 32 galaxies have only upper limits ranging from 2 to 10 mJy at 21 cm. Ulvestad & Wilson (1984) have divided radio structures into 5 classes (Table 9 and Fig. 30).

Table 9 summarizes the properties of the total radio source for each of the 29 galaxies in the sample, plus Mkn 926, 1048 and 1261. Eight of the 29 objects contain type L radio sources, and almost all exhibit aligned components straddling the optical continuum nucleus (Fig. 30). The linear sizes of the radio sources range from below a few hundred parsecs to a few kiloparsecs, comparable in scale with the forbidden line region. The radio sources in Sy 1 are systematically smaller than those in Sy 2.

In addition, the differences between polarization and radio axis position angles, has been reported (Ulvestad and Wilson 1984). The differences are 10° for Sy 1, Mkn 926; 27° and 53° for the Sy 1.5, Mkn 5 and NGC 5548; and 67° and 73° for Sy 2, Mkn 78 and Mkn 573. There is a tendency for Sy 2 to have much larger positioon angle differences than Sy 1, and these data tentatively support Antonucci's (1983) finding of a relation between radio axes and optical polarization vector directions: in Sy 1, these directions tend to be aligned, while they tend to be perpendicular in Sy 2.

Wilson (1982) indicated further that a number of arguments favour nuclear ejection models to explain the linear radio structure of Seyferts.

(1) The nearby Seyferts with linear radio structure are view closed to "face-on". For example, the angle between the disc and the plane of the sky is i=39° for NGC 1068 (Burbidge et al. 1959), i=21° for NGC 4151 (Simkin 1975). It indiceates that the structures are truly aligned and are not caused by projection effects.

(2) The radio components in double sources are commonly elongated along the

radio axis (Fig. 30).

(3) The radio structure of NGC 4151 (Fig. 31) is strongly suggestive of quasi-continuous nuclear ejection (Ulvestad et al 1981).

However, because double radio sources are not, in general, found outside the optical isophotes of Seyferts (de Bruyn & Wilson 1976), the beam or plasmoids must not escape the nuclear environment (Kpc scale). The most natural means of achieving this is to "disrupt" the beam or "halt" the plasmoids by friction with the dense interstellar medium in the inner part of the spiral (Wilson & Willis 1980). Models of this type can be checked by finding more objects with curved radio structure in spirals. As long as the ejection is close to the plane of the galaxy, the 's' shape defined by the radio emission should curve in the opposite sense to that defined by the normal spiral arms.

As for Sy 1, there is a number of gas clouds in the BLR. Although the filling factor of the gas clouds is small, they can exert a tremendous ram pressure due to their high density and velocity ($\rho v^2 \approx 1000$ dyns/cm^2). Thus, the gas may be capable of disrupting or stopping the progress of jets from the galaxy nuclei. Such a interaction could do more than just reduce the average radio source size. Therefore, Sy 1 contain smaller radio sources than Sy 2. It might also account for the lower radio powers in the Sy 1, since bulk energy in a jet could be spent in generating turbulence and heating rather than being converted to radio emission (Ulvestad & Wilson 1984). It is plausible, but we can not rule out other possibility.

As described in Section 2.4.1, Seyferts radio spectra generally are power laws which have indices $-1.0 < \alpha < -0.5$, although a few have flat spectra with $\alpha \simeq 0$. The radiation mechanism is, therfore, non-thermal and presumably synchrotron. Generally speaking, there is a magnetic field in the beam. In the beginning near the Seyfert core, the magnetic field is parallel to the beam. Then, as the beam expands, field becomes perpendicular to the beam. When the relativistic electrons coming from the Seyfert nuclei inject into the beam, they may produce radio radiation, i.e., synchrotron radiation. This picture seems to be appropriate to

Seyferts.

According to the radio properties of Seyferts, Wilson (1982) considered Seyfert nuclei as "mini radio galaxies". Their radio luminosities are several orders of magnitude below radio-loud QSOs.

2.4.3. Jet production

As described above, radio observations of Sy 1 show the presence of jets and beams. Here we constrain ourselves to discuss the jet production, and assume the Sy 1 core to be a massive black hole.

As we know, material preferentially escapes along "directions of least resistance". These directions are likely to be related to a rotation axis within the galactic nucleus. One class of possibilities involves the 'twin exhaust' nozzle (Blandford & Rees 1974; Rees 1978) in which buoyant material surrounded by a rotating gravitationally bound cloud escapes via two beams. The confinement is provided by a gravitationally bound cloud in the central potential well; within this cloud lies a source of gas which is very buoyant (in the sense that its value of 'P/ρ' for exceeds the gravitational binding energy) and may be relativistic. If the gravitationally bound cloud is flattened, owing to rotation and/or the shape of the potential well, the buoyant fluid emerges along the minor axis. If a steady flow pattern establishes itself, its form is calculable provided that the $P(\rho)$ relation for the buoyant fluid is known. A nozzle forms where the external pressure drops to about half the stagnation pressure; further out, the flow is supersonic, and the channel slowly broadens as the external pressure drops off. This general mechanism does not require any pressure anisotropy in the fluids concerned.

The width of the channel adjusts itself so that there is pressure balance across the walls. The channel cross-section is proportional to the energy flux

carried by the jets, and varies inversely with the pressure in the external cloud.

The "twin-exhaust" configuration bases on purely hydrodynamical processes. Another different possibility utilises the anisotropic stress from an ordered magnetic field. If such a field is initially aligned along the rotation axis of a disc, it can exert a strong torque and generate outflow along the field lines which will be directed along the rotation axis (Blandford 1976).

It is now unclear whether jet is basically a hydrodynamical process or whether a crucial role may be played by electromagnetic effects, anisotropic radiation pressure, etc. In particular, the radio observation shows the misalignment of the radio axis with the spin axis of galaxy disc (Wilson 1982; Ulvestad & Wilson 1984). These are all interesting and open questions.

2.5 X-ray emission

2.5.1 General properties

In the last few years, the study of Seyfert nuclei with X-ray astronomy has developed rapidly. By now Seyfert 1 galaxies have been established as a class of strong X-ray emitters. In this section we describe their general X-ray properties.

The 2-10 Kev X-ray luminosities of galactic nuclei range from $L \lesssim 10^{36}$ erg/s for our own Galaxy nucleus to $L_x \gtrsim 10^{46}$ erg/s for QSOs. Sy 1's cover a wide range of X-ray luminosities (10^{42}-10^{45} erg/s), overlapping those of QSOs.

Sy 1's also show variability in X-rays. For example, Mkn 509 may be variable by a factor of 2 in the 2-10 Kev band over two weeks (Dower et al. 1980). Data taken at the same time in the 13-60 Kev band show a similar decrease in flux over the two weeks of observations (Dil et al. 1979). Elvis (1976) and Tananbaum et al. (1978) reported a flare with a factor of 2 increase in less than 3 days for NGC 4151 in the 2-6 Kev band. Ward et al. (1978) have shown that X-ray emission from MCG 8-11-11 is variable by a factor of $\gtrsim 3$ on a time scale 1 month in the 2-10 Kev band. X-ray emission variable on time scales from $\sim$150 sec to $\sim 10^3$ sec, corresponding to a 0.5-4.5 Kev luminosity, has been discovered for NGC 4051 (Marshall et al. 1983). NGC 6814 also showed variability on the time scale of 100 sec in the 3-20 Kev band (Tennant et al. 1981; Tennant & Mushotzky 1983). The shape of the X-ray spectrum appears to remain fairly constant while the intensity varies. As we know, observations of rapid X-ray variability place strong constraints on the size of the "central engineé. The variability of 100 sec implies an upper limit to the size of the X-ray source of 3×10^{12} cm which is the Schwarzschild radius ($2GM/C^2 = R_g$) of $10^7 M_0$ black hole. The smallness of the emitting region, together with the greatness of the power emitted jet strong constraints on models for the energy source. On the other hand, rapid X-ray variability seems to be rare among Seyfert 1"s: most AGNs do not vary on timescales ranging from minutes to a few hours by more than 10% (Tennant & Mushotzky 1983).

Another important property is that hard X-ray 2 - 165 Kev observations of many Sy 1 (Rothschild et al. 1983) show that the spectrum is surprisingly well represented by a single power law with index $\alpha = 0.62 \pm 0.04$ (Fig. 32). No spectral break is required, although increasingly sharp spectral changes could be fitted above $\sim$50 Kev. At lower energies, the 0.75-4.5 Kev spectra of Sy 1 which have $L_x > 10^{43.5}$ erg/s in 2 - 10 Kev band are in gneeral well fitted by a single model consisting of a power law plus absorption by cold gas. The average spectral index $\langle\alpha\rangle$ is 0.66 ± 0.36 (Petre et al. 1984). At much higher energies, ballon-borne observations of NGC 4151 and a few other active galaxies (Schonfelder 1982; Perotti et al. 1981) suggest that a flat spectrum continues to about a Mev, beyond which it steepens. But more, and better quality, spectra in the range from 100 Kev to 10 Mev are needed before we can safely conclude that the spectral break does occur at $\sim$1 Mev, although this seems likely on the basis of prsent data.

In order to explain these observational results, several possible mechanisms of X-ray radiation have been suggested. We shall discuss these mechanisms in Section 2.5.3.

2.5.2 Various relations

In the present section, we shall discuss correlations between the X-ray luminosity and observed properties in other wave bands, and briefly discuss some possible inference.

(1) X-ray versus optical continuum

A first indication of a correlation between the apparent nuclear magnitude and X-ray flux of Sy 1's was pointed out by Elvis et al. (1978; cf. Fig.33). The evidence for this correlation was strengthened by new data of Kriss et al. (1980) who also attempted to subtract out from the observed optical flux, the contribution of star-light (see Fig. 34). The correlation coefficient for data in Fig. 34 is 0.64 corresponding to a probability of 5.10^{-4} of occurring by chance from an uncorrelated distribution.

From the analysis of a large sample of radio-quiet quasars, Zamorani (1984) concluded that there is a well defined correlation between X-ray and optical luminosities over a range of at least four orders of magnitude, with a continuity in the X-ray properties from low luminosity Seyfert galaxies to the most luminous quasars.

(2) X-ray versus infrared continuum

For Sy 1 a relation between the 3.5 μm (or 10 μm) and 2 - 10 Kev X-ray flux was first pointed out by Elvis et al (1978) (Fig. 35a, b). With additional infrared data McAlary et al (1979) have further strengthened this correlation (Fig. 36).

Since Neugebauer et al (1976) and Rieke (1978) indicated that many Seyfert galaxies have significant stellar contribution to infrared flux, Kriss et al (1980) followed Penston et al (1974) and removed the stellar contribution in 3.5 μm flux. Fig. 37 shows their result. A strong correlation is still present, but not nearly as tight as that originally found by McAlary et al (Fig. 36). In addition, for comparison, they have computed spectral indices α_{IO} (from 3.5μm to 4400 Å) and β_{OX} (from optical to X-ray). Fig. 38 shows that α_{IO} tends to be flatter than the β_{OX}, indicating a break in the ultraviolet. The two indices are uncorrelated. On the other hand, the β_{OX} of Sy 2 is larger than that of Sy 1, i.e., Sy 2 tend to have a smaller ratio L_x/L_{opt}.

Lawrence & Elvis (1982) have used a larger sample than previous works, and found that $L_{3.5\ m}$ is roughtly proportional to L_{HX}, but $L_{10\,\mu m}$ decreases less than linearly with decreasing L_{HX} (Fig. 36). They have interpreted this as meaning that IR continuum is made up of two parts, an extension of non-thermal continuum and thermal radiation from dust at temperature $\sim$ a few hundred degrees. The slope α then characterizes the relative contribution of the thermal component.

(3) X-ray versus 21 cm flux

Fig 35c (Elvis et al 1978) show that only weak correlations exist between

the 21 cm radio and X-ray flux.

(4) X-ray versus H_β FWZI

A correlation of emission line width with X-ray luminosity, at a confidence level of a few percent, was first noted by Elvis et al (1978) and again by Wilson (1979). Using the full sample of Seyferts Kriss et al (1980) have plotted Fig. 40. For Sy 1 alone the correlation is significant at a level of only a few percent. However, other upper limits on Sy 2 strong suggest that this correlation is real.

(5) X-ray versus optical emission line intensities

Fig 41a-d give plots of the flux densities in H_α, H_β, He II λ4686Å (a high excitation line) and [O III]λ5007Å against X-ray flux density. There are significant correlations between H_α and 2-10 Kev flux densities and between H_β and 2 Kev X-ray flux. A subsequent analysis, based on more data (Lawrence & Elvis (1982) has strengthened Kriss et al. results. H_β is proportional to L_{HX}. However, [O III] decreases much more slowly with decreasing L_{HX} than would be expected from a simple photoionization model. They think that either the NLR also has a flattened configuration, or its filling factor is a sensitive function of either L_{HX} or the radial distance from the continuum source.

(6) X-ray versus the H_β/[O III]λ5007 ratio

Grindlay et al (1980) have demonstrated a correlation between the H_β/[O III] ratio and the X-ray luminosity of Sy 1 which holds for their X-ray selected QSOs as well (Fig. 42). Kriss et al (1980) presented further data on the relation in Fig. 43, extended it to lower X-ray luminosities with their Sy 2 observations. For the Sy 1 alone the relation is not very tight. However, if the Sy 2 are included, the correlation is dramatically improved.

2.5.3 Possible mechanisms

First of all, we discuss the implications of various correlations of X-ray versus other wavebands which were mentioned above. The correlation of emission line width with X-ray luminosity in Seyferts requires the permitted line region to be associated with the source of the X-ray emission. This is strengthened by correlations of X-ray flux with optical emission line intensities. The influence

of the X-ray continuum radiation may even be important in the larger forbidden line region, as is demonstrated by the H_β/[O III] correlation with the X-ray luminosity. The particular physical process involved, however, is still unclear.

Since the non stellar continua in the optical and the infrared are correlated with the X-ray flux, the global spectral characteristics of all Seyfert galaxies must be similar (Kriss et al 1980). This suggests that the same physical process is operating in all of them, and that the source of the X-ray emission is associated with the region producing the non stellar continua in the optical and infrared. We know that thermal radiation from dust may play a significant role in the infrared emission of Seyfert galaxies. The correlation of the infrared excees with X-ray flux may be interpreted as evidence that X-ray heating of dust is important.

In particular, the X-ray selected QSOs of Grindlay et al (1980) fit optical/ /X-ray correlation, and it is plausible that such radio quiet QSOs are closely related to the Seyfert phenomenon.

In most of the above correlations, there is a smooth progression from the Sy 1 to the lower X-ray flux levels of the Sy 2, suggesting that Sy 2 are intrinsically less luminous examples of the same process, although the spectra of Sy 2 are significantly steeper than those of the Sy 1. Of course, this suggestion is still controversial.

On the basis of the above correlation analyses and of the properties of X-ray radiation, described in the above subsections, several models have been suggested.

(1) Synchrotron radiation and synchrotron self-compton emission

Many authors (e.g. Stein & Weedman 1976; Neugebauer et al. 1976; Elvis et al. 1978; Cavaliere & Morrison 1980; Tennant et al. 1981; Rees 1981; Tenant & Mushotzky 1983; Fabia 1983) have discussed this mechanism. Non-thermal continuum radiation of Seyfert nuclei indicates that relativistic electrons are present. These relativistic electrons could have been accelerated by a magnetic field or shocks (Fig. 44) near a massive central object. Concerning the shock acceleration possibility, Rothchild et al. (1983) noted that the value of the spectral index of the mean of their 11 Seyfert galaxies,

α_x = 0.62, as well as the dispersion around the mean, 0.15, are very similar to the values $\langle\alpha_{3c}\rangle = 0.77 \pm 0.15$ found for 3CR radio sources, to the radio-optical index of flat-spectrum radio sources $\langle\alpha_{ro}\rangle = 0.69 \pm 0.1$, to the radio spectral index of jets $\langle\alpha_{jet}\rangle = 0.6 \pm 0.15$, and to the index of radio emission from disks of spiral galaxies $\langle\alpha_{sp}\rangle = 0.7 \pm 0.12$. Since the radio emission from these objects is due to relativistic electrons, they have inferred a relativistic particle index $\gamma = 2\alpha + 1 \simeq 2.3$, a value consistent with the index of the injection spectrum of cosmic rays in our Galaxy, and concluded that the X-ray spectrum is also likely due to relativistic particles. The similarity of the energy spectrua argues for a common mechanism, such as shocks, for accelerating electrons. From the X-ray data they argue that the shock should be relatively weak, i.e., Mach number less than 5. As we know, motion of the relativistic electrons in the magnetic field may produce X-ray emission, through the synchrotron process. The main objection to this mechanism is the very short radiation lifetime of the relativistic electrons. That is, the electron radiation lifetime t_γ is much less than $t_c = R/V$ which is the electron transit time across the source at a velocity $V \leq C$, because $t_\gamma = m_e c^2 / \gamma \sigma_T W$ range from 10^3 sec to under 1 sec (where σ_T is Thomson cross section, $W = B^2/4$ energy density of magnetic field) Cavaliere & Morrison 1980). Due to this, relativistic electrons must be reaccelerated at sites spread throughout the volume and re-used several times during a time-scale R/C.

The origin of X-rays in galactic muclei by synchrotron self-Compton radiation has been discussed by many authors (e.g. schnopper et al. 1977; Elvis et al. 1978; Rees 1981; Rothschild et al. 1983; Fabian 1983). It is suggested that X-rays are produced by inverse Compton scattering of lower energy photons generated by synchrotron radiation. Inverse Compton scattering between photons and electrons will generate radiation of frequency $\nu_c \sim 4/3\, \gamma^2 \nu_s$ (where ν_s is frequency of synchrotron). There is not only first-order scattering, but also there can be higher-order scatterings. So even γ-rays of energy 10^3 Mev can be produced. This mechanism receives support from the observed correlations of the X-ray power with both the infrared and the optical power (Section 2.5.2). An obvious prediction is that variability at infrared,

optical and X-ray waveband should also be correlated. Again there is a problem with the life-time of relativistic electrons. Models involving a re-acceleration of electrons have been discussed by Blanford & Rees (1978) and Cavaliere & Morrison (1980). Indeed, the available electric and magnetic fields could be fully able to reaccelerate the electrons in the X-ray emitting region.

(2) Thermal bremsstrahlung

The broad emission lines of Sy 1 imply that individual clouds in the BLR are moving at speeds of several thousand km/s. Shocks involving this kind of velocity automatically yield gas at temperature $T_e \geq 10^8$ K (Rees 1981). The clouds giving the optical emission lines ($T_e \simeq 10^4$ K) may be in pressure balance with a hot and more rarefied gas ($T_e \gtrsim 10^8$ K). The X-ray can originate via thermal bremsstrahlung in this gas of high temperature. The power radiated in the 2-10Kev band is given by $L_x = 2.4 \times 10^{-27} T^{\frac{1}{2}} n_e^2 V$ erg/s (Tennant et al 1981), Where n_e is the electron desity (cm^{-3}) and V the volume of the gas. For Sy 1, in general, assuming $L_x \sim 10^{44}$erg/s and $V \sim 4 \times 10^{51} cm^3$, the electron density is found to be $n_e \sim 3 \times 10^7 cm^{-}$ which is resonable. However, some spectra of Sy 1 in the X-ray waveband, such as Mkn 509, are not well fitted by a thermal bremsstrahlung (Mushotzky et al 1980). In addition, if shock heating were essential, and the thermal bremsstrahlung played an important role in X-ray emission, one might expect a relation between the width of the Balmer lines and X-ray power, in fact only a weak relation exists.

(3) Comptonisation

If photons of energy $h\nu$ are scattered by electrons with temperature T_e such that $kT_e \gg h\nu$, then each time a photon is scattered its energy changes by a fration $\sim \pm (kT_e / m_e c^2)^{\frac{1}{2}}$; averaged over scatterings, there is a systematic mean gain in photon energy of $\delta\nu/\nu = kT_e / m_e c^2$. After many scatterings, a Wien law would be established. Katz (1976) calculated the spectrum of radiation emerging from an optically thick sphere ($\tau_{es} > 1$). The emergent spectrum depends essentia-

lly on the parameter $Y = \tau_{es}^2 (KT_e/m_e c^2)$: if $Y \ll 1$, nothing much happens; if $Y \gg 1$, a Wien law is set up; but in the intermediate case where $Y \simeq 1$, the spectrum has an approximate power-law form. This mechanism can be applied to accretion discs in X-ray sources.

As mentioned in 2.5.1, 2-165 Kev X-ray observations show that many Sy 1 have a single power law spectrum without any turnover. This seems to rule out $Y \gg 1$ possibility. Shapiro et al. (1976) and Katz (1976) showed that the resultant spectrum is a power law for energies below KT_e with an exponential falloff at higher energies. According to the observational results which are obtained up to date, $T_e \sim$ a few 10^9K, τ_{es} is less than a few.

"Comptonisation flares" would occur if there were an impulsive change in the temperature of a large fraction of the gas or in the soft-photon source. And the hot gas that could give rise to Comptonised X-ray would be closer to the central object than the optical emission-line region. So maybe it is possible to explain the X-ray flares of the Sy NGC 6814 on timescales about 100 sec.

Furthermore, the emission line clouds can be excited by a continuum spectrum extending into the X-ray band. The clouds closer to the central continuum than those yielding optical lines could be excited by continuum X-rays to high ionization levels, so that even Fe could be almost completely stripped of electrons (Rees 1981). If this is the case, we can expect a variability of ironlines following the X-ray variability.

In summary, it is still an open question whether the X-rays that constitute the ionizing flux are due to synchrotron/Compton processes, or are due to Comptonisation, etc. To settle this question, 100Kev-10Mev observations of Sy 1 are needed.

2.5.4 Basic energy source

Rees (1978) has summarized current ideas on the nature of the primary power source in active galaxies. By use of his "Flow diagram" (Fig. 45), one can discuss this problem briefly.

On the basis of observational data, such as optical apparent magnitude, radio flux, X-ray flux, redshift and variability, etc., most interpretations of AGNs invoke a mass of 10^6-$10^9 M_\odot$ in a region $\leq$ 1 pc in size. In summary, there are three kinds of models about the primary power soruce (Fig. 45):

(1) dense star cluster;

(2) massive stars, "spinars", or "magnetoids";

(3) accretion onto massive black holes.

Generally speaking, model (3) has the advantage of a far greater efficiency ($\simeq$ 10%) in converting the rest mass into electromagnetic radiation, (Lynden-Bell 1969, 1978; Rees 1978). In addition, an evolution (1)($\rightarrow$(2)) $\rightarrow$(3), or (2)$\rightarrow$(3), seems inexorable. Finally high luminosity flares on a timescale of $\sim$ 100 sec (Tennant et al. 1981; Tennant & Mushotzky 1983) seem hardly compatible with models other than (3).

2.6 Sy 1 and Sy 1.5

The most thorough discussion of the relationship of Sy 1.5 with Sy 1 and Sy 2 has been given by Cohen (1983). He obtained high-quality optical spectra of 14 Sy 1.5, and compared quantitatively their broad-line spectra with the spectra of Sy 1 and their narrow-line spectra with the spectra of Sy 2. He stressed that the classification can be deceiving if it leads to the belief that Sy 1.5 have equal proportions of Sy 1-type and Sy 2-type properties. In fact, most of Sy 1.5 have properties which are very similar to Sy 1, despite a more noticeable narrow-line component in the Balmer lines. The luminosity, equivalent width, and line ratios of the broad lines of Sy 1.5 are more or less the same as those of Sy 1. Except for a few cases, the amount of emission in the narrow component of the Balmer lines is only a small fraction of that in the broad lines. The average narrow-line ratios are very similar to those of Sy 2, but Sy 1.5 have much stronger high-ionization lines. Cohen concluded that "many Sy 1.5 are fairly representative of Sy 1. In fact, they should probably not be called intermediate Seyfert galaxies at all."

Now we shall develop the comparisons of essential properties between Sy 1 and Sy 1.5 in different wavebands or in different ways in order to get a definite conclusion.

2.6.1 X-ray luminosity

(1) HX(2-10Kev) luminosity distribution (HXLD)

Taking Lawrence & Elvis sample (1982), and plotting the HXLD of Sy 1.5 and Sy 2 in Fig. 46, we found that Sy 1 and Sy 1.5 were detected at luminosity $L_{HX} \sim 10^{42}-10^{45}$ ergs/s whereas only 5 Sy 2 were detected with luminosity $L_{HX} \sim 10^{42}-10^{43}$ ergs.s, and most of the Sy 2 have not been detected in HX(2-10Kev) at all. Sy 1.5 are similar to Sy 1 and strong HX sources. But Sy 2 are very weak HX sources. This is an important difference between Sy 1.5 and Sy 2 since L_{HX} is a key parameter which describes activity and physical situation of the nuclei.

(2) SX (0.5-4.5Kev) luminosity distribution (SXLD)

The observational data are summarized by Lawrence & Elvis (1982). Sy 1.5 SXLD approaches Sy 1 SXLD. Sy 2 have lower soft X-ray luminosity than Sy 1.5 in most cases (Fig. 47).

(3) $\langle \alpha_{ox} \rangle$

α_{ox}, the energy index connecting the optical with the X-ray band, is defined as

$$\alpha_{ox} = \frac{-\log[L_x/L_{op}]}{\log(\nu_x/\nu_{op})} = -\frac{\log[L_{2kev}/L_{4400}]}{2.85}$$

Taking Kriss et al. data (1980), we have calculated α_{ox} for each source and plotted the α_{ox} distributions in Fig. 48. Then we have got mean values $\langle \alpha_{ox} \rangle_{\text{nuclear}}$ and $\langle \alpha_{ox} \rangle_{\text{total}}$ without internal reddening correction, and found

$$\langle \alpha_{ox} \rangle_{\text{nuclear, Sy1}} \approx \langle \alpha_{ox} \rangle_{\text{nuclear, Sy1.2 \& Sy1.5}} \sim 1.20 \pm 0.01$$

$$\langle \alpha_{ox} \rangle_{\text{total, Sy1}} \approx \langle \alpha_{ox} \rangle_{\text{total, Sy1.2 \& Sy1.5}} \sim 1.30 \pm 0.03$$

In both cases Sy 1.5 have slightly smaller values of $\langle \alpha_{ox} \rangle$ than Sy 1 have.

In particular, the 2-165 Kev observations of Rothschild et al. (1983) and the 0.75-4.5 Kev observations of Petre et al. (1984) have shown that the X-ray spectra of Sy 1.5 are not evidently different from those of Sy 1. Therefore, we may say that Sy 1.5 have X-ray properties similar to Sy 1, and are different from Sy 2.

2.6.2 UV-radiation

In Figs. 50a-d we have plotted the distributions of equivalent width (EW) for prominent UV-radiation lines, C IV, L_α, C III] and Mg II. There

are no big differences between Sy 1.5 and Sy 1. The distribution of the continuum luminosity at 1550Å, M_{1550}, (Fig. 50e) shows that Sy 1.5 have almost the same continuum luminosity range as Sy 1. From Fig. 50f we can see the C IV/C III] ratio distribution of Sy 1.5 is analogous to that of Sy 1. It means that Sy 1 and Sy 1.5 have nearly the same ionization parameter since the C IV/ C III] ratio is a very sensitve indicator the ionization parameter (Davidson 1977; Davidson & Detzer 1979; Ferland & Mushotsky 1982). The above facts demonstrate that Sy 1 and Sy 1.5 both have the similar properties in UV-radiation.

2.6.3 Color index distribution (CID)

Using our sample (Cheng et al. 1983) and plotting Fig. 51, 52 we found CID of Sy 1.5 is similar to that of Sy 1, but evidently, most of Sy 1.5 are bluer than Sy 2. Their axial ratio, b/a, distribution are not different for the three subclasses of objects.

2.6.4 Redshift distribution (RSD)

On the basis of observational data collected by us (see Table 2), Fig. 53, 54 have been drawn, and show that RSD of Sy 1 is wider than those of Sy 1.5 and Sy 2 respectively. At small red shifts ($Z \lesssim 0.02$) the number of Sy 2 is relatively larger than those of Sy 1 and Sy 1.5.

2.7 QSO and miniquasar

The similarities between the nuclei of Seyfert and QSOs, in particular, the radioquiet ones, have been stressed repeatedly. The evidence for continuity between these two classes of objects is summarized below.

2.7.1 Redshift and luminosity

In order to determine luminosity of an object, we have to know its distance. For distant Seyferts and QSOs we need firstly demostrate whether or not their redshifts are cosmological. Normal methods which one can use are angular diameter-redshift diagrams and magnitude-redshift diagrams. For QSOs, we can see the Miley's (1971) and Fang et al (1977) papers. For Seyfert galaxies, Khachikian & Weedman

(1974) have ploted logCZ - logθ (Fig. 55); an apparent magnitude-redshift diagram for non-violent variable Sy 1 and low-redshift, radio-weak quasars is shown in Fig. 56 (Cheng et al 1981). These are empirical evidence that Sy 1 and QSOs have cosmological redshifts.

Now we can calculate the luminosities of Seyfert 1 nuclei (cheng et al. 1984) and QSOs and compare them. There is an overlap in luminosity between Sy 1 nuclei and QSos as stressed by Khachikian and Weedman (1977) who have compared the powers emitted in broad hydrogen lines to avoid problems with contaminattion by star light (in turn, the broad-line luminosity is roughtly proportional to the luminosity of the nonthermal continuum (Weedman 1976)). In fact it turns out to be impossible to make a clear-cut distinction between high luminosity Seyferts and low luminosity QSOs. The Sy 1 nuclei cover a luminosity range of 10^3, and most QSOs are less than 10 times bright than the brightest Sy 1. The entire phenomeon, from the faintest Sy 1 to the brightest QSOs, covers a factor of 10^5 in luminosity. Thus the bolometric luminosities range from 10^{43}ergs/s to 10^{48}ergs/s (for $q_o = 0$ and $H_o = 50$ km/s/Mpc).

2.7.2 Continuum spectrum

Considering Seyferts and QSOs together, there appear to be four distinct possible continuum sources. They are

(1) normal stellar emission;

(2) an infra-red source, probably dust;

(3) a nonthermal power-law spectrum in the visual and infrared;

(4) perhaps, thermal emission from an accretion disc in the violet and UV band.

Sy 1 and QSOs all are X-ray emitters. We have found that 0.5-4.5Kev X-ray luminosities range from 2×10^{41}ergs.s to 3×10^{44}ergs.s for Sy 1 (Lawrence & Elvis 1982), and from 10^{43}ergs/s to 10^{47}ergs/s for QSOs (Tananbaum et al. 1979). There is an overlap in X-ray luminosity.

At present, X-ray spectra are available for several Sy 1. Unfortunately, information on QSO spectra is very limited. The available data however (Petre et al.(1984) again suggest a similarity between QSOs and Sy 1.

2.7.3 Emission-line spectrum

Wu et al (1983) have observed 20 Seyfert galaxies, and made a comparison of the emission line properties between QSOs and Sy 1. They found that there is an inverse correlation between the continuum luminosity at 1450 Å and the equivalent width of C IV λ1550 for QSOs and Sy 1. A reasonable interpretation is that the covering factor increases as luminosity decreases. This is consistent with the fact that the L_α and C IV equivalent width for Sy 1 are a factor of 2 larger than those for high redshift QSOs. They also found that the I(C IV λ1550)/I(C III] λ1909) ratio is about 2 for high redshift QSOs and 5 for Sy 1. That means that Sy 1 have a higher ionization parameter than high redshift QSOs. There is not satisfactory explanation for this result yet.

2.7.4 Other properties

As discussed in previous sections, there are many similarities between QSOs and Sy 1, such as continuum spectrum, UV-excess, X-ray radiation, emission lines, morphology and polarization properties, etc. An additional property they have in common is variability. The optical variability of Seyferts has already been mentioned. As for QSOs, from the data in "THE ASIAGO CATALOGUE OF QUASI STELLAR OBJECTS" (Barbieri et al 1982) which contains 2004 objects found in the literature published before Dec. 31, 1981, we estimate that about 13% of QSOs are optical variables. They can ondergo a substantial change in optical luminosity within a few weeks, which is more or less the same as for Sy 1.

The above discussion supports the following classification scheme (Woljer & Setti, 1981)

Quasars Blue continuum (U-B excess in continuum in rest frame)

Broad emission lines

$M_V < -24$

Subclasses:

QSO: "Optical quasars" Log R < 1.5 , $R = \frac{F(5GHz)}{F(2500A)}$ (in rest frame)

QSR: "Radio quasars" Log R > 1.5

Subdivided in

Seep (radio) spectrum $\alpha < -0.7$, $F_\nu \propto \nu^\alpha$

Flat (radio) spectrum $\alpha > -0.5$

Sy 1 Blue nuclei of galaxies

Emission lines; total width of H lines $>$ 3000km/s

$M_V > -24$

$M_V = -24$ has been chosen as the dividing line, since this is the magnitude of Fairall 9 which seems to represent an approriate transition case between "fuzzy" quasars and more typical Seyferts (Woltjer & Setti 1981).

No wonder, a lot of astronomers call Sy 1 nuclei "Miniquasar".

However, there are two facts which need to be taken into account. First, as mentioned in 2.7.3 most of Sy 1 have larger I(C IV λ 1550)/I(C III] λ 1909) ratio than high redshift quasars. What is the reason for this? Second, some QSOs have considerable absorption lines, and some QSOs have absorption lines with multiple redshifts. However, only a few Sy 1 have absorption lines which can be observed, and only Mkn 231 seems to have absorption lines with three different values of redshifts. Maybe, this will provide some evidence on the origin of absorption lines of QSOs.

2.8 Conclusion and discussion

On the basis of observational results and theoretical analysis which are already know, a crude diagram of the Sy 1 structure can be given (Rees 1981) (Fig. 57).

A typical Sy 1 galaxy consists of a bright nucleus and a spiral galaxy. The nucleus has strong non-stellar blue or ultraviolet continuum. Its spectrum has strong broad permitted lines which extend to high ionization levels, and narrower forbidden lines. Continuum sources are opitcally unresolved; On the basis of variability, the dimension of continuum source is smaller than about 10^{-2}pc. The size of the BLR is about 1 pc. The sizes of the NLR range from tens to hundreds pc. Both UV and IR excesses appear in the continuum spectra of Sy 1. Radio structures show jets and beams, but do not extend outside the NLR. Most of Sy 1 are X-ray sources. X-ray emission can vary on timescale of a few hours to weeks, and has even been observed to be as rapid as $\sim$100 seconds, indicating that it comes from a very small region.

The basic similarities between Sy 1 and Sy 1.5 tell us that they are manifestations of much the same phenomenon. As mentioned by Cohen (1983), it appears that there are probably no "pure" Sy 1, bare broad-line regions wihtout surrounding narrow-line regions.

The comparisons between Sy 1 and optically selected quasars show that Sy 1 is really a "Miniquasaré. This fact provides the opportunity of studying the quasar phenomenon in relatively nearby objects.

Along the problems which still await a solution we recall the following.

Seyfert evolution: Is there an evolutionary relation between Sy 1 and Sy 2? Are Sy 1.5 a transition stage or not? If so, do either Sy 1 or Sy 2 evolve to Sy 1.5? A particularly puzzling result, in this respect is the finding of Khachikian et al. (1983) who reported that the Sy 1.5Mkn 6 has occasionally turned into an Sy 2.

Dust: many observational results show that Sy 1 contain dust. However, its amount and distribution are not known. Better IR data are definitely needed. Maybe Sy 1 extinction curves are somewhat different from that of our own Galaxy. Maybe we should find out better reddening indicators. Theoretical studies are also important. We shall go into details of this subject in Chapter III.

3000 Å hump: The possibility that the 3000Å hump is produced by an accretion disk surrounding a massive black hole needs to be further explored.

X-ray spectral index: The hard X-ray spectral index of Sy 1 is 0.62 0.15, and is almsot the same as that of many classes of radio sources. This value of the spectral index seems to have some special meaning that we do not know yet.

I(C IV λ1550/I(C III] λ1909) ratio: Most of Sy 1 have higher C IV/C III] ratios than those of QSOs. Someone proposed that the best explanation is that the ionization parameter is different. The difference amounts to a factor of about 2.5. Why is the ionization parameter different?

In addition, a satisfactory model for the geometry and the dynamics of the BLR and of the NLR is still lacking.

CHAPTER III INTERNAL REDDENING OF SEYFERT 1 GALAXIES

As discussed in section 2.2.5, dust reddening is an important component in explaining the steep Balmer decrements of Sy 1's.

Recalling Chapter II, the optical spectra of Sy 1 exhibit four or five major components: the starlight of the underlying galaxy, the variable non-thermal continuum, the 3000Å hump perhaps originated from an accretion disc, the broad permitted emission lines and the narrow emission lines. As we know, these various components may originate in different regions. Naturally, one will ask how the reddening affects the different radiation components. This question is obviously related to the understanding of the distribution of dust in Sy 1. In this Chapter we shall examine the reddenings of continua, of the BLR and of the NLR of a large number of Seyfert galaxies.

3.1 Continuum reddening of Seyfert 1 nuclei

The amount of reddening due to dust associated with AGNs has long been the subject of considerable debate and the matter is still far from being settled (Grandi 1983). Cheng, Danese & De Zotti (see below) have tackled this problem, we take as a starting point the two important discoveries:

(1) the paucity of optically discovered nearly edge-on Seyfert galaxies, relative to a compaison sample of normal spirals (Keel 1980; Doroshenko & Terebizh 1980);

(2) the correlation of the ratio of H_β to hard X-ray luminosities with the axial ratio b/a of the AGNs (Lawrence & Elvis 1982).

Mon. Not. R. astr. Soc. (1983) **204**, *Short Communication*, 13P–18P

Continuum reddening of Seyfert 1 nuclei

F. Z. Cheng *ISAS, Strada Costiera 11, I-34014 Trieste, Italy*
L. Danese *Istituto di Astronomia, Vicolo dell'Osservatorio 5, I-35100 Padova, Italy*
G. de Zotti* *Institute of Astronomy, Madingley Road, Cambridge CB3 0HA*

Received 1983 April 20; in original form 1983 March 4

Summary. We show that the observed colours of Seyfert 1 nuclei are tightly correlated with the inclination of the surrounding galaxies. This allows us to derive simple expressions giving the average reddening of their continuum as a function of the axial ratio. The resulting values of $E(B-V)$ substantially exceed those for starlight.

1 Introduction

The determination of nuclear luminosities of Seyfert galaxies is hampered by two factors: contamination by starlight and internal extinction. While successful methods for singling out the nucleus from the underlying galaxy have been derived by Sandage (1973) and applied to Seyferts by Khachikian & Weedman (1974) and Véron (1979), the correction for internal extinction is still matter of considerable debate (Gaskell 1982; Malkan 1983).

In addition, most of the previous work has concentrated on emission lines whose reddening is not necessarily the same as that of the continuum (Costero & Osterbrock 1977; Koski 1978; Clavel *et al.* 1980; Malkan & Oke 1983). The only direct way of estimating the latter in Seyfert 1 galaxies hinges upon observations of the 2175 Å absorption dip, whose origin is not well understood (*cf.* Savage & Mathis 1979). This feature also shows considerable variation in our own Galaxy and a standard galactic UV extinction law could well not be applicable to Seyfert 1 nuclei.

In this paper we approach the problem following the principles of Holmberg (1958, 1975), i.e. assuming that the obscuring region has a flattened configuration, parallel to the disc of the surrounding galaxy, as is strongly suggested by the paucity of edge-on optically discovered Seyferts (Keel 1980) and by the correlation of the ratio of Hβ to hard X-ray luminosities with the inclination of the galaxy (Lawrence & Elvis 1982). In Section 2 we show that the distributions of colour indices do conform to those expected in the presence of a thin, uniform absorbing layer in the equatorial plane of the galaxy and we determine

*Permanent address: Unita' di ricerca GNA/CNR di Padova, c/o Istituto di Astronomia, Vicolo dell'Osservatorio 5, I-35100 Padova, Italy.

the corresponding empirical absorption laws. In Section 3 we discuss some evidence of an increase of reddening with decreasing luminosity. In Section 4 we compare our estimates of the reddening of the continuum with those of the reddening of emission lines. Section 5 contains our conclusions.

2 Empirical reddening laws

A careful search in the literature has yielded a sample of 73 type 1 or intermediate Seyfert galaxies for which both complete optical photometry and axial ratios are available. The sample includes 54 out of the 69 Seyfert 1s identified in the first nine Markarian lists. Small aperture photometric data have been selected whenever possible. Our primary source for axial ratios was Keel (1980); additional values have been taken, in order of decreasing preference, from Lawrence & Elvis (1982), the *Second Reference Catalogue* (de Vaucouleurs, de Vaucouleurs & Corwin 1976), the *ESO/Uppsala Catalog* (Lauberts 1982) and the Markarian lists.

A plot of the $(B-V)_c$ colours [subscript c denotes correction for reddening within our own Galaxy, using the Burstein & Heiles (1973) method] as a function of the axial ratio b/a shows (Fig. 1) that the data points are distributed, without exception, on the red side of a sharply defined boundary line on which $(B-V)_c$ is a linear function of b/a, at least for $b/a \gtrsim 0.3$:

$$(B-V)_c = 0.05 + 0.79\,(1 - b/a). \tag{1}$$

A quick check confirms that for objects lying close to this line the contamination by the underlying galaxy is small at least within the aperture used for observations; actually most of these objects have an extremely bright nucleus: a few examples are Mkn 509, ESO 141 –

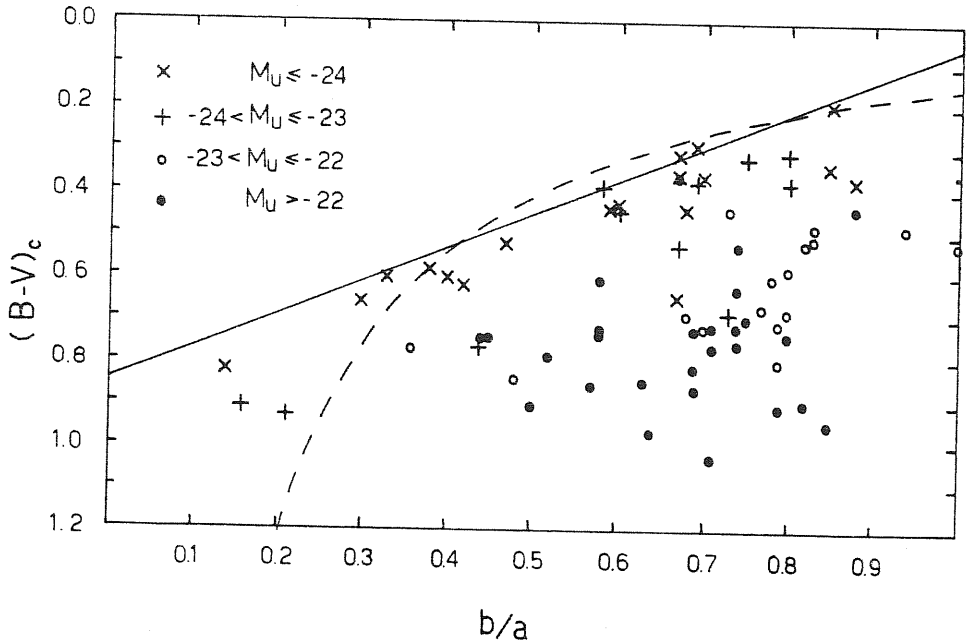

Figure 1. Distribution of $(B-V)_c$ as a function of the axial ratio. The straight line represents equation (1), the dashed curve equation (4). Values of M_U correspond to $H_0 = 50\ \mathrm{km\ s^{-1}\ Mpc^{-1}}$.

G55, Akn120 and 3C120. We are therefore entitled to interpret equation (1) as the exact analogue of the absorption law originally derived by Holmberg (1958, 1975) for normal galaxies. If, following Sandage (1973), we assume an intrinsic nuclear colour $(B-V)_Q = 0$, we have

$$E(B-V) = (B-V)_c = 0.05 + 0.79\,(1 - b/a). \tag{2}$$

For comparison, Holmberg's result for early-type spirals reads, in his photometric system:

$$E(pg-pv) = 0.11 + 0.19\,(1 - b/a). \tag{3}$$

Thus the absorption correction for Seyfert nuclei turns out to be generally much larger than that for starlight.

A good fit to the data can also be obtained using the functional form appropriate to the case of a thin uniform absorbing layer in the equatorial plane of the galaxy:

$$E(B-V) = +0.15 + 0.25\,(a/b - 1). \tag{4}$$

Using the standard value of the ratio $E(U-B)/E(B-V) = 0.8$ (Savage & Mathis 1979) and assuming an intrinsic nuclear colour $(U-B) = -1.1$, we obtain

$$(U-B)_c = -1.06 + 0.63\,(1 - b/a) \tag{5}$$

or

$$(U-B)_c = -0.98 + 0.2\,(a/b - 1). \tag{6}$$

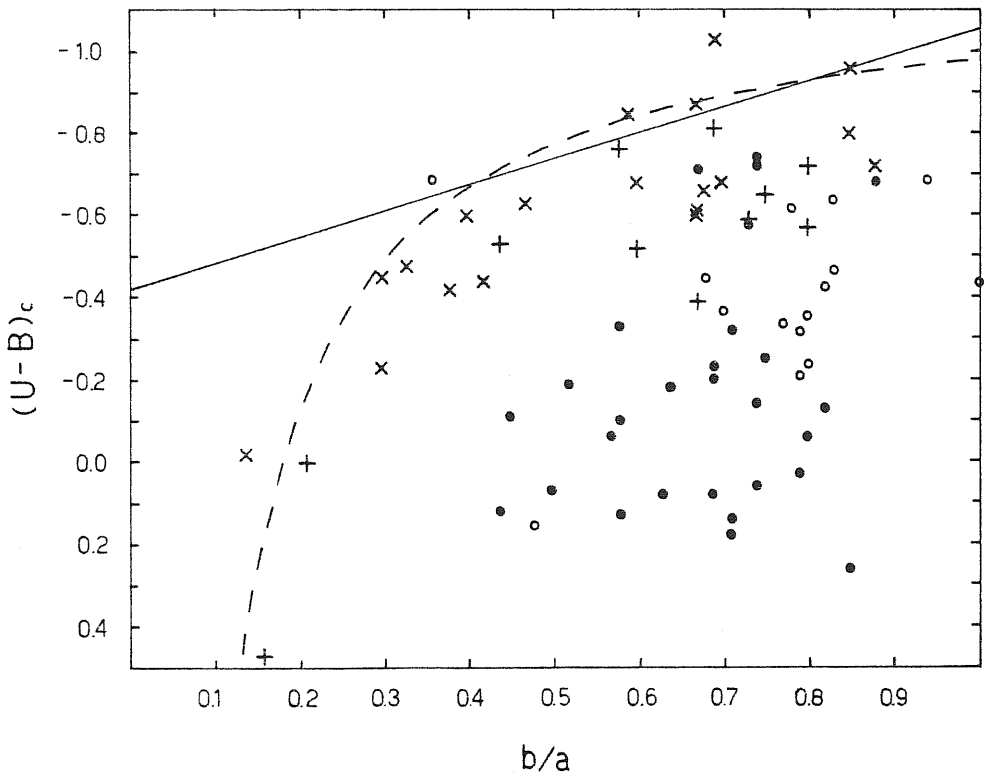

Figure 2. Distribution of $(U-B)_c$ as a function of the axial ratio. The continuous line represents equation (5), the dashed one, equation (6). Symbols have the same meaning as in Fig. 1.

Again both expressions are consistent with the observations which, however, seem to favour the second one (*cf.* Fig. 2). The fact that the boundary of the data point distribution is not as sharply defined as in Fig. 1 is not surprising: the U band is more sensitive to the '3000 Å bump' as well as to variability.

Note that the consistency of equations (5) and (6) with the corresponding ones for $(B-V)_c$ can be regarded as a successful check of the reddening laws (2) and (3); in fact it means that the estimates of $E(B-V)$ provided by these equations are bound to agree with those that can be independently obtained, whenever the contamination by the underlying galaxy is negligible, from the $(B-V)_c$ versus $(U-B)_c$ diagram, using the standard extinction curve.

3 Does reddening correlate with luminosity?

While the above results imply that Seyferts contain substantial amounts of dust, current observations indicate that the latter is much less abundant in QSOs (*cf.*, e.g. Soifer & Neugebauer 1981). This may suggest that reddening correlates with absolute magnitude, being larger for lower luminosity objects. To investigate this problem further we have computed the absolute nuclear magnitude of all objects in our sample using Sandage's (1973) 'colour given' method, straightforwardly generalized to include the internal reddening correction as given by equation (2). Following Véron (1979) we have assumed the underlying galaxies to have intrinsic colours $(U-B)_g = 0.3$ and $(B-V)_g = 0.8$. We have then grouped the objects into several absolute magnitude bins, marked with different symbols in Figs 1 and 2.

A remarkable luminosity segregation shows up in these figures, less luminous objects being confined at larger and larger distances from the boundary line. At the present stage, however, it is impossible to tell to what extent such segregation is due to increasing contamination by starlight. On the other hand, if a fair number of nuclei with $M_U \simeq -23 \div -22$ ($H_0 = 50\,\mathrm{km\,s^{-1}\,Mpc^{-1}}$) dominate the underlying galaxy contributions in the apertures used for observations, $E(B-V)$ might, on the average, be increasing with absolute magnitude by as much as $\Delta E(B-V) \approx 0.1\,\Delta M_U$.

4 Comparison with emission line reddening estimates

Fig. 3 shows the reddening estimates for 22 type-1 and 1.5 Seyferts, obtained by Lacy *et al.* (1982) and Malkan (1983) on the basis of emission line ratios $[E(B-V)_{EL}]$, plotted against their axial ratios. Whenever more than one value of $E(B-V)_{EL}$ is given, we have taken their arithmetic mean; 3C 227 has been omitted because no estimate of b/a is available for it. The continuous line represents equation (2).

Two points are worth noting:

(i) There is some indication of a correlation between $E(B-V)_{EL}$ and b/a. The formal value of the correlation coefficient (unweighted data) is $r = -0.53$, corresponding to a 1 per cent probability that the data could have come from an uncorrelated population. This result, however, rests heavily upon one single, and uncertain, point (associated with IC 4329A) located near to the upper left corner in Fig. 3; without it, r drops to -0.21; correlations as strong would arise in 37 per cent of samples from an uncorrelated population. On the other hand, from the colours of 3C 227 (Sandage 1973), a bright nucleus surrounded by a faint envelope, and our equations (2), (4), (5) and (6) we would predict quite a small value of b/a; the result of Lacy *et al.* (1982), $E(B-V)_{EL} = 0.49 \pm 0.09$ would then somewhat strengthen the case for a correlation.

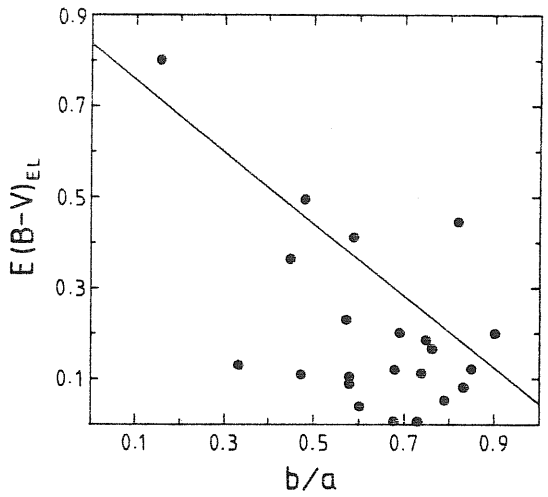

Figure 3. Distribution of emission line reddenings as a function of the axial ratio. The straight line represents equation (2).

(ii) The values of $E(B-V)_{EL}$ tend to lie below our estimates for the continuum. The uncertainties are so large, however, that the two reddenings may still be equal.

5 Conclusions

The main results of this paper can be summarized as follows.

(a) There is clear evidence of a correlation between the colours of Seyfert 1s and their axial ratios, which is straightforwardly interpreted in terms of internal reddening of the continuum. This interpretation is further supported by a comparison of the distributions of $(B-V)$ and $(U-B)$.

(b) The implied values of $E(B-V)$ are quite large. They reach several tenths of a magnitude for $b/a \leqslant 0.5$, thus naturally accounting for the paucity of edge-on Seyferts in optically selected samples (Keel 1980).

(c) There is some indication of an increase of reddening with decreasing optical luminosity of the nucleus, consistent with the notion of a small dust absorption in quasars.

(d) Our continuum reddening estimates generally exceed those obtained for emission lines. The uncertainties, however, are so large that any firm conclusions are premature.

Our results have a number of obvious implications; in particular the luminosity function of Seyfert 1 nuclei and several correlations involving their continuum luminosity need to be reconsidered. Work in these directions is in progress.

Acknowledgments

GDZ thanks the Institute of Astronomy, University of Cambridge, and especially Professor M. Rees, for their generous hospitality and for financial support. He acknowledges information discussions with M. Gaskell, M. Ward and A. Lawrence. We are grateful to the referee for useful comments, to Mrs N. Tate and to Mr R. Sword for help with the manuscript and the figures. Work supported in part by the National Research Council (CNR) of Italy, through grant PSN 81-037.

References

Burstein, D. & Heiles, C., 1978. *Astrophys. J.*, **225**, 40.
Clavel, J., Benvenuti, P., Cassatella, A., Heck, A., Penston, M. V., Selvelli, P. L., Beeckmans, F. & Macchetto, F., 1980. *Mon. Not. R. astr. Soc.*, **192**, 769.
Costero, R. & Osterbrock, D. E., 1977. *Astrophys. J.*, **211**, 675.
de Vaucouleurs, G., de Vaucouleurs, A. & Corwin, H., 1976. *Second Reference Catalogue of Bright Galaxies*, University of Texas Press.
Gaskell, C. M., 1982. *Publ. astr. Soc. Pacific*, **94**, 891.
Holmberg, E., 1958. *Medd. Lund Obs. Ser. II, No. 136.*
Holmberg, E., 1975. In *Stars and Stellar Systems*, Vol. 9, p. 123, eds Sandage, A., Sandage, M. & Kristian, J., University of Chicago Press.
Keel, W. C., 1980. *Astr. J.*, **85**, 198.
Khachikian, E. Ye. & Weedman, D. W., 1974. *Astrophys. J.*, **192**, 581.
Koski, A. T., 1978. *Astrophys. J.*, **223**, 56.
Lacy, J. H., Soifer, B. T., Neugebauer, G., Matthews, K., Malkan, M., Becklin, E. E., Wu, C.-C., Boggess, A. & Gull, T. R., 1982. *Astrophys. J.*, **256**, 75.
Lauberts, A., 1982. *The ESO/Uppsala Survey of the ESO (B) Atlas*, ESO Publications.
Lawrence, A. & Elvis, M., 1982. *Astrophys. J.*, **256**, 410.
Malkan, M. A., 1983. *Astrophys. J.*, **264**, L1.
Malkan, M. A. & Oke, J. B., 1983. *Astrophys. J.*, **265**, 92.
Sandage, A., 1973. *Astrophys. J.*, **180**, 687.
Savage, B. D. & Mathis, J. S. 1979. *A. Rev. Astr. Astrophys.*, **17**, 73.
Soifer, B. T. & Neugebauer, G., 1981. In *Infrared Astronomy, IAU Symp. 96*, p. 329, eds Wynn-Williams, C. G. & Cruikshank, D. P., Reidel, Dordrecht, Holland.
Véron, P., 1979. *Astr. Astrophys.*, **78**, 46.

3.2 Reddening of BLR

The standard method to measure the reddeining of emission line regioons is to use two more accessible lines of different wavelength whose relative intensities are known a priori or can be calculated with sufficient accuracy. Then, the amount of reddening is estimated from the observed line ratios and an assumed extinction curve.

Comparing violet and infrared lines of Seyfert galaxies Wampler (1968b, 1971) showed that the narrow lines at least, and probably the broad lines too, were substantially reddened. However Wampler (1968a) found that the observed L_α/H_β ratio could not be explained by reddening alone and he proposed that collisional and self-absorption effects were important. The work of Shields (1974) and subsequent workers has verified that significant Balmer optical depths and collisional effects can indeed produce steep Balmer decrements and a low L_α/H_β ratio. It is currently widely concluded that steep broad-line Balmer decrements do not necessarily imply any reddening at all. Although O I and He II imply about the same amount of reddening as deduced from a simple interpretation of the hydrogen line ratio (Netzer & davidson 1979; Gaskell 1981) the theoretical ratios of these lines have been called into question by Grandi (1983) and the reddening they imply could be spurious. Grandi (1983) has in fact concluded that there could be no useful line ratios at all for deducing reddening for BLR of quasar-like objects.

Last year at the Liège conference Netzer (1983) indicated again that close examination of the data suggests that all larger wavelength lines are observed to be stronger than the shorter wavelength ones, compared with theoretical predictions; the most noticeable discrepancies are in the strength of helium lines. He concluded that the easiest way to reconcile theory and observation is to admit substantial amounts of reddening by dust.

This debated question has been recently discussed in detail by De Zotti and Gaskell (1984). These authors present a compilation of axial ratios and published-broad and narrow-line Balmer decrements for 109 Seyfert galaxies

of all classes among which 75 sources are SY 1 and Sy 1.5. They have plotted Fig. 58a-d which show the BLR decrements versus inclination. The data have been divided into four luminosity groups as indicated in the figures (magnitudes are taken from Cheng, Danese and de Zotti (1983b) and are corrected for inclination according to Eq. 1 of Cheng et al. (1983a). Their results are as follows:

(1) For the lower luminosity classes the axial ratios and BLR Balmer decrements are correlated at greater than 90% confidence;

(2) Only the highest luminosity group shows no correlation;

(3) For the entire sample the probability of the correlation arising by chance is 10^{-5}.

These results clearly indicate that there is reddening by dust confined to the planes of the galaxies. The scatter in Fig. 58 is explained as due to the known (quite large) errors in both a/b and (H_α/H_β). a/b is uncertain by 30% (due to measuring errors) and $\log(H_\alpha/H_\beta)$ is uncertain by 0.15 due to "known" variability (de Zotti and Gaskell 1984). A decrease of reddening with increasing luminosity is also suggested by the data.

When they assume that the dust is in plane parallel layers around the broad line regions of Seyferts (as in Fig. 59a) and fit an equation of the form: $E(B-V) = E_0\, a/b$, the BLR H_α/H_β ratios give $E_0 = 0.15 \pm 0.04$ (i.e. a pole-on reddening of 0.15 in E(B-V)). Cheng, Danese and de Zotti (1983) found that a good fit to the nuclear colours of the brighter Seyferts could be obtained with a similar equation and a pole-on reddening of 0.15. The agreement between these two totally independent estimates of the pole-on reddening is strong support for both the nonthermal continuum and the BLR being reddened by the same external dust with a pole-on reddening E_0 of 0.15.

In addition, de Zotti and Gaskell (1984) find that the mean intrinsic BLR $(H_\alpha/H_\beta)_0$ ratio ($<(H_\alpha/H_\beta)_0>$) is certainly less than 3.8 and could be less than 2.6! This result supports Collin-Souffrin, Dumont and Tully (1982) conclusion that BLR have densities of about 10^{10}-10^{11} cm^{-3} rather than 10^{8}-$10^{9.5}$ cm^{-3}.

3.3 Reddening of NLR

For the NRL there are more line ratios available and it has long been common practice to determine reddenings of NLR in AGNs using the departures of the various observed line ratios from the expected theoretical value in Menzel-Baker case B. In particular the narrow-line Balmer decrements were frequently used as reddening indicators.

In recent years, however, this procedure has been challenged by several workers (see discussion in Gaskell 1982). In order to check whether or not NLR Balmer decrements can be used as indicators of reddening, Gaskell (1982) compared reddenings estimated from NLR Balmer decrements of AGNs with those derived from other less suspect ratios, such as transaural/nebular line ratios of [S II] and [O II], [S II] λ4071/1.03μ ratio and He II recombination lines. He found good agreement between the various reddening estimates, implying the intrinsic Balmer decrement of NLR is within 10% of the case-B value, and that when estimating physical conditions and abundance from narrow-li,e strengths one can safely use dereddened line strengths corrected by means of the Balmer decrement.

de Zotti and Gaskell (1984) have estimated the anrrow-line H_α/H_β ratios for 26 intermediate Seyferts. They cautioned that it is hard to assess the systematic and random errors in these rations since they depend on the phylosophy of the person who did the de-blending in each case, and that the errors in the NLR H_α/H_β ratios are certainly much greater than in BLR H_α/H_β ratios and are perhaps on the order of 50% or a factor of two in many cases.

Their first result is that the NLR decrement of Sy 2 is steeper on average than the decrement of intermediate Seyferts. The median decrement for Sy 2 is 5.1 while the median NLR decrement for intermediate Seyferts is 4.2.

According to recent theoretical results (Halpern 1982; Halpern & Steiner 1983;

Gaskell & Ferland 1984) the intrinsic $H\alpha/H\beta$ is usually close to 3.1 under NLR conditions. The steep observed NLR decrements must be due to reddening. If this is the case the difference of median NLR decrement between Sy 2 and intermediate Seyferts implies line-of-sight reddening, E(B-V), higher by 0.18 mag. in Sy 2, than that in NLR of intermediate Seyferts. This confirms the result found by Gaskell (1984) using forbidden line ratios to compare the reddening of Seyferts with and without BLRs. Although there seems to be good evidence for the NLR of Sy 2 having more dust than intermediate Seyferts. This conclusion is supported by the observed fact that, in comparison with Sy 1, intermediate Seyferts have higher symmetry of forbidden lines (Heckman and Balick 1979). We can anticipate that emission lines of Sy 2 should have higher degrees of polarization than those of intermediate Seyferts.

Comparing the BLR and the NLR Balman decrements, de Zotti and Gaskell (1984) found that there is only a weak correlation between them. There is thus little support for the common assumption that the BLR and NLR have the same reddening due to dust external to both regions. BLR decrements also appear to be systematically steeper than NLR decrements. This however may well be the selection effect favouring the reporting of NLR measurements in BRL objects when the broad lines are weak compared to the narrow lines since "de-blending" will be easier in these cases.

The NLR decrements for Sy 2 and Sy 1.5 almost do not correlate with axial ratio (a/b). It means that the dust in NLR of Sy 1 and Sy 1.5 cannot be in a simple plane layer parallel to the disc of the underlying galaxies (de Zotti & Gaskell (1984). This result is consistent with that of Keel (1980) who has already shown that Sy 2 are not preferrentially seen as face-on as Sy 1 are.

3.4 Conclusion and Discussion

3.4.1 Conclusion

From the correlation of broad-band colours of Seyfert 1 with the inclination of the lost galaxy, Cheng, Danese and de Zotti (1983a,b) derived a simple reddening law:

$$E(B-V) = 0.25(a/b - 1) + 0.15$$

De Zotti & Gaskell (1984) deduced an essentially identical relationship from broad line Balmer decrements; they also found some evidence of a decrease of reddening with increasing luminosity, an indication of which was noted by Cheng, Danese and de Zotti (1983a,b) too.

Danese & de Zotti (1984) demostrated that the reddening law given by Cheng et al (1983a) accounts quantitatively for the distribution of axial ratios in optically selected samples of Sy 1, as well as for the correlation of the ratio of H_β to hard X-ray luminosities with the axial ratio b/a of the galaxy (Lawrence & Elvis 1982).

Additional evidences for extinction in Sy 1 are discussed by Rudy (1984) who again suggests that dust is unlikely to play a major role in high luminosity QSOs.

$(H_\alpha/H_\beta)_{narrow}$ should be "reistated" as an indicator of reddening for the NLR of AGNs, but with an assumed intrinsic value of about 3.1 (Halpern 1982; Halpern & Steiner 1983; Gaskell 1984; Gaskell & Ferland 1984). The steep observed NLR decrements must be due to reddening and dust can not be in a simple plane parallel to the disc of underlying galaxy. The reddening of the NLR in AGNs may not be the same as that of BLR. The reddenings of the NLR of Sy 2 are mostly higher than those of the NLR of Sy 1.5 (de Zotti & Gaskell 1984).

3.4.2 Discussion

1) Possible models for the distribution of the dust

(a) Reddening of the BLR.

Plane parallel layer in the plane of the galaxy (Fig. 59a)

Assuming a finite thickness of the dust plane, de Zotti and gaskell (1984) have adopted a reddining law of the form:

$$E(B-V) = E_0 \left(\frac{1-b_0^2}{(b/a)^2 - b_0^2}\right)^{\frac{1}{2}} \qquad \text{with } b_0=0.1 \text{ (see RCBG2).}$$

Fitting this to the BIR data they have obtained the pole-on reddening, $E_0=0.15\pm0.04$, and the mean unreddened Balmer decrement, $\langle (H_\alpha/H_\beta)_0 \rangle = 2.6$ ($\pm$ 20%).

Flattended "dough-nut" distribution (Fig. 59b)

After inspecting Fig. 58b-d more carefully de Zotti and Gaskell (1984) suggested that a curve may be a better fit to the data than stright line. The sort of curve needed would arise very naturally if there were a "hole" in the dust at the very center of the Seyfert. The "doughnut" model makes different predictions about the amount of reddening and the intrinsic $(H_\alpha/H_\beta)_{broad}$ from the simple uniform disc model. In particular, in the "doughnut" model the face-on Sy 1 would be showing completely unreddened continua and BLRs. If so the intrinsic BLR decrement would be $(H_\alpha/H_\beta)_0 =$ = 3.8.

(b) Reddening of the NLR

Dust "two-shape" distribution (Fig. 59c)

As mentioned in section 2.2.4, on the basis of analysis of narrow-line profiles Heckman et al (1981) suggested that the NIR consists of gas and dust flowing radially with respect to the nucleus. Taking this opinion into account, we suggest as follows, (i) dust associated with NLR clouds; (ii) NLR has an ellipsoidal configuration, (iii) "dough-nut" embedded in the NLR

i.e., dust "two-shape" distribution. Obviously, this model leads to following conclusions: (a) E_c may still be 0.15; (b) The BLR $(H_\alpha/H_\beta)_c < 3.8$; (c) The BLR decrements are steeper than the NIR decrements, which are consistent with the result given by de Zotti & Gaskell (1984); (d) The NIR reddening should slightly be correlated with the axial ratio b/a.

(2) Does reddening correlated with luminosity?

Moshotzky (1982) found that the column density measured from low-energy X-ray absorption was greater for lower luminosity Seyferts. Lawrence & Elvis (1982) indicated that the X-ray covering factor is a smoothly decreasing function of the hard X-ray luminosity. They also found that the infrared excess of Seyferts (interpreted as thermal reradiation by dust) increases with decreasing hard X-ray luminosity. Therefore, the X-ray and IR observation appear to show luminosity dependent reddening.

Cheng, Danese and de Zotti (1983a, b) also found evidence for a luminosity dependent reddening of the continuum

$$\Delta E(U-B)_N \approx 0.2\ (M_u + 24.5)\ (1-b/a)$$

Some indications that the BLR reddening increases with decreasing luminosity with $\Delta E(B-V) \approx -0.06\,\Delta M_B$ for b/a = 0.5 were also noted by de Zotti and Gaskell (1984). Further work on this subject is in progress.

(3) The λ 2200 dust absorption feature

The absence or weakness of absorption at λ 2200 in AGNs have been mentioned by many authors, and has been taken as an indication of low reddening (cf. McKee & Petrosian 1974; Gaskell 1981). For example, Grandi (1982) argued that the reddenings really are that low, and that the standard broad-line reddening indicators are in error. As discussed by de Zotti & Gaskell, a thorough study of the BLR of NGC 3783 is against this idea. Ward & Morris (1984) show that the P8/H6, O I λ 8446/λ1304 and He II λ 4686/λ1640 ratios are all consistent with E(B-V) = 0.25.

This is in good agreement with our prediction from the axial ratio, but much greater than the reddening, E(B-V)=0.10, deduced from λ2200. This fact also shows that O I and He II line ratios are good indicators of reddening.

There are two kinds of explanations for the low λ2200 reddening. The first one is that a mean galactic extinction curve might not be applicable to the environment of a Seyfert nucleus. According de Zotti & Gaskell's estimates (1984), the λ2200 feature is systematically weaker in most Seyferts than in our Galaxy, but perhaps "normal" in a few.

The second one is that there is excess emission in the spectrum of QSOs and Seyferts around 2200 (Gaskell 1981), de Zotti and Gaskell (1984) pointed out that the excess shown in the detailed modelling of the Fe II emission (the"3000 Å hump") by Netzer and Wills (1983) and Wills, Netzer and Will (1984) is exactly that needed to reconcile the λ2200 reddening with those implied by the Balmer decrements. Taking this excess into account, Wills (1983) got for IZw 1 a colour excess E(B-V) = 0.21, which is very close to our prediction. Other observers had either ignored Fe II emission altogether or else assumed that it stopped at λ2300. As shown by de Zotti and Gaskell (1984), if the λ2200 reddenings are corrected by 0.10 in E(B-V) every discrepancy with estimates from orientations disappear (Fig. 60).

(4) Can internal reddening explain all emission line ratios?

Obviously, although internal reddenings strongly affect the emission line ratios, it can not explain all line ratios by itself. As discussed in section 2.2.5, for example, reddening by dust external to the galactic nuclei cannot entirely explain both the P_α/H_β and L_α/H_β ratios. As far as the L /H ratio is concerned several additional effects must be taken into account such as collisional excitation of H_β, de-excitation of L_α and self-absorption from the level n=2 under the high-density conditions of Seyfert nuclei. Therefore, to explain all line ratios we have to consider both internal reddening and other physical processes. We would like to indicate again that $(H_\alpha/H_\beta)_{broad}$, O I λ8446/ λ1340 and He II λ4686/ λ1640 ratios are good indicators of reddening in the BLR and that $(H_\alpha/H_\beta)_{narrow}$, [O II] and [S II] are good indicators of the reddening in the NLR.

CHAPTER IV THE RATIO OF X-RAY TO OPTICAL LUMINOSITY FOR AGNs

In this Chapter we can see how the internal reddening affects the ratio of X-ray to optical luminosity for AGNs.

Mon. Not. R. astr. Soc. (1984) **208**, 799–811

The ratio of X-ray-to-optical luminosity for active galactic nuclei

F. Z. Cheng *ISAS, Strada Costiera 11, I-34014 Trieste, Italy*

L. Danese *Istituto di Astronomia, Vicolo dell'Osservatorio 5, I-35100 Padova, Italy*

G. De Zotti* *Institute of Astronomy, Madingley Road, Cambridge CB3 0HA*

F. Lucchin *Dipartimento di Fisica, Via Marzolo 8, I-35100 Padova, Italy*

Received 1983 October 13; in original form 1983 June 7

Summary. We show that the apparent enhancement of the average ratio of X-ray to optical luminosity for Seyfert 1 nuclei, in comparison with radio quiet QSOs, may be largely, if not totally, due to internal reddening. Estimates of the average optical to X-ray energy index, α_{ox}, for five independent samples covering, altogether, over three orders of magnitude in optical luminosity, are all consistent with $\bar{\alpha}_{ox} \simeq 1.55$ and a dispersion $\sigma \simeq 0.15$. A comparison of optical and X-ray counts adds support to this conclusion.

1 Introduction

Among the first remarkable results of the X-ray studies of Seyfert 1 galaxies (Elvis *et al.* 1978; Tananbaum *et al.* 1978) was the evidence for a correlation between the X-ray and the optical emission, suggesting that the luminous non-thermal continuum, previously known to extend from far *IR* to *UV*, spans over at least three more decades in frequency. Subsequently, extensive *Einstein* observations also have established such a correlation for quasars (Tananbaum *et al.* 1979; Ku, Helfand & Lucy 1980; Zamorani *et al.* 1981).

The ensuing attempts to specify the relationship between the optical (l_o) and the X-ray (l_x) luminosities, however, have not yet reached a generally agreed conclusion. Investigations following a suggestion by Zamorani *et al.* (1981) have led to claims that the ratio l_x/l_o is systematically increasing with decreasing l_o (Reichert *et al.* 1982; Zamorani 1982; Avni & Tananbaum 1982). On the other hand, Kriss & Canizares (1982) warned that this result may be subject to selection effects and Margon, Chanan & Downes (1982) showed that observations of X-ray selected QSOs could also be matched with a model assuming a constant l_x/l_o. In addition, a comparison of the X-ray detection rates of optically selected

* Permanent address: Unita di Ricerca GNA/CNR di Padova, c/o Istituto di Astronomia, Vicolo dell' Osservatorio 5, I-35100 Padova, Italy.

QSOs (Ku *et al.* 1980; Zamorani *et al.* 1981) led Kembhavi & Fabian (1982) to suggest that l_x/l_o might rather decrease with decreasing optical luminosity.

As a matter of fact, the significance of the correlation between l_x/l_o and l_o is marginal if we consider only QSOs. It becomes much greater if we add Seyfert 1s for which current estimates (Kriss, Canizares & Ricker 1980; Setti & Woltjer 1982) yield significantly larger values of l_x/l_o. Unfortunately, however, the determination of l_x/l_o for Seyfert 1s require several corrections which are necessarily crude in the present data situation and, moreover, have been at least partly overlooked so far. Spurious correlations may be easily introduced by the fact that corrections are generally larger for lower-luminosity objects as well as by unrecognized selection effects.

In this paper, after a quantitative discussion of the relevant corrections (Section 2) and of the effects of X-ray thresholds (Section 3) we analyse the distributions of l_x/l_o for all the available samples (Section 4). In Section 5 we consider the additional information provided by X-ray source counts. The results of this comparative study are summarized in Section 6.

2 Luminosities of Seyfert 1 nuclei

2.1 OPTICAL LUMINOSITIES

The determination of the optical luminosities of Seyfert 1 nuclei is complicated by two factors: contamination by the underlying galaxy and internal reddening. The amount of internal extinction has long been the subject of considerable debate and the matter is still far from being settled (*cf.* Grandi 1983). On the other hand, several pieces of evidence for substantial obscuration by a flattened dusty region parallel to the plane of the surrounding galaxy, but still close to the nucleus, have been accumulating in the last few years. These include

(a) the paucity of optically discovered nearly edge-on Seyfert galaxies, relative to a comparison sample of normal spirals (Keel 1980; Doroshenko & Terebizh 1980),

(b) the correlation of the ratio of Hβ to hard X-ray luminosities with the axial ratio b/a of the galaxy (Lawrence & Elvis 1982),

(c) the correlation of the broad-band colours of the nuclei with b/a (Cheng, Danese & De Zotti 1983).

The last authors found that the variation of the colour excess with b/a can be expressed, at least for nuclei with $-24 \geq M_U \geq -25$ ($H_0 = 50$ km s^{-1} Mpc^{-1}), by

$$E(U-B)_N = 0.63(1 - b/a). \tag{1}$$

They also found some indications that, for fainter nuclei, the reddening correction might increase with increasing magnitude by as much as

$$\delta E(U-B)_N = 0.2(M_U + 24.5)(1 - b/a). \tag{2}$$

Nuclei much brighter than $M_U = -25$, on the other hand, show little if any evidence of internal extinction (*cf.* e.g. Soifer & Neugebauer 1981).

It is easily seen that the reddening law derived by Cheng *et al.* (1983) can account quantitatively for the findings (a) and (b); in addition, it is fully consistent with the amounts of reddening of broad lines as a function of axial ratio deduced by De Zotti & Gaskell (in preparation) from Balmer decrements. In view of all that, we will use it to correct for internal extinction.

A successful method for subtracting out the contribution of the underlying galaxy, referred to as the 'colour-given' method, has been devised by Sandage (1973) and Khachikian & Weedman (1974). It is based on the assumption that both the nuclei and the galactic discs have all more or less the same intrinsic colours, $(U-B)_N$ and $(U-B)_G$, respectively. Thus the nuclear contribution to the total observed magnitude can be inferred from the observed colours of the nucleus plus the galaxy, $(U-B)_C$, after having corrected the intrinsic colours of the two components for the effect of redshift and for reddening. The method is most conveniently applied in the U band where the nuclei are brighter relative to the galactic discs than in B or in V.

The ratio between the intensity of the nucleus, I_N, and that of the galaxy, I_G, is given by

$$a(U) = \frac{I_N(U)}{I_G(U)} = \frac{1 - \mathrm{dex}\{-0.4[(U-B)_C - (U-B)_{G,c}]\}}{\mathrm{dex}\{-0.4[(U-B)_C - (U-B)_{N,c}]\} - 1} \tag{3}$$

where

$$(U-B)_{G,c} = (U-B)_G + E(U-B)_g + E(U-B)_G + K(U)_G - K(B)_G \tag{4a}$$

$$(U-B)_{N,c} = (U-B)_N + E(U-B)_g + E(U-B)_N + K(U-B)_N \tag{4b}$$

In actual calculations the following assumption have been adopted:

(*a*) $(U-B)_N = -1$, the blue limit of the $U-B$ distribution of quasars and Seyfert 1 galaxies (Sandage 1973; Khachikian & Weedman 1974)

(*b*) $(U-B)_G = 0.1$, the effective aperture colour for a face-on Sa or Sab galaxy (de Vaucouleurs & de Vaucouleurs 1972)

(*c*) reddening within our own Galaxy, $E(B-V)_g$, estimated for each object using the maps of Burstein & Heiles (1982) and a ratio $E(U-B)/E(B-V) = 0.8$ (Savage & Mathis 1979)

(*d*) internal reddening of starlight $E(U-B)_G = 0.50 \log(a/b)$, appropriate to a morphological type $T = 1$ (de Vaucouleurs & de Vaucouleurs 1972)

(*e*) K-corrections have been neglected. In addition, whenever equation (1), or equation (1) + equation (2), give $(U-B)_{N,c} > (U-B)_C$ we have set $E(U-B)_N = (U-B)_C - (U-B)_N - E(U-B)_g - K(U-B)_N$.

(*f*) The apparent magnitude of the nucleus is then

$$U_N = U_C + 2.5 \log[1 + 1/a(U)], \tag{5}$$

where U_C is the observed magnitude (nucleus + galaxy). Finally the absolute nuclear magnitude is obtained from

$$M_U = U_N - A_{U,g} - A_{U,N} - K(U)_N - 5 \log z - 43.89, \tag{6}$$

where the numerical constant corresponds to $H_0 = 50\,\mathrm{km\,s^{-1}\,Mpc^{-1}}$. Also, we have taken $A_U = 6.125\,E(U-B)$ (Savage & Mathis 1979) and $K(U)_N = 1.25 \log(1+z)$, corresponding to an optical spectral index $\alpha_o = 0.5$ (Richstone & Schmidt 1980).

2.2 SOFT X-RAY LUMINOSITIES

It has been demonstrated by Lawrence & Elvis (1982) that the ratio of hard (2–10 keV) to soft (0.5–4.5 keV) X-ray luminosities, L_{HX}/L_{SX}, which is approximately constant for $L_{HX} \geq 10^{44}\,\mathrm{erg\,s^{-1}}$, at lower luminosities smoothly increases with decreasing L_{HX}, in keeping with the findings in low luminosity galaxies of large X-ray absorbing columns

(Maccacaro *et al.* 1982b; Mushotzky 1982) which anti-correlate with L_{HX} (Mushotzky 1982). A least-squares fit to the data collected by Lawrence & Elvis gives

$$\log (L_{HX}/L_{SH}) = 19.53 - 0.439 \log L_{SX} \qquad (\log L_{SX} < 44). \tag{7}$$

Taking into account that in the absence of absorption and for an X-ray spectral index $\alpha_x = 0.65$ we have $\log (L_{HX}/L_{SX}) = 0.26$, when only soft X-ray data are available we adopt as a first order approximation to the intrinsic luminosity at 2 keV, l_x:

$$\log l_x = 1.51 + 0.561 \log L_{SX} \qquad (\log L_{SX} < 44) \tag{8a}$$

$$\log l_x = \log L_{SX} - 17.99 \qquad (\log L_{SX} \geqslant 44). \tag{8b}$$

3 The effect of X-ray selection

X-ray flux limited observations will obviously preferentially select objects with larger values of l_x/l_o, i.e. with smaller values of the two point energy index introduced by Tananbaum *et al.* (1979),

$$\alpha_{ox} = -\log (l_x/l_o)/\log (\nu_x/\nu_o) \tag{9}$$

relating the monochromatic luminosity at 2 keV ($\nu_x = 4.836 \times 10^{17}$ Hz), l_x, to the monochromatic luminosity at 2500 Å ($\nu_o = 1.199 \times 10^{15}$ Hz), l_o, both in erg s^{-1} Hz^{-1}.

In the absence of any optical threshold, the expected sample mean, $\langle \alpha_{ox} \rangle$, as a function of the absolute magnitude M_B is given by (dropping the subscripts ox to simplify the notation)

$$\langle \alpha \rangle = \frac{\int d\alpha\, N(> S_x, M_B, \alpha)\, \alpha}{\int d\alpha\, N(> S_x, M_B, \alpha)} \tag{10}$$

where S_x is the X-ray flux limit at 2 keV in erg cm^{-2} s^{-1} Hz^{-1}, $N(> S_x, M_B, \alpha)$ is the number of objects in the sample per unit interval of M_B and α_{ox}:

$$N(> S_x, M_B, \alpha) = f(\alpha \mid M_B)\, \rho_o(M_B, 0) \int_0^{V_m} dV\, F(M_B, z)$$

$$= 4\pi f(\alpha \mid M_B)\, \rho_o(M_B, 0)\, \Omega \int_0^{D_m} dD\, \frac{D^2 F(M_B, z)}{(1+z)^3 [2(\Omega z + 1)^{1/2} + \Omega - 2]}, \tag{11}$$

$f(\alpha \mid M_B)$ is the distribution of function of α_{ox} [which may depend on absolute magnitude, but is assumed to be independent of redshift: although a dependence of α_{ox} on z is not excluded by the available data, no clear evidence for it has been found so far, *cf.* Avni & Tananbaum (1982)]. $\rho_o(M_B, 0)$ is the local optical luminosity function, $F(M_B, z)$ is the evolution function defined as the ratio of the luminosity function at the redshift z, $\rho(M_B, z)$ to $\rho_o(M_B, 0)$, D is the luminosity distance (Weinberg 1972, p. 485),

$$\log D_m = \tfrac{1}{2}[\log l_o - \log (4\pi S_x) - \alpha \log (\nu_x/\nu_o) + (1 - \alpha_x) \log (1 + z_m)], \tag{12}$$

z_m is the redshift corresponding to D_m and l_o is related to M_B by: $\log l_o = 20.53 - 0.4\, M_B$ (Schmidt 1968).

Although in general $\langle\alpha\rangle$ is a complicated function of M_B, even if $\bar{\alpha}$ is a constant, its behaviour can be simply understood considering a few limiting cases. So long as the effective volume element $dV_e = dV F(M_B, z)$ has an Euclidean form ($dV_e = 4\pi D^2\, dD$), and the K-correction term in equation (12) can be neglected ($\alpha_x \cong 1$), equation (10) simplifies to

$$\langle\alpha(M_B)\rangle = \frac{\int f(\alpha \mid M_B)\, \alpha \exp\left[-\tfrac{3}{2}\, \alpha \ln (\nu_x/\nu_o)\right] d\alpha}{\int f(\alpha \mid M_B) \exp\left[-\tfrac{3}{2}\, \alpha \ln (\nu_x/\nu_o)\right] d\alpha} \tag{13}$$

where the 'guillotine factor', cutting down the distribution on the large α_{ox} side, is clearly visible. Note also that in this case $\langle\alpha\rangle$ is independent of the X-ray flux limit and is a function of M_B only if $f(\alpha)$ is.

If $f(\alpha)$ is a Gaussian with mean $\bar{\alpha}$ and dispersion σ, equation (13) yields

$$\langle\alpha\rangle = \bar{\alpha} - \tfrac{3}{2} \ln (\nu_x/\nu_o)\, \sigma^2 \cong \bar{\alpha} - 9\sigma^2. \tag{14}$$

Under the same assumptions the expectation value of the sample dispersion, s, turns out to be:

$$s^2 = \frac{\int d\alpha f(\alpha)[\alpha - \langle\alpha\rangle]^2 \exp\left[-\tfrac{3}{2}\, \alpha \ln (\nu_x/\nu_o)\right]}{\int d\alpha f(\alpha) \exp\left[-\tfrac{3}{2}\, \alpha \ln (\nu_x/\nu_o)\right]} = \sigma^2. \tag{15}$$

Thus while the sample dispersion is an unbiased estimator of the true dispersion, the sample mean $\langle\alpha\rangle$ may be considerably smaller than $\bar{\alpha}$.

It is also interesting to notice that equations (13)–(15) do not apply only when the redshifts involved are $\ll 1$, as for example in the case of hard X-ray samples, but also in the case of moderate evolution [i.e. $F(M, z) \propto (1+z)^{4+\epsilon}$, the value of ϵ depending on the density parameter Ω: for $\Omega z \ll 1$, $\epsilon = 0$]. A stronger evolution increases the difference between $\langle\alpha\rangle$ and $\bar{\alpha}$. If, for illustration, we take $F(M, z) = (1+z)^4\, D^n$ and $\Omega z \ll 1$, we obtain an equation strictly analogous to equation (14), the only difference being that the coefficient of σ^2 increases by a factor $(n+3)/3$. This effect, coupled with the strongly luminosity-dependent evolution suggested by optical data (Schmidt & Green 1983), might account at least in part for the peculiar luminosity distribution of active galactic nuclei in X-ray selected samples (*cf.* e.g. Margon *et al.* 1982).

So far we have assumed that the integration limit D_m is fixed by the X-ray threshold. As the optical luminosity increases, however, a larger and larger fraction of sources will be visible in X-rays up to the distance $D_{\max}$, fixed by the shape of the evolution function and by the geometry of the Universe, beyond which the contribution to the integral in equation (10) is small. Correspondingly the X-ray selection effect will become less and less important and $\langle\alpha\rangle$ will approach $\bar{\alpha}$. More precisely, the X-ray selection will only affect those sources whose α_{ox} exceeds

$$\alpha_{\min}(l_o) = \frac{\log l_o - \log (4\pi S_x) - 2 \log D_{\max} + (1 - \alpha_x) \log (1 + z_{\max})}{\log (\nu_x/\nu_o)}\,; \tag{16}$$

its role becomes, therefore, quite modest if $\alpha_{\min} > \bar{\alpha}$.

Figs 1 and 2 show the full shapes of $\langle\alpha\rangle$ as a function of M_B for various optical evolution functions (see captions) and $\log S_x = -30.5$ or -31.25, roughly the limiting fluxes of the

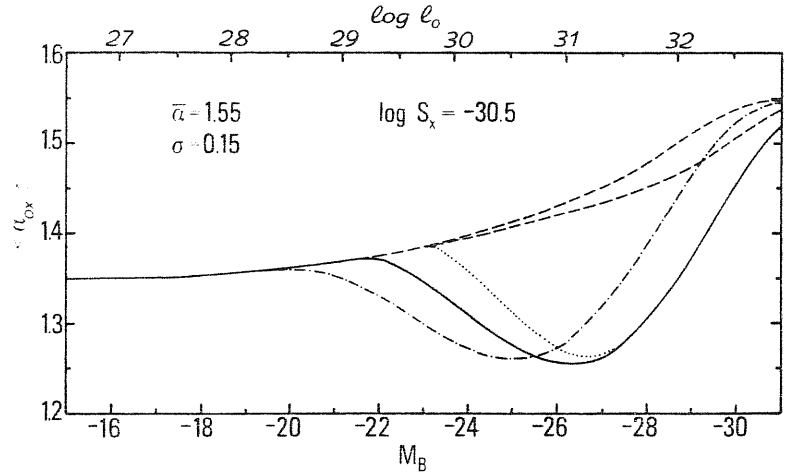

Figure 1. Graph of $\langle \alpha_{ox} \rangle$ as a function of optical luminosity. The dashed curves correspond to no evolution and $\Omega = 1$ (upper curve) or $\Omega = 0.2$. The dotted, solid and dot–dashed lines refer to Schmidt & Green (1983) models HL1, HH1 and HH5, respectively with a redshift cut-off $z_{max} = 3.5$.

Einstein medium sensitivity (Maccacaro *et al.* 1982a) and deep (Giacconi *et al.* 1979) surveys.

If the sample selection includes also an optical threshold, say B, the upper integration limit in equation (11) is replaced by the minimum between D_m [equation (12)] and D'_m given by

$$\log D'_m = 0.2\,(B - M_B) + 0.5\,(1 - \alpha_o)\log(1 + z_m) + 19.49 \tag{17}$$

where α_o is the optical spectral index. The condition for the X-ray limit to be relevant is, for $\alpha_o \cong \alpha_x$,

$$\bar{\alpha} \gtrsim \alpha_l = \frac{-\log S_x - 0.4B - 19.55}{\log(\nu_x/\nu_o)}\,. \tag{18}$$

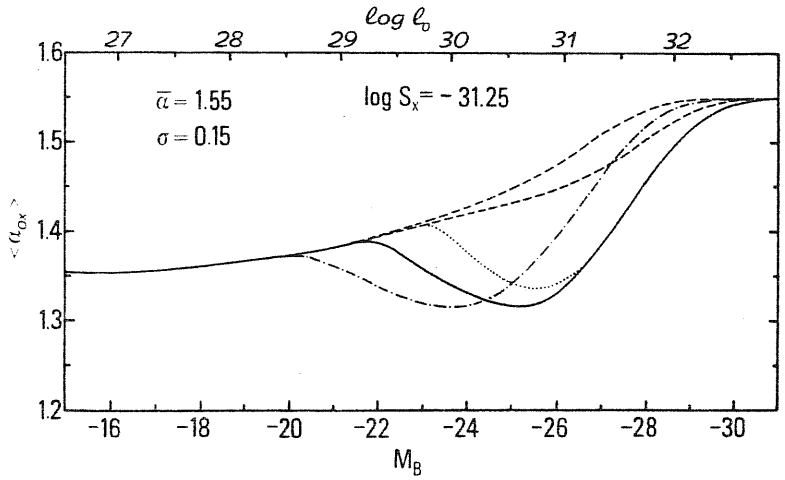

Figure 2. Same as in Fig. 1 but for an X-ray flux limit $\log S_x = -31.25$.

4 Estimates of $\bar{\alpha}$ from various samples

4.1 THE SAMPLE OF PICCINOTTI *et al.* (1982)

This sample is particularly useful because of its completeness above a well defined X-ray threshold, of its almost complete optical identifications and because its hard X-ray luminosities are not affected by photoelectric absorption. We have derived the nuclear optical luminosities at 2500 Å both with (l'_o) and without (l_o) allowance for the possible increase of reddening with decreasing optical luminosity [equation (2)], of all but one the objects classified as Seyfert 1s. The exception is NGC 7213 whose colours (McAlary *et al.* 1983) are redder than those assumed for the underlying galaxy, so that the colour-given method could not be applied. The X-ray luminosities at 2 keV, l_x, have been derived from the first pass (2–10 keV) luminosities listed by Piccinotti *et al.* (1982) assuming $\alpha_x = 0.65$. The relevant data and results are listed in Table 1.

If α_{ox} is uncorrelated with l_o we have $\langle\alpha'_{ox}\rangle = 1.31$; $\sigma' = 0.13$, $\langle\log l'_o\rangle = 29.29$ when equation (2) is taken into account; $\langle\alpha_{ox}\rangle = 1.23$, $\sigma = 0.17$, $\langle\log l_o\rangle = 29.06$, otherwise.

As noted in Section 3, so long as only redshifts $\ll 1$ are involved any dependence of α on l_o is directly reflected on $\langle\alpha\rangle$. If the reddening is independent of optical luminosity, a correlation between α_{ox} and $\log l_o$, significant at the $\cong 0.7$ per cent confidence level

Table 1. The sample of Piccinotti *et al.* (1982).

Name	U	U-B	θ(")	$E(U-B)_g$	z	b/a	Refs.	log l_o	log l'_o	log l_x	α_{ox}	α'_{ox}
III Zw 2	15.38	−0.70	10.1	0.06	0.090	0.66	1,a	30.15	30.08	27.09	1.18	1.15
F 9	12.30	−1.01	9.6	0	0.045	0.80	2,b	30.11	30.11	26.40	1.42	1.42
NGC 526A	15.08	−0.34	22.5	0	0.0189	0.67	3,c	28.54	28.97	25.87	1.02	1.19
Mkn 590	14.75	+0.03	25	0	0.027	0.79	4,d	28.23	28.61	25.94	0.88	1.02
3C 120	14.10	−0.75	15	0.11	0.033	0.59	5,d	29.72	29.72	26.31	1.31	1.31
H 0557-385	16.19	−0.23	-	0.03	0.0344	0.35	6,e	29.25	29.57	26.19	1.18	1.30
NGC 3783	13.64	−0.53	17.7	0.04	0.0092	0.80	3,f	28.47	28.78	25.16	1.27	1.39
NGC 4151	11.80	−0.72	13.5	0	0.0033	0.74	7,d	28.37	28.69	24.76	1.39	1.51
NGC 4593	14.07	−0.03	15.4	0.01	0.0085	0.78	3,f	27.72	28.23	25.05	1.03	1.22
MCG 6-30-15	14.48	+0.16	22.9	0.03	0.0077	0.58	3,g	27.53	28.43	24.84	1.03	1.38
IC 4329A	14.88	+0.09	17.7	0.04	0.016	0.30	3,f	28.97	29.44	25.80	1.22	1.40
NGC 5548	13.56	−0.64	13.5	0	0.019	0.83	7,d	29.02	29.19	25.86	1.21	1.28
ESO 103-G35	15.02	−0.63	13.6	0.06	0.013	0.36	3,g	28.82	28.82	25.32	1.34	1.34
ESO 141-G55	13.30	−0.99	17.7	0.04	0.037	0.69	3,g	29.62	29.62	26.32	1.27	1.27
Mkn 509	12.42	−0.93	17	0.03	0.036	0.85	8,h	30.03	30.03	26.38	1.40	1.40
NGC 7213	13.12	+0.47	22.5	0	0.0059	0.95	3,i	—	—	24.51	—	—
NGC 7469	12.84	−0.72	13.5	0.04	0.017	0.58	7,d	29.71	29.71	25.65	1.56	1.56
MCG 2-58-22	14.30	−0.59	25	0.02	0.048	0.67	8,d	29.83	29.86	26.60	1.24	1.25

Note

Whenever similarly accurate photometric data at different apertures θ are available, we have preferred those with $\theta \cong 10''$ because smaller aperture data may require significant corrections for focusing, diffraction and seeing effects (*cf.* McAlary *et al.* 1983). In addition the mean effective aperture (de Vaucouleurs *et al.* 1976) of galaxies in the sample is also likely to be close to 10" so that the average aperture corrections to their intrinsic colours is probably small.

References for photometry and redshifts. 1. Markarian & Lipovetskii (1972). 2. Griersmith & Visvanathan (1979). 3. McAlary *et al.* (1983). 4. Doroshenko & Terebizh (1979). 5. Weedman (1973). 6. Fairall, McHardy & Pye (1982). 7. Zasov & Lyutyi (1973). 8. Stein & Weedman (1976). 8. Doroshenko & Terebizh (1981).

References for axial ratios. a. Hutchings *et al.* (1982). b. Su & Simkin (1980). C. Vorontsov-Velyaminov & Arhipova (1974). d. Keel (1980). e. Our estimate from the plate in Fairall *et al.* (1982). f. Simkin, Su & Schwarz (1980). g. Lauberts (1982). h. Lawrence & Elvis (1982). i. de Vaucouleurs *et al.* (1976).

(correlation coefficient $r = 0.62$), is suggested by the data. A least-squares fit gives $\langle\alpha\rangle = 1.29 + 0.13\ (\log l_o - 29.5)$ in the luminosity interval $28 \leqslant \log l_o \leqslant 30.4$ with a rms residual $\sigma = 0.13$. From equation (14) it then follows

$$\bar{\alpha} = 1.44 + 0.13\ (\log l_o - 29.5) \tag{19}$$

consistently above the results of Avni & Tananbaum (1982) and Zamorani (1982).

On the other hand, if equation (2) holds, any evidence of a correlation disappears (the correlation coefficient drops to $r = 0.15$) and from equation (14) we have $\bar{\alpha} = 1.47$.

4.2 THE SETTI & WOLTJER–VERON SAMPLE

Setti & Woltjer (1982) pointed out that X-ray observations are available for all but one of the Seyfert 1 nuclei brighter than $U_N \cong 15.1$ in the first five Markarian lists (Veron 1979). These objects then constitute a well-defined optically selected sample suitable for deriving an estimate of the distribution of α_{ox} largely free from X-ray selection effects. The relevant data are summarized in Table 2. There are two differences with respect to the sample originally analysed by Setti & Woltjer (1982): Mkn 291 has been omitted because better photometric data (McAlary *et al.* 1983) have shown that its apparent nuclear magnitude is well below the adopted limit; contrariwise, Mkn 279 has been added to the sample.

Soft X-ray data have been corrected for photoelectric absorption according to equation (8a); however, when the corrected luminosities exceeded the hard X-ray upper limits of Elvis *et al.* (1978), the nominal values of the latter were adopted. Uncorrected X-ray luminosities are also listed (in brackets) in Table 2. In the case of NGC 3516, for which no direct X-ray observations are available, we have used the conservative completeness limit of the *HEAO-1 A2* all sky survey (1.4 *R*15 counts; Piccinotti *et al.* 1982). Negligible

Table 2. The Setti & Woltjer-Veron sample.

Name	U	$U-B$	$\varepsilon^{(*)}$	$E(U-B)_g$	z	b/a	Refs.	$\log L_o$	$\log L'_o$	$\log L_x$	Refs.	α_{ox}	α'_{ox}
Mkn 9	14.49	−0.64	15	0.05	0.040	0.94	1,a	29.25	29.30	25.87 (25.44)	A	1.30	1.32
Mkn 10	14.48	−0.55	15	0.06	0.029	0.40	1,a	29.90	29.91	<25.83	B	>1.56	>1.57
Mkn 79	13.96	−0.78	10	0.07	0.022	0.69	2,a	29.34	29.34	25.67	C	1.41	1.41
Mkn 279	14.70	−0.45	15	0	0.031	0.68	1,a	29.17	29.40	26.06	C	1.19	1.28
Mkn 290	14.94	−0.62	15	0	0.031	0.86	1,b	28.84	29.01	26.08 (25.81)	A	1.06	1.12
Mkn 304	14.16	−0.86	17	0.02	0.067	–	3,–	30.06	30.04	25.83 (25.35)	A	1.62	1.62
Mkn 335	13.56	−0.70	15	0.02	0.025	0.80	1,a	29.40	29.51	25.57	D	1.47	1.51
Mkn 352	14.59	−0.66	15	0.02	0.015	0.67	1,b	28.84	29.04	25.50	A,B	1.28	1.36
Mkn 376	14.59	−0.58	10.1	0.09	0.056	0.68	4,a	30.05	30.01	26.56	B	1.34	1.33
Mkn 478	14.07	−0.84	10.1	0	0.079	0.85	4,b	30.12	30.09	<26.56	B	>1.37	>1.35
Mkn 486	14.53	−0.68	10.1	0	0.039	0.60	4,a	29.68	29.77	<25.24(<24.31)	A	>1.70	>1.74
Mkn 506	14.87	−0.55	17	0.04	0.043	0.73	4,a	29.47	29.59	26.07 (25.80)	A	1.30	1.35
NGC 3516	12.89	−0.23	24	0.02	0.0090	0.75	5,a	28.58	28.93	<25.01	E	>1.37	>1.50
NGC 4051	14.03	−0.33	10	0	0.0024	0.58	6,a	27.32	28.29	23.5	F,B	1.46	1.84
NGC 4151	11.80	−0.72	13.5	0	0.0033	0.74	6,a	28.37	28.69	24.76	E	1.39	1.51

Note
See note to Table 1.

References for photometry and redshifts. 1. Weedman (1973). 2. Dibai (1970). 3. Markarian & Lipovetskii (1972). 4. Khachikian & Weedman (1974). 5. de Vaucouleurs & de Vaucouleurs (1968). 6. Zasov & Lyutyi (1973).

References for axial ratios. a. Keel (1980). b. Adams (1977).

References for X-ray luminosities. (A) Kriss *et al.* (1980). (B) Elvis *et al.* (1978). (C) McHardy *et al.* (1981). (D) Dower *et al.* (1980). (E) Piccinotti *et al.* (1982). (F) Lawrence & Elvis (1982).

contamination $[a(U)\rightarrow\infty]$ and $E(U-B)_N = (U-B) - E(U-B)_g - (U-B)_N = 0.12$ have been assumed for Mkn 304, a stellar object for which no b/a is available.

Including the lower limits to α_{ox} at their nominal values and assuming α_{ox} to be uncorrelated with optical luminosity, we find $\bar{\alpha} = 1.454$, $\sigma = 0.185$, $\langle \log l'_o \rangle = 29.40$ if we allow for an increase of reddening with absolute magnitude [equation (2)], or $\bar{\alpha} = 1.39$, $\sigma = 0.16$, $\langle \log l_o \rangle = 29.225$, otherwise. The quoted values of $\bar{\alpha}$ may be somewhat underestimated as 4 out of the 15 values of α_{ox} we have used are actually lower limits. No significant evidence for a correlation of α_{ox} with luminosity is found in either case (correlation coefficient $r = -0.13$ or $r = 0.28$, respectively). The discrepancy with the result of Setti & Woltjer (1982), $\bar{\alpha} \cong 1.24$, is due to the fact that these authors have adopted the absolute nuclear magnitudes derived by Veron (1979) without allowing for internal reddening.

4.3 SERENDIPITOUS X-RAY SOURCES

The analysis of the available samples of optically indentified serendipitous X-ray sources (Grindlay *et al.* 1980; Chanan, Margon & Downes 1981; Kriss & Canizares 1982; Reichert *et al.* 1982) is complicated by the fact that their X-ray and optical limits are not well defined. Zamorani (1982) has found that the union of the first three samples quoted above shows clear signs of incompleteness for $S_x \leqslant 5 \times 10^{-31}$ erg cm^{-2} s Hz and for $B > 18$. Reichert *et al.* (1982) state similar completeness limits for their sample.

There are, in total, 32 objects within these limits. The data listed in the discovery papers, taken at face value, give $\langle \alpha_{ox} \rangle = 1.31$, $\langle \log l_0 \rangle = 29.67$. Although the majority of these objects have relatively low X-ray and optical luminosities and would probably need the corrections discussed in Section 2, we have not attempted to apply them since essential pieces of information such as $(U-B)$ colours and axial ratios are partially or totally lacking. Rather, we have tried to estimate the error in the above result by computing the average α_{ox} for the subset of 11 objects which are so luminous that such corrections are likely to be small ($\log l_o > 30$, $\log L_{SX} > 44$); we find: $\langle \alpha_{ox} \rangle = 1.39$, $\langle \log l_o \rangle = 30.51$.

On the other hand, if we insert the adopted optical and X-ray limits in equation (18) we find $\alpha_l = 1.36$, somewhat below our previous estimates of $\bar{\alpha}$; this suggests that the above values of $\langle \alpha_{ox} \rangle$ are significantly affected by the X-ray selection. Indeed, using the evolutionary models of Schmidt & Green (1983) and assuming $\bar{\alpha} = 1.55$, $\sigma = 0.15$ we would predict $\langle \alpha_{ox} \rangle$ to be in the range 1.38–1.4 for $\langle \log l_o \rangle \cong 30.5$.

4.4 THE SAMPLES OF KU *et al.* (1980) AND ZAMORANI *et al.* (1981)

The distribution of α_{ox} for active galactic nuclei in these samples has been analysed by several authors, using different approaches. As far as optical (as opposed to radio) quasars are concerned, the main results can be summarized as follows. Ku *et al.* (1980) obtained $\bar{\alpha} = 1.52 \pm 0.03$ for a composite sample including data from Tananbaum *et al.* (1979), Marscher *et al.* (1979) and Chanan *et al.* (1981) in addition to their own observations. Zamorani *et al.* (1981) did not explicitly estimate α (they rather computed $\alpha_{ox}^{\rm eff}$, corresponding to $\langle l_x/l_o \rangle$), but from the maximum likelihood probability distribution shown in their fig. 3 it follows $\bar{\alpha} \cong 1.6$. Both groups find an enhanced average α_{ox} for high redshift ($z > 1$) QSOs, the increase being significant at the 4 per cent confidence level, according to Zamorani *et al.* (1981); the results quoted by Ku *et al.* (1980), though formally of higher statistical significance, are likely to be biased by the inclusion in their sample of 26, mostly low z, X-ray selected nuclei.

Kembhavi & Fabian (1982) pointed out that to account for the sharp reduction in the detection rate of radio quiet QSOs above $V = 18$, $\bar{\alpha}$ must be $\geqslant 1.55$, a conclusion independently reached by Cavaliere *et al.* (1981b) as well, and suggested that a decrease of $\bar{\alpha}$ with increasing optical luminosity might also be required. On the other hand Setti & Woltjer (1982) pointed out that absolute magnitudes of detected objects are confined to $M_B > -26$ and $M_B < -29$, with a gap in between; the fast decrease of the detection rate with increasing apparent magnitude may then be understood as a consequence of the rather peculiar selection of the overall optical sample.

Confining ourselves to the sample of Zamorani *et al.* (1981), which has a considerably lower fraction of upper limits, we notice that all six sources with absolute luminosity in the range $30 < \log l_o < 30.75$ and seven out of 10 in the range $32.15 < \log l_o < 32.6$ have been detected. The corresponding average values of α_{ox}, treating upper limits as detections, and of $\log l_o$ are $\bar{\alpha} = 1.53$, $\langle \log l_o \rangle = 30.39$ and $\bar{\alpha} = 1.54$, $\langle \log l_o \rangle = 32.25$, respectively.

4.5 THE SAMPLE OF MARSHALL *et al.* (1983)

Marshall *et al.* (1983) have taken deep exposures with the *Einstein Observatory* of a complete sample consisting of 10 optically selected, faint ($B < 19.2$) QSOs, five of which have been detected. All objects have apparent magnitudes in the range $18.25 \leqslant B \leqslant 19.16$, with $\langle B \rangle = 18.77$. Inserting this value in equation (18), together with an estimated X-ray threshold $S_x = 10^{-31}$ erg cm^{-2} s^{-1} Hz^{-1} at 2 keV), we find that this sample is probing the distribution of α_{ox} below $\alpha_l \cong 1.52$, which is in fact close to the maximum α_{ox} (=1.58) of detected sources. A 50 per cent detection rate would then imply $\bar{\alpha} \cong \alpha_l \cong 1.52$. As a check of this result we can predict the average value of α_{ox} for detected sources on the assumption of a Gaussian distribution: $\langle \alpha_{ox} \rangle = \bar{\alpha} - (2/\pi)^{1/2}\sigma$. With $\bar{\alpha} = 1.52$ and $0.15 \leqslant \sigma \leqslant 0.2$ we have $1.4 \geqslant \langle \alpha_{ox} \rangle \geqslant 1.36$, in satisfactory agreement with the observed value, $\langle \alpha_{ox} \rangle = 1.35 \pm 0.08$.

5 Estimate of $\bar{\alpha}$ from source counts

The counts of optically selected QSOs in the apparent magnitude interval $15 \leqslant B \leqslant 19.5$ can be fitted by a power law (Braccesi *et al.* 1980; Schmidt & Green 1983):

$$N(>S_o) \propto \exp(-0.4aB_o)(S_o/\bar{S}_o)^{-a} \tag{20}$$

where $S_o = \bar{S}_o \exp(-0.4B)$ is the monochromatic flux at 2500 Å, $\bar{S}_o = 2.8 \times 10^{-20}$ erg cm^{-2} s Hz^{-1} (Schmidt 1968), $a \cong 2.25$ and $B_o \cong 18.5$.

If the ratio l_x/l_o does not depend on l_o, the X-ray counts will also obey a power law with the same slope in the flux density interval

$$S_{o\,\min}(\nu_x/\nu_o)^{-\bar{\alpha}} \leqslant S_x \leqslant S_{o\,\max}(\nu_x/\nu_o)^{-a} \tag{21}$$

where $S_{o\,\min}$ and $S_{o\,\max}$ are the optical fluxes corresponding to $B = 19.5$ and 15, respectively. Here and in the following we assume, for simplicity, the spectral indices in the optical and in the X-ray bands to be approximately equal. For a Gaussian distribution of α_{ox} we obtain (*cf.* also Cavaliere *et al.* 1981a):

$$N(>S_x) \propto \exp(-0.4aB)(S_x/\bar{S}_x)^{-a} \quad \text{sources square deg}^{-1} \tag{22}$$

with

$$\bar{S}_x = \bar{S}_o(\nu_x/\nu_o) - \bar{\alpha} + \frac{a}{2}\sigma^2 \ln(\nu_x/\nu_o). \tag{23}$$

It then follows

$$\bar{\alpha} - \tfrac{1}{2}\sigma^2 a \ln(\nu_x/\nu_o) = \frac{-\log S_x - \log[N(>S_x)]/a + \log \bar{S}_o - 0.4 B_o}{\log(\nu_x/\nu_o)}. \tag{24}$$

Using the results of the medium sensitivity survey (Maccacaro *et al.* 1982a), $N(>S_M) = 1.26$ sources square deg^{-1}; $S_M \cong 2.3 \times 10^{-31}$ erg cm^{-2} s^{-1} Hz^{-1}, we find

$$\bar{\alpha} - \tfrac{1}{2}\sigma^2 a \ln(\nu_x/\nu_o) = 1.40 \tag{25}$$

which, for $0.15 \leqslant \sigma \leqslant 0.20$, yields $1.55 \leqslant \bar{\alpha} \leqslant 1.67$. The data of the deep survey, $N(>S_E) \cong 19.2$ sources square deg^{-1}, $S_E = 5.3 \times 10^{-32}$ erg cm^{-2} s^{-1} Hz^{-1} (Giacconi *et al.* 1979) give essentially the same results: $1.59 \leqslant \bar{\alpha} \leqslant 1.67$.

6 Conclusions

The most striking outcome of the discussion in Sections 4 and 5 is that determinations of $\bar{\alpha}$ and σ from 5 independent samples, characterized by different selection criteria and covering different ranges of optical luminosity as well as from X-ray source counts, yield remarkably similar results. Actually all available data spanning over three orders of magnitude in optical luminosity seem to be consistent with $\bar{\alpha} \cong 1.55$, $\sigma = 0.15$ (*cf.* Fig. 3), implying that the apparent enhancement of the ratio l_x/l_o for Seyfert galaxies, emphasized by several authors (Setti & Woltjer 1982; Reichert *et al.* 1982; Zamorani 1982; Avni &

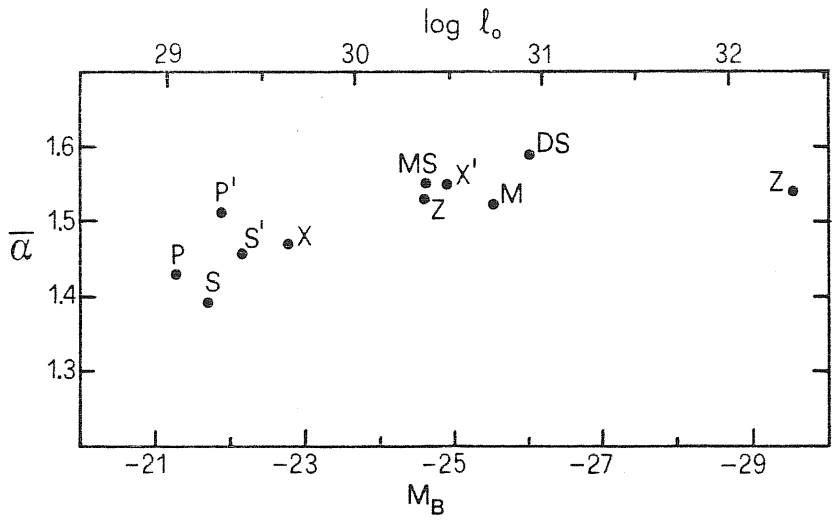

Figure 3. Estimates of $\bar{\alpha}$ from various samples. P and P': Piccinotti *et al.* (1982), assuming $\sigma = 0.15$; S and S': Setti-Woltjer–Veron; X and X': serendipitous X-ray sources; Z: Zamorani *et al.* (1981); M: Marshall *et al.* (1983); MS and DS: medium sensitivity and deep survey counts ($\sigma = 0.15$). The points labelled P' and S' have been obtained assuming a reddening correction increasing with magnitude according to equation (2); X' refers to the subsample of high luminosity serendipitous sources (see text).

Tananbaum 1982) might well be the effect of internal reddening. Note that neglecting the latter may easily lead to a serious underestimate of optical luminosities of Seyfert nuclei not only because the extinction correction may be quite large but also because the contribution of the underlying galaxy to the total magnitude, derived using the colour-given method, is overestimated.

Some residual evidence for a correlation between α_{ox} and l_o has been found only in the sample of Piccinotti *et al.* (1982). It is not unambiguous, however, as it entirely disappears if the reddening increases with decreasing optical luminosity in the way that some optical data already suggest (Cheng *et al.* 1983).

A still open problem is set up by the rather peculiar luminosity and redshift distributions of X-ray selected active galactic nuclei (*cf.* e.g. Margon *et al.* 1982), which have also been interpreted as indirect evidence for higher l_x/l_o at lower luminosities. An alternative explanation is suggested in Section 3: in the presence of the strongly luminosity dependent evolution which seem to be required by optical data (Schmidt & Green 1983), the effect of the X-ray threshold is, in turn, luminosity dependent (*cf.* Fig. 1) and becomes particularly severe just for $M_B \simeq -26$. This view is somewhat supported by the finding (Section 4) that the average α_{ox} for X-ray selected sources is consistent with the global value of $\bar{\alpha}$. It remains to be seen, however, whether the redshift and luminosity distributions can be matched in detail. Work on this problem is under way.

Acknowledgments

GDZ thanks the Institute of Astronomy, University of Cambridge and especially Professors M. Rees and A. Fabian for their generous hospitality. He acknowledges useful discussions with Professor A. Fabian, Drs M. Gaskell and A. Lawrence. We are indebted to the referee for comments that helped to improve the presentation of the paper. Work supported in part by the National Research Council of Italy through grant PSN 81-037.

References

Adams, T. F., 1977. *Astrophys. J. Suppl.*, **33**, 19.
Avni, Y. & Tananbaum, H., 1982. *Astrophys. J.*, **262**, L17.
Braccesi, A., Zitelli, V., Bonoli, F. & Formiggini, L., 1980. *Astr. Astrophys.*, **90**, L10.
Burstein, D. & Heiles, C., 1982. *Astrophys. J.*, **87**, 1165.
Cavaliere, A., Danese, L., De Zotti, G. & Franceschini, A., 1981a. *Astr. Astrophys.*, **97**, 269.
Cavaliere, A., Danese, L., De Zotti, G. & Franceschini, A., 1981b. *Space Sci. Rev.*, **30**, 101.
Chanan, G. A., Margon, B. & Downes, R. A., 1981. *Astrophys. J.*, **243**, L5.
Cheng, F. Z., Danese, L. & De Zotti, G., 1983. *Mon. Not. R. astr. Soc.*, **204**, 13P.
de Vaucouleurs, G. & de Vaucouleurs, A., 1968. *Astr. J.*, **73**, 858.
de Vaucouleurs, G. & de Vaucouleurs, A., 1972. *Mem. R. astr. Soc.*, **77**, 1.
de Vaucouleurs, G., de Vaucouleurs, A. & Corwin, H., 1976. *Second Reference Catalogue of Bright Galaxies*, University of Texas Press, Texas.
Dibai, E. A., 1970. *Astrofiz.*, **6**, 350 (*Astrophysics*, **6**, 185).
Doroshenko, V. T. & Terebizh, V. Yu., 1979. *Pis'ma Astr. Zh.*, **5**, 571 (*Soviet Astr. Letters*, **5**, 305).
Doroshenko, V. T. & Terebizh, V. Yu., 1980. *Astrofiz.*, **16**, 393.
Doroshenko, V. T. & Terebizh, V. Yu., 1981. *Astrofiz.*, **17**, 667 (*Astrophysics*, **17**, 358).
Dower, R. G., Griffiths, R. E., Bradt, H. V., Doxsey, R. E. & Johnston, M. D., 1980. *Astrophys. J.*, **235**, 355.
Elvis, M., Maccacaro, T., Wilson, A. S., Ward, M. J., Penston, M. V., Fosbury, R. A. E. & Perola, G. C., 1978. *Mon. Not. R. astr. Soc.*, **183**, 159.
Fairall, A. P., McHardy, I. M. & Pye, J. P., 1982. *Mon. Not. R. astr. Soc.*, **198**, 13P.
Giacconi, R., Bechtold, J., Branduardi, G., Forman, W., Henry, J. P., Jones, C., Kellogg, E., van der Laan, H., Liller, W., Marshall, H., Murray, S. S., Pye, J., Schreier, E., Sargent, W. L. W., Seward, F. & Tananbaum, H., 1979. *Astrophys. J.*, **234**, L1.

Grandi, S. A., 1983. *Astrophys. J.*, **268**, 591.
Griersmith, D. & Visvanathan, N., 1979. *Astr. Astrophys.*, **79**, 329.
Grindlay, J. E., Steiner, J. E., Forman, W. R., Canizares, C. R. & McClintock, J. E., 1980. *Astrophys. J.*, **239**, L43.
Hutchings, J. B., Crampton, D., Campbell, B., Gower, A. C. & Morris, S. C., 1982. *Astrophys. J.*, **262**, 48.
Keel, W. C., 1980. *Astrophys. J.*, **85**, 198.
Kembhavi, A. K. & Fabian, A. C., 1982. *Mon. Not. R. astr. Soc.*, **198**, 921.
Khachikian, E. Ye & Weedman, D. W., 1974. *Astrophys. J.*, **192**, 581.
Kriss, G. A. & Canizares, C. R., 1982. *Astrophys. J.*, **261**, 51.
Kriss, G. A., Canizares, C. R. & Ricker, G. R., 1980. *Astrophys. J.*, **242**, 492.
Ku, W. H. M., Helfand, D. J. & Lucy, L. B., 1980. *Nature*, **288**, 323.
Lauberts, A., 1982. *The ESO/Uppsala Survey of the ESO(B) Atlas*, ESO publications, Garching.
Lawrence, A. & Elvis, M., 1982. *Astrophys. J.*, **256**, 410.
Maccacaro, T., Feigelson, E. D., Fener, M., Giacconi, R., Gioia, I. M., Griffiths, R. E., Murray, S. S., Zamorani, G., Stocke, J. & Liebert, J., 1982a. *Astrophys. J.*, **253**, 504.
Maccacaro, T., Perola, G. C. & Elvis, M., 1982b. *Astrophys. J.*, **257**, 47.
Margon, B., Chanan, G. A. & Downes, R. A., 1982. *Astrophys. J.*, **253**, L7.
Markarian, B. E. & Lipovetskii, V. A., 1972. *Astrofiz.*, **8**, 155 (*Astrophysics*, **8**, 89).
Marscher, A. P., Marshall, F. E., Mushotzky, R. F., Dent, W. A., Balonek, T. J. & Hartman, H. F., 1979. *Astrophys. J.*, **233**, 498.
Marshall, H. L., Tananbaum, H., Zamorani, G., Huchra, J. P., Braccesi, A. & Zitelli, V., 1983. *Astrophys. J.*, **269**, 42.
McAlary, C. W., McLaren, R. A., McGonegal, R. J. & Maza, J., 1983. *Astrophys. J., Suppl.*, **52**, 341.
McHardy, I. M., Lawrence, A., Pye, J. P. & Pounds, K. A., 1981. *Mon. Not. R. astr. Soc.*, **197**, 893.
Mushotzky, R. F., 1982. *Astrophys. J.*, **256**, 92.
Piccinotti, G., Mushotzky, R. F., Boldt, E. A., Holt, S. S., Marshall, F. E., Serlemitsos, P. J. & Shafer, R. A., 1982. *Astrophys. J.*, **253**, 485.
Reichert, G. A., Mason, K. O., Thorstensen, J. R. & Bowyer, S., 1982. *Astrophys. J.*, **260**, 437.
Richstone, D. E. & Schmidt, M., 1980. *Astrophys. J.*, **235**, 377.
Sandage, A., 1973. *Astrophys. J.*, **180**, 687.
Savage, B. D. & Mathis, J. S., 1979. *A. Rev. Astr. Astrophys.*, **17**, 73.
Schmidt, M., 1968. *Astrophys. J.*, **151**, 393.
Schmidt, M. & Green, R. F., 1983. *Astrophys. J.*, **269**, 352.
Setti, G. & Woltjer, L., 1982. *Astrophysical Cosmology*, eds. Brück, H. A., Coyne, G. V. & Longair, M. S., p. 315, Pontificiae Academiae Scientiarum Scripta Varia, Città del Vaticano.
Simkin, S. M., Su, H. J. & Schwarz, M. P., 1980. *Astrophys. J.*, **237**, 404.
Soifer, B. T. & Neugebauer, G., 1981. *IAU Symp. 96, Infrared Astronomy*, eds. Wynn-Williams, C. G. & Cruikshank, D. P., p. 329, Reidel, Dordrecht, Holland.
Stein, W. A. & Weedman, D. W., 1976. *Astrophys. J.*, **205**, 44.
Su, H. J. & Simkin, S. M., 1980. *Astrophys. J.*, **238**, L1.
Tananbaum, H., Avni, Y., Branduardi, G., Elvis, M., Fabbiano, G., Feigelson, E., Giacconi, R., Henry, J. P., Pye, J. P., Soltan, A. & Zamorani, G., 1979. *Astrophys. J.*, **234**, L9.
Tananbaum, H., Peters, G., Forman, W., Giacconi, R., Jones, C. & Avni, Y., 1978. *Astrophys. J.*, **223**, 74.
Veron, P., 1979. *Astr. Astrophys.*, **78**, 46.
Vorontsov-Velyaminov, B. A. & Arhipova, V. P., 1974. *Morfologiceskii Katalog Galaktik. Vol. V*, Moscow State University, Moscow.
Weedman, D. W., 1973. *Astrophys. J.*, **183**, 29.
Weinberg, S., 1972. *Gravitation and Cosmology*, Wiley, New York.
Zamorani, G., 1982. *Astrophys. J.*, **260**, L31.
Zamorani, G., Henry, J. P., Maccacaro, T., Tananbaum, H., Soltan, A., Avni, Y., Liebert, J., Stocke, J., Strittmatter, P. A., Weymann, R. J., Smith, M. G. & Condon, J. J., 1981. *Astrophys. J.*, **245**, 357.
Zasov, A. V. & Lyutyi, M. V., 1973. *Astr. Zh.*, **50**, 233 (*Soviet Astr.*, **17**, 169).

CHAPTER V THE OPTICAL LUMINOSITY FUNCTION OF SEYFERT 1 NUCLEI

Review

The luminosity function is defined as the number density of sources as function of their absolute luminosity. Several estimates of Seyfert optical luminosity function are already in the literature (Sargent 1972; Huchra and Sargent 1973; Sramek and Weedman 1978; veron 1979; Terebizh 1980; Meurs 1982). Since most of the Seyfert galaxies have redshift $Z \leqslant 0.1$, they were considered as sources which are uniformly distributed in an Euclidean space.

Sargent (1972) used only 8 Seyfert (with $m_p \leqslant 16.5$) from the first two Markarian lists, assuming H_o = 75 km/s/mpc and found that the space density of very luminous Seyfert galaxies is about 1.3×10^{-6} mag^{-1} at $M_p = -21$. On the basis of the V/V_{max} test, devised by Schmidt (1968), he has shown that the markarian survey is complete to about $m_{pg} = 15.5$; at $m_{pg} = 16.5$ the sample appears to be incomplere by roughly a factor of 5. This work was extended by Huchra and Sargent (1973) to include 31 Seyfert galaxies (with $m_p \leqslant 15.5$) from the first four Markarian lists. Fig. 61 illustrates their results. They pointed out that at $M_p = -23$ essentially all galaxies are Markarian Seyfert galaxies.

These authors have built the luminosity function of Seyfert galaxies, using the total (nucleus plus underlying galaxy) luminosity. As described in Chapter I and II, Sy 1 is a more or less normal spiral galaxy plus a bright, compact, often variable nucleus with a strong UV excess. When the nucleus is much brighter than the underlying galaxy, the total luminosity is about equal to that of the nucleus; but; when the nucleus is faint, the luminosity is that of the galaxy. Moreover, as we know, Sy 1 nuclei have nonthermal spectra, while the underlying galaxies, normal spirals, have essentially black-body spectra. Particularly, in the V band, the luminosity of Sy 1 nucleus is contaminated by the underlying galaxies. This point was particularly stressed by Veron (1979) who obtained a preliminary estimate of the luminosity function of Seyfert nuclei using the "colour-given"

method (Sandage 1973) to estimate the nuclear magnitudes of Seyfert 1's in the first 5 Markarian lists of Fig. 62.

Sramek & Weedman (1978) have used the fluxes of hydrogen emission line H_β, F_β, as luminosity indicators to build the luminosity function of local QSOs and Sy 1 nuclei, since the emission lines are not contaminated by starlight from any galactic envelope. Data of the fluxes of Sy 1 nuclei, F_β, come from the paper by Weedman (1976). The results are given by Table 9.

Terebizh's (1980) much larger sample included 121 Seyferts but was less homogeneous. Besides Seyfert galaxies in the first 11 Markarian lists, his sample contained, for example, Seyferts from the 3C and 4C radio source catalogues as well.

Meurs (1982) used a sample of 90 Seyferts to build luminosity functions. Of those objects, 86 Seyferts come from the first 9 lists of Markarian survey, 4 from Zwicky catalogues.

Meurs pointed out that the Markarian Seyferts surely is imcomplete both at faint and bright apparent magnitudes (Fig. 63); it seems to be rather complete in the range $m_p \sim 14 \div 15$. The incompleteness at faint magnitudes is obviously due to the greater difficulty in recognizing Seyferts; on the other hand, objects brighter than $m_p = 13$ have usually been omitted from Markarian lists (Markarian 1967).

MEurs estimates of luminosity function of Seyferts are given in Table 10 and Fig. 64.

Meurs also presented a comparison of the Seyfert luminosity function with those of other objects of interest (see Fig. 65), field galaxies (Felten 1977), optically selected QSOs (local) (Braccesi et al 1980), Markarian galaxies in general (Huchra and Sargent 1973) and Markarian Seyfert galaxies (meurs 1982). According to Fig. 65, the Seyfert galaxies comprise about 8% of all Markarian galaxies between $M_{B(0)} = -20 \div -21$. This fraction increases to about 20% between $M_{B(0)} = -21 \div -22$. At $M_{B(0)} > -22$ nearly all the field galaxies are Markarian Seyferts.

Altogether the Seyferts comprise 1.1% of all galaxies with the same absolute magnitudes.

The Seyfert galaxies luminosity function shows an interesting behaviour at its bright end. It does not fall off as fast as the field galaxy curve, but is considerably flattened and seems to join the luminosity function for local QSOs.

All the estimates mentioned above have some planes (cf. Cheng et al. 1984). A new derivation of the local luminosity function of Seyfert 1 nuclei, incorporating corrections for previouslu overlooked biases is presented in the next section.

ecf418gz4

THE OPTICAL LUMINOSITY FUNCTION OF SEYFERT 1 NUCLEI

Cheng Fu-zhen[1,2], L. Danese[3], G. De Zotti[3,4] and A. Franceschini[3]

[1] I.S.A.S., Strada Costiera 11, I-34014 Trieste, Italy

[2] Center for Astrophysics, University of Science and Technology of China, Hefei, Anhui, China*

[3] Istituto di Astronomia, Vicolo dell'Osservatorio, 5, I-35100 Padova, Italy*

[4] ESO, Karl-Schwarzschild-Str. 2, D-8046 Garching bei München, FRG

Proofs to: Dr. L. Danese

* Permanent address

Summary

We have collected from the literature all confirmed Seyfert 1 and 1.5 galaxies in the area covered by the first nine Markarian lists and we have estimated their nuclear magnitudes in two independent ways. We have then defined a "homogeneous" subsample suitable for deriving the luminosity function with the method described by Neyman & Scott (1974). Our derivation incorporates corrections for incompleteness, for random errors in the nuclear magnitudes and for the effect of binning. The resulting luminosity function matches remarkably well that of optically selected QSOs at $M_B=-23$ ($H_o=50$), flattens out somewhat at $M_B=-21.5$, but does not show clear evidence of a leveling off down to $M_B=-18$; it also compares very favourably with the local luminosity function of X-ray selected active galactic nuclei. Our results agree with those of previous investigations for $M_B>-20$; at higher luminosities we differ from some recent estimates by factors of up to ten.

1. Introduction

Any attempt to determine the local luminosity function of Seyfert nuclei faces with several serious difficulties. The first one concerns the estimate of nuclear magnitudes themselves, given that observations include contributions from the host galaxies, which may be dominant when nuclei are not particularly bright. The second is related to the definition of a suitable sample, i.e. of a sample whose incompleteness is fully understood and can be properly taken into account. A third difficulty follows from the fact that the, presumably large, errors associated with the estimated magnitudes may seriously affect the luminosity distributions (Eddington 1913); a detailed appraisal of the amplitude of uncertainties is needed to evaluate the appropriate corrections.

The aim of this paper is to improve over previous investigations by carefully taking into account all the problems listed above, which have been, at least partly, overlooked so far. Special care has been taken to minimize the effect of each source of errors and to obtain reliable estimates of the overall uncertainties on nuclear magnitudes.

The plan of the paper is the following. In Section 2 we present the sample we have used. Section 3 deals with the problem of estimating nuclear magnitudes. In Section 4 we describe our procedure for deriving the luminosity function. In Section 5 we discuss our results and we compare them with those of previous investigations.

2. The sample

We have confined ourselves to Seyfert 1 and 1.5 galaxies (as defined by Weedman (1977) and Osterbrock (1977)), which apparently have fundamentally uniform properties. In fact, there are probably no "pure" Seyfert 1 galaxies, without narrow components of the permitted lines, and the broad lines of type

1.5 objects are very similar to those of type 1 in luminosity, equivalent widths and line ratios (Cohen 1983). In addition, an analysis of the data compiled by Cheng, Danese & De Zotti (1983b) and Lawrence and Elvis (1982) shows that the two Seyfert types have very similar distributions of broad-band colours and of X-ray to optical luminosity ratios. Hence the spectra of the nuclear emissions must also be similar, consistently with Shuder's (1981) result that a power law ionizing continuum with approximately constant slope accounts for the emission line spectra of a wide class of active nuclei.

On the other hand, the relationships with Seyfert 1's of Seyfert types 1.8, 1.9, and 2, of emission line radio-galaxies and of "Liners" is not clear, at least to us; thus, we have chosen not to include these objects in our sample.

As is well known, the primary source of Seyferts is the Markarian survey. In particular, extensive spectrophotometric studies have been carried out of Seyfert candidates in the first nine Markarian lists (Markarian 1967, 1969 a,b; Markarian & Lipovetskii 1971, 1972, 1973, 1974, 1976 a,b) so that there is a good chance that most, if not all, Seyfert 1 and 1.5 have been identified.

Shown in Fig. 1 is our subjective definition of the boundaries of the region covered by the first 9 Markarian lists and the distribution in galactic coordinates of all objects in our sample. The area of this region is 3.39 sr, or $1.11\ 10^4$ sq. deg. In the following, however, we will employ an effective solid angle, Ω, incorporating a correction for the fact that, due to the absorption within our own galaxy, the limiting magnitude is a function of the direction (Kiang 1976; Felten 1976). Using the extinction law of de Vaucouleurs and Buta (1983) we find $\Omega=1.86$ for the U band and $\Omega=2.01$ for the B band.

We have collected from the literature (up to the end of 1983), and included in our sample, all objects lying in this area and classified as

Seyfert 1 or 1.5 on the basis of reasonably high quality spectra; we have omitted all objects referred to as possibly or probably being Seyfert 1's.

Altogether our sample comprises 88 objects, 68 of which have been discovered during the Markarian survey (one of them, however, belongs to the 10th list and a second one to the 14th (Markarian, Lipovetskii & Stepanian 1977, 1979)). Of the remaining 20, 12 are relatively nearby galaxies which compensate for the fact that bright galaxies were systematically excluded from Markarian lists (Markarian 1967) and 5 come from Zwicky lists of compact galaxies. UBV photometry for all but four of these objects is available in the literature.

The relevant data on our sample are given in Table 1, whose content is mostly self-explanatory. We need only to add that, whenever a choice has been possible, we have normally selected the smallest aperture photometry. The index C stands for "combination", i.e.: nucleus + galaxy. The reddening within our own galaxy, $E(B-V)_g$, has been deduced, for each object, from the maps of Burstein & Heiles (1982).

3. Estimates of nuclear magnitudes

A successful method for separating the nuclear and the host galaxy contributions to observed magnitudes, referred to as the "colour-given" method, has been devised by Sandage (1973). It is based on the assumption that both the nuclei and the surrounding galaxies have all approximately the same intrinsic colours so that the observed colours directly reflect the luminosity ratios. Details on our application of this method are given in sub-section 3.2. In sub-section 3.3 we compare the nuclear magnitudes derived using the colour-given method with those obtained subtracting out the contribution of an appropriate template galaxy ("galaxy-given" method). Our choice for the parameters characterizing the galaxies hosting Seyfert 1 nuclei is justified in the next sub-section.

Note that all distance-dependent quantities have been converted to H_o=50 km s^{-1} Mpc^{-1}.

3.1 Properties of host galaxies

It has long been known that the overwhelming majority of Seyfert nuclei reside in spiral, or SO, galaxies (de Vaucouleurs 1974; Adams 1977; Heckman 1978). The nearby Seyfert 1 galaxies of Simkin, Su & Schwarz (1980) which have revised type T listed in the Second Reference Catalog (de Vaucouleurs, de Vaucouleurs & Corwin 1976) are distributed over $0 \leq T \leq 4$ with a peak at T=1÷2. The multicolour surface photometry of 20 Markarian Seyferts by Yee (1983) has shown that the colours of the underlying galaxies are comparable to those of normal spirals in the range Sa to Sbc; in fact disregarding objects with uncertain colour, the average B-V of his galaxies hosting a Seyfert 1 nucleus is ≈0.7.

In view of the above, we assume as typical the effective aperture colours of Sa/Sab galaxies, reduced to face-on (de Vaucouleurs & de Vaucouleurs 1972):

$$(B-V)_{G,0} = 0.7 \quad , \quad (U-B)_{G,0} = 0.1 \qquad (1)$$

As for the total absolute magnitude of the template galaxy we have taken

$$M_B = -21 \ , \qquad (2)$$

which is the average magnitude of galaxies with Seyfert 1 nuclei in Yee's (1983) sample and almost coincides with Holmberg's (1975) determination of the mean absolute magnitude of Sa-Sb galaxies. Also, the above value of M_B is

close to the average magnitude of galaxies underlying the low redshift, X-ray selected quasars of Malkan, Margon & Chanan (1984), $M_B \simeq -21.45$ (correcting the quoted disk magnitudes by -0.4 mag. to take into account the contribution from the bulge), and to the average magnitude of galaxies with $0 \leq T \leq 4$ in Boroson's (1981) sample, $M_B \simeq -21.35$.

The median scale length of exponential disks of the Seyfert galaxies studied by Yee (1983) is, omitting the objects with very uncertain disk parameters, r_o=6 kpc, in good agreement with the median values of r_o for the galaxies with $0 \leq T \leq 4$ in the samples of Schweizer (1976), r_o=5.2 kpc, and Boroson (1981) r_o=6.6 kpc (after correcting for the distance scale).

If we assume an average bulge-to-disk luminosity ratio =0.5 (the average value for galaxies in the Boroson (1981) sample) the effective diameter D_e (i.e. the diameter of the isophote enclosing half the total flux) is

$$D_e \simeq 2\, r_o \simeq 12 \text{ kpc} . \qquad (3)$$

The above value of D_e, the magnitude-aperture curves of de Vaucouleurs (1977) and the colour-aperture curves of de Vaucouleurs & Corwin (1977) for T=2, have been used to estimate the aperture corrections for each object in our sample.

The face-on colours have been converted into those appropriate for a galaxy of inclination i using the relations given by de Vaucouleurs & de Vaucouleurs (1972):

$$E(B-V)_{G,i} = -0.25 \log(b/a) \qquad (4)$$

$$E(U-B)_{G,i} = -0.5 \log(b/a) \qquad (5)$$

where b/a is the axial ratio.

Finally we have adopted the K-corrections, $K(B-V)_G$ and $K(U-B)_G$, for Sab galaxies given by Pence (1976).

3.2 The colour-given method

As shown by Sandage (1973) the ratio of the intensity of the nucleus to that of the galaxy, within a given aperture, can be inferred from the observed colours, $(U-B)_C$ or $(B-V)_C$, if the intrinsic colours of the two components are known. For example, the intensity ratio in the B band is given by:

$$a_B = \frac{I_N(B)}{I_G(B)} = \frac{1-\mathrm{dex}\{0.4[(B-V)_G - (B-V)_C]\}}{\mathrm{dex}\{0.4[(B-V)_N - (B-V)_C]\} - 1} \qquad (6)$$

where

$$(B-V)_G = (B-V)_{G,0} + E(B-V)_g + E(B-V)_{G,i} + K(B-V)_G \qquad (7)$$

$$(B-V)_N = (B-V)_{N,0} + E(B-V)_g + E(B-V)_{N,i} \quad . \qquad (8)$$

The corrections for reddening within our own galaxy, $E(B-V)_g$, are given for each object in Table 1. The other terms in the right-hand side of eq. (7) are discussed in the previous sub-section.

We have attributed to the nuclei the intrinsic colours

$$(B-V)_{N,0} = 0 \quad , \quad (U-B)_{N,0} = -1 \quad , \qquad (9)$$

which correspond to the blue limits of the colour distributions of Seyfert 1 galaxies (Khachikian & Weedman 1974; cf. also Sandage 1973).

Their reddening within the host galaxy has been estimated using the formula derived by Cheng, Danese & De Zotti (1983a):

$$E(B-V)_{N,i} = \begin{cases} 0.25\ (a/b - 1) + 0.15 & \text{for } a/b < 4 \\ 0.9 & \text{for } a/b \geq 4 \end{cases} \qquad (10)$$

Since the nuclear continuum is apparently well represented by a power law over the frequency range of interest here the effect of redshift on nuclear colours (K-correction) has been neglected.

Given the luminosity ratio a_B, the nuclear B magnitude follows from the equation

$$B_N = B_C + 2.5 \log(1 + 1/a_B) \ . \qquad (11)$$

Of course this method works properly if the observed colour is redder than that of the nucleus and bluer than that of the galaxy. Whenever $(B-V)_C \leq (B-V)_N$ we have neglected the contribution from the galaxy (i.e. we have taken $B_N = B_C$. If $(B-V)_G \leq (B-V)_C$, the method cannot be applied.

The nuclear U magnitudes, U_N, have been computed in a strictly analogous way. The nucleus-to-galaxy intensity ratio a_U has been derived from eq. (6) after having replaced (B-V) with (U-B); $E(U-B)_g$ and $E(U-B)_{N,i}$ have been obtained multiplying the corresponding E(B-V) by 0.75.

3.3 Results and error estimates

Listed in Table 2 are the nuclear U and B magnitudes of all objects in our sample, derived using the colour-given method and the observed (U-B) or (B-V) colours, respectively. Also given there are the independent estimates

obtained subtracting out from the observed fluxes the expected contributions from the template galaxy defined in sub-section 3.1, computed taking into account aperture, inclination and K-corrections ("galaxy-given" method). Of course the latter method could not be applied for the few objects whose total (i.e. nucleus + galaxy) observed luminosity is lower than that of our template galaxy.

As a first consistency check, we have compared the colour-given nuclear magnitudes relying on (U-B) colours with those relying on (B-V) colours. Disregarding the nuclei with $U_N > 16.5$ or $M_U > -18$ (both limits being appreciably looser than those defining the final sample used to construct the luminosity function, cf. Sect. 5) we find an average difference $\simeq 0.14$ mag. with a dispersion of $\simeq 0.4$ mag.

A comparison with the results of the galaxy-given method yields, again for U_N (colour-given) < 16.5, M_U (colour-given) < -18: $\langle U_N$ (colour-given) $-$ U_N (galaxy-given) $\rangle \simeq 0.03$ with a dispersion $\sigma \simeq 0.36$. Similarly, for $B_N < 17$, $M_B < -18$ we find: $\langle B_N$ (colour-given) $- B_N$ (galaxy-given) $\rangle \simeq -0.06$ with a dispersion $\sigma \simeq 0.4$.

As a third test, we have compared the nuclear magnitudes deduced using the colour-given method with those derived by Yee (1983), for 11 Seyfert 1 galaxies, on the basis of detailed multicolour surface photometry. To this end we have used Yee's vgr magnitudes integrated within a 10" diameter aperture (except for Mkn 374 whose v-g colour is too red to permit the application of the colour-given method; its nuclear magnitude has been estimated from the U-B colour in Table 1); conversions to the UBV system have been done following Thuan & Gunn (1976). We find: $\langle B_N$ (colour-given) $- B_N$ (Yee) $\rangle = -0.09$ with a dispersion $\sigma = 0.47$.

The above results are reassuring about the general validity of the colour-given method; they also indicate that the rms errors on estimated

nuclear magnitudes are ≈0.5 mag. in the B band and somewhat smaller (≈0.4 mag., say) in the U band, where the nuclei are more prominent.

4. Derivation of the luminosity function

4.1 Definition of a "homogeneous" sample

The problem of deriving a luminosity function, up to a multiplicative constant, from an incomplete sample, as Markarian's notoriously is, has been solved by Neyman & Scott (1961, 1974) under the assumption that it is possible to construct a "homogeneous" sub-sample such that the probability for an object to be included in it depends solely on apparent magnitude.

We expect that the sample listed in Table 1 is plagued by at least two sources of "inhomogeneity":

1) when the luminosity of the nucleus is too low in comparison with that of the surrounding galaxy, its Seyfert properties may go unnoticed;
2) at the opposite extreme, distant objects whose nuclei are particularly prominent may appear starlike and as such be excluded from the Markarian lists.

The luminosity distribution of objects in Table 1 suggests that the first effect is important for $M_B \leq -18$.

As for the second effect, an inspection of Schmidt & Green (1983) Table 1 indicates that the fraction of objects showing an associated nebulosity on the prints of the Palomar Sky Survey Atlas drops rapidly above $z=0.07 \div 0.08$. Indeed, the redshift distribution of the highest luminosity nuclei ($-24 \leq M_B \leq -23$) in our Table 1 shows a clear deficiency at $z \geq 0.08$. There are no objects in the range $0.08 \leq z \leq 0.11$ while at least 8 ± 3.6 are expected on the basis of the observed number for $z<0.08$, assuming a uniform distribution and $B_{lim}=16$; in fact there are 6 quasars with $-23 \geq M_B \geq -24$ and $B<16$ in the

Schmidt and Green (1983) sample, which covers a smaller area and also excludes objects whose starlike component is not dominant.

It has been proven by Neyman & Scott (1961) that a necessary condition for a sample to be "homogeneous" is that the apparent and the absolute magnitudes of objects are mutually independent. In a strictly analogous way it can be proven that the apparent magnitudes must also be uncorrelated with the ratio a (eq. (6)) between the luminosities of the nucleus and of the host galaxy, and with the axial ratio b/a.

To test the hypothesis of no correlation we have computed Kendall's τ and Spearman's r rank-order correlation coefficients for several assumed limiting magnitudes. As is well known (cf., e.g., Siegel 1956) τ has a Gaussian distribution with mean zero and standard deviation

$$\sigma_K = \left[\frac{4\,N + 10}{9\,N\,(N-1)}\right]^{1/2}, \qquad (12).$$

N being the number of data points.

As an example, we give in Table 3 the values of τ/σ_K measuring the significance of correlations between the apparent U magnitudes of the nuclei, derived with the colour-given method, and the absolute magnitude M_U, the intensity ratios a_U and the axial ratios b/a (the Spearman's rank test yields essentially the same results). It can be seen that if we confine ourselves to $-18.5 > M_U \geq M_c$, with

$$M_c = U_{lim} - 5 \log z_c - 43.89 \qquad (13)$$

and $z_c = 0.08$ or 0.07, it is possible, by suitably choosing U_{lim}, to define subsamples for which all τ/σ_K are appreciably smaller than 2, so that correlations are only marginally significant.

(The significance of the correlations is considerably higher for the unrestricted sample, as a consequence of its larger "inhomogeneity".)

Similar conclusions hold for the B band, too.

4.2 Corrections for incompleteness

After having defined a reasonably "homogeneous" subsample, we can proceed to estimate the corrections for incompleteness following the procedure described by Neyman & Scott (1974).

If the space density is uniform, the luminosity distribution $\eta(M)$ (giving the number of objects of absolute magnitude M per unit dM) is related to the luminosity function $\Psi(M)$ by

$$\eta(M) = \frac{\Omega}{4\pi} V_e(M,m_1)\Psi(M) \qquad (14)$$

where Ω is the effective solid angle covered by the survey (see Sect. 2), m_1 is the limiting apparent magnitude,

$$V_e(M,m_1) = \int_{-\infty}^{m_1} dm \frac{dV}{dm} p(m) \quad , \qquad (15)$$

p(m) is the probability of inclusion in the sample (which is a function only of the apparent magnitude for "homogeneous" samples) and

$$\frac{dV}{dm} = \frac{4\pi}{3} 0.6 \ln 10 \, \mathrm{dex}\,[0.6(m-25-M)] \quad \mathrm{Mpc}^3 \qquad (16)$$

is the Euclidean volume element.

Following Terebizh (1980) we approximate p(m) with the ratio of the observed counts to those expected in the case of a uniform space distribution:

$$p(m) = \frac{n_{obs}(m)}{n_{un}(m)} = \frac{n_{obs}(m)}{n_{un}(m_1)} \text{ dex } [0.6(m_1-m)] \qquad (17)$$

where m_1 is some reference apparent magnitude.

Substituting (16) and (17) into (15) we find

$$V_e(M,m_1) = V(M,m_1) \frac{N_{obs}(<m_1)}{N_{un}(<m_1)} \qquad (18)$$

where $V(M,m_1)$ is the accessible volume:

$$V(M,m_1) = \frac{4\pi}{3} \text{ dex } [0.6(m_1-25-M-A)] \text{ Mpc}^3 \ , \qquad (19)$$

A being the extinction within our own galaxy.

Note that the correction for incompleteness does not affect the shape of the luminosity function but simply amounts to a multiplicative factor, $F_i=N_{un}/N_{obs}$. It is thus mistaken to apply corrections depending on the apparent magnitude as it has been done in some recent investigations.

applied, following Huchra & Sargent (1973), the V/V_{max} test (Schmidt 1968) succes sively increasing the assumed limiting magnitude m_1 in steps of 0.05 mag. starting at U = 14 or B = 14.8; whenever $\langle V/V_{max} \rangle < 0.5$ (the value appropriate for a uniform distribution in an Euclidean space) we have added at the limiting magnitude the integer number of objects that brings $\langle V/V_{max} \rangle$ closest to 0.5.

In the presence of a redshift cutoff, z_c, the upper limit to m_1 is the minimum between the limiting magnitude defining the sample, m_{lim}, and

$$m_c = M + 5 \log z_c + 43.89 \ . \qquad (20)$$

As a consequence F_i is, in general, a function of absolute magnitude.

4.3 The effect of errors on the luminosity distribution

Because of the errors affecting the estimated nuclear magnitudes (we neglect errors in the distances), the observed luminosity distribution may be considerably different from the true one (Eddington 1913).

Let $g(M,M')dM'$ be the probability that, because of errors, a source of absolute magnitude M is observed with an absolute magnitude between M' and M'+dM'. The observed luminosity distribution $\eta(M')$ is related to the true luminosity function $\Psi(M)$ by:

$$\eta(M') = \frac{\Omega}{4\pi} V_e(M',m_1) \int dM \Psi(M) g(M,M') \quad . \tag{21}$$

We assume g(M,M') to be a Gaussian with mean M and dispersion σ=0.4 mag. in the U band and σ=0.5 mag. in the B band.

An additional complication arises because, in practice, we bin the data so that the observed quantity is:

$$N_{obs}(\bar{M}) = \frac{1}{2\Delta M} \int_{\bar{M}-\Delta M}^{\bar{M}+\Delta M} \eta(M')dM' \quad . \tag{22}$$

The integral equation (22), with $\eta(M')$ given by eq. (21) has been solved for the luminosity function $\Psi(M)$ using the iterative technique of Lucy (1974). (The standard developments into Eddington series (Trumpler & Weaver 1953), which require the calculation of derivatives of the poorly defined function $N_{obs}(M)$, are impractical in this case.) The stability of the solution has been tested using a number of different starting approximations

for $\Psi(M)$. The corrections for the effect of errors are obviously larger when $\Psi(M)$ is steeper; however, they never exceed 40%.

The statistical errors associated to $\Psi(M)$ have been computed from the formula

$$\sigma(\Psi(M))/\Psi(M) = (1 - N_{obs}/N_{tot})^{1/2} N_{obs}^{-1/2} \qquad (23)$$

which follows from the binominal character of the distribution of the number of objects in each bin (see, e.g., Trumpler & Weaver 1953); N_{obs} is the number of objects in a bin, N_{tot} the total number of objects in the sample.

5. Results and discussion

In Tables 4 and 5 we give our estimates of the space densities of Seyfert 1 and 1.5 nuclei, based on samples defined by $z \leq 0.08$, $M_B < -18$ or $M_U < -18.5$, $B_{lim} = 17.0$ or $U_{lim} = 16.3$. For the B-band we give the results based on both the (U-B) and the (B-V) colours. The quoted errors include, added in quadrature, the contributions from uncertainties in the values of the parameters (that we estimate to be a factor of 1.3, see below) as well as from statistical fluctuations (eq. (23)).

We have carried out several checks on the stability of our results. Tables 4 and 5 show that the $\Psi(M)$ derived using the colour-given method is in very good agreement with that obtained with the galaxy-given method; also the results in the U and in the B bands, which are based on partly different data, are fully consistent with each other. In addition, we have tested the effect of varying the assumed B_{lim} between 15.4 and 17.1 and U_{lim} between 15 and 16.5 , of changing the assumed colours of the galaxy and of the nucleus by 0.2 mag., of varying z_c by +/-0.01 and of changing the size of bins: the variations in the derived space densities never exceeded 30%.

The uncertainty in the normalization of the luminosity function, estimated using different procedures to derive the incompleteness factor (subsection 4.2), is ≅25%.

In Fig. 2 our results are shown in comparison with those obtained by Veron (1979), Terebizh (1980) and Meurs (1982). Veron's luminosity function has been converted to the B band using the nuclear colour $(B-V)_N=0.2$ adopted in his paper. (Note that the space densities in Veron's Table 1 must be corrected downwards by a factor of 2 (Veron 1984, private communication); on the other hand, the densities in his Fig. 2 are per half-magnitude intervals.) The transformation $B=m_p+0.11$, suggested by Meurs (1982), has been used to convert the blue photographic magnitudes used by Terebizh and Meurs. Terebizh's results have been adjusted to $H_o=50$.

The various estimates plotted in Fig. 2 agree with each other for $M_B>-20$. At higher luminosities, Meurs' and Terebizh's results lie systematically above ours, the difference reaching a factor ≈8 in the range $-21\geq M_B\geq-22$. This is partly due to their use of total, as opposed to nuclear, magnitudes; shifting their curves to the left by ≈1 mag. would considerably mitigate the discrepancy. Contrariwise, Veron's estimates are systematically low; for $M_B<-21$, they differ from ours by a factor ≈10.

On the whole, we do find evidence of a flattening of the luminosity function for $M_B\geq-21.5$, at variance with Veron; we do not see, however, any clear indication of a leveling off at low luminosities, as suggested by Meurs.

Figure 2 also shows that our local luminosity function matches very well with that derived by Schmidt & Green (1983) for QSOs. The curve plotted in this figure refers to their model HL1, which assumes no evolution for $M_B>-23.26$. We note, in passing, that the restriction to $z\leq0.08$ does not guarantee that the effect of evolution is negligible. On the contrary, the local density of sources in our highest luminosity bin could be overestimated by a factor of up to 1.6 if Schmidt & Green (1983) evolution models hold.

In Fig. 3 we compare our results with a recent estimate of the local luminosity function of X-ray selected active galactic nuclei, obtained by Danese, De Zotti & Franceschini (1984) taking into account the data from both the HEAO-1 A2 all sky survey (Piccinotti et al. 1982) and the Einstein medium sensivity survey (Maccacaro et al. 1982; Stocke et al. 1983), and extrapolated using an optical-to-X-ray spectral index $\alpha_{ox}=1.3$, appropriate for an average absolute magnitude (uncorrected for internal reddening) $M_B=-21$ (cf. Avni & Tananbaum 1982).

The X-ray luminosity function includes the contributions of all classes of active nuclei (excepting BL Lacs), so that it is not a surprise that at low luminosities it lies above the optical one which comprises only type 1 and 1.5 Seyferts. At higher luminosities, where the latter objects dominate the space density of X-ray selected active nuclei, the two luminosity functions agree remarkably well.

G. De Zotti acknowledges useful discussions with Dr. P. Veron. He also wishes to thank the European Southern Observatory and, in particular, Prof. G. Setti, for their generous hospitality and financial support. We are grateful to Miss B. Sjöberg for carefully typing the manuscript and to Mr. J.M. Leclercqz for drawing the figures. Work supported in part by CNR grant PSN 83-014 and by MPI grant 12.02.06.

References

Adams, T.F., 1977. Astrophys. J. Suppl., 33, 19.

Avni, Y. & Tananbaum, H., 1982. Astrophys. J., 262, L17.

Boroson, T., 1981. Astrophys. J. Suppl., 46, 177.

Burstein, D. & Heiles, C., 1982. Astr. J., 87, 1165.

Cheng, F.Z., Danese, L. & De Zotti, G., 1983a. Mon. Not. R. astr. Soc., 204, 13 P.

Cheng, F.Z., Danese, L. & De Zotti, G., 1983b. Mem. Soc. astr. It., 54, 675.

Cohen, R.D., 1983. Astrophys. J., 273, 489.

Danese, L., De Zotti, G. & Franceschini, A., 1984. Astr. Astrophys., submitted.

Davidson, K. & Kinman, T.D., 1978. Astrophys. J., 225, 776.

de Vaucouleurs, G., 1974. In IAU Symp. No. 58, Formation and Dynamics of Galaxies, ed. J.R. Shakeshaft, Reidel, Dordrecht, p. 332.

de Vaucouleurs, G., 1977. Astrophys. J. Suppl., 33, 211.

de Vaucouleurs, G. & Buta, R., 1983. Astr. J., 88, 939.

de Vaucouleurs, G. & Corwin, H., 1977. Astrophys. J. Suppl., 33, 219.

de Vaucouleurs, G. & de Vaucouleurs, A., 1968. Astr. J., 73, 858.

de Vaucouleurs, G. & de Vaucouleurs, A., 1972. Mem. R. astr. Soc., 77, 1.

de Vaucouleurs, G., de Vaucouleurs, A. & Corwin, H., 1976. Second Reference Catalogue of Bright Galaxies, University of Texas Press, Austin.

Dibai, E.A., 1970. Astrofizika, 6, 350 (Astrophys., 6, 185).

Dibai, E.A., Doroshenko, V.T. & Pòstnov, K.A., 1981. Pis'ma Astr. Zh., 7, 527 (Soviet Astr. Letters, 7, 295).

Doroshenko, V.T. & Terebizh, V.Yu., 1979. Pis'ma Astr. Zh., 5, 571 (Soviet Astr. Letters, 5, 305).

Doroshenko, V.T. & Terebizh, V.Yu., 1981. Astrofizika, 17, 667 (Astrophys., 17, 358).

Eddington, A.S., 1913. Mon. Not. R. astr. Soc., 73, 359.

Felten, J.E., 1976. Astrophys. J., 207, 700.

Heckman, T., 1978. Publ. astr. Soc. Pacific, 90, 241.

Holmberg, E., 1975. In Stars and Stellar Systems, Vol. 9, p.123, eds. Sandage, A., Sandage, M. & Kristian, J., University of Chicago Press, Chicago.

Huchra, J.P., 1976. Astr. J., 81, 952.

Huchra, J.P. & Sargent, W.L.W., 1973. Astrophys. J., 186, 433.

Huchra, J.P., Wyatt, W.F. & Davis, M., 1982. Astr. J., 87, 1628.

Keel, W.C., 1980. Astr. J., 85, 198.

Khachikian, E.Ye. & Weedman, D.W., 1974. Astrophys. J., 192, 581.

Kiang, T., 1976. Mon. Not. R. astr. Soc., 174, 425.

Kinman, T.D., 1983. Mon. Not. R. astr. Soc., 202, 53.

Koski, A.T., 1978. Astrophys. J., 223, 56.

Lauberts, A., 1982. The ESO/Uppsala Survey of the ESO(B) Atlas, ESO Publications, Garching bei München.

Lawrence, A. & Elvis, M., 1982. Astrophys. J., 256, 410.

Lucy, L.B., 1974. Astr. J., 79, 745.

Maccacaro, T., Feigelson, E.D., Fener, M., Giacconi, R., Gioia, I.M., Griffiths, R.E., Murray, S.S., Zamorani, G., Stocke, J. & Liebert, J., 1982. Astrophys. J., 253, 504.

Malkan, M.A., Margon, B. & Chanan, G.A., 1984. Astrophys. J., in press.

Markarian, B.E., 1967. Astrofizika, 3, 55 (Astrophys., 3, 24).

Markarian, B.E., 1969a. Astrofizika, 5, 443 (Astrophys., 5, 206).

Markarian, B.E., 1969b. Astrofizika, 5, 581 (Astrophys., 5, 286).

Markarian, B.E. & Lipovetskii, V.A., 1971. Astrofizika, 7, 511 (Astrophys., 7, 299).

Markarian, B.E. & Lipovetskii, V.A., 1972. Astrofizika, 8, 155 (Astrophys., 8, 89).

Markarian, B.E. & Lipovetskii, V.A., 1973. Astrofizika, 9, 487 (Astrophys., 9, 283).

Markarian, B.E. & Lipovetskii, V.A., 1974. Astrofizika, 10, 307 (Astrophys., 10, 185).

Markarian, B.E. & Lipovetskii, V.A., 1976a. Astrofizika, 12, 389 (Astrophys., 12, 241).

Markarian, B.E. & Lipovetskii, V.A., 1976b. Astrofizika, 12, 657 (Astrophys., 12, 429

Markarian, B.E., Lipovetskii, V.A. & Stepanian, D.A., 1977. Astrofizika, 13, 225 (Astrophys., 13, 116).

Markarian, B.E., Lipovetskii, V.A. & Stepanian, D.A., 1979. Astrofizika, 15, 549 (Astrophys., 15, 363).

McAlary, C.W., McLaren, R.A., McGonegal, R.J. & Maza, J., 1983. Astrophys. J. Suppl., 52, 341.

McClure, R.D. & van den Bergh, S., 1968. Astr. J., 73, 1008.

Meurs, E.J.A., 1982. Ph.D. thesis, Sterrewacht Leiden.

Neyman, J. & Scott, E.L., 1961. Proc. 4th Berkeley Symp. Math. Stat. and Prob., 3, 261, University of California Press, Berkeley.

Neyman, J. & Scott, E.L., 1974. In IAU Symp. No. 63, Confrontation of Cosmological Theories with Observational Data, ed. M.S. Longair, p. 129.

Nilson, P., 1973. Uppsala General Catalogue of Galaxies, Nova Acta Regiae Societatis Scientiarum Upsaliensis Ser. V:A. Vol. 1.

Osterbrock, D.E., 1977. Astrophys. J., 215, 733.

Osterbrock, D.E. & Dahari, O., 1983. Astrophys. J., 273, 478.

Pence, W., 1976. Astrophys. J., 203, 39.

Penfold, J.E., 1979. Mon. Not. R. astr. Soc., 186, 297.

Penston, M.V., Penston, M.J., Selmes, R.A., Becklin, E.E. & Neugebauer, G., 1974. Mon. Not. R. astr. Soc., 169, 375.

Peterson, B.M., Fricke, K. & Biermann, P., 1981. Publ. astr. Soc. Pacific, 93, 281.

Piccinotti, G., Mushotzky, R.F., Boldt, E.A., Holt, S.S., Marshall, F.E., Serlemitsos, P.J. & Shafer, R.A., 1982. Astrophys. J., 253, 485.

Sandage, A., 1973. Astrophys. J., 180, 687

Schmidt, M., 1968. Astrophys. J., 151, 393.

Schmidt, M., & Green, R.F., 1983. Astrophys. J., 269, 352.

Schweizer, F., 1976. Astrophys. J. Suppl., 31, 313.

Shuder, J.M., 1981. Astrophys. J., 244, 12.

Siegel, S., 1956. Non-Parametric Statistics for the Behavioural Sciences, McGraw-Hill, New York.

Simkin, S.M., Su, H.J. & Schwarz, M.P., 1980. Astrophys. J., 237, 404.

Stein, W.A. & Weedman, D.W., 1976. Astrophys. J., 205, 44.

Stocke, J.T., Liebert, J., Gioia, I.M., Griffiths, R.E., Maccacaro, T., Danziger, I.J., Kunth, D. & Lub, J., 1983. Astrophys. J., 273, 458.

Terebizh, V.Yu., 1980. Astrofizika, 16, 45 (Astrophys., 16, 36).

Thuan, T.X. & Gunn, J.E., 1976. Publ. astr. Soc. Pacific, 88, 543.

Trumpler, R.J. & Weaver, H.F., 1953. Statistical Astronomy, University of California Press, Berkeley.

Ulvestad, J.S. & Wilson, A.S., 1983. Astr. J., 88, 253.

Veron, P., 1979. Astr. Astrophys., 78, 46.

Veron-Cetty, M.-P. & Veron, P., 1984. ESO Scientific Report No. 1, ESO Publications, Garching bei München

Veron-Cetty, M.-P., Veron, P. & Tarenghi, M., 1982. Astr. Astrophys., 113, 46.

Weedman, D.W., 1973. Astrophys. J., 183, 29.

Weedman, D.W., 1977. A. Rev. Astr. Astrophys., 15, 69.

Weedman, D.W., 1978. Mon. Not. R. astr. Soc., 184, 11 P.

Weedman, D.W. & Khachikian, E.Ye., 1969. Astrofizika, 5, 113 (Astrophys., 5, 51).

Yee, H.K.C., 1983. Astrophys. J., 272, 473.

Zasov, A.V. & Lyutyi, M.V., 1973. Astr. Zh., 50, 233 (Soviet Astr., 17, 169).

Table 1. The sample

Name	Type	z	Ap(")	V_C	$(B-V)_C$	$(U-B)_C$	b/a	Ref.	$E(B-V)_g$
Mkn 6	1.5	0.018	15	14.17	0.97	0.02	0.50	A, 1, a	0.08
Mkn 9	1	0.040	15	14.59	0.54	-0.64	0.94	B, 1, b	0.03
Mkn 10	1	0.029	15	14.55	0.67	-0.55	0.40	B, 1, b	0.03
Mkn 40	1	0.021	15	15.39	0.82	-0.23	0.69	B, 1, a	0.
Mkn 42	1	0.024	15	15.45	0.79	-0.19	0.52	B, 2, b	0.
Mkn 50	1	0.023	14.3	15.24	0.76	-0.14	0.74	B, 3, a	0.
Mkn 69	1	0.076	25	15.93	0.52	-0.44	1.0	B, 4, b	0.
Mkn 79	1.5	0.022	10	14.27	0.47	-0.78	0.69	C, 5, b	0.06
Mkn 106	1	0.122	10	16.22	0.22	-0.90	0.95	D, 5, c	0.01
Mkn 110	1	0.036	15	15.37	0.76	-0.67	0.70	B, 1, a	0.01
Mkn 124	1	0.057	25	15.33	0.61	-0.47	0.33	B, 5, b	0.01
Mkn 141	1	0.039	15	14.98	0.71	-0.32	0.79	B, 1, b	0.02
Mkn 142	1	0.045	10	15.77	0.44	-0.58	0.73	B, 5, b	0.
Mkn 205	1	0.070	15	15.24	0.40	-0.94	0.85	E, 1, c	0.02
Mkn 231	1	0.041	15	13.84	0.84	0.15	0.48	B, 1, b	0.01
Mkn 236	1	0.052	17	15.48	0.66	-0.45	0.30	B, 6, b	0.
Mkn 279	1.5	0.031	15	14.46	0.69	-0.45	0.68	C, 1, b	0.02
Mkn 290	1	0.031	15	14.96	0.60	-0.62	0.86	B, 1, a	0.01
Mkn 291	1	0.036	25	15.51	0.64	-0.08	0.58	B, 7, b	0.02
Mkn 304	1	0.067	17	14.66	0.36	-0.86	0.95	B, 6, c	0.05
Mkn 315	1.5	0.039	14.2	14.83	0.97	-0.08	0.82	A, 8, b	0.06
Mkn 335	1	0.025	15	13.85	0.41	-0.70	0.80	B, 1, b	0.03
Mkn 352	1	0.015	15	14.81	0.44	-0.66	0.67	B, 1, a	0.03
Mkn 358	1	0.046	17	15.23	0.79	-0.32	0.70	B, 6, b	0.02
Mkn 359	1	0.017	11.7	14.22	0.67	-0.21	0.68	F, 9, b	0.01
Mkn 372	1.5	0.031	17	14.81	1.05	-0.03	0.81	A, 1, b	0.10
Mkn 374	1	0.044	17	14.61	0.70	-0.38	0.42	B, 1, b	0.08
Mkn 376	1	0.056	10.1	14.62	0.55	-0.58	0.68	B, 6, b	0.09
Mkn 382	1	0.034	10.1	15.50	0.51	-0.63	0.88	B, 6, b	0.04
Mkn 464	1	0.051		16.12	0.83	-0.77	0.79	B, 10, b	0.
Mkn 474	1	0.041	17	15.25	0.97	-0.18	0.64	B, 6, b	0.
Mkn 478	1	0.079	10.1	14.58	0.33	-0.84	0.85	B, 6, a	0.
Mkn 486	1	0.039	10.1	14.78	0.43	-0.68	0.60	B, 6, b	0.01
Mkn 493	1	0.031		14.99	0.59	-0.51	0.83	F, 10, b	0.

Table 1 (continued)

Name	Type	z	Ap(")	V_C	$(B-V)_C$	$(U-B)_C$	b/a	Ref.	$E(B-V)_g$
Mkn 504	1	0.036	10.1	15.78	0.85	-0.47	0.44	B, 6, b	0.03
Mkn 506	1.5	0.043	17	14.68	0.74	-0.55	0.73	C, 6, b	0.03
Mkn 509	1	0.036	17	13.32	0.23	-0.93	0.85	B, 11, d	0.04
Mkn 530	1	0.029	17	14.01	0.72	-0.21	0.80	B, 1, b	0.03
Mkn 541	1	0.041	15.7	15.14	0.93	-0.15	0.69	B, 12, b	0.02
Mkn 543	1	0.026		14.68	0.65	-0.09	0.83	G, 10, b	0.
Mkn 584	1	0.078		15.24	0.65	-0.49	0.80	G, 10, b	0.
Mkn 590	1.5	0.027	25	13.81	0.91	0.03	0.79	D, 4, b	0.
Mkn 595	1	0.028		14.69	0.77	-0.40	0.63	H, 10, b	0.
Mkn 618	1	0.034	25	14.26	0.52	-0.47	0.60	D, 4, b	0.05
Mkn 634	1	0.066	25	15.31	0.67	-0.34	0.77	F, 4, e	0.
Mkn 662	1.5	0.055	25	15.37	0.69	-0.24	0.70	F, 4, c	0.
Mkn 668	1	0.079	25	14.92	0.77	0.14	0.71	G, 7, b	0.
Mkn 699	1	0.034	25	15.11	0.71	-0.19	0.85	M, 7, c	0.01
Mkn 704	1.5	0.029	25	14.28	0.60	-0.40	0.38	C, 4, b	0.01
Mkn 705	1	0.028	25	14.51	0.51	-0.41	0.82	G, 4, b	0.01
Mkn 707	1	0.051		15.98	0.61	-0.70	0.80	B, 10, f	0.03
Mkn 716	1.5	0.056		16.2:	0.65:	-0.4:	0.90	F, 13(*), c	0.
Mkn 734	1	0.050	25	14.81	0.32	-0.65	0.75	G, 4, b	0.01
Mkn 739E	1	0.030	25	14.08	0.78	-0.02	0.89	H, 4, f	0.
Mkn 766	1	0.013	25	13.55	0.72	0.06	0.74	G, 4, b	0.01
Mkn 771	1	0.064	25	14.93	0.38	-0.66	0.70	G, 4, f	0.02
Mkn 783	1	0.067	25	15.55	0.49	-0.50	0.75	F, 4, c	0.01
Mkn 813	1	0.111	25	15.27	0.15	-0.79	0.95	F, 4, c	0.01
Mkn 817	1.5	0.032	25	13.86	0.31	-0.57	0.80	C, 4, b	0.01
Mkn 841	1.5	0.036	25	14.48	0.37	-0.65	0.90	C, 7, c	0.
Mkn 845	1	0.046	25	15.15	0.82	-0.02	0.14	F, 7, b	0.01
Mkn 849	1	0.082		16.7:	0.65:	-0.4:	0.27	F, 14(*), b	0.
Mkn 871	1	0.034	25	14.50	0.70	-0.20	0.30	G, 7, b	0.03
Mkn 876	1	0.129	25	15.29	0.47	-0.66	0.75	G, 15, c	0.02
Mkn 877	1	0.115		15.46	0.17	-1.0	0.95	F, 10, c	0.03
Mkn 885	1	0.025	25	14.56	0.82	-0.17	0.60	F, 15, c	0.02
Mkn 975	1	0.050		14.95	0.70	-0.50	0.61	F, 10, b	0.04
Mkn 1392	1	0.036	36	14.35	0.99	0.14	0.33	I, 16, g	0.01

Table 1 (continued)

Name	Type	z	Ap(")	V_C	$(B-V)_C$	$(U-B)_C$	b/a	Ref.	$E(B-V)_g$
NGC 2639	1	0.011		11.76	0.89	0.37	0.66	J, 17, h	0.02
NGC 3227	1.5	0.003	10.4	13.43	0.86	0.02	0.45	C, 18, b	0.
NGC 3516	1	0.009	24	12.40	0.72	-0.23	0.75	B, 19, b	0.02
NGC 4051	1	0.002	10	13.63	0.73	-0.33	0.58	B, 20, b	0.
NGC 4151	1.5	0.003	13.5	11.99	0.53	-0.72	0.74	B, 20, b	0.
NGC 4235	1	0.007	15	13.60	1.10	0.50	0.13	G, 21, b	0.
NGC 5273	1	0.004	23	13.24	0.83	0.16	0.82	J, 22, i	0.
NGC 5548	1.5	0.019	13.5	13.72	0.48	-0.64	0.83	C, 20, b	0.
NGC 5940	1	0.034		14.90	0.66	-0.20	1.0	J, 10, i	0.
NGC 7469	1.5	0.017	13.5	13.12	0.44	-0.72	0.58	C, 20, b	0.03
0048+29	1	0.036		14.1:	0.5:	-0.55:	1.0	J, 23(+), j	0.0
2237+07	1	0.025		13.85:	0.55:	-0.5:	0.89	J, 23(+), j	0.0
I Zw 1	1	0.061	17	14.07	0.43	-0.67	0.88	B, 6, b	0.03
II Zw 1	1	0.054	17	15.17	0.56	-0.37	0.67	B, 6, b	0.01
II Zw 136	1	0.062	17	14.53	0.29	-0.90	0.47	B, 1, a	0.03
III Zw 2	1	0.090	10.1	15.56	0.52	-0.70	0.66	B, 6, i	0.04
VII Zw 118	1	0.080		15.11	0.62	-0.60	0.95	F, 10, c	0.04
Ton 524A	1	0.060	15	16.18	0.51	-0.47	0.83	B, 4, b	0.
Tol 1059+105	1	0.034		15.63	0.80	-0.56	0.80	G, 10, c	0.
X Comae	1	0.092	25	16.65	0.58	-0.36	0.80	B, 4, b	0.01

Notes to Table 1.

(*) We have used the relation: $B = m_{pg} + 0.34$ (Huchra 1976); the values of $(B-V)_C$ and $(U-B)_C$ have been derived from tentative colour - absolute magnitude relations for objects in the present sample.

(+) We have used the relation: $B = m_p + 0.11$ (Meurs 1982); for colours see the previous note.

Sources of Seyfert types.

A. Koski (1978)

B. Weedman (1977)

C. Cohen (1983)

D. Osterbrook (1977)

E. Weedman (1973)

F. Osterbrook & Dahari (1983)

G. Weedman (1978)

H. Ulvestad & Wilson (1983)

I. Huchra, Wyatt & Davis (1982)

J. Veron-Cetty & Veron (1984)

References for photometry and redshifts.

1. Weedman (1973)
2. Weedman & Khachikian (1969)
3. Penfold (1979)
4. Doroshenko & Terebizh (1979)
5. Dibai (1970)
6. Khachikian & Weedman (1974)
7. Doroshenko & Terebizh (1981)
8. Peterson, Fricke & Biermann (1981)
9. Davidson & Kinman (1978)
10. Veron-Cetty & Veron (1984)
11. Stein & Weedman (1976)
12. McAlary et al. (1983)
13. Markarian & Lipovetskii (1976a)
14. Markarian & Lipovetskii (1976b)
15. Dibai, Doroshenko & Postnov (1981)
16. Kinman (1983)
17. de Vaucouleurs, de Vaucouleurs & Corwin (1976)
18. Penston et al. (1974)
19. de Vaucouleurs & de Vaucouleurs (1968)
20. Zasov & Lyutyi (1973)
21. Veron-Cetty, Veron & Tarenghi (1982)
22. McClure & van den Bergh (1968)
23. Nilson (1973)

References for axial ratios.

a. Adams (1977)

b. Keel (1980)

c. Our estimate from blue Palomar Sky Survey prints

d. Lawrence & Elvis (1982)

e. Markarian & Lipovetskii (1974)

f. Markarian & Lipovetskii (1976a)

g. Kinman (1983)

h. de Vaucouleurs, de Vaucouleurs & Corwin (1976)

i. Lauberts (1982)

j. Nilson (1973)

Table 2. Estimates of nuclear magnitudes (H_o = 50 km $s^{-1}Mpc^{-1}$).

Name	Colour-given				Galaxy-given	
	U_N	B_N	M_U	M_B	U_N	B_N
Mkn 6	15.61	-	-19.56	-	15.31	15.67
Mkn 9	14.34	15.11	-22.56	-21.79	14.28	15.06
Mkn 10	14.70	15.96	-21.50	-20.24	14.82	15.63
Mkn 40	16.59	-	-18.92	-	-	-
Mkn 42	16.61	18.32	-19.18	-17.47	18.70	-
Mkn 50	16.63	16.47	-19.07	-19.23	16.91	-
Mkn 69	16.49	17.07	-21.81	-21.22	16.31	16.99
Mkn 79	13.74	14.87	-21.86	-20.74	13.84	14.87
Mkn 106	15.49	16.43	-23.83	-22.89	15.54	16.53
Mkn 110	15.50	18.00	-21.17	-18.67	15.88	17.87
Mkn 124	15.45	16.73	-22.22	-20.94	15.59	16.29
Mkn 141	15.78	17.05	-21.06	-19.80	15.66	16.32
Mkn 142	15.81	16.55	-21.34	-20.61	15.92	16.94
Mkn 205	14.61	15.82	-23.51	-22.30	14.68	15.77
Mkn 231	16.43	16.88	-20.52	-20.08	14.94	14.82
Mkn 236	15.69	17.13	-21.78	-20.34	15.91	16.67
Mkn 279	14.88	16.27	-21.46	-20.08	14.85	15.59
Mkn 290	14.77	15.34	-21.58	-21.00	14.79	15.69
Mkn 291	16.85	16.84	-19.82	-19.83	17.40	-
Mkn 304	13.82	14.79	-24.20	-23.22	13.85	14.80
Mkn 315	16.42	-	-20.42	-	15.88	16.20
Mkn 335	13.03	13.70	-22.85	-22.18	13.01	13.80
Mkn 352	14.53	15.34	-20.24	-19.43	14.76	16.11
Mkn 358	16.45	17.16	-20.76	-20.04	16.39	17.11
Mkn 359	15.22	16.00	-19.82	-19.04	15.04	15.58
Mkn 372	16.38	-	-19.96	-	16.08	16.56
Mkn 374	15.31	-	-21.80	-	15.30	15.90
Mkn 376	14.06	14.70	-23.57	-22.93	13.99	14.69
Mkn 382	15.33	16.38	-21.21	-20.17	15.51	16.72
Mkn 464	16.23	20.79	-21.20	-16.64	16.84	-
Mkn 474	16.68	16.85	-20.27	-20.11	16.45	16.95
Mkn 478	14.08	15.08	-24.30	-23.30	14.10	14.99

Table 2 (continued)

Name	Colour-given U_N	Colour-given B_N	Colour-given M_U	Colour-given M_B	Galaxy-given U_N	Galaxy-given B_N
Mkn 486	14.27	15.13	-22.57	-21.71	14.30	15.11
Mkn 493	15.35	16.52	-21.00	-19.82	15.52	16.71
Mkn 504	16.14	18.29	-20.53	-18.38	16.39	17.57
Mkn 506	14.92	16.77	-22.14	-20.29	14.92	15.73
Mkn 509	12.23	13.40	-24.44	-23.27	12.25	13.26
Mkn 530	15.06	16.18	-21.14	-20.02	14.64	15.02
Mkn 541	16.61	-	-20.34	-	16.45	17.05
Mkn 543	15.45	17.05	-20.51	-18.92	16.76	-
Mkn 584	15.73	16.78	-22.62	-21.57	15.52	16.12
Mkn 590	16.39	-	-19.66	-	15.37	15.48
Mkn 595	15.11	16.77	-21.02	-19.36	15.16	16.02
Mkn 618	14.58	14.94	-21.97	-21.60	14.49	15.13
Mkn 634	16.18	17.05	-21.81	-20.94	15.88	16.39
Mkn 662	16.49	17.25	-21.10	-20.34	16.25	16.77
Mkn 668	20.52	17.14	-17.85	-21.24	16.02	15.88
Mkn 699	16.42	17.53	-20.13	-19.02	16.83	-
Mkn 704	14.58	14.94	-21.62	-21.26	14.67	15.39
Mkn 705	14.99	15.74	-21.13	-20.39	15.08	16.09
Mkn 707	17.23	17.71	-20.20	-19.71	17.78	-
Mkn 716	16.99	17.97	-20.72	-19.74	17.62	-
Mkn 734	14.56	15.20	-22.83	-22.18	14.56	15.39
Mkn 739E	16.27	18.69	-19.93	-17.51	15.24	15.37
Mkn 766	15.82	16.08	-18.64	-18.38	15.58	16.10
Mkn 771	14.66	15.38	-23.26	-22.54	14.64	15.42
Mkn 783	15.78	16.41	-22.24	-21.61	15.69	16.40
Mkn 813	14.64	15.49	-24.47	-23.63	14.61	15.45
Mkn 817	13.76	14.27	-22.65	-22.15	13.68	14.41
Mkn 841	14.37	15.17	-22.30	-21.50	14.41	15.36
Mkn 845	16.23	17.31	-20.98	-19.90	16.16	16.41
Mkn 849	16.99	18.18	-21.47	-20.28	17.32	18.16
Mkn 871	15.10	16.22	-21.45	-20.32	15.10	15.56
Mkn 876	15.13	15.93	-24.31	-23.52	15.03	15.74
Mkn 877	14.50	15.63	-24.70	-23.57	14.52	15.59

Table 2 (continued)

Name	Colour-given				Galaxy-given	
	U_N	B_N	M_U	M_B	U_N	B_N
Mkn 885	15.77	18.54	-20.11	-17.34	16.08	17.62
Mkn 975	15.15	16.39	-22.23	-21.00	15.12	15.83
Mkn 1392	16.60	-	-20.07	-	15.94	15.97
NGC 2639	-	-	-	-	14.20	13.56
NGC 3227	15.08	17.20	-16.19	-14.07	15.18	16.04
NGC 3516	13.38	14.75	-20.28	-18.91	13.10	13.57
NGC 4051	14.36	15.70	-16.04	-14.70	15.11	-
NGC 4151	11.86	13.13	-19.42	-18.15	11.92	12.86
NGC 4235	16.83	-	-16.57	-	16.08	15.82
NGC 5273	16.35	-	-15.55	-	-	-
NGC 5548	13.71	14.76	-21.58	-20.53	13.72	14.60
NGC 5940	14.71	16.00	-21.84	-20.55	14.57	15.28
NGC 7469	12.70	13.59	-22.34	-21.45	12.76	13.62
0048 + 29	14.15	15.16	-22.52	-21.51	14.15	15.03
2237 + 07	14.00	15.01	-21.88	-20.88	14.22	15.48
I Zw 1	13.82	14.71	-24.00	-23.11	13.73	14.47
II Zw 1	15.72	16.25	-21.83	-21.31	15.53	16.09
II Zw 136	13.78	14.95	-24.07	-22.91	13.81	14.80
III Zw 2	15.24	16.21	-23.43	-22.45	15.25	16.06
VII Zw 118	15.15	16.30	-23.26	-22.10	15.02	15.73
Ton 524A	16.57	17.24	-21.21	-20.54	16.72	17.85
Tol 1059 + 105	16.09	20.40	-20.46	-16.14	16.92	-
X Comae	17.36	17.78	-21.35	-20.93	17.22	17.89

Table 3. Correlations between the apparent nuclear magnitude U_N, the intensity ratio a_U, the absolute nuclear magnitude M_U and the axial b/a: values of τ/σ_K for several limiting magnitudes U_{lim}.

U_{lim}	$M_U<-18.5, z<0.08$			$M_U<-18.5, z<0.07$		
	U,M_U	U,a_U	U,b/a	U,M_U	U,a_U	U,b/a
15.0	-0.71	-0.07	-0.98	-0.25	-0.18	-0.96
15.1	-0.29	-0.98	-0.83	0.03	-1.04	-0.83
15.2	0.10	-1.09	-0.40	0.31	-1.04	-0.23
15.3	1.48	-2.23	-0.87	1.40	-2.15	-0.76
15.4	1.95	-2.70	-0.86	2.03	-2.53	-0.70
15.5	1.65	-2.07	-1.19	1.78	-1.98	-1.16
15.6	1.99	-1.48	-0.86	1.88	-1.47	-0.79
15.7	1.96	-0.82	-1.27	1.73	-0.89	-1.26
15.8	1.82	-1.19	-1.34	1.38	-1.43	-1.10
15.9	2.26	-2.44	-0.87	1.28	-2.28	-0.02
16.0	2.35	-2.32	-0.76	1.48	-1.97	-0.13
16.1	2.35	-2.44	-0.24	1.35	-1.76	-0.22
16.2	1.42	-2.44	0.63	0.83	-2.01	-0.10
16.3	1.69	-1.54	-0.25	1.04	-1.25	-0.72
16.4	2.13	-2.52	0.44	2.63	-2.37	0.38
16.5	2.05	-3.43	0.97	2.33	-3.13	0.80
16.6	2.85	-3.30	0.56	1.80	-2.75	0.89
16.7	3.69	-3.69	-0.15	2.43	-2.92	-0.27
16.8	3.20	-3.72	-0.07	2.13	-3.03	-0.68
16.9	2.45	-3.20	-0.31	1.64	-2.74	-0.63
17.0	2.47	-3.22	-0.18	1.74	-2.69	-0.69

Table 4. Local luminosity function of Seyfert 1 and 1.5 nuclei in the B band (H_o=50 km s^{-1} Mpc^{-1})

M_B	log $\Psi(M_B)$ (Mpc^{-3} mag^{-1})		
	Colour-given		Galaxy-given
	(U-B)	(B-V)	
-18.5	-5.58(+0.26,-0.53)	-5.11(+0.22,-0.37)	-5.14(+0.26,-0.53)
-19.5	-5.43(+0.17,-0.22)	-5.46(+0.18,-0.24)	-5.37(+0.17,-0.22)
-20.5	-5.82(+0.15,-0.16)	-5.75(+0.14,-0.16)	-5.54(+0.14,-0.14)
-21.5	-6.24(+0.13,-0.14)	-6.44(+0.15,-0.17)	-6.19(+0.14,-0.15)
-22.5	-7.26(+0.20,-0.31)	-6.93(+0.17,-0.22)	-6.87(+0.17,-0.21)
-23.5	-7.27(+0.19,-0.27)	-7.34(+0.20,-0.30)	-7.20(+0.19,-0.27)

Table 5. Local luminosity function of Seyfert 1 and 1.5 nuclei in the U band (H_o = 50 km s^{-1} Mpc^{-1}).

M_U	log $\Psi(M_U)$ (Mpc^{-3} mag^{-1})	
	Colour-given	Galaxy-given
-19.5	-5.43(+0.22,-0.38)	-5.30(+0.19,-0.27)
-20.5	-5.56(+0.17,-0.21)	-5.61(+0.16,-0.20)
-21.5	-5.76(+0.13,-0.14)	-5.80(+0.14,-0.15)
-22.5	-6.31(+0.14,-0.16)	-6.25(+0.14,-0.15)
-23.5	-7.06(+0.19,-0.27)	-7.16(+0.21,-0.31)
-24.5	-7.28(+0.21,-0.31)	-7.16(+0.19,-0.27)

Figure Captions

Fig. 1 Distribution in galactic coordinates of all objects in our sample and assumed boundaries of the region covered by the first 9 Markaraian lists.

Fig. 2 Comparison of the present estimate of the local luminosity function of Seyfert 1 and 1.5 nuclei with those obtained by Veron (squares), Terebizh (open circles) and Meurs (filled circles). Plotted are the geometric means of the space densities (colour-given method) listed in Table 4. Error bars are shown only for our results. The dashed line displays the local luminosity function of QSOs associated with the evolution model HL1 of Schmidt and Green (1983).

Fig. 3 Comparison of the present luminosity function (cf. caption to Fig. 2) with a recent estimate of the local luminosity function of X-ray selected active galactic nuclei (Danese, De Zotti & Franceschini 1984); see text for details.

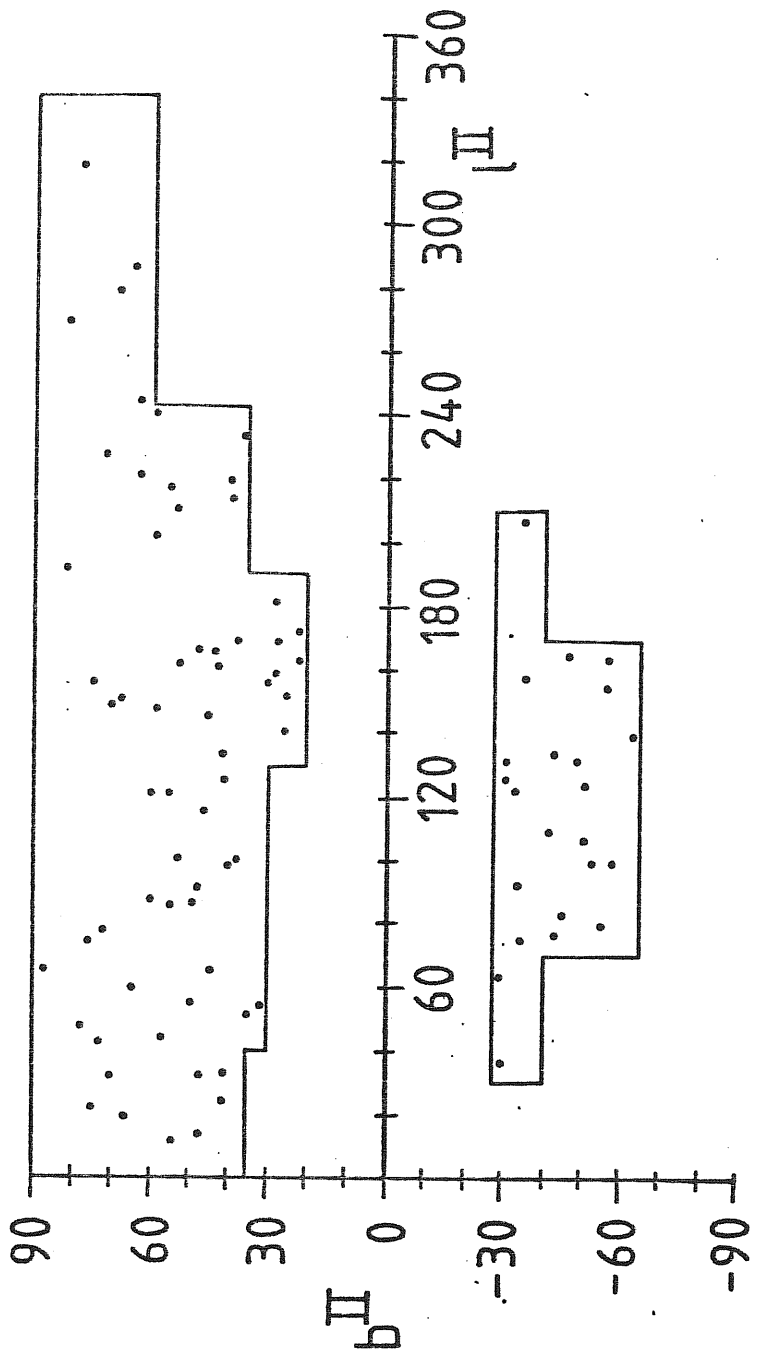
90
60
30
0
-30
-60
-90
b^{II}
60
120
180
240
300
360
l^{II}

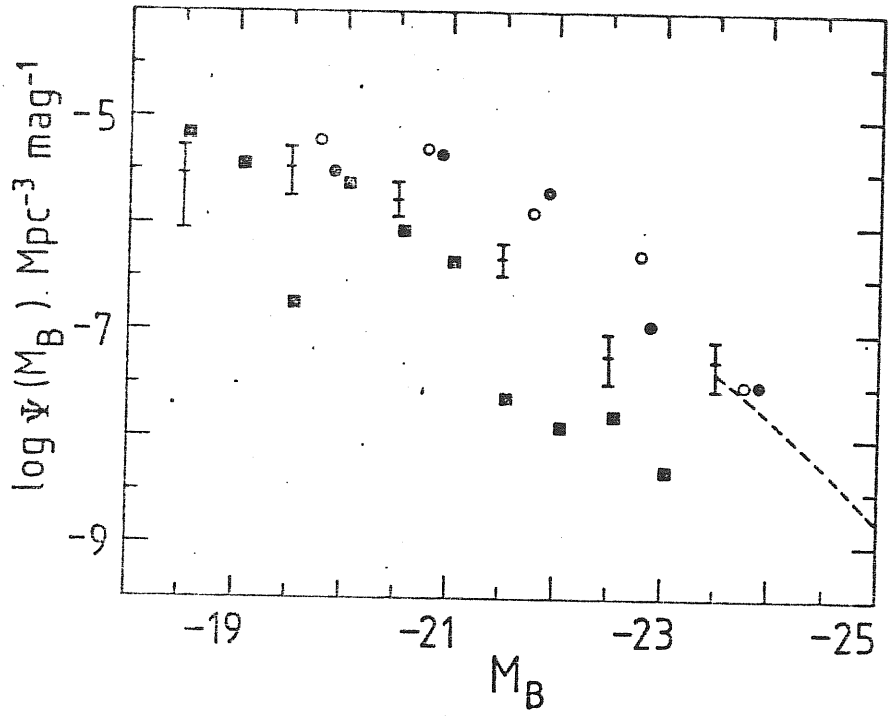
log Ψ (M_B) Mpc^-3 mag^-1
-5
-7
-9
-19
-21
-23
-25
M_B

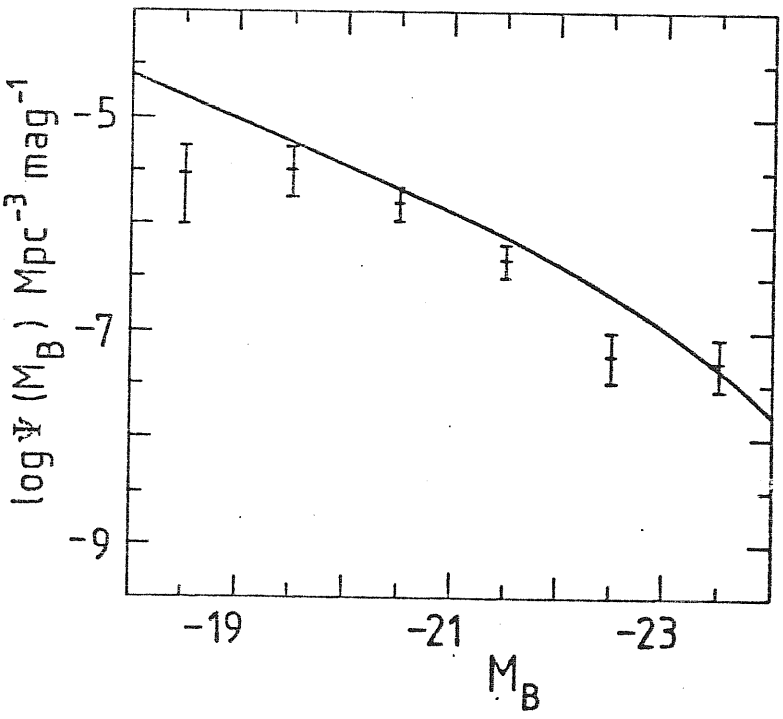
log Ψ (M_B) Mpc^-3 mag^-1
-5
-7
-9
-19
-21
-23
M_B

CHAPTER VI MAIN CONCLUSIONS

In this thesis we have described in some detail the observational properties of Sy 1 galaxies and discussed possible interpretations of the data. The main new results presented here concern: 1) the problem of internal reddening; 2) the ratio of x-ray to optical luminosity of AGNs; 3) the local luminosity function of Seyfert 2 nuclei.

Our main conclusions are:

(1) Reddening by dust certainly play an important role. We have presented evidence for an absorbing layer in the equatorial plane of the lost galaxy and have derived a simple reddening law for the nuclear continuum.

(2) The BRL of Sy 1 has the same internal reddening as the continuum source.

(3) Taking the internal reddening into account, the estimates for five independent samples show that the average optical to X-ray energy indexes are more or less the same, i.e., the ratio of X-ray to optical luminosity for AGNs, on the average, is unrelated to their optical luminosities.

(4) The local luminosity function of Sy 1 nuclei matches remarkably well that of optically selected QSOs at $M_B \approx -23$ (Schmidt and Green 1983); it also compares very favourably with a recent determination of the local luminosity function of X-ray selected AGNs (danese et al 1984).

ACKNOWLEDGEMENT

I would like to express my heartfelt appreciation to my supervisors Prof. L.Danese and Prof. C.De Zotti for their introducing into this interesting field and also for their enthusiastic instruction.

I wish to thank following Profs. M.Abramowicz, S.Bonomentto, G.Barbaro, B.Cester, C.Chiosi, L.Danese, C.De Zotti, F.de Felice, J.C.Miller, L.Sedmak, R.Stalio, P.Selvelli and B.W.Tolman. I have benefited greatly their lectures.

I am grateful to Profs. P.Budinich, L.Fonda, N.Dallaporta, D.W.Sciama, M.Hack and SISSA Committee for fellowship and their invaluable encouragement during the course of my study and work in Italy.

The SISSA, ICTP and Trieste Observatory staffs and libraries are gratefully acknowledged for their helpful services.

Thanks are also given to Prof. L.Rosino and Padova Observatory staffs for their much help and hospitalities during the coure of the work in Padova.

Finally, I thank Ms. Alex Meehan and Ms. Lidia Bogo very much for carefully typing the manuscript.

REFERENCES

Abell, G.O., Eastmond, T.S. and Jenner, D.C., Ap. J., 222(1978) L1.

Adam, G., A.Ap.Suppl., 31(1978)151.

Adam, G., Private conmunication, 1982

Adams, T.F., Ap.J.,Suppl. Series, 33(1977)19.

Adams, M.T. & Rudnick, L., A.J., 82(1977)857.

Adams, T.F. & Weedman, D.W., Ap.J., 199(1975)19.

Afanasev, V.L. et al, Soviet. AJ. Letters, 5(1979a)144.

Afanasev, V.L. et al, Astrophys, 16(1979b)119.

Alcaino, G., A.Ap.Suppl., 26(1976)261.

Anderson, K.S., Ap.J., 162(1970)743.

Anderson, K.S., Ap.J., 189(1974)191.

Angel, J.R.P. et al, Ap.J.Letters, 206 (1976)L5.

Anguita, A.C. & Pedreros, M., A.J., 82(1977)102.

Antonucci, R.R.J., Nature, 303(1983)158.

Apparao, K.V. et al, Nature, 273(1978)450.

Арп Ох, В.А. et al, АСТРОФИЗИКА, 18(1982)216.

Arakerian, M.A., Publ. Byurkan. Obs., 47(1975)3.

Arakerian, M.A., Dibai, E.A. and Esipov, V.F., Astrophys, 6(1970a)14.

Arakerian, M.A., Dibai, E.A. and Markarian, B.E., Astro. TSIRK, 568(1970b)1.

Arakelian, M.A. et al, Astrophys, 7(1971)102.

Arakelian, M.A. et al, Astrophys, 9(1973)183.

Arakelian, M.A. et al, Astrophys, 11(1975)254.

Arakelian, M.A. et al, Astrophys, 12(1976a)122.

Arakelian, M.A. et al, Astrophys, 12(1976b)456.

Arakelian, M.A. et al, Astro. TSIRK, 586(1970c)1.

Allen, D.A. et al, M.N.R.A.S., 184(1978)303.

Arkhipova, V.P. & Esipov, V.F., Soviet. AJ. Letters, 5 (1979)90.

Arp, H., Ap.J.Suppl.Ser., 14(1966)1.

Arp, H., Ap.J., 152(1968)1101.

Arp, H., Ap.Letters, 9(1971)1.

Arp, H., Ap.J., 218(1977)70.

Arp, H., Ap.J., 250(1981)31.

Arp, H. & Khachikian, E.E., Astrophys, 9(1975)308.

Auriemma, C. et al, A.Ap., 57(1977)41.

Anderson, K.S. & Kraft, R.P., Ap.J., 158(1969)859.

Baldwin, J.A., Ap.J., 201(1975)26.

Baldwin, J.A., M.N.R.A.S., 178(1977)678.

Balzano, V.A. & Weedman, D.W., Ap.J., 243(1981)756.
Barbieri, C., Ap.Letters, 14(1973)231.
Barbieri, C. et al, Mem.S.A.It., 1982, Vol.53, N°3.
Barbieri, C. & Romano, G., A.Ap., 50(1976)15.
Blandford, R.D., M.N.R.A.S., 176(1976)465.
Blandford, R.D. & Rees, M.J., M.N.R.A.S., 169(1974)395.
Blandford, R.D. & Rees, M.J., in "Proc. Pittsburg Conferece on BL Lac Objects", ed. A. Wolfe, 1978, p.328.
Blumenthal, G.R. & Mathews, W.G., Ap.J., 198(1975)517.
Boksengberg, A. & Netzer, H., Ap.J., 212(1977)37.
Boksengberg, A. & Sargent, W.L.W., Ap.J., 198(1975)31.
Boksengberg, A. et al, M.N.R.A.S., 173(1975)381.
Boksengberg, A. et al, M.N.R.A.S., 178(1977)451.
Boksengberg, A. et al, in "Proc. of Second European IUE Conferece", PIXVII, Tubingen, Germany(1980).
Bolton, J.G. & Ekers, J., Australian. J.Phys., 19(1966a)275.
Bolton, J.G. & Ekers, J., Australian. J. Phys., 19(1966b)471.
Bolton, J.G. & Ekers, J., Australian. J. Phys., 19(1966c)559.
Bolton, J.G. & Kinman, T., Ap.J., 145(1966)951.
Bolton, J.G. & Wall, J.V., Australian. J. Phys., 23(1970)789.
Bolton, J.G. et al, Australian. J. Phys., 24(1971)889.
Bolton, J.G. et al, Ap.J., 144(1966)1229.
Bolton, J.G., Shinmmins, A.J. and Wall, J.V., Australian. J. Phys. Suppl., N34(1975)1.
Bond, H.E., Kron, R. and Spinrad, H., Ap.J., 213(1977)1.
Borchkhadze, T.M. & West, R.M., Astrophys, 13(1977)358.
Borchkhadze, T.M. & West, R.M., Astrophys, 16(1980)233.
Braccesi, A. et al, A.Ap., 85(1980)80.
Bradt, H.V. et al, Ap.J., 226(1978)L111.
Bregman, J.D. & Witteborn, F.C., Ap.J., 281(1984)L17.
Burbidge, E.M., Ap.J., 149(1967)L51.
Burbidge, E.M., Ap.J., 152(1968)L111.
Burbidge, E.M. & Kinman, T., Ap.J., 145(1966)654.
Burbidge, E.M. & Strittmatter, P.A., Ap.J., 172(1972)L37.
Burbidge, E.M. et al, Ap.J., 178(1972)L43.
Burbidge, G.R., Nature, Phys. Sci., 246(1973)17.
Burbidge, G.R. & Burbidge, E.M., 222(1969)735.
Burbidge, G.R. et al, Rev. Mod. Phys., 35(1963)947.
Burbidge, E.M. et al, Ap.J., 130(1959)26.
Braccesi, A. et al, Ap.J., 152 (1968) L105.

Caldwell, N. & Phillips, M.M., Ap.J., 244(1981)447.
Canizares, J.P. et al, Ap.J. Letters, 226(1978)L69.
Cannon, R.D. et al, Ap.J., 193(1974)43.
Capriotti, E. et al, Ap.J., 230(1979)681.
Capriotti, E.R. et al, Ap.J., 241(1980)903.
Carter, D. & Malin, D.F., M.N.R.A.S., 203(1983)49p.
Cavaliere, A. & Morrison, P., Ap.J. Letters, 238(1980)L63.
Cavaliere, A. et al, A.Ap., 97(1981)269.
Cheng, F.Z. et al, Acta. Astrophys. Sinica, 1(1981)24.
Eng. Trns. in China Astron. Astrophys., 5(1981)24.
Cheng, F.Z., Danese, L. and de Zotti, G., M.N.R.A.S., 204(1983)13p.
Cheng, F.Z., Danese, L. and de Zotti, G., Mem. S.A.It., Vol 54°N°3(1983)675.
Cheng, F.Z. et al, M.N.R.A.S., 208(1984)799.
Cheng, F.Z. et al, "Proc. of Symposium on X-ray Astronomy '84 in Bologna, Italy", in press
Cheng, F.Z. et al, M.N.R.A.S., 1985, in press
Chavira, E., Bol. Obs. Tonantzintla Y Tacubaya, 2,N17(1958)15.
Chavira, E., Bol. Obs. Tonantzintla Y Tacubaya, 2,N18(1959)3.
Chi-Chao Wu, et al, Ap.J., 247(1981)449.
Clarke, M., Bolton, J. and Shimmins, A., Australian. J. Phys., 19(1966)375.
Cohen, R.D., 1981, UCSC Ph.D. Thesis.
Cohen, R.D., Ap.J., 273(1983)489.
Cohen, M.M. et al, Mem. Roy. Astron. Soc., 84(1977)1.
Condon, J.J et al, A.J., 81(1976)913.
Condon, J.J et al, Ap.J., 246(1981)624.
Collin-Souffrin, S., Dumont, S. and Tully, J., A.Ap., 106(1982)362.
Cristiani, S. & Tarenghi, M., A.Ap., 132 (1984) 351.
Cromwell, R. & Weymann, R.J., Ap.J. Letters, 159(1970)L147.
Crutri, R.M. et al, Ap.J., 280(1984)521.
Clements, E.D., M.N.R.A.S., 204 (1983) 811.

Danese, L. & de Zotti, G., preprint, 1984.
Danzinger, I.J. & Goss, V.M., M.N.R.A.S., 200(1983)27p.
Danzinger, I.J., Fosbury, R.A.E. and Penston, M.V., M.N.R.A.S., 179(1977)41p.
Davidson, K., Ap.J., 218(1977)20.
Davidson, K. & Kinman, T.D., Ap.J., 225(1978)776.
Davidson, K. & Netzer, H., Rev. Mod. Phys., 51(1979)715.
Davies, R.D., M.N.R.A.S., 161(1973)25p.
de Bruyn, A.G., Highlights of Astronomy, 5(1980)631.
de Bruyn, A.G. & Wilson, A.S., A.Ap., 53(1976)93.

de Bruyn, A.G.& Wilson, A.S., A.Ap., 64 (1978a) 433.
de Bruyn, A.G.& Wilson, A.S., A.Ap., 64 (1978b) 444.
Denisyuk, E.K. & Lipovetski, V.A., Astrophys, 10 (1974) 195.
Denisyuk, E.K. & Lipovetski, V.A., Soviet.AJ.Letters, 3 (1977) 3.
De Zotti, G., Acta Cosmologica, 11 (1982) 65.
De Zotti, G. & Gaskell, C.M., preprint, 1984.
de Vaucouleurs, G. & de Vaucouleurs A., A.J., 73 (1968) 850.
Dibai, E.A., Astrophys, 6 (1970) 185.
Dibai, E.A. & Shakhovskoy, N.M., Astro.Tsirk., No 375 (1966) 1.
Dibai, E.A. et al, Soviet.AJ.Letters., 7 (1981) 295.
Dil, S. et al, Bull.AAS., 11 (1979) 467.
Disney, M.J., Ap.J., 181 (1973) L55.
Disney, M.J. & Cromwell, R.H., Ap.J., 164 (1971) L35.
Doroshenko, V.T. & Terebizh, V.Y., Soviet.AJ.Letters., 5 (1979) 305.
Doroshenko, V.T. & Terebizh, V.Y., Astrofiz, 16 (1980) 393.
Doroshenko, V.T. & Terebizh, V.Y., Astrophys, 17 (1981) 358.
Dower, R.G. et al, Ap.J., 235 (1980) 355.
Dressler, A. & Gunn, J.E., Ap.J., 270 (1983) 7.
Dressler, A. & Sandage, A., Publ.Astro.Soc.Pacific., 90 (1978) 5.

Elvis, M., M.N.R.A.S., 177 (1976) 7p.
Elvis, M. et al, M.N.R.A.S., 183 (1978) 129.

Fabian, A.C., Highlights of Astronomy, R.M. West (ed), Vol 6, 1983 by the IAU, 447.
Fabian, A.C. et al, Space Sci.Rev., 30 (1981) 113.
Fairall, A.P., Publ.Astron.Soc.Pacific 80 (1968) 235.
Fairall, A.P., M.N.R.A.S.South Africa, 37 (1978) 41.
Fairall, A.P., M.N.R.A.S., 191 (1980a) 391.
Fairall, A.P., M.N.R.A.S., 192 (1980b) 389.
Fairall, A.P., M.N.R.A.S., 196 (1981) 417.
Fairall, A.P., M.N.R.A.S., 203 (1983) 47.
Fairall, A.P., Mchardy, I.M. and Pye, J.P., M.N.R.A.S., 198 (1982) 13p.
Fang Lizhi et al, Act.Astron.Sinica, 17 (1976) 134.
Eng.Trans. in China Astron., 1 (1977) 278.
Fanti, C. et al, A.Ap.Suppl., 19 (1975) 143.
Feldman, F.R., Marshall, F.E. and Phillipps, M.M., IAU Circ 3293 (1978) (18.10.78).
Feldman, F.R. et al, Ap.J., 256 (1982) 427.
Felten, J.E., A.J., 82 (1977) 861.
Ferland, G.J. & Mushotzky, R.F., Ap.J., 262 (1982) 564.

Foltz, C.B. et al, Ap.J., 250 (1981) 508.
Ford, K. & Rubin, V., Ap.J., 145 (1966) 357.
Fosbury, R.A.E. & Wall, J.V., M.N.R.A.S., 189 (1979) 79.
Fairall, A.P., Lowe, L. and Dobbie, P.J.K., 1983, A Catalogue of Galaxies South of Declination -30°
Garrison, R.F. & Walborn, N.R., J.Roy.Astron.Soc.Canada, 68 (1974) 117.
Gaskell, C.M., 1981, Ph.D. thesis, University of Califoria, Santa Cruz.
Gaskell, C.M., Pub.Astron.Soc.Pacific, 94 (1982) 891.
Gaskell, C.M., Ap.Letters, 24 (1984) 43.
Gaskell, C.M. & De Zotti, G., B.A.A.S., 15 (1983) 988.
Gaskell, C.M. & Ferland, G.J., Pub.Astron Soc.Pacific, 96 (1984) 393.
Ghigo, F.D. et al, A.J., 87 (1982) 1438.
Gioia, E.M. et al, Ap.J., 271 (1983) 524.
Glaspey, J.W. et al, Ap.J., 203 (1976) 335.
Goodrich, R.W. & Osterbrock, D.E., Ap.J., 269 (1983) 416.
Grandi, S.A., Ap.J., 215 (1977) 446.
Grandi, S.A., Ap.J., 221 (1978) 501.
Grandi, S.A., Ap.J., 255 (1982) 25.
Grandi, S.A., M.N.R.A.S., 204 (1983a) 691.
Grandi, S.A., Ap.J., 268 (1983b) 591.
Grandi, S.A. & Phillips, M.N., Ap.J., 239 (1980) 475.
Greenstein, J. & Oke, J.B., Publ.Astron.Soc.Pacific, 82 (1970) 898.
Greenstein, J. & Schmidt, M., Ap.J., 140 (1964) 1.
Griersmith, D., A.J., 85 (1980) 789.
Griffin, R., A.J., 68 (1963) 421.
Griffiths, R.E. et al, Ap.J., 230 (1979) L21.
Grindlay, J.E. et al, Ap.J. (Letters), 239 (1980) L43.

Halpern, J.P., 1982, Ph.D. thesis, Harvard University.
Halpern, J.P. & Steiner, J.E., Ap.J. (Letters), 269 (1983) L37.
Haro, G., Bol.Obs.Tonantzintla y Tacubaya, No14 (1956) 16.
Haro, G. & Luyten, W., Bol.Obs.Tonantzinta y Tacubaya, 3 (1962) 37.
Harris, D.E. et al, A.Ap., 111 (1982) 299.
Hawarden, T.G. et al, M.N.R.A.S., 186 (1979) 495.
Hayes, M.J.C. et al, Space Sci. Rev., 30 (1981) 39.
Heckman, T.A. et al, Ap.J., 247 (1981) 403.
Heckman, Y.M. & Balick, B., A.Ap., 79 (1979) 350.
Henry, J.P. et al, Ap.J., 272 (1983) 434.
Hodge, D.W., A.J., 73 (1968) 846.

Holmberg, E.B. et al, A.Ap.Suppl., 27 (1977) 295.
Huchra, J.P., Ap.J.Suppl., 35 (1977) 171.
Huchra, J.P., Ap.J., 238 (1980) L11.
Huchra, J.P. & Sargent, W.L.W., Ap.J., 186 (1973) 433.
Huchra, J.P., Wyatt, W.F. and Davis, M., A.J., 87 (1982) 1628.
Humason, M.L. et al, A.J., 61 (1956) 97.
Hunstead, R.W. et al, Proc. Astron. Soc. Astralia, 4 (1982) 447.
Hutchings, J.B. et al, Ap.J., 247 (1981) 743.
Hutchings, J.B. et al, Ap.J., 262 (1982) 48.
Hutchings, J.B. et al, Ap.J., 280 (1984) 41.
Heckman, T.M. et al, Ap.J., 262 (1982) 529.

Iriarte, B. & Chavira, E., Bol.Obs.Tonantzintla y Tucabaya 2, No.16 (1957) 3.

Jauncey, D.L. et al, Ap.J., 219 (1978) L1.
Jones, T.W. & Stein, W.A., Ap.J., 197 (1975) 297.

Katgert, J.K., A.Ap.Suppl., 31 (1978) 409.
Katz, J., Ap.J., 206 (1976) 910.
Kazaryan, M.A., Astrofizika, 15 (1979) 5.
Kazaryan, M.A., Astrofizika, 19 (1983) 411.
Kazaryan, M.A. & Khachikyan, E.E., Astrophys, 17 (1981) 354.
Kazaryan, M.A. et al, Astro. Tsir, 813 (1974) 2.
Kell, W.C., A.J., 85 (1980) 198.
Kell, W.C., Ap.J., 269 (1983a) 466.
Kell, W.C., Ap.J.Suppl.Ser., 52 (1983b) 229.
Keel, W.C., & Weedman, D.W., A.J., 83 (1978) 1.
Kellemann, K.I., In External Galaxies and Quasi-Stellar Objects, IAU Symp., 44, ed. D.S. Evans (1972) p190.
Kempe, J.C. et al, Ap.J. (Letters), 215 (1977) L107.
Khachikian, E.Ye. & Weedman, D.W., Astrophys, 7 (1971) 231.
Khachikian, E.Ye. & Weedman, D.W., Ap.J., 192 (1974) 581.
Khachikian, E.Ye. & Weedman, D.W., in "Redshifts and Expansion of the Universe", IAU Colloq., 37, ed. C.Balkowski & B. Westerlund (1977).
Khachikian, E.Ye. et al, Astrophys, 18 (1983) 308.
Kinman, T.D., M.N.R.A.S., 202 (1983) 53.
Kinman, T.D. et al, Ap.J., 147 (1967) 848.
Kinman, T. & Burbidge, E.M., Ap.J., 148 (1967) L59.

Kojoian, G. et al, Bull.Amer.Astron.Soc., 14 (1982) 947.
Kollatschny, W. & Fricke, K.J., A.Ap., 125 (1983) 276.
Kollatschny, W. & Fricke, K.J., A.Ap., 135 (1984) 171.
Kollatschny, W. et al, A.Ap., 119 (1983) 80.
Kopylov, I.M. et al, Astrophys, 10 (1974) 305.
Kopylov, I.M. et al, Astrophys, 12 (1976) 119.
Koski, A.T., Ap.J., 223 (1978) 56.
Kriss, G.A. et al, Ap.J., 242 (1980) 492.
Kriss, G.A. & Canizares, C.R., Ap.J., 261 (1982) 51.
Kristian, J. & Sandage, A., Ap.J., 162 (1970) 391.
Krolik, J.H. et al, Ap.J., 249 (1981) 422.
Krolik, J.H. & Vrtilek, J.M., Ap.J., 279 (1984) 521.
Kunth, D., 1981, private communication (Mkn 1395).
Kunth, D. & Sargent, W.L.W., A.Ap., 76 (1979a) 50.
Kunth, D. & Sargent, W.L.W., A.Ap.Suppl., 36 (1979) 259.

Lacy, J.H. et al, Ap.J., 256 (1982) 75.
Lauberts, A., 1982, The ESO/UPPSALA Survey of the ESO(B) Atlas, ESO Publications.
Laustsen, S., Sky and Telescope 53 (1977) 102.
Lawrence, A. & Elvis, M., Ap.J., 256 (1982) 410.
Lebofsky, M.J. & Rieke, G.H., Ap. J., 229 (1979) 111.
Lebofsky, M.J. & Rieke, G.H., Nature, 284 (1980) 410.
Lewis, D.W., McAlpine, G.M. and Koski, A.T., Bull. American. Astron. Soc., 10 (1978) 388.
Lindblad, P.D., 1978, Astronomical Papers Dedicated to Stroemgren, ed. REIZ p403.
Longair, M.S. & Gunn, J.E., M.N.R.A.S., 170 (1975) 121.
Lorre, J., Ap.J., 222 (1978) L99.
Lynden-Bell, D., Nature, 223 (1969) 690.
Lynden-Bell, D., Physica Scripta, 17 (1978) 185.
Lynds, C.R., Ap.J., 147 (1967) 396.
Lynds, C.R. et al, Ap.J., 142 (1965) 1667.
Lyutyi, V.M., Sov.Astron.AJ., 16 (1973) 263.
Lyutyi, V.M., Astrophys.Space Phys.Rev., 1 (1981) 61.
Lyutyi, V.M. & Pronik, V.I., in "Variable Stars and Stellar Evolution", ed. L. Plaut, Dordrecht: Reidel, (1975) p591.

MacAlpine, G.M. et al, Ap.J.Suppl., 35 (1977a) 203.
MacAlpine, G.M. et al, Ap.J.Suppl., 34 (1977b) 95.
MacAlpine, G.M. et al, Ap.J.Suppl., 35 (1977c) 197.

Maltby, P., Matthews, T.A. and Moffet, A.T., Ap.J., 137 1963) 153.
Malkan, M.A., Ap.J., 268 (1983) 582.
Malkan, M.A. & Sargent, W.L.W., Ap.J., 254 (1982) 22.
Markarian, B.E., Astrophys, 3 (1967) 24.
Markarian, B.E., Astrophys, 5 (1969a) 206.
Markarian, B.E., Astrophys, 5 (1969b) 286.
Markarian, B.E. & Lipovetski, V.A., Astrophys, 7 (1971) 299.
Markarian, B.E. & Lipovetski, V.A., Astrophys, 8 (1972) 89.
Markarian, B.E. & Lipovetski, V.A., Astrophys, 9 (1973) 283.
Markarian, B.E. & Lipovetski, V.A., Astrophys, 10 (1974) 185.
Markarian, B.E. & Lipovetski, V.A., Astrophys, 12 (1976a) 241.
Markarian, B.E. & Lipovetski, V.A., Astrophys, 12 (1976b) 429.
Markarian, B.E., Lipovetski, V.A. and Stepanian, D.A., Astrophys, 13 (1977a) 116.
Markarian, B.E., Lipovetski, V.A. and Stepanian, D.A., Astrophys, 13 (1977b) 215.
Markarian, B.E., Lipovetski, V.A. and Stepanian, D.A., Astrophys, 15 (1979a) 130.
Markarian, B.E., Lipovetski, V.A. and Stepanian, D.A., Astrophys, 15 (1979b) 235.
Markarian, B.E., Lipovetski, V.A. and Stepanian, D.A., Astrophys, 15 (1979c) 363.
Markarian, B.E., Lipovetski, V.A. and Stepanian, D.A., Soviet AJ Letters, 5 (1979d) 269.
Markarian, B.E., Lipovetski, V.A. and Stepanian, D.A., Astrophys, 16 (1980a) 1.
Markarian, B.E., Lipovetski, V.A. and Stepanian, D.A., Astrophys, 16 (1980b) 353.
Markarian, B.E., Lipovetski, V.A. and Stepanian, D.A., Astrophys, 17 (1981) 321.
Markarian, B.E., Lipovetski, V.A. and Stepanian, D.A., Astrophys, 19 (1983a) 14.
Markarian, B.E., Lipovetski, V.A. and Stepanian, D.A., Astrophys, 19 (1983b) 129.
Marshall, F.E, et al, Ap.J., 269 (1983) L31.
Martin, P.G. et al, Ap.J., 266 (1983) 470.
Martin, P.G. et al, Ap.J. (Letters), 209 (1976) L21.
Martin, P.G. et al, Ap.J., 255 (1982) 65.
Matthews, T.A. & Sandage, A., Ap.J., 138 (1963) 30.
Matthews, T.A. et al, Ap.J., 140 (1964) 35.
Mathis, J.S., Ap.J., 162 (1970) 761.
Mc Alary, C.W. et al, Ap.J., 234 (1979) 471.
Mc Alary, C.W. et al, Ap.J.Suppl., 52 (1983) 341.
Mc Clure, R.D. & van der Bergh, S., A.J., 73 (1968) 1008.
Mc Grimsey, B.Q. et al, A.J., 80 (1975) 895.
Meurs, E.J.A., 1982, Ph.D. Thesis, Leiden University.
Meurs, E.J.A. & Wilson, A.S., A.Ap.Suppl., 45 (1981) 99.
Miller, H.R., Publ.Astron.Soc.Pacific., 90 (1978) 661.
Miller, H.R., Publ.Astron.Soc.Pacific., 91 (1979a) 624.
Miller, H.R., A.Ap.Suppl., 35 (1979b) 387.
Miller, H.R., Ap.J., 227 (1979c) 52.

Miller, J.S., Ann.Rev.A.Ap., 12 (1974) 331.
Miley, G.K., M.N.R.A.S., 152 (1971) 477.
Minkowski,R., A.J., 73 (1968) 842.
Morgan, W.W., Publ.Astron.Soc.Pacific, 70 (1958) 364.
Morgan, W.W., Ap.J., 153 (1968) 27.
Morgan, W.W. & Dreiser, R., Ap.J., 269 (1983) 438.
Morgan, W.W. et al, in "Study Week On the Nuclei of Galaxies", ed. D.O'connell, 1971, p27.
Mushotzky, R.F., Ap.J., 256 (1982) 92.
Mushotzky, R.F. et al, Ap.J., 235 (1980) 377.
Markarian, B.e. & Stepanian, D.A., Astrophys, 19 (1984) 354.
Martin, P.G. et al, Ap.J., 266 (1983) 470.
Netzer, H., M.N.R.A.S., 171 (1975) 395.
Netzer, H., 24th International Astrophysical Colloquium Proceeding, 1983.
Netzer, H. & Wills, B.J., Ap.J., 275 (1983) 445.
Neugebauer, G. et al, Ap.J., 205 (1976) 29.
Neugebauer, G. et al, Ap.J., 230 (1979) 79.

O'connell, R.W. & Kingham, K.A., Publ.Astron.Soc.Pacific, 90 (1978) 244.
Oke, J.B., J.Roy.Astron.Soc.Canada, 72 (1978) 121.
Oke, J.B. & Sargent, W.L.W., Ap.J., 151 (1968) 807.
Oke, J.B. et al, Publ.Astron.Soc.Pacific, 92 (1980) 758.
Olsen, E.T., A.J., 75 (1970) 764.
Osmer, P.S. & Smith, M.G., Ap.J.Suppl.Ser., 42 (1980) 333.
Osmer, P.S., Smith, M.G. and Weedman, D.W., Ap.J., 189 (1974) 187.
Osterbrock, D.E., Ap.J., 160 (1970) 25.
Osterbrock, D.E., In Nuclei of Galaxies, ed. D.J.K. O'connell, 1971, p151.
Osterbrock, D.E., Ap.J., 215 (1977) 733.
Osterbrock, D.E., Active Galactic Nuclei, ed. C. Hazad & S. Mitton, 1979, p25.
Osterbrock, D.E., Ap.J., 246 (1981a) 676.
Osterbrock, D.E., Ap.J., 249 (1981b) 462.
Osterbrock, D.E., Q,Jl R.astr.Soc., 25 (1984) 1.
Osterbrock, D.E., Bull.Amer.Astron.Soc., 14 (1982) 910.
Osterbrock, D.E. & Dahari, O., Ap.J., 273 (1983) 478.
Osterbrock, D.E. & Grandi, S.A., Ap.J., 228 (1979) L59.
Osterbrock, D.E. & Koski, A.T., M.N.R.A.S., 176 (1976) 61p.
Osterbrock, D.E. & Miller, J.S., Ap.J., 197 (1975) 535.
Osterbrock, D.E. & Phillips, M.M., Publ.Astron.Soc.Pacific, 89 (1977) 251.
Osterbrock, D.E. & Shuder, J.M., Ap.J.Suppl., 49 (1982) 149.

Osterbrock, D.E. et al, Ap.J., 206 (1976) 898.
Osterbrock, D.E. et al, Publ.Astron.Soc.Pacific, 90 (1978) 493.
Ozernoy, L.M., Circular.Astr.Acad. de Ciencias, Moscu, No581 (1970) 58.
Ozernoi, L., Chertoprud, V.E. and Chuvekhin, S.D., Soviet AJ., 13 (1970) 1029.
Osterbrock, D.E., Bull.Amer.Astron.Soc., 11 (1979a) 637.

Pelat, D. & Alloin, D., A.Ap., 81 (1980) 172.
Pelat, D. et al, ESO Preprint, No98 (1980) 5+34pp.
Penfold, J.E., M.N.R.A.S., 186 (1979) 297.
Penston, M.V., "Objects of Hing Redshifts", eds. G.O.Abell & P.J.E.Peebles, 1980, p247.
Penston, M.V. et al, M.N.R.A.S., 169 (1974) 357.
Penston, M.V. et al, M.N.R.A.S., 180 (1977) 19.
Penston, M.V. et al, M.N.R.A.S., 189 (1979) 459.
Penston, M.V. et al, M.N.R.A.S., 196 (1981) 857.
Penston, M.V. et al, M.N.R.A.S., 208 (1984) 347.
Perola, G.C., Mem.S.A.It., 54,No 2 (1983) 385.
Peterson, B.A. & Bolton, J.G., Ap.Letters, 13 (1973) 187.
Peterson, B.A. et al, Ap.Letters, 17 (1976) 137.
Peterson, B.A. et al, Ap.J., 232 (1979) 400.
Peterson, B.A. et al, Publ.Astron.Soc.Pacific, 93 (1981) 281.
Peterson, B.A. et al, Ap.J.Suppl., 49 (1982) 469.
Peterson, B.A. et al, Ap.J., 279 (1984) 529.
Petre, R. et al, Ap.J., 280 (1984) 499.
Petrosian, A.R. et al, Astrophys, 14 (1978) 36.
Petrosian, A.R. et al, Astrophys, 15 (1979) 250.
Phillips, M.M., Ap.J.Suppl., 38 (1978) 187.
Phillips, M.M., Ap.J., 266 (1983) 485.
Piccinotti, G. et al, Ap.J., 253 (1982) 485.
Pineda, F. et al, IAU Circ., 3202 (1978).
Puschell, J.J., Publ.Astron.Soc.Pacific, 90 (1978) 652.
Pravdo, S.H. et al, Ap.J., 251 (1981) 501.

Rafanelli, P. & Schulz, H., A.Ap., 117 (1983) 109.
Rees, M.J., Physics Scripta, 17 (1978) 193.
Rees, M.J., Space Sci.Rev., 30 (1981a) 87.
Rees, M.J., Proc. of Internat. School and Workshop on Plasma Astrophys., 1981b, p267.
Rees, M.J., "Exagalactic Radio Sources", IAU Symp., No 97 (1982) 211.

Rees, M.J. & Sargent, W.L.W., Comment Astrophys.Space Phys. 4 (1972) 7.
Reichert, G.A. et al, Ap.J., 260 (1982) 437.
Ricker, G.R. et al, Nature, 271 (1978a) 35.
Ricker, G.R. et al, 21th Cospar Meeting, Innsbruck, ed, Baity and Peterson, 1978b,p281.
Rieke, G.H., Ap.J., 226 (1978) 550.
Roche, P.F. et al, M.N.R.A.S., 207 (1984) 35.
Rodgers, A.W. et al, Ap.J., 225 (1978) 768.
Rose, J.A. & Searle, L., Ap.J., 253 (1982) 556.
Rothschild, R.E. et al, Ap.J., 269 (1983) 423.
Rubin, V.C., Ap.J., 191 (1974) 645.
Rubin, V.C., Ap.J., 238 (1980) 808.
Rubin, V.C. & Ford, W.K., Ap.J., 154 (1968) 431.
Rubin, V.C. et al, Ap.J., 177 (1972) 31.
Rudy, R.J., Preprint (1984).
Rudy, R.J. et al, 253 (1982) 53.

Sandage, A., Ap.J., 139 (1964) 416.
Sandage, A., Ap.J., 141 (1965) 1560.
Sandage, A., Ap.J., 145 (1966) 1.
Sandage, A., Ap.J., 144 (1966a) 1234.
Sandage, A., Ap.J., 146 (1966b) 13.
Sandage, A., Ap.J., 150 (1967a) L9.
Sandage, A., Ap.J., 150 (1967b) L145.
Sandage, A., Ap.J., 150 (1967c) L177.
Sandage, A., in "Nuclei of Galaxies", ed. D.J.K.O'Connell, 1971, p271.
Sandage, A., Ap.J., 178 (1972) 25.
Sandage, A., Ap.J., 180 (1973) 357.
Sandage, A., Ap.J., 180 (1973a) 687.
Sandage, A., A.J., 83 (1978) 904.
Sandage, A.R. et al, Ap.J., 157 (1969) 55.
Sandage, A. & Brucato, R., A.J., 84 (1979) 472.
Sandage, A. & Luyten, W., Ap.J., 148 (1967) 767.
Sandage, A. & Tammann, G.A., 1981, A Revised Shapley-Ames Catalogue of Bright Galxies, Carnegie Institution of Washington Publication.
Sandage, A. et al, Ap.J., 142 (1965) 1307.
Sandage, A. & Wyndham, J., Ap.J., 141 (1965) 328.
Sanders, R.H. & Bania, T.M., Ap.J., 204 (1976) 341.
Sargent, W.L.W., Ap.J., 159 (1970a) 765.
Sargent, W.L.W., Ap.J., 160 (1970b) 405.

Sargent, W.L.W., 1971, In Nuclei of Galaxies, ed. D.J.K. O'Connell, p81.
Sargent, W.L.W., Ap.J., 173 (1972) 7.
Sargent, W.L.W., Ap.J., 212 (1977) L105.
Sargent, W.L.W. & Searle, L., Ap.J., 162 (1970) L155.
Savage, A., Bolton, J.G. and Wright,A.E., M.N.R.A.S., 179 (1977) 135.
Schewer, P.A.G. & Redhead, A.C.S., Nature, 277 (1979) 182.
Schilizzi, R.T., Mem.Roy.Astron.Soc., 79 (1975) 75.
Schmidt, M., Ap.J., 141 (1965) 1.
Schmidt, M., Ap.J., 151 (1968) 393.
Schmidt, M., Ap.J., 162 (1970) 371.
Schmidt, M., Ap.J., 176 (1972) 273.
Schmidt, M., Ap.J., 193 (1974) 505.
Schmidt, M. & Green, R.F., Ap.J., 269 (1983) 352.
Schmidt, G.D. & Miller, J.S., Ap.J., 240 (1980) 759.
Schmidt, G.D. & Miller, J.S., Ap.J., 253 (1982) 53.
Schmidt-Kaler, T., A.J., 72 (1967) 526.
Schnopper,H.M. et al, Ap.J., (Letters), 215 (1977) L7.
Schnopper,H.M. et al, Nature, 275 (1978) 719.
Schwartz, D.W., (COSAR)"X-Ray Astronomy", eds. W.A. Baity & L.E.Peterson, Pergaman Press, Oxford and New York, 1979, p453.
Schwarzschild, M., Ap.J., 182 (1973) 357.
Schulz, H. & Rafanelli, P., A.Ap., 103 (1981) 216.
Scott, R.L. et al, A.J., 81 (1976) 7.
Searle, L. & Bolton, J., Ap.J., 154 (1968) L101.
Seaton, M.J., M.N.R.A.S., 170 (1975) 475.
Sersic, J.L., "Extragalactic Astronomy", D.Reidel Pub.Com., Dordrecht, Holland, 1982.
Seyfert, C.K., Ap.J., 97 (1943) 28.
Shields, G.A., Ap.J., 191 (1974) 309.
Shields, G.A., Ap.Letters, 18 (1977) 119.
Shields, G.K., Nature, 272 (1978) 706.
Shields, G.A. et al, Ap.J., 176 (1972) 75.
Shuder, J.M., Ap.J., 240 (1980) 32.
Shuder, J.M., Ap.J., 259 (1982) 48.
Shuder, J.M. & Osterbrock, D.E., Ap.J., 250 (1981) 55.
Simkin, S.M., Ap.J., 200 (1975) 567.
Simkin, S.M. et al, Ap.J., 237 (1980) 404.
Smith, H.E. & Spinrad, H., Ap.J., 236 (1980) 419.
Smith, H.E. et al, Ap.J., 206 (1976) 345.
Smith, H.A. et al, Ap.J., 274 (1983) 571.

Smith, M.G., Ap.J., 202 (1975) 591.
Smith, M.G. et al, Ap.J.Suppl.Ser., 32 (1976) 217.
Snijders, M.A.J. et al, Proc. of Second European IUE Conference, Tubingen, Germany, 1980, p279.
Souffrin, S., A.Ap., 1 (1969) 305.
Spinrad, H. & Smith, H.E., Ap.J., 206 (1976) 355.
Sramek, R.A. & Tovmassian, H.M., Ap.J., 196 (1975) 339.
Sramek, R.A. & Tovmassian, H.M., Ap.J., 191 (1974) L13.
Sramek, R.A. & Weedman, D.W., Ap.J., 221 (1978) 468.
Stauffer, J.R., Ap.J., 262 (1982) 66.
Stauffer, J.R., Schild, R. and Keel, W., Ap.J., 270 (1983) 465.
Stein, W.A. & Weedman, D.W., Ap.J., 205 (1976) 44.
Steiner, J.E. et al, Ap.J., 259 (1982) 482.
Stocke, J. et al, Ap.J., 252 (1981) 69.
Stockton, A.N., A.J., 73 (1968) 887.
Stone, R.P.S., Ap.J.Suppl.Ser., 48 (1982) 395.
Stoughton, R. & Osterbrock, D.E., Publ.Astron.Soc.Pacific, 92 (1980) 117.
Su, H.J. & Simkin, S.M., Ap.J., 238 (1980) L1.
Sulentic, J.W., A.J., 81 (1976) 582.

Tananbaum, H. et al, 223 (1978) 74.
Tennant, A.F. & Mushotzky, R.F., Ap.J., 264 (1983) 92.
Tennat, A.F. et al, ApJ., 251 (1981) 15.
Terebizh, V.Y., Astrophys, 16 (1980) 36.
Theys, J.C. & Spiegel, E.A., Ap.J., 208 (1976) 650.
Thompson, I. et al, Ap.J., 229 (1979) 909.
Thompson, I. et al, M.N.R.A.S., 192 (1980) 53.
Tohlin, J.E. & Osterbrock, D.E., Ap.J., (Letters), 210 (1976) L117.
Tsvetanov, Z.I., Soviet AJ Letters, 7 (1981) 421.

Ulrich, M.H., Ap.J., 163 (1971) 441.
Ulrich, M.H., Ap.J., 181 (1973) 51.
Ulrich, M.H., A.Ap., 40 (1975) 337.
Ulrich, M.H. et al, M.N.R.A.S., 192 (1980) 561.
Ulrich, M.H. et al, M.N.R.A.S., 206 (1984) 221.
Ulvestad, J.S. & Wilson, A.S., 1983, "Radio Structure of Seyfert Galaxies. V. A Flux Limited Sample of Markarian Seyferts".
Ulvestad, J.S. & Wilson, A.S., Ap.J., 278 (1984) 544.

Van der Bergh, S., J.Roy.Astron.Soc.Canada, 69 (1975) 105.
Van der Kruit, P.C., A.Ap., 15 (1971) 110.
Vanderriest, C. & Lelievre, G., A.Ap., 56 (1977) 71.
de Vaucouleurs, S.G., Ap.J.Suppl.Ser., 5 (1961) 233.
de Vaucouleurs, S.G., Ap.J., 139 (1964) 899.
de Vaucouleurs, S.G. & de vaucouleurs, A., A.J., 73 (1968) 858.
de Vaucouleurs, S.G. & de Vaucouleurs, A., Ap.J., 197 (1975) L1.
de Vaucouleurs, S.G. & de Vaucouleurs, A., Mem.Roy.Astron.Soc., 77 (1972) 1.
de Vaucouleurs, S.G. et al, Second Reference Catalogue of Bright Galaxies, 1976.
de Vaucouleurs, S.G. et al, A.J., 83 (1978) 1331.
Veron, P., Nature, 272 (1978) 430.
Veron, P., A.Ap., 78 (1979) 46.
Veron, P., In "Physical Cosmology", eds. R. Balian et al. Les Houches, Session XXXII, North-Holland Pub.Com., 1980, p295.
Veron, M. P. & Veron, P., unpublished.
Veron-Cetty, M.P. & Veron, P., 1984, ESO Scientific Report, No 1.
Veron, M.P. et al, A.Ap., 98 (1981) 34.
Veron-Cetty, M.P. et al, A.Ap., 113 (1982) 46.
Veron, P. et al, A.Ap., 91 (1981) 71.
Visvanathan, N. & Oke, J.B., Ap.J. (Letters), 152 (1968) L165.

Wade, C.M., A.J., 73 (1968) 876.
Walker, M.F., A.J., 71 (1966) 184.
Walker, M.F., Ap.J., 151 (1968) 71.
Wall, J.V. & Connon, R.D., Australian J.Phys.Astrophys.Suppl., No 31, 1973.
Walsh, D. et al, M.N.R.A.S., 189 (1979) 667.
Wampler, E.J., Ap.J., 147 (1967) 1.
Wapler, E.J., Ap.J., 153 (1968a) 19.
Wampler, E.J., Ap.J.Letters, 154 (1968b) L53.
Wampler, E.J., Ap.J., 164 (1971) 1.
Wampler, E.J. et al, Ap.J., 276 (1984) 403.
Ward, M.J. & Wilson, A.S., A.Ap., 70 (1978) L79.
Ward, M.J. et al, A.Ap., 59 (1977) L19.
Ward, M.J. et al, Ap.J., 223 (1978) 788.
Ward, M.J. et al, M.N.R.A.S., 199 (1982) 953.
Wasilewski, A.J., Publ.Astron.Soc.Pacific, 93 (1981) 560.
Wasilewski, A.J., Ap.J., 272 (1983) 68.
Weedman, D.W., Ap.J., 159 (1970) 405.
Weedman, D.W., Ap.J., 183 (1973) 29.
Weedman, D.W., Ap.J., 208 (1976) 30.

Weedman, D.W., Q.JL.R.astro.Soc., 17 (1976) 227.
Weedman, D.W., Ann.Rev.A.Ap., 15 (1977) 69.
Weedman, D.W., M.N.R.A.S., 184 (1978) 11p.
Weedman, D.W. & Khachikian, E.E., Astrophys, 5 (1969) 51.
Wegner, G., Ap.S.S., 60 (1979) 15.
Wehinger, P.A. & Wyckoff, S., M.N.R.A.S., 181 (1977) 211.
West, R.M. et al, A.Ap.Suppl., 31 (1978a)55.
West, R.M. et al, A.Ap., 62 (1978b)L13.
West, R.M. et al, A.Ap., 65 (1978c) 151.
West, R.M. et al, 1980, "The Peculiar Seyfert Galaxy ESO o12-G21", ESO preprint N101.
West, R.M. et al, A.Ap.Suppl., 46 (1981) 57.
Westerlund, B.E. & Smith, L., Austral.J.Phys., 19 (1966) 181.
Westerlund, B.E. & Wall, J., A.J., 74 (1969) 335.
Weymann, R.J., Ap.J., 160 (1970) 31.
Wilkes, B.J. et al, Proc.Astron.Soc.Astralia, 5 (1983) 2.
Williams, R.E. & Weymann, R.J., A.J., 73 (1968) 895.
Wills, B.J., Nature, 251 (1974) 691.
Wills, B.J., A.J., 81 (1976) 1031.
Wills, B.J., Liege Astrophysical Colloquia, 24 (1983) 458.
Wills, B.J. & Wills, D., Ap.J.Suppl.Ser., 41 (1979) 689.
Wills, B.J. et al, A.J., 78 (1973) 521.
Wills, B.J., Netzer, H. and Wills, D., Ap.J., 1984 in press.
Wills, D. & lynds, R., Ap.J.Suppl., 36 (1978) 317.
Wills, D. & Wills, B.J., Ap.J., 190 (1974) 271.
Wilson, A.S., P c.R.Soc.London,A, 366 (1979) 461.
Wilson, A.S., in "Extragalactic Radio Sources" IAU Symp. No 97, 1982, p179.
Wilson, A.S & Willis, A.G., Ap.J., 240 (1980) 429.
Wilson, A.S. & Meurs, E.J.A., 1982, preprint.
Wilson, A.S. et al, A.J., 86 (1981) 1289.
Wing, R.F., A.J., 78 (1973) 684.
Woltjer, L., Ap.J., 130 (1959) 38.
Woltjer, L., A.J., 73 (1968) 914.
Woltjer, L. & Setti, G., Proc. of the Vatican Study Week on "Cosmology and Fundamental Physics", 1981.
Wright, A.E. et al, Ap.J., 211 (1977a) L115.
Wright, A.E. et al, Australia J. Phys. Suppl., 41 (1977b) 1.
Wu, C.C. et al, Ap.J., 266 (1983) 28.
Wyckoff, S. et al, Ap.J., 247 (1981) 750.
Wyndham, J., A.J., 70 (1965) 384.
Wyndham, J., Ap.J., 144 (1966) 459.

Yee, H., Ap.J., 241 (1980) 894.

Zamorani, G.,"VLBI and Compact Radio Sources" Symp. by the IAU, 1984, eds. R. Fanti et al, p85.

Zasov, A.V. & Lyutyi, N.V., Soviet Astron AJ, 17 (1973) 169.

Zotov, N. & Tapia, S., Ap.J., 229 (1979) L5.

Zwicky, F., Ap.J., 143 (1966) 192.

Zwicky, F. et al, Publ.Astron.Soc.Pacific, 82 (1970) 93.

Table 1 Measured Relative Line Fluxes

name	class	narrow lines			broad lines	
		[OIII] λ5007	H_β λ4861	H_α λ6563	H_α λ6563	H_β λ4861
Mkn 423	1.9	1.00	0.15	0.70	4.47	0.45
Mkn 516	1.8	1.00	0.29	3.61	3.56	0.50
Mkn 609	1.8	1.00	0.18	1.12	3.04	0.39
Mkn 1018	1.9	1.00	0.08	0.37	3.37	0.38
VZw 317	1.9	1.00	0.35	0.74	4.53	0.30

TABLE 3

SEYFERT 1 GALAXIES

Object	Class	b/a	V_R (km s^{-1})	FWZI of H (km s^{-1})	Log Lx(2-10 kev) (erg s^{-1})	Reference
NGC 1566	S	0.79	1170	4800		2
NGC 4051	S	0.77	700	6000 (Hβ)		3
NGC 6814	S	0.93	1440	6000	42.63	7,12
FA 51	S	0.47	4150	7500 (Hβ)	43.28	4,14
Mkn 358	S	0.7	13750	7800		1
MCG 8-11-11	S	0.75	6150	8000	43.94	5,12
Mkn 10	S	0.4	8790	12300		1
ESO 141-G55	S	0.65	11300	9400 (Hβ)	44.05	6
Mkn 618	S	0.5	10200	9600		1
NGC 3227	S	0.67	1000	11600	42.56	1,13
ESO 103-G35	RS	0.2	3990	6000 (Hα)	43.36	8
Mkn 382	RS	0.85	10200	7200		1
NGC 7469	RS	0.71	5020	8200	43.80	1,12
NGC 4151	RS	0.88	990	9000 (Hβ)	42.56	10,12
Mkn 590	RS	0.85	8100	11200	43.89	1,14
NGC 3783	RS	0.80	2740	9900 (Hβ)	43.23	9,12
Mkn 374	RS	0.5	13200	13200		1
Mkn 79	RS	0.65	6580	14600	43.80	1,12
Mkn 236	RS	0.8	15600	14000		1
Mkn 541	RR	0.55	12300	10100	43.92	1,12
ESO 113-IG45	RR	0.8	13830	10650 (Hβ)	44.34	6
Mkn 506	RR	0.65	12900	12000		1
NGC 7213	RR	0.9	1770	13000 (Hα)	42.50	11,14
NGC 3516	RR	0.66	2780	15200		1
3C 120	DR	0.6	9900	15000	44.43	1,12
NGC 5548	DR	0.71-0.88	4990	15100	43.40	1,12
Mkn 279	DR	0.55	9220	17700	44.24	1,9
MCG-2-58-22	DR	0.8	14380	22700 (Hβ)	44.72	6
Mkn 352	A	0.64	4500	13400		1
Mkn 290	A?		9240	13000		1
Mkn 110	A?		10800	13100		1
Mkn 504	A?	0.75	10800	12900		1
Mkn 486	A?		11700	13400		1
Mkn 509	A?	0.75	10650	14000	44.40	1,12
Mkn 376	A?	0.7	16800	19200	44.61	1,12
3C 382	A?		17580	25000	44.72	1,14
3C 390.3	A?		17100	18000	44.69	1,12
3C 445	A?		17000	14000	44.63	1,14

Reference

1. Osterbrock 1977
2. Martin 1974
3. Anderson 1970
4. Martin et al. 1978
5. Ward et al. 1977
6. Ward et al. 1978
7. Ulrich 1971
8. Phillips et al. 1979
9. Elvis et al. 1978
10. Boksenberg et al. 1975
11. Phillips 1979
12. Tananbaum et al. 1978
13. Griffiths et al. 1979
14. Marshall et al. 1979

TABLE 2

NAME	ALPHA	DELTA	TYPE	Z	V	B-V	U-B	AP	REFERENCES
UM 16	0 0 36.3	4 28 13	s2	0.058	17.0				144 317
MKN 335	0 3 45.2	19 55 29	s1	0.025	13.85	0.41	-0.70	15.0	152 287
MKN 334	0 0 35.6	21 40 54	s2?		14.62	0.68	-0.08	14.2	56 195
III ZW 2	0 7 56.7	10 41 47	s1	0.089	15.56	0.52	-0.70	10.1	118 42
UM 228	0 18 27.1	0 36 10	s2	0.098	17.0				143 76
ZW 0033+45	0 33 36.9	45 23 24	s1	0.048	15.3				132
MKN 955	0 35 2.0	0 0 21	s2	0.035	15.0				158 7
S10721	0 35 49.8	41 12 21	s1	0.072	17.0				30 184
MKN 957	0 39 9.8	40 5 5	s2	0.073	15.5				158 127
ES0012-G21	0 39 16.0	-79 30 54	s1	0.031	14.73	0.57	-0.25		297
IV ZW 29	0 39 32.3	40 3 10	s1	0.102	16.0				319 288
M 31	0 40 0.3	41 0 3	s2	0.000	10.5				213
PKS 0044+030	0 44 31.4	3 3 33	s1?	0.624	16.0				59 193
MKN 1146	0 44 42.2	14 25 50	s1	0.039	15.28	0.84	-0.38		160 272 163
MKN 1147	0 45 58.1	10 3 58	s1	0.036	16.0				160 182
MKN 348	0 46 4.9	31 41 4	s2	0.014	14.59	0.95	0.17	15.0	152 105 249
0048+29	0 48 53.1	29 7 46	s1	0.036	14.5				106
MKN 1148	0 49 16.5	17 9 41	s1	0.064	17.0				160 163
I ZW 1	0 50 57.8	12 25 20	s1	0.061	14.07	0.43	-0.67	17.0	290 118
TON S180	0 54 42.0	-22 38 0	s1	0.062	14.41	0.18	-0.94		53 272
0055.3+01	0 55 14.9	1 4 2	s2?	0.057	16.4	1.10	0.0	24.0	119
MKN 352	0 57 9.1	31 33 28	s1	0.015	14.81	0.44	-0.66	15.0	152 288
TOL 0109-38	1 9 9.8	-38 20 56	s2	0.011	14.12	0.88	0.12		246 272
MKN 975	1 11 12.4	13 0 26	s1.5	0.050	14.95	0.70	-0.50		158 272 6
MKN 1152	1 11 21.8	-15 6 39	s1.5	0.052	15.0	0.80	-0.28		160 272 163
MKN 1	1 13 19.6	32 49 33	s2	0.016	14.84	0.90	0.09	15.0	149 288 271
MKN 565	1 13 28.4	4 1 51	s?	0.021	13.5				154 144
F 294	1 13 45.0	-50 27 0	s2	0.017					79
PKS 0116+08	1 16 24.2	8 14 10	s2	0.594	20.7				303 234
II ZW 1	1 19 26.5	- 1 18 5	s1.5	0.054	15.17	0.56	-0.37	17.0	290 118
PG 0119+229	1 19 57.0	22 54 35	s1	0.053	15.41				239
NGC 513	1 21 42.0	33 33 0	s2	0.016	13.4				106
NGC 526A	1 21 42.0	-35 20 0	s1	0.018	14.60	0.97	0.09		97 272 200
ESO 113-IG45	1 21 51.2	-59 3 59	s1	0.045	13.44	0.31	-0.87	22.0	298
MKN 993	1 22 42.7	31 52 36	s2	0.017	14.12	0.91			158 72 6
MKN 358	1 23 45.0	31 21 25	s1	0.042	15.23	0.79	-0.32	17.0	152 290
MKN 359	1 24 50.3	18 55 12	s1	0.017	14.22	0.67	-0.21	11.7	152 63
MKN 1157	1 30 38.8	35 24 43	s2	0.015	15.5				160 183

TABLE 2

NAME	ALPHA	DELTA	TYPE	Z	V	B-V	U-B	AP	REFERENCES
PHL 1033	1 31 7.8	3 42 13	s1	0.255	18.70	-0.2	-0.3		145 98 238
PHL 1049	1 32 31.7	7 43 47	s1	0.147	17.26	0.61	-0.70		226 238
3C 48.0	1 34 49.8	32 54 20	s1?	0.367	16.20	0.42	-0.58		170 214 94
V ZW 85	1 37 35.7	31 59 38	s2	0.065	15.8				133
MKN 573	1 41 22.9	2 5 56	s2	0.017	14.07	0.83	0.02		154 272 7
UM 146	1 52 42.0	6 21 0	s1.5	0.017	14.5				145 199 183
MKN 1014	1 57 15.8	0 9 10	s1	0.163	15.69	0.46	-0.77		159 272 7
MKN 584	1 57 51.1	2 25 40	s1	0.078	15.24	0.65	-0.49		154 272 126
NGC 788	1 58 36.0	- 7 3 0	s2	0.013	13.2				106
3C 57	1 59 30.3	-11 47 0	s1?	0.670	16.4	0.14	-0.73		38 217 237
MKN 1018	2 3 42.6	- 0 31 47	s1	0.043	14.65	1.12	0.11		159 272 6
3C 59	2 4 8.8	29 16 30	s1	0.109	16.				176 288
F 377	2 9 2.0	-49 55 50	s2	0.046					80
MKN 590	2 12 0.4	- 0 59 57	s1.5	0.027	13.80	0.67	-0.55		179 272 125
AKN 79	2 14 19.7	38 10 59	s2	0.020	13.6				13 19
MKN 1400	2 17 42.0	7 59 0	s1	0.029	15.5				165 183
3C 67.0	2 21 18.1	27 36 38	s2	0.310	18.6				315 233
F 296	2 23 49.0	-63 26 50	s1						79
MKN 1040	2 25 16.5	31 5 18	s1.5	0.016	14.74	0.97	0.07	10.0	281 204
MKN 1044	2 27 38.2	- 9 13 11	s1	0.016	14.08	0.47	-0.71		159 272 6
MKN 1179	2 30 26.9	27 43 4	s1	0.038	16				160 91
NGC 985	2 32 10.5	- 9 0 21	s1	0.043	14.28	0.36	-0.95		268
NGC 1019	2 35 52.3	1 41 32	s1	0.024	14.95	0.76	-0.29		223 272
MKN 595	2 38 55.8	6 58 27	s1	0.028	14.69	0.77	-0.40		154 272 126
NGC 1068	2 40 7.0	- 0 13 31	s2	0.003	10.82	0.97	-0.03	15.0	118 192 227
4U 0241+61	2 41 0.6	62 15 27	s1	0.044	16.4				11
Q 0242-387	2 42 38.4	-38 47 37	s2	0.120	17.8				177
UKS0242-724	2 42 53.9	-72 29 30	s1	0.102	15.86	0.48	-0.89		9 272
NGC 1097	2 44 12.0	-30 29 6	s2	0.004	12.26	0.90	0.19	14.3	140 291 272
MKN 1187	2 45 37.3	13 43 39	s1	0.045	15.5				160 163
MKN 372	2 46 31.4	19 5 50	s1.5	0.031	14.81	1.05	-0.03	17.0	152 287
MKN 1058	2 46 47.0	34 46 54	s2	0.018	15.5				159 7
NGC 1144	2 52 38.5	- 0 23 7	s2	0.029	13.3				106
MKN 1066	2 56 49.8	36 37 21	s2	0.012	14.01	0.95		25.0	159 72 7
V ZW 317	3 1 0.0	31 11 0	s1	0.058	16.5				181
NGC 1229	3 6 0.0	-23 8 0	s2	0.035					199
4C 39.11	3 9 12.6	39 5 16	s1	0.161	18.2				5
MKN 1073	3 11 42.8	41 51 3	s2	0.023	14.18	0.87	-0.08	25.0	72 159 7
PKS 0312-77	3 12 56.3	-77 3 0	s1	0.223	16.10	0.16	-0.77		10 3 109
MKN 609	3 22 57.3	- 6 19 9	s2	0.032	14.12	0.60	-0.29		155 272 181

TABLE 2

NAME	ALPHA	DELTA	TYPE	Z	V	B-V	U-B	AP	REFERENCES
MKN 612	3 28 10.1	- 3 18 28	s2	0.020	15.5				155 7
NGC 1358	3 31 10.8	- 5 15 30	s2	0.013	13.05	1.05	0.51	37.3	199 95
NGC 1365	3 31 42.0	-36 18 18	s1	0.006	12.95	0.68	-0.04		135 269 138
NGC 1386	3 34 52.0	-36 9 54	s2	0.002	12.80	0.94	0.40		198 272 199
A 0335+09	3 35 57.1	9 48 27	s2?						56
PKS 0336-35	3 36 51.6	-35 32 30	s2	0.113	19.				52
III ZW 55	3 38 38.3	- 1 27 30	s2	0.025	15.22	0.84	0.17	11.0	231
3C 93.0	3 40 51.6	4 48 22	s1	0.357	19.17	0.35	-0.50		55 244 306
PKS 0353+027	3 53 22.4	2 47 43	s1?	0.602	18.6				245
3C 98.0	3 56 10.2	10 17 32	s2	0.031	15.3				148 236
3C 109.0	4 10 54.9	11 4 41	s1	0.306	18.01	0.95	-0.16		315 220 45
IE 0412-0803	4 12 27.0	- 8 3 8	s1	0.039	14.91	0.75	-0.55		253
3C 111.0	4 15 0.6	37 54 19	s1?	0.048	18.05	1.7			139 233
NGC 1566	4 16 53.3	-55 3 23	s1	0.004	13.17	0.76	-0.04	8.5	178 286 288
CARAFE NEB	4 26 34.4	-48 1 23	s2	0.016	14.89	1.18	0.84		100 272
F 303	4 29 33.0	-53 43 0	s1	0.038					79
3C 120	4 30 31.6	5 14 59	s1	0.033	14.27	0.58	-0.75	15.0	287 24 130
MKN 618	4 34 0.0	-10 28 36	s1	0.035	14.26	0.52	-0.47	25.0	71 155 65
NGC 1667	4 46 10.2	- 6 24 24	s2	0.015	12.86	0.80	0.13		271 199
F 239	4 47 58.0	-57 44 45	s2	0.023					78
NGC 1685	4 50 3.9	- 3 1 53	s2	0.014	15.18	1.03	0.12		272
IE 0449-184	4 49 26.3	-18 23 55	s2	0.338	18.5				254
0456+04	4 56 30.0	4 54 0	s1	0.019	14.0				106
X 0459+034	4 59 31.3	3 27 35	s1	0.016	15.				89
NGC 1808	5 6 0.0	-37 34 42	s?	0.003	12.55	0.98	0.23		87 275 272
UGC 3255	5 7 7.9	7 25 16	s2	0.019	15.6				106
AKN 120	5 51 9.7	- 0 12 16	s1	0.033	13.73	0.44	-0.52	25.0	71 72 203
PKS 0518-45	5 18 18.2	-45 49 48	s1	0.034	15.77	0.87	-0.31		62 300 236
NGC 2110	5 49 46.4	- 7 28 2	s2	0.007	15.2				44
0550-66	5 50 34.3	-66 37 34	s1	0.075	17.0				60
MCG 8-11-11	5 51 9.7	46 25 51	s1	0.020	14.10	0.90	-0.34	25.0	71 172 282
3A 0557-383	5 56 21.2	-38 20 15	s1	0.034	14.5				81
MKN 3	6 9 48.4	71 3 11	s2	0.014	13.34	1.15	0.15	15.0	149 287 286
F 251	6 26 32.0	-63 19 30	s?						78
MKN 6	6 45 43.9	74 29 10	s1.5	0.019	14.17	0.97	0.02	15.0	127 287 149
MKN 620	6 45 37.5	60 54 13	s2	0.006	12.5				155 106
MKN 374	6 55 34.5	54 15 57	s1	0.044	14.61	0.70	-0.38	17.0	152 287
F 265	6 56 6.0	-65 29 45	s?	0.030					78
0700+63	7 0 46.3	63 38 8	s1	0.152					99

TABLE 2

NAME	ALPHA	DELTA	TYPE	Z	V	B-V	U-B	AP	REFERENCES
VII ZW 118	7 2 24.1	64 40 39	s1	0.079	15.11	0.62	-0.60		132 272 183
MKN 376	7 10 36.2	45 47 7	s1	0.056	14.62	0.55	-0.58	10.1	152 290 288
4C 65.08	7 19 6.0	65 10 43	s?	0.218	18.7				57 279
MKN 9	7 32 42.2	58 52 56	s1	0.039	14.59	0.54	-0.64	15.0	287 149 290
3C 184.1	7 34 25.1	80 33 24	s2	0.119	17.				315 48
PKS 0736+01	7 36 42.5	1 44 0	s1	0.191	16.47	0.43	-0.77		35 221 188
MKN 78	7 37 56.8	65 17 42	s2	0.038	14.58	0.99	-0.31	15.0	151 287 15
MKN 79	7 38 47.3	49 55 41	s1.5	0.022	14.27	0.47	-0.78	10.0	151 67 14
MKN 10	7 43 7.4	61 3 25	s1	0.030	14.55	0.67	-0.55	15.0	149 287
IE0745+5545	7 45 8.2	55 45 27	s1	0.174	17.84	0.57	-0.86		129
MKN 382	7 52 3.6	39 19 7	s1	0.034	15.50	0.51	-0.63	10.1	152 290 288
MKN 1210	8 1 27.0	5 15 22	s2	0.013	15.				161 122
3C 192.0	8 2 35.5	24 18 27	s2	0.060	15.5				315 48
MKN 1212	8 4 2.5	27 16 16	s?	0.041	15.				161 164
MKN 622	8 4 21.0	39 8 59	s2	0.023	14.08	0.82	0.22	25.0	155 71 7
MKN 1218	8 35 13.2	25 4 18	s1	0.028	15.				161 91
VII ZW 244	8 38 32.0	77 3 59	s1	0.131	15.68	0.40	-0.70		132 272 239
NGC 2639	8 40 3.0	50 23 10	s1	0.011	11.76	0.89	0.37		106 270 115
E 0849+080	8 49 34.0	8 4 15	s1	0.063	16.0				205
MKN 1220	8 51 49.9	17 52 50	s1	0.064	16.5				161 164
MKN 704	9 15 39.4	16 30 59	s1.5	0.029	14.28	0.60	-0.40	25.0	58 71 66
MKN 106	9 16 18.6	55 34 20	s1	0.122	16.22	0.22	-0.90	10.0	67 232 151
MKN 110	9 21 44.4	52 30 8	s1	0.036	15.37	0.76	-0.67	15.0	287 151
MKN 705	9 23 20.0	12 57 4	s1	0.028	14.51	0.51	-0.41	25.0	71 66 289
PKS 0925-203	9 25 33.6	-20 21 45	s1	0.348	16.40	0.07	-0.87		39 2 194
MCG 5-23-16	9 31 20.0	27 33 0	s2	0.044	16.				183
MKN 707	9 34 26.5	1 19 14	s1	0.051	15.98	0.61	-0.70		239 272 288
0934+547	9 34 42.0	54 42 0	s2	0.100					167
0936+562	9 36 12.0	56 15 0	s1	0.117					167
MKN 403	9 37 55.7	21 27 43	s2	0.024	15.4				153 7
NGC 2992	9 43 18.0	-14 5 48	s1	0.007	13.78	1.06	0.40		49 275 199
3C 227.0	9 45 6.5	7 39 17	s1	0.086	16.33	0.98	-0.36		315 288 218
MKN 124	9 45 24.3	50 43 29	s1	0.056	15.33	0.61	-0.47	25.0	151 67 14
A 0945-30	9 45 28.4	-30 42 57	s2	0.008	13.70	1.05	0.45		240 272
MKN 1239	9 49 46.3	- 1 22 36	s1	0.019	14.39	0.60	-0.33		161 272 164
NGC 3031	9 51 27.3	69 18 8	s1	0.000	11.63	1.12	0.72		224 243
NGC 3081	9 57 10.0	-22 35 10	s2	0.007	13.56	0.90	0.26		272 199
NGC 3080	9 57 14.2	13 17 5	s1	0.035	15.01	0.67	-0.36		162 183 106
3C 234.0	9 58 57.4	29 1 38	s1	0.185	17.27	0.94	-0.41		96 221 236
1001-37	10 1 11.0	-37 10 0	s1	0.023	15.29	0.96	-0.08		27 272

TABLE 2

NAME	ALPHA	DELTA	TYPE	Z	V	B-V	U-B	AP	REFERENCES
MKN 715	10 2 5.2	15 1 21	s?	0.082	15.80	0.99	-0.34		156 71 6
MKN 716	10 7 27.5	23 21 19	s1.5	0.057	16.5				156 184 66
F 427	10 7 44.0	-42 33 30	s2	0.032					80
PG 1011-040	10 11 49.2	- 4 3 43	s1	0.058	15.49				239
MKN 720	10 15 0.6	7 13 17	s1	0.045	15.27	0.85	-0.22		156 272 6
MKN 141	10 15 39.3	64 13 6	s1	0.039	14.98	0.71	-0.32	15.0	151 287 14
NGC 3227	10 20 46.8	20 7 8	s1.5	0.003	13.43	0.86	0.02	10.4	58 192 212
MKN 142	10 22 23.0	51 55 50	s1	0.045	15.77	0.44	-0.58	10.0	67 151 288
TON 524A	10 28 46.4	29 2 27	s1	0.060	16.18	0.51	-0.47	15.0	108 71 288
NGC 3281	10 29 37.0	-34 35 48	s2	0.011	14.00	1.16	0.59		272 199
MKN 34	10 30 51.5	60 17 22	s2	0.051	14.76	1.06	0.07	15.0	149 288
1038+580	10 38 12.0	57 1 0	s1.5	0.067					167
NGC 3362	10 42 17.0	6 51 45	s2	0.028	15.				31 77
NGC 3393	10 46 0.0	-24 53 48	s2	0.012					272
4C 61.20	10 49 22.4	61 41 18	s1	0.422	16.48	0.18	-0.70		305 302 307
TOL 1049+064	10 49 35.0	6 25 45	s2	0.051	17.				31 77
MKN 1269	10 52 29.5	40 43 16	s1.5	0.120	17.				161 183
MKN 634	10 55 20.6	20 45 18	s1	0.066	15.31	0.67	-0.34	25.0	183 71 7
ESO 215-G14	10 57 7.0	-51 10 30	s2	0.019					42 293 82
A 1058+45	10 58 42.5	45 55 22	s2	0.029	14.1				106
MKN 728	10 58 24.0	11 19 0	s2	0.036	15.53	0.95	0.26	25.0	183 71 91
TOL 1059+105	10 59 21.0	10 33 48	s1	0.034	15.63	0.80	-0.56		31 272
PKS 1101-325	11 1 8.2	-32 35 5	s1	0.354	16.30	-0.01	-0.81		190 2 312
NGC 3516	11 3 22.8	72 50 20	s1	0.009	12.40	0.72	-0.23	24.0	267 4 288
ESO 438-G9	11 8 22.0	-28 13 42	s1	0.024					123 168
1116+583A	11 16 0.0	58 20 0	S?						
MKN 734	11 19 10.9	12 0 46	s1	0.049	14.81	0.32	-0.65	25.0	71 161 183
NGC 3660	11 21 0.5	- 8 23 16	s2	0.011	11.9				124
MKN 40	11 22 47.8	54 39 26	s1	0.020	15.39	0.82	-0.23	15.0	287 288 149
MKN 423	11 24 7.6	35 31 34	s1?	0.032	14.29	0.75	0.09	25.0	153 71 180
MKN 1298	11 26 43.6	- 4 7 36	s1	0.060	14.61	0.36	-0.77		161 272 164
1127+575	11 27 0.0	57 34 0	S						168
MKN 1447	11 27 42.0	49 51 0	s1.5	0.096	16.				165 183
MKN 176	11 29 55.4	53 13 35	s2	0.027	14.61	0.89	0.30	15.0	151 287 231
MKN 738	11 33 19.4	28 28 25	s?	0.039	15.30	0.67	0.04	25.0	156 71 6
MKN 739E	11 33 52.7	21 52 22	s1	0.030	14.08	0.78	-0.02	25.0	156 71 263
1136+579	11 36 6.0	57 59 0	s1	0.116					167
NGC 3783	11 36 33.0	-37 27 41	s1	0.009	13.49	0.68	-0.53	17.7	146 178 288
1136+595	11 36 12.0	59 30 0	s1	0.114					167
1136+594	11 36 24.0	59 28 0	s1.5	0.060					167
1136+34	11 36 35.9	34 12 28	s1?						56
1125+581	11 25 8.0	58 6 0	s2	0.051					167
1133+572	11 33 2.0	57 14 0	s2	0.051					167

TABLE 2

NAME	ALPHA	DELTA	TYPE	Z	V	B-V	U-B	AP	REFERENCES
MKN 744	11 37 4.9	32 11 11	s2	0.010	13.74	0.88	0.20	25.0	156 71 183
MKN 745	11 37 20.6	17 13 55	s?	0.010	14.62	0.39	-0.06	25.0	71 156 6
3C 263.0	11 37 9.3	66 4 28	s1	0.652	16.32	0.18	-0.56		228 85
WAS 26	11 38 40.0	22 14 0	s1	0.063	14.9				285
MKN 1457	11 44 36.0	52 43 0	s2	0.049	15.0				165 183
PKS 1146-037	11 46 23.9	- 3 47 30	s1	0.341	16.90	0.06	-0.74		36 2 312
PG 1149-110	11 49 30.9	-11 5 34	s1	0.049	15.46				239
MKN 42	11 51 5.7	46 29 24	s1	0.024	15.45	0.79	-0.19	15.0	149 290
NGC 3982	11 53 52.8	55 24 18	s2	0.003	11.7				199
NGC 3998	11 55 20.9	55 43 55	s1	0.004	12.1				70
I SZ 96	11 58 6.0	-20 34 0	s1	0.062	15.05	0.82	-0.01		272 208
MKN 1310	11 58 40.7	- 3 23 58	s1	0.019	16.5				162 164 183
NGC 4051	12 0 36.4	44 48 35	s1	0.002	13.63	0.73	-0.33	10.0	192 288
AKN 347	12 1 56.3	20 35 40	s2	0.022	14.44	0.99	0.37	25.0	13 71 20
GQ COM	12 2 8.9	28 10 54	s1	0.165	15.60	0.04	-0.96		40
PKS 1203+011	12 3 14.4	1 10 54	s?	0.104	18.2				36 312
NGC 4117	12 5 12.0	43 24 0	s2	0.003	14.3				106
MKN 198	12 6 43.2	47 20 7	s2	0.024	14.73	0.82	0.07	15.0	151 287 261
NGC 4151	12 8 1.0	39 41 2	s1.5	0.003	11.99	0.53	-0.72	13.5	64 317 185
NGC 4156	12 8 18.2	39 45 3	s2	0.022	14.32	0.69	-0.20		26 265
1213.6+51	12 13 38.7	51 6 12	s1.5	0.031	14.90	1.08	0.25	36.0	166 119
NGC 4235	12 14 36.7	7 28 9	s1	0.007	13.6	1.10	0.50	15.0	275 1
MKN 766	12 15 55.6	30 5 26	s1	0.012	13.55	0.72	0.06	25.0	289 71 66
PKS 1216-10	12 16 3.4	-10 3 56	s2	0.087	16.				61 235
MKN 1320	12 16 34.9	- 1 31 50	s1.5	0.103	15.				162 91 183
MKN 205	12 19 33.8	75 35 18	s1	0.070	15.24	0.40	-0.94	15.0	25 287
MKN 50	12 20 50.7	2 57 22	s1	0.023	15.24	0.76	-0.14	14.3	118 189 230
1222+04	12 22 48.0	4 37 52	s1	0.076	17.0				257
NGC 4388	12 23 15.0	12 56 18	s2	0.008	13.90	0.80	-0.06		275 199
3C 273	12 26 33.2	2 19 43	s1	0.158	12.8	0.21	-0.95		94 214 273
TON 1542	12 29 33.1	20 26 3	s1	0.064	14.93	0.38	-0.66	25.0	71 54 280
PKS 1233-24	12 32 59.4	-24 55 44	s1	0.355	17.18	0.36	-0.74		32 300 50
NGC 4593	12 37 4.6	- 5 4 11	s1	0.009	13.15	0.80	-0.19	15.5	275 137
TOL 1238-364	12 38 12.0	-36 29 0	s2	0.011	13.50	0.65	0.02		247 272 191
PG 1244+026	12 44 2.1	2 38 31	s1	0.048	16.15				239
MKN 231	12 54 5.0	57 8 38	s1	0.041	13.84	0.84	0.15	15.0	150 287 17
X COM	12 57 57.7	28 40 10	s1	0.092	16.65	0.58	-0.36	25.0	29 71 288
MKN 236	12 58 18.0	61 55 26	s1	0.052	15.48	0.66	-0.45	17.0	290 288 150
NGC 4922B	12 59 0.0	29 35 0	s2	0.024	15.0				106

TABLE 2

NAME	ALPHA	DELTA	TYPE	Z	V	B-V	U-B	AP	REFERENCES
MKN 783	13 0 30.4	16 40 34	s1	0.068	15.55	0.49	-0.50	25.0	156 71 183
NGC 4941	13 1 37.0	- 5 17 0	s2	0.003	13.0				116
NGC 4945	13 2 32.4	-49 12 0	s2	0.002	14.4				266 272
B 312	13 4 52.1	37 28 38	s1	0.184	16.97	0.41	-0.74		43
II SZ 10	13 10 28.0	-10 51 48	s1	0.034	15.15	0.33	-0.88		239 272 208
NGC 5033	13 11 9.2	36 51 30	s1	0.003	12.03	0.93	0.37	22.0	110 275 242
1318+605	13 18 8.0	60 31 0	s1.5	0.099	16.5				167
MKN 1347	13 20 24.9	8 25 19	s1	0.050	15.5				162 183
NGC 5135	13 22 57.0	-29 34 24	s2	0.013	13.35	0.64	-0.08		272 199
E 1327+321	13 27 25.0	32 8 17	s1	0.093	17.3				205
NGC 5194	13 27 45.7	47 27 16	s2	0.001	13.47	0.91	0.39		117 209
MKN 789	13 29 55.4	11 21 44	s1?						56
3C 287.1	13 30 20.5	2 16 8	s1	0.215	18.27	0.92	-0.15		315 218 288
MCG-6-30-15	13 33 1.5	-34 2 30	s1	0.006	13.58	0.95	0.34		272 201
1335+39	13 35 28.4	39 24 31	s2	0.020	14.2				106
NGC 5252	13 35 44.0	4 47 43	s2	0.022	14.25	0.98	0.26		272 77
MKN 266SW	13 36 14.7	48 29 6	s2	0.028	13.42	0.77	0.06		150 104 196
MKN 268	13 38 54.0	30 37 49	s2	0.041	14.66	0.94	0.28	15.0	287 17
MKN 270	13 39 41.4	67 55 27	s2	0.009	14.05	0.92	0.31	15.0	287 17 118
NGC 5273	13 39 55.1	35 54 21	s1	0.003	13.12	0.89	0.44		256 250
PKS 1340+05	13 40 12.4	5 19 38	s1	0.133	17.8				55 92
TON 730	13 41 36.8	25 53 55	s1	0.088	15.91	0.57	-0.84		108 215
MKN 273	13 42 51.7	56 8 14	s2	0.038	14.91	0.77	0.10	15.0	292 287 169
MKN 69	13 43 51.2	29 53 9	s1	0.076	15.93	0.52	-0.44	25.0	149 71 288
TOL 1344+038	13 44 40.0	3 54 0	s2	0.023	16.				31 77
IC 4329A	13 46 27.9	-30 3 41	s1	0.014	14.44	0.96	0.51		69 288
TOL 1347+023	13 47 22.0	2 20 15	s1	0.033	17.0				31 77
TOL 1350-383	13 50 6.0	-38 20 0	s2	0.060	15.				247 191
NGC 5347	13 51 4.0	33 44 12	s2	0.008	12.7				199
TOL 1351-375	13 51 18.0	-37 32 0	s1	0.052	15.37	1.25	0.10		247 31 191
MKN 662	13 51 46.4	23 40 32	s1.5	0.055	15.37	0.69	-0.24	25.0	183 71 7
MKN 279	13 51 53.6	69 33 13	s1.5	0.031	14.46	0.69	-0.45	15.0	58 287 17
MKN 463NE	13 53 39.8	18 36 58	s2	0.051	14.22	0.79	-0.10	25.0	153 71 65
MKN 464	13 53 45.5	38 49 7	s1	0.051	16.12	0.83	-0.77		153 272 65
OQ 208	14 4 45.6	28 41 29	s1	0.077	15.35	0.78	-0.05		311 48
1405.2-30	14 05 12.5	-30 9 44	s1.5?	0.023	15.50	0.57	-0.21	15.0	119
I ZW 81	14 6 24.0	49 5 0	s1	0.051	16.5				231
3C 295.6	14 9 36.3	57 27 34	s1	0.473	20.31				73 102
NGC 5506	14 10 38.8	- 2 58 22	s2	0.007	14.38	0.87	0.14		309 272
MKN 673	14 15 43.7	26 38 34	s2	0.036	15.				155 197

TABLE 2

NAME	ALPHA	DELTA	TYPE	Z	V	B-V	U-B	AP	REFERENCES
NGC 5548	14 15 43.5	25 22 1	s1.5	0.019	13.72	0.48	-0.64	13.5	58 4 288
PKS 1417-19	14 17 2.6	-19 14 42	s1	0.119	16.66	0.94	-0.48		33 300 45
MKN 471	14 20 46.9	33 4 37	s2	0.034	14.42	0.85	0.08	17.0	153 118 18
MKN 813	14 25 5.8	20 3 17	s1	0.131	15.01	0.22	-0.89		157 272 66
B2 1425+26	14 25 21.9	26 45 38	s1	0.366	15.68	0.20	-0.73		108 90
MKN 1383	14 26 33.8	1 30 27	s1	0.086	14.87	0.34	-1.04		162 272 183
NGC 5643	14 29 24.0	-43 59 0	s2	0.003	13.60	0.97	0.40		291 199
NGC 5674	14 31 22.5	5 40 38	s2	0.025	13.7				106
MKN 816	14 31 40.8	52 59 28	s?	0.089	16.5				157 7
MKN 474	14 33 6.1	48 52 47	s1	0.041	15.25	0.97	-0.18	17.0	153 118 28
MKN 817	14 34 57.9	59 0 39	s1.5	0.033	13.86	0.31	-0.57	25.0	157 71 66
MKN 686	14 35 19.7	36 47 2	s2	0.014	13.39	0.88	0.27	29.0	104 183 7
MKN 477	14 39 2.5	53 43 4	s2	0.038	14.61	0.72	-0.18	25.0	72 220 318
NGC 5728	14 39 37.0	-17 2 18	s2	0.009	13.40	0.94	0.30		211 275 199
MKN 478	14 40 4.6	35 39 7	s1	0.079	14.58	0.33	-0.84	10.1	153 125 118
3C 303.0	14 41 24.8	52 14 18	s?	0.141	17.29	1.08	-0.17		315 222
ESO 273-IG04	14 45 26.0	-43 34 24	s2	0.037	14.72	0.95	0.18		41 272
3C 305.0	14 48 17.4	63 28 36	s2	0.042	13.74				315 101
PG 1448+273	14 48 58.6	27 21 42	s1	0.065	15.01				239
MKN 830	14 49 7.3	58 52 4	s1	0.210	16.0				157 187
MKN 841	15 1 36.3	10 37 56	s1.5	0.036	14.48	0.37	-0.65	25.0	72 66 58
MKN 1392	15 3 26.0	3 54 0	s1.5	0.036	14.35	0.99	0.14	36.0	119 273
MKN 845	15 6 12.6	51 38 37	s1	0.042	15.15	0.82	-0.02	25.0	183 72 28
1506.3-00	15 6 20.1	-00 0 24	s1.5?	0.054	15.10	1.01	-0.14	24.0	119
MKN 1395	15 8 35.0	4 28 59	s1		15.5				162 131
PKS 1510-08	15 10 8.9	- 8 54 48	s1	0.361	16.52	0.17	-0.74		35 47
B2 1512+37	15 12 46.8	37 1 55	s1	0.370	15.5				176 46
MKN 688	15 14 18.0	19 16 0	s1?						12
3C 318.0	15 17 50.6	20 26 54	s2	0.752	20.9	1.03			314 248
MKN 849	15 17 50.8	28 45 23	s1	0.079	17.				157 66
1518+593	15 18 18.0	59 19 0	s1	0.079					167
NGC 5929	15 24 18.9	41 50 41	s2	0.008	14.0				106
MKN 854	15 24 37.4	43 34 15	s1	0.156	17.5				157 187
MKN 1098	15 27 37.9	30 39 23	s1	0.035	15.5				160 183
NGC 5940	15 28 51.3	7 37 38	s1	0.033	14.90	0.66	-0.20		106 272
E 1530-085	15 30 37.0	- 8 31 22	s2	0.023	15.7				205
4C 35.37	15 31 45.2	35 54 21	s1	0.156	17.8				176 288
1532+01/2	15 32 20.6	1 40 10	s1	0.310					301
1533+14	15 33 32.8	14 40 57	s2	0.020	14.7				106
MKN 290	15 34 44.8	58 4 0	s1	0.029	14.96	0.60	-0.62	15.0	287 17

TABLE 2

NAME	ALPHA	DELTA	TYPE	Z	V	B-V	U-B	AP	REFERENCES
MKN 486	15 35 20.7	54 43 22	s1	0.039	14.78	0.43	-0.68	10.1	153 118 125
MKN 860	15 37 19.0	25 6 34	s?	0.023	14.80	0.77	0.10	25.0	157 72 6
MKN 291	15 52 54.1	19 20 16	s1	0.035	15.51	0.64	-0.08	25.0	72 288 17
MKN 1102	15 55 27.7	41 41 11	s2	0.035	16.5				160 122
MKN 1103	15 55 41.0	41 40 28	s2	0.034	16.				160 122
E 1556+259	15 56 15.0	25 59 15	s1	0.070	17.1				205
E 1556+274	15 56 25.2	27 25 39	s1	0.090	16.9				205
MKN 493	15 57 16.3	35 10 15	s1	0.031	14.99	0.59	-0.51		153 272 183
3C 327.0	15 59 55.7	2 6 12	s2	0.104	16.31	1.39	0.28		315 221 236
MKN 871	16 6 15.5	12 27 44	s1	0.034	14.50	0.70	-0.20	25.0	289 72 66
MKN 876	16 13 36.2	65 50 37	s1	0.129	15.29	0.47	-0.66	25.0	289 68 66
1614 +35	16 14 40.1	35 49 50	S1?						
H 1613+06	16 15 18.2	6 11 12	s1	0.038	15.66	0.89	-0.30		202 272 56
3C 332.0	16 15 47.1	32 29 50	s1	0.152	16.				315 48
MKN 877	16 17 56.5	17 31 35	s1	0.114	15.46	0.17	-1.00		157 272 66
MKN 699	16 22 5.3	41 11 48	s1	0.034	15.11	0.71	-0.19	25.0	263 72 175
MKN 1498	16 26 48.0	51 53 0	s1.5	0.056					166
MKN 883	16 27 47.1	24 33 7	s2	0.038	15.14	0.95	-0.24		183 272 66
MKN 885	16 29 42.9	67 29 6	s1	0.026	14.56	0.82	-0.17	25.0	183 68 7
VII ZW 653	16 36 0.0	85 36 0	s1	0.063	16.3				133
NGC 6251	16 37 56.9	82 38 18	s2	0.024					243
NGC 6221	16 48 25.0	-59 8 0	s2	0.004	13.45	0.96	0.17		74 291 274
NGC 6240	16 50 27.8	2 28 55	s2	0.024	13.37	0.94	0.56		86 22
MKN 504	16 59 10.4	29 28 44	s1	0.036	15.58	0.85	-0.47	10.1	118 18 288
UGC 106838	17 2 24.7	- 1 28 23	s1	0.031	15.55	1.29	0.22		310 272
NGC 6300	17 12 18.0	-62 45 48	s2	0.003	13.1				74 199
ARP 1028	17 17 56.3	49 1 58	s1	0.025	14.7				23 251
V 396HER	17 20 37.7	24 39 6	s1	0.175	16.38	0.47	-0.89		40
MKN 506	17 20 45.6	30 55 40	s1.5	0.043	14.68	0.74	-0.55	17.0	118 58 125
PKS 1733-56	17 33 21.5	-56 32 16	s2	0.098	17.				107
MKN 507	17 48 55.8	68 43 5	s2	0.053	15.45	0.88	0.19	10.1	118 273
KAZ 102	18 3 37.4	67 37 54	s1	0.136	15.78	0.26	-0.84		111 112 113
3C 380.0	18 28 13.5	48 42 40	s1	0.691	16.81	0.24	-0.59		229 217 142
1831+731	18 31 28.6	73 10 56	s1	0.123	15.5				304
3C 381.0	18 32 24.5	47 24 40	s1	0.161	17.24	1.40			315 221 219
3C 382.0	18 33 12.0	32 39 18	s1	0.059	15.39	1.11	-0.10		315 221 288
ESO 103-G35	18 33 22.0	-65 28 18	s1	0.013	14.84	0.85	-0.63	13.6	146 103 84
ESO 103-G56	18 38 27.0	-64 9 15	s1	0.011					169 82
ESO 140-G43	18 40 14.6	-62 24 58	s1	0.014	14.10	0.73	-0.17		296
KAZ 163	17 4 18.0	68 38 00	s1	0.063	16.5	0.64			111

TABLE 2

NAME	ALPHA	DELTA	TYPE	Z	V	B-V	U-B	AP	REFERENCES
F 334	18 44 11.0	-53 12 30	s2	0.018					79
3C 390.3	18 45 37.6	79 43 6	s1	0.057	15.38	0.68	-0.69		315 288
PKS 1912-549	19 12 35.2	-55 0 8	s1	0.398	16.49	0.09	-0.81		278 3 109
ESO 141-G55	19 16 57.0	-58 45 52	s1	0.037	13.95	0.34	-0.99	17.7	283 146
F 513	19 18 25.0	-74 4 0	s2	0.070					80
NGC 6814	19 39 55.4	-10 26 37	s1	0.005	13.80	1.19	-0.20	25.0	68 288
F 339	20 7 59.0	-57 14 0	s1	0.054					79
NGC 6890	20 14 48.0	-44 58 0	s2	0.008	14.02	0.97	0.37		291 199
F 341	20 16 13.0	-52 47 0	s2	0.016					79
F 348	20 33 24.0	-50 15 50	s2	0.008					79
MKN 509	20 41 26.2	-10 54 17	s1	0.035	13.12	0.23	-0.93	17.0	288 252 125
MKN 896	20 43 44.5	- 2 59 46	s1	0.027	14.61	0.66	-0.28		183 272 6
PKS 2048-57	20 48 12.1	-57 15 25	s2	0.011	13.60	1.09	0.38		51 291 199
PKS 2128-12	21 28 52.7	-12 20 20	s1	0.501	15.99	0.13	-0.67		120 241
II ZW 136	21 30 1.2	9 55 1	s1	0.061	14.53	0.29	-0.90	17.0	287 75
IC 5135	21 45 18.0	-35 11 0	s2	0.016	13.87	0.62	0.02		74 291 199
MKN 516	21 53 52.9	7 7 43	s1?	0.028	15.01	0.86	0.15		154 272 181
NGC 7172	21 59 7.2	-32 6 36	s2	0.008	13.61	1.07	0.59		210 95 270
E 2204+468	22 4 26.0	46 50 4	s1	0.163	19.7				205
NGC 7212	22 4 33.9	9 59 20	s2	0.026					284
NGC 7213	22 6 12.0	-47 25 0	s1	0.006	12.09	1.02	0.47		313 272 270
PKS 2206-237	22 6 32.1	-23 46 37	s2	0.087	17.0				39 92
PG 2209+184	22 9 30.2	18 27 1	s1	0.070	15.86				239
MKN 304	22 14 45.8	13 59 20	s1	0.067	14.66	0.36	-0.86	17.0	152 118
3C 445.0	22 21 14.8	- 2 21 26	s1	0.057	15.77	1.16	-0.17		96 218 236
F 357	22 23 39.0	-70 39 0	s2	0.028					79
NGC 7314	22 33 0.2	-26 18 32	s1	0.006	13.11	0.84	0.36		271 250
NGC 7319	22 33 46.0	33 42 59	s2	0.022	14.8				106
MKN 915	22 34 7.3	-12 48 17	s1.5	0.025	14.61	0.99	-0.03	15.0	183 72 7
2237+07	22 37 46.5	7 47 34	s1	0.025	14.3				106
MKN 917	22 38 48.1	31 54 30	s2	0.025	14.10	0.85	0.24	25.0	72 7 158
AKN 564	22 40 18.3	29 27 48	s1	0.025	14.16	0.70	-0.33		259 13 21
MR 2251-178	22 51 25.9	-17 50 54	s1	0.068	14.11	0.52	-0.86		206 207 273
MKN 1126	22 58 10.0	-13 11 15	s1.5	0.010	14.33	0.86	0.11		160 272 163
PKS 2300-18	23 0 23.5	-18 57 36	s1	0.129	17.82	0.62	-0.19		33 300 241
NGC 7469	23 0 44.4	8 36 16	s1.5	0.017	13.12	0.44	-0.72	13.5	288 316 58
MKN 315	23 1 35.7	22 21 16	s1.5	0.040	14.83	0.97	-0.08	14.2	127 195
MKN 926	23 2 7.2	- 8 57 2[illegible]	s1.5	0.047	14.21	0.68	-0.59	25.0	58 72 283

TABLE 2

NAME	ALPHA	DELTA	TYPE	Z	V	B-V	U-B	AP	REFERENCES
PG 2304+042	23 4 30.1	4 16 41	s1	0.042	15.44				239
IE 2304-2259	23 4 57.5	-22 59 19	s2	0.193					253
NGC 7496	23 6 59.3	-43 41 57	s2	0.050	16.60	0.87	-0.94		277 8
ESO 148-IG02	23 12 51.0	-59 19 36	s2	0.044	14.73	0.48	-0.10		296
NGC 7582	23 15 38.3	-42 38 39	s2	0.005	13.57	0.87	0.17		291 277 87
NGC 7590	23 16 10.0	-42 30 42	s2	0.005	13.76	0.96	0.36		291 272
NGC 7603	23 16 22.9	- 0 1 47	s1	0.029	14.01	0.72	-0.21		154 288
PKS 2322-12	23 22 43.7	-12 23 56	s2	0.082	17.2				236 96
NGC 7672	23 25 0.0	12 7 0	s2	0.013	14.8				106
MKN 533	23 25 24.4	8 30 13	s2	0.029	14.36	0.83	-0.02		154 271 7
NGC 7682	23 26 30.7	3 15 28	s2	0.017	14.3				106 24
UM 163	23 27 58.0	- 2 44 20	s1		14.86	0.92	-0.23		145 272
MKN 930	23 29 29.5	28 40 18	s2	0.018	15.				266 122
PKS 2344+09	23 44 3.9	9 14 5	s1	0.677	15.97	0.26	-0.60		120 121
IE23486+198	23 48 41.3	19 47 5	s1	0.045					90
MKN 541	23 53 28.4	7 14 41	s1	0.040	15.14	0.93	-0.15	15.7	179 146 125
IC 1515	23 53 36.0	- 1 16 0	s2	0.023					199
PKS 2356-61	23 56 29.4	-61 11 41	s2	0.096	16.				299 61
MKN 543	23 59 52.5	3 4 27	s1	0.026	14.68	0.65	-0.09		154 272 126

REFERENCES TO TABLE 2

1. Abell et al. 1978
2. Adam 1978
3. Adam 1982
4. Adams 1977
5. Adams & Rudnick 1977
6. Afanasjev et al. 1977a
7. Afanasjev et al. 1979b
8. Alcaino 1976
9. Allen et al. 1978
10. Anguita & Pedreros 1977
11. Apparao et al. 1978
12. Aptekx et al. 1982
13. Arakelian 1975
14. Arakelian et al. 1970a
15. Arakelian et al. 1970b
16. Arakerian et al. 1970c
17. Arakerian et al. 1971
18. Arakerian et al. 1973
19. Arakerian et al. 1975
20. Arakerian et al. 1976a
21. Arakerian et al. 1976b
22. Arkhipova & Esipov 1979
23. Arp 1966
24. Arp 1968
25. Arp 1971
26. Arp 1977
27. Arp 1981
28. Arp & Khachikian 1975
29. Barbieri 1973
30. Barbieri & Romano 1976
31. Bohuski et al. 1978
32. Bolton & Ekers 1966a
33. Bolton & Ekers 1966b
34. Bolton & Ekers 1966c
35. Bolton & Kinman 1966
36. Bolton & Wall 1970
37. Bolton et al. 1971
38. Bolton et al. 1966
39. Bolton et al. 1975
40. Bond et al. 1977
41. Borchkhadze & West 1977
42. Borchkhadze & West 1980
43. Braccesi et al. 1968
44. Bradt et al. 1978
45. Burbidge 1967
46. Burbidge 1968
47. Burbidge & Kinman 1966
48. Burbidge & Strittmatter 1972
49. Burbidge et al. 1972
50. Burbidge & Burbidge 1969
51. Caldwell & Phillips 1981
52. Carter & Malin 1983
53. Chavira 1958
54. Chavira 1959
55. Clarke et al. 1966
56. Clements 1983
57. Cohen et al. 1977
58. Cohen 1983
59. Condon et al. 1976
60. Cristiani & Tarenghi 1983
61. Danziger & Goss 1983
62. Danziger et al. 1977
63. Davidson & Kinman 1978
64. Davies 1973
65. Denisyuk & Lipovetski 1974
66. Denisyuk & Lipovetski 1977
67. Dibai 1970
68. Dibai et al. 1981
69. Disney 1973
70. Disney & Cromwell 1971
71. Doroshenko & Terebizh 1979
72. Doroshenko & Terebizh 1981
73. Dressler & Gunn 1983
74. Dressler & Sandage 1978
75. Fairall 1968
76. Fairall 1978
77. Fairall 1980a
78. Fairall 1980b
79. Fairall 1981
80. Fairall 1983
81. Fairall et al. 1982
82. Fairall et al. 1983
83. Fanti et al. 1975
84. Feldman et al. 1978
85. Ford & Rubin 1966
86. Fosbury & Wall 1979
87. Garrison & Walborn 1974
88. Gaston 1983
89. Chigo et al. 1982
90. Gioia et al. 1983
91. Goodrich & Osterbrock 1983
92. Grandi 1983 a
93. Greenstein & Oke 1970
94. Greenstein & Schmidt 1964
95. Griesmith 1980
96. Griffin 1963
97. Griffiths et al. 1979
98. Haro & Luyten 1962
99. Harris et al. 1982
100. Hawarden et al. 1979
101. Heckman et al. 1982
102. Henry et al. 1983
103. Holmberg et al. 1977
104. Huchra 1977
105. Huchra 1980
106. Huchra et al. 1982
107. Hunstead et al. 1982
108. Iriarte & Chavira 1957
109. Jauncey et al. 1978
110. Katgert 1978
111. Kazaryan 1979
Kazaryan 1983
112. Kazaryan & Khachikyan 1981
113. Kazaryan et al. 1974
114. Keel 1980
115. Keel 1983a
116. Keel 1983b
117. Keel & Weedman 1978
118. Khachikian & Weedman 1974

119. Kinman 1983
120. Kinman et al. 1967
121. Kinman & Burbidge 1967
122. Kojoian et al. 1982
123. Kollatschny & Fricke 1983
124. Kollatschny et al. 1983
125. Kopylov et al. 1974
126. Kopylov et al. 1976
127. Koski 1978
128. Kriss et al. 1980
129. Kriss & Canizares 1982
130. Kristian & Sandage 1970
131. Kunth 1981
132. Kunth & Sargent 1979a
133. Kunth & Sargent 1979b
134. Lauberts 1982
135. Laustsen 1977
136. Lawrence & Elvis 1982
137. Lewis et al. 1978
138. Lindblad 1978
139. Longair & Gunn 1975
140. Lorre 1978
141. Lynds 1967
142. Lynds et al. 1965
143. Mac Alpine et al. 1977a
144. Mac Alpine et al. 1977b
145. Mac Alpine et al. 1977c
146. Mc Alary et al. 1983
147. Mc Clure & van der Bergh 1968
148. Maltby et al. 1963
149. Markarian 1967
150. Markarian 1969a
151. Markarian 1969b
152. Markarian & Lipovetski 1971
153. Markarian & Lipovetski 1972
154. Markarian & Lipovetski 1973
155. Markarian & Lipovetaki 1974
156. Markarian & Lipovetski 1976a
157. Markarian & Lipovetski 1976b
158. Markarian et al. 1977a
159. Markarian et al. 1977b
160. Markarian et al. 1979a
161. Markarian et al. 1979b
162. Markarian et al. 1979c
163. Markarian et al. 1979d
164. Markarian et al. 1980
165. Markarian et al. 1981
166. Markarian et al. 1983a
167. Markarian et al. 1983b
168. Markarian & Stepanyan 1984
169. Martin et al. 1983
170. Matthews & Sandage 1963
171. Meurs 1982
172. Miller 1979
173. Mushotzky et al. 1980
174. Neugebauer et al. 1976
175. O'connell & Kingham 1978
176. Olsen 1970
177. Osmer & Smith 1980
178. Osmer et al. 1974
179. Osterbrock 1977
180. Osterbrock 1979
181. Osterbrock 1981
182. Osterbrock 1982
183. Osterbrock & Dahari 1983
184. Osterbrock & Grandi 1979
185. Osterbrock & Koski 1976
186. Osterbrock & Phillips 1977
187. Osterbrock et al. 1978
188. Ozenoi et al. 1970
189. Penfold 1979
190. Penston & Bolton 1973
191. Penston et al. 1977
192. Penston et al. 1974
193. Peterson et al. 1976
194. Peterson et al. 1979
195. Peterson et al. 1981
196. Petrosian et al. 1977
197. Petrosian et al. 1979
198. Phillips & Frogel 1980
199. Phillips et al. 1983
200. Piccinotti et al. 1982
201. Pineda et al. 1978
202. Provdo et al. 1981
203. Puschell 1978
204. Rafanelli & Schulz 1983
205. Reichert et al. 1982
206. Ricker et al. 1978a
207. Ricker et al. 1978b
208. Rodgers et al. 1978
209. Rose & Searle 1982
210. Rubin 1974
211. Rubin 1980
212. Rubin & Ford 1968
213. Rubin et al. 1972
214. Sandage 1964
215. Sandage 1965
216. Sandage 1966a
217. Sandage 1966b
218. Sandage 1967a
219. Sandage 1967b
220. Sandage 1967c
221. Sandage 1972
222. Sandage 1973
223. Sandage 1978
224. Sandage et al. 1969
225. Sandage & Brucato 1979
226. Sandage & Luyten 1967
227. Sandage & Tammann 1981
228. Sandage et al. 1965
229. Sandage & Wyndham 1965
230. Sargent 1970a
231. Sargent 1970b
232. Sargent 1972
233. Sargent 1977
234. Savage et al. 1977
235. Schilizzi 1975
236. Schmidt 1965
237. Schmidt 1968
238. Schmidt 1974

119. Kinman 1983
120. Kinman et al. 1967
121. Kinman & Burbidge 1967
122. Kojoian et al. 1982
123. Kollatschny & Fricke 1983
124. Kollatschny et al. 1983
125. Kopylov et al. 1974
126. Kopylov et al. 1976
127. Koski 1978
128. Kriss et al. 1980
129. Kriss & Canizares 1982
130. Kristian & Sandage 1970
131. Kunth 1981
132. Kunth & Sargent 1979a
133. Kunth & Sargent 1979b
134. Lauberts 1982
135. Laustsen 1977
136. Lawrence & Elvis 1982
137. Lewis et al. 1978
138. Lindblad 1978
139. Longair & Gunn 1975
140. Lorre 1978
141. Lynds 1967
142. Lynds et al. 1965
143. Mac Alpine et al. 1977a
144. Mac Alpine et al. 1977b
145. Mac Alpine et al. 1977c
146. Mc Alary et al. 1983
147. Mc Clure & van der Bergh 1968
148. Maltby et al. 1963
149. Markarian 1967
150. Markarian 1969a
151. Markarian 1969b
152. Markarian & Lipovetski 1971
153. Markarian & Lipovetski 1972
154. Markarian & Lipovetski 1973
155. Markarian & Lipovetaki 1974
156. Markarian & Lipovetski 1976a
157. Markarian & Lipovetski 1976b
158. Markarian et al. 1977a
159. Markarian et al. 1977b
160. Markarian et al. 1979a
161. Markarian et al. 1979b
162. Markarian et al. 1979c
163. Markarian et al. 1979d
164. Markarian et al. 1980
165. Markarian et al. 1981
166. Markarian et al. 1983a
167. Markarian et al. 1983b
168. Markarian & Stepanyan 1984
169. Martin et al. 1983
170. Matthews & Sandage 1963
171. Meurs 1982
172. Miller 1979
173. Mushotzky et al. 1980
174. Neugebauer et al. 1976
175. O'connell & Kingham 1978
176. Olsen 1970
177. Osmer & Smith 1980
178. Osmer et al. 1974
179. Osterbrock 1977
180. Osterbrock 1979
181. Osterbrock 1981
182. Osterbrock 1982
183. Osterbrock & Dahari 1983
184. Osterbrock & Grandi 1979
185. Osterbrock & Koski 1976
186. Osterbrock & Phillips 1977
187. Osterbrock et al. 1978
188. Ozenci et al. 1970
189. Penfold 1979
190. Penston & Bolton 1973
191. Penston et al. 1977
192. Penston et al. 1974
193. Peterson et al. 1976
194. Peterson et al. 1979
195. Peterson et al. 1981
196. Petrosian et al. 1977
197. Petrosian et al. 1979
198. Phillips & Frogel 1980
199. Phillips et al. 1983
200. Piccinotti et al. 1982
201. Pineda et al. 1978
202. Provdo et al. 1981
203. Puschell 1978
204. Rafanelli & Schulz 1983
205. Reichert et al. 1982
206. Ricker et al. 1978a
207. Ricker et al. 1978b
208. Rodgers et al. 1978
209. Rose & Searle 1982
210. Rubin 1974
211. Rubin 1980
212. Rubin & Ford 1968
213. Rubin et al. 1972
214. Sandage 1964
215. Sandage 1965
216. Sandage 1966a
217. Sandage 1966b
218. Sandage 1967a
219. Sandage 1967b
220. Sandage 1967c
221. Sandage 1972
222. Sandage 1973
223. Sandage 1978
224. Sandage et al. 1969
225. Sandage & Brucato 1979
226. Sandage & Luyten 1967
227. Sandage & Tammann 1981
228. Sandage et al. 1965
229. Sandage & Wyndham 1965
230. Sargent 1970a
231. Sargent 1970b
232. Sargent 1972
233. Sargent 1977
234. Savage et al. 1977
235. Schilizzi 1975
236. Schmidt 1965
237. Schmidt 1968
238. Schmidt 1974

239. Schmidt & Green 1983
240. Schnopper et al. 1978
241. Searle & Bolton 1968
242. Shuder 1980
243. Shuder & Osterbrock 1981
244. Smith & Spinrad 1980
245. Smith et al. 1976
246. Smith 1975
247. Smith et al. 1976
248. Spinrad & Smith 1976
249. Sramek & Tovmassian 1974
250. Stauffer 1982
251. Stauffer et al. 1983
252. Stein & Weedman 1976
253. Steiner et al. 1982
254. Stocke et al. 1981
255. Stockton 1968
256. Stone 1982
257. Stoughyon & Osterbrock 1980
258. Tananbaum et al. 1978
259. Terebizh 1980
260. Tsvesanov 1981
261. Ulrich 1971
262. Ulrich 1975
263. Ulvestad & Wilson 1983
264. Vanderriest & Lelievre 1977
265. de Vaucouleurs 1961
266. de Vaucouleurs 1964
267. de Vaucouleurs & de Vaucouleurs 1968
268. de Vaucouleurs & de Vaucouleurs 1975
269. de Vaucouleurs & de Vaucouleurs 1972
270. de Vaucouleurs et al. 1976
271. de Vaucouleurs et al. 1978
272. Veron & Veron unpublished
273. Veron-Cetty & Veron 1984
274. Veron et al. 1981
275. Veron-Cetty et al. 1982
276. Veron 1979
277. Veron et al. 1981
278. Wall & Connon 1973
279. Walsh et al. 1979
280. Wampler 1967
281. Ward & Wilson 1978
282. Ward et al. 1977
283. Ward et al. 1978
284. Wasilewski 1981
285. Wasilewski 1983
286. Weedman 1970
287. Weedman 1973
288. Weedman 1977
289. Weedman 1978
290. Weedman & Khachikian 1969
291. Wegner 1979
292. Wehinger & Wyckoff 1977
293. West 1979
294. West et al. 1978a
295. West et al. 1978b
296. West et al. 1978c
297. West et al. 1980
298. West et al. 1981
299. Westerlund & Smith 1966
300. Westerlund & Wall 1969
301. Wilkes et al. 1983
302. Wills 1974
303. Wills 1976
304. Wills & Wills 1979
305. Wills et al. 1973
306. Wills & Lynds 1978
307. Wills & Wills 1974
308. Wills & Wills 1976
309. Wilson et al. 1976
310. Wilson et al. 1981
311. Wing 1973
312. Wright et al. 1977a
313. Wright et al. 1977b
314. Wyndham 1965
315. Wyndham 1966
316. Zasov & Lyutyi 1973
317. Zasov & Tapia 1979
318. Zwicky 1966
319. Zwicky et al. 1970

TABLE 4

LINE PROFILE CLASSIFICATIONS AND WIDTHS

Galaxy	Profile	Seyfert	Hβ FWHI	Hβ FWOI	Hα FWHI	Hα FWOI	HI FWHI	HI FWOI
Mk 10	s	1	2400	9300	2400	15300	2400	12300
Mk 40	s	1	2000	13300	1900	9100	2000	11200
Mk 69	s	1	1500	11100	1500	8200	1500	9600
Mk 79	s	1.2	5200	12200	3300	17100	4200	14600
Mk 106	sa	1	3700	15700	3300	14200	3500	15000
Mk 110	sa	1	2500	13000	2200	13200	2400	13100
Mk 124	s	1	1400	9800	1400	7500	1400	8600
Mk 141	sa	1.2	5300	12300	2300	14900	3800	13600
Mk 142	s	1	1700	12300	1100	9100	1400	10700
Mk 236	sa	1.2	4900	13000	3700	15100	4300	14000
Mk 279	a	1	6200	18500	4100	16900	5200	17700
Mk 290	sa	1	2500	13000	2500	13000	2500	13000
Mk 291	s	1	1100	8300	500	5200	800	6800
Mk 304	a	1	5900	15400	4700	22100	5300	18800
Mk 335	s	1	1700	10500	1400	9500	1600	10000
Mk 352	sa	1	3800	12500	3100	14300	3400	13400
Mk 358	s	1	2000	7500	1300	8200	1600	7800
Mk 374	a	1.2	4600	10600	3100	15800	3800	13200
Mk 376	a	1	5900	18100	4900	20200	5400	19200
Mk 382	s	1	1500	7400	1400	6900	1400	7200
Mk 478	s	1	1700	10200	1400	9700	1600	10000
Mk 486	s	1	2000	14200	1900	12700	2000	13400
Mk 504	s	1	2300	13900	1900	11900	2100	12900
Mk 506	sa	1.5	3400	12500	3600	11300	3500	12000
Mk 509	s	1	3600	15100	2900	12900	3200	14000
Mk 541	sa	1	3300	10200	2600	10000	2900	10100
Mk 590	s	1.5	3700	9300	3100	13000	3400	11200
Mk 618	s	1	2200	10500	2100	8700	2200	9600
NGC 3227	s	1.2	2500	11800	2400	11400	2400	11600
NGC 3516	s	1	6800	14800	4300	15500	5600	15200
NGC 5548	s	1.5	3700	15400	3300	14900	3500	15100
NGC 7469	sa	1	1900	8500	1700	7800	1800	8200
I Zw 1	s	1	1400	9600	1200	8200	1300	8900
II Zw 1	sa	1.5	1500	11200	1900	12600	1700	11900
II Zw 136	s	1	2300	11400	2200	10100	2200	10800
III Zw 2	a	1	5700	15800	4100	17400	4900	16600
3C 120							2000	15000
3C 227							2500	14000
3C 382							18000	25000
3C 390.3							13000	18000
3C 445							3000	14000

Table 5 RELATIVE EMISSION?LINE INTENSITIES IN SEYFERT 1 GALAXIES

Line	Mk 236	Mk 279	Mk 290	Mk 291	Mk 304	Mk 335	Mk 352	Mk 358	Mk 374
3727 [O II]	0.085	0.10	0.054	0.46	0.008	≤0.01	<0.007	0.10	...
4340 Hγ	~0.34	0.37	0.33	0.40	0.28	0.48	0.47	0.44	0.43
4363 [O III]	~0.037	0.014	0.027	0.10	0.007	0.019	...	<0.026	0.034
4570 Fe II	0.30	0.15	0.096	0.45	0.16	0.22	0.20	0.48	0.52
4686 He II	0.37	0.16	0.16	0.88	0.15	0.33	0.44	0.60	0.28
4861 Hβ	1.00	1.00	1.00	1.00	1.00	1.00	1.00	1.00	1.00
4959 [O III]	0.14	0.062	0.20	0.32	0.022	0.076	0.046	0.15	0.14
5007 [O III]	0.46	0.20	0.63	0.97	0.066	0.23	0.11	0.43	0.43
5190 Fe II	0.37	0.081	0.046	0.51	0.068	0.10	0.027	0.15	0.14
5320 Fe II		0.078	0.060		0.11	0.11	0.095	0.33	0.22
5876 He I	0.22	0.15	0.18	0.20	0.16	0.16	0.15	0.093	0.25
6087 [Fe VII]	...	≤0.008	0.018	...	≤0.004	...	...	...	0.13
6300 [O I]	0.033	0.026	0.021	0.10	≤0.003	...	...	<0.042	...
6364 [O I]	...	...	0.008	...	...	...	...	...	...
6369 Fe II	...	...	...	...	...	...	...	0.089	...
6548 [N II]	0.024	0.004	0.016	0.35	0.008:	...	...	0.042	...
6563 Hα	3.45	2.89	3.32	4.53	2.98	2.60	2.66	2.82	3.25
6583 [N II]	0.073	0.11	0.048	1.07	0.025:	<0.34	...	0.14	0.027
6716 [S II]	0.057	0.028:	0.022	0.29	0.004	...	...	0.17	0.021
6731 [S II]	0.061	0.028:	0.019	0.18	0.008	...	...		0.021

TABLE 6

EMISSION-LINE WIDTHS

OBJECT	FWOI (km s^{-1})	FWHM (km s^{-1})			
	Hα	Hα	Hβ	Hγ	He I λ5876
NGC 4051.....	6070	620	990	1240	...
III Zw 77	10100	680	840	620	...
Mrk 79.....	17400	4000	4950	...	...
Mrk 279	19400	6230	6860[a]	...	...
			7260[b]		
Mrk 290	11800	2140	2550	2640	...
	23600[c]				
Mrk 304	21500	4530	5160	4540	6470
Mrk 335	9560	1120	1350	1490	1550
Mrk 359	4050	480	480	...	620
Mrk 374	14600	3200	5060	...	...
Mrk 486	11200	1840	1630	2080	...
Mrk 704	12700	5230	6750	...	...
Mrk 771	16800	3590	3830	3800	4730
Mrk 817	19400	4140	4300	3880	6410
Mrk 876	27400	6500	5390[d]	...	...
			6070[b]		
Mrk 926	25800	6800	6360	...	...
Mrk 1040.....	10400	1590	1830	...	...
Mrk 1383	22200	4290	4600	3400	...
Akn 564	5910	600	720	790	730
MCG 8-11-11 ...	9880	2920	3630	3600	...

[a] 1980.
[b] 1981.
[c] Mrk 290 may have a faint blue wing to Hα.
[d] 1978.

TABLE 7

[O III] λ5007 Emission Line Profile Parameters

Galaxy	Class	PA/Length	W80	W50	W20	C80	C50	C20	AI_{20}
		(°/")		(km s^{-1})			(km s^{-1})		
(1)	(2)	(3)	(4)	(5)	(6)	(7)	(8)	(9)	(10)
NGC 1275.....	NRG	90/12	460	1360±10	2400	245	4920	-80	0.27±0.01
NGC 2992.....	S2	120/17	140	260±15	450	-10	2375	-15	0.03±0.06
NGC 3227.....	S1	45/12	260	540±10	900	50	--	5	0.10±0.03
NGC 4051.....	S1	45/12	110	210±10	420	20	595	-35	0.29±0.05
NGC 4151.....	S1	45/6.5	190	460±5	760	32	905	20	0.03±0.10
NGC 4235.....	S1	120/6.5	270	400±40	710	0	2220	80	-0.23±0.12
NGC 5548.....	S1	135/6.5	190	380±10	640	15	5030	-45	0.20±0.03
NGC 7469.....	S1	90/12	240	390±10	670	10	4790	-60	0.21±0.04
NGC 7603.....	S1	90/9	170	330±25	670	5	8785	-105	0.33 0.07
Mrk 3.....	S2	153/6.5	495	850±5	1385	50	4050	-95	0.22±0.01
Mrk 6.....	S1	153/6.5	240	560±10	1230	65	5680	0	0.10±0.01
Mrk 10.....	S1	45/12	160	360±20	520	-5	--	5	-0.03±0.07
Mrk 34.....	S2	45/6.5	250	570±10	820	25	15270	0	0.04±0.03
Mrk 40.....	S1	155/6.5	130	220±10	360	5	6175	-20	0.15±0.06
Mrk 42.....	S1	153/12	100	160±20	260	10	7395	-25	0.30±0.13
Mrk 78.....	S2	153/6.5	870[a]	1030±10	1440	0[a]	11285	-105	0.20±0.01
Mrk 79.....	S1	153/14	210	360±10	530	-10	6635	-15	0.02±0.04
Mrk 176.....	S2	153/12	260	490±10	1100	20	7930	-80	0.18±0.02
Mrk 268.....	S2	45/12	310	530±30	1070	20	--	-50	0.12±0.06
Mrk 270.....	S2	45/9	180	380±10	600	-30	3125	15	-0.16±0.04
Mrk 279.....	S1	45/6.5	280	580±30	1470	20	9070	-310	0.44±0.04
Mrk 290.....	S1	45/6.5	240	380±10	530	10	13115	-10	0.09±0.04
Mrk 298.....	S2	100/6.5	210	410±15	620	35	10285	-40	0.25±0.04
Mrk 463.....	S2	45/14	220	540±10	980	50	15040	-80	0.26±0.02
Mrk 504.....	S1	45/6.5	90	170±20	290	0	10790	0	0.00±0.12
Mrk 609.....	S2	90/12	290	450±25	940	5	10225	-100	0.22±0.05
Mrk 766.....	S1	45/12	120	240±10	480	15	3868	-20	0.17±0.04
3C 98.....	NRG	170/12	130	230±15	370	10	9020	-10	0.12±0.08
3C 111.....	BRG	153/6.5	70	260±35	750	5	14710	40	-0.10±0.10
3C 192.....	NRG	45/4	190	330±35	420	-25	17805	15	-0.20±0.15
3C 305.....	NRG	57/14	370	740±15	1090	50	12445	-100	0.26±0.03
3C 382.....	BRG	45/6.5	220	490±25	830	0	17370	-20	0.05±0.06
3C 390.3[b].....	BRG	150/3.9	250	410±10	780	10	16640	-5	0.03±0.02
Cyg A.....	NRG	150/6.5	200	340±10	550	10	16795	5	0.01±0.03
OQ 208.....	BRG	155/6.5	180	420±25	840	-10	22970	-60	0.12±0.06
IC 4329 A....	S1	135/4	230	570±20	870	25	4780	55	-0.08±0.05

[a]The values for W80 and C80 for the Mrk 78 profile were actually derived at the ~67% intensity level because of its unusual double-peaked shape.

[b]Comparison of the spectrum in Fig. 1 (obtained 1980 May) with that in Osterbrock, Koski, and Phillips (1976) shows that the broad Hβ component has faded appreciably relative to the narrow [O III] and Hβ lines. A spectrum of Hα, also obtained during the 1980 May observations, shows the same effect. The notch in the broad Hα profile, seen in the Osterbrock et al. spectrum, now nearly descends to the level of the continuum. Further monitoring of the profiles of the broad lines in this object would be worthwhile.

TABLE 8

Comparison of Narrow Line and Systemic Velocities

Galaxy	C50 − V_{SYS} (km s^{-1})	C50 References	V_{SYS} References
NGC 1068 ...	−150	Pelat and Alloin 1980	Heckman *et al.* 1978
NGC 1275 ...	−280	This paper	Rubin *et al.* 1977
NGC 3227 ...	−180	Rubin and Ford 1968	Rubin and Ford 1968
NGC 4051 ...	−105	This paper	Heckman *et al.* 1978
NGC 4151 ...	−90	This paper	Heckman *et al.* 1978
NGC 5548 ...	−175	This paper	Heckman *et al.* 1978
NGC 6764 ...	−50	Rubin *et al.* 1975	Heckman *et al.* 1978
IC 4329 A ...	−60	This paper	Wilson and Penston 1979
Mrk 79	−10	This paper	Heckman *et al.* 1978

TABLE 9a

LOCAL QUASAR LUMINOSITY FUNCTION Φ

log F_B	z	V (Gpc^3)	log Φ
41.2.....	0.0039	3.49×10^{-5}	+4.46
41.6.....	0.0071	2.10×10^{-4}	+3.68
42.0.....	0.0132	1.35×10^{-3}	+2.87
42.4.....	0.0245	0.86×10^{-2}	+2.07
42.8.....	0.0447	4.81×10^{-2}	+1.32
43.2.....	0.0813	2.90×10^{-1}	+0.54
43.6.....	0.1514	1.75	−0.24
44.0.....	0.2691	0.86 × 10	−0.93
44.4.....	0.5000	4.50 × 10	−1.65

TABLE 9b

VOLUME DENSITIES OF LOCAL QUASARS

log F_B (Table 9a)	Local Density*	Local Density Φ (Table 9a)
44.4	0.025	0.022
44.0	0.38	0.117
43.6	1.62	0.58
43.2	7.12	3.47
42.8	12.9 (35)	20.9
42.4	63.8 (851)	117
42.0	(4,467)	741
41.6	(7,762)	4790
41.2	(10,715)	28,800

* Values given are from Schmidt (1970) or from Huchra and Sargent (1973), in parentheses, and are in number Gpc^{-3}; 1 Gpc = 10^3 Mpc.

Table 10 Space densities of Seyfert galaxies (Mpc^{-3} mag^{-1}).

	all Seyferts		type 1		type 2	
M_p (1)	log ϕ (2)	$n(M_p)$ (3)	log ϕ (4)	$n(M_p)$ (5)	log ϕ (6)	$n(M_p)$ (7)
-19	-5.85	(1)			-5.85	(1)
-20	-5.09	(6)	-5.52	(3)	-5.30	(3)
-21	-5.13	(24)	-5.35	(12)	-5.52	(12)
-22	-5.53	(34)	-5.69	(25)	-6.03	(9)
-23	-6.78	(8)	-6.96	(6)	-7.25	(2)
-24	-7.51	(5)	-7.51	(5)		

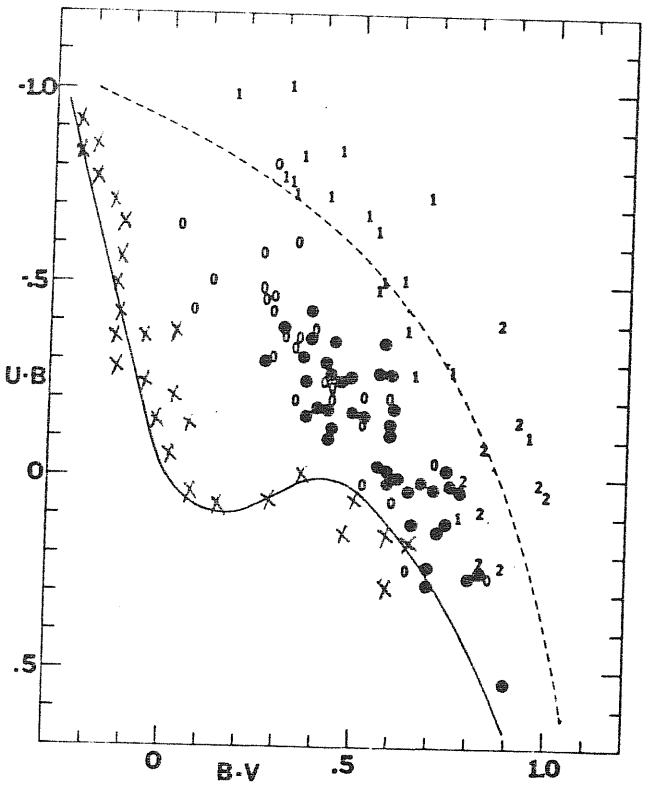

FIG. 1.—Color-color diagram for galaxies in table 1; observed colors listed in the table plotted after correcting for galactic reddening. *Filled circles*, BN (bright nucleus) galaxies; *open circles*, D (diffuse) galaxies; *numbers "1,"* Seyfert galaxies of type 1; *numbers "2,"* Seyfert galaxies of type 2. *Dashed curve*, Sandage's locus of the color changes expected as a galaxy like M31 (*lower right*) is increasingly dominated by the superposed light from a typical QSO.

Cross (X), open cluster.

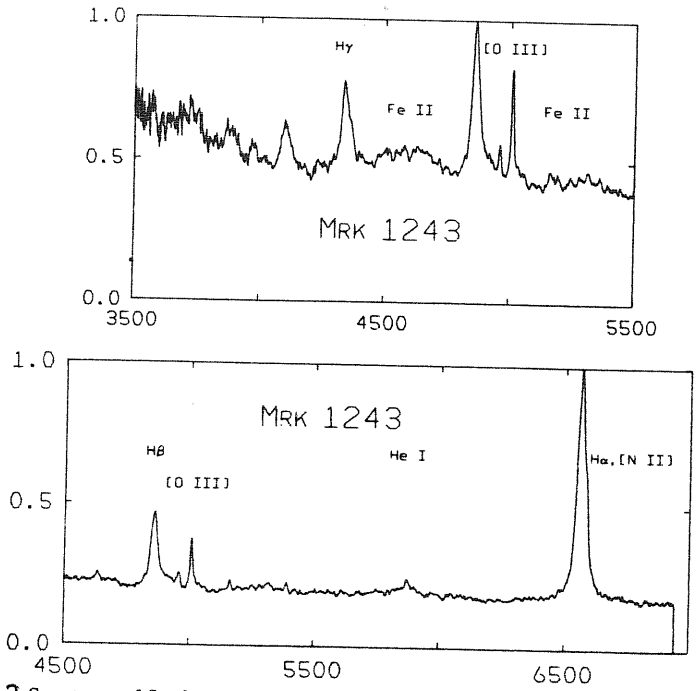

FIG. 2.—Spectrum of Seyfert 1 galaxy Mrk 1243, *above*, λλ3500–5500; *below*, λλ4500–7000 in the rest system of the object. *Vertical scale*, relative energy flux in flux units per unit wavelength interval; *horizontal scale*, wavelength in Angstrom units.

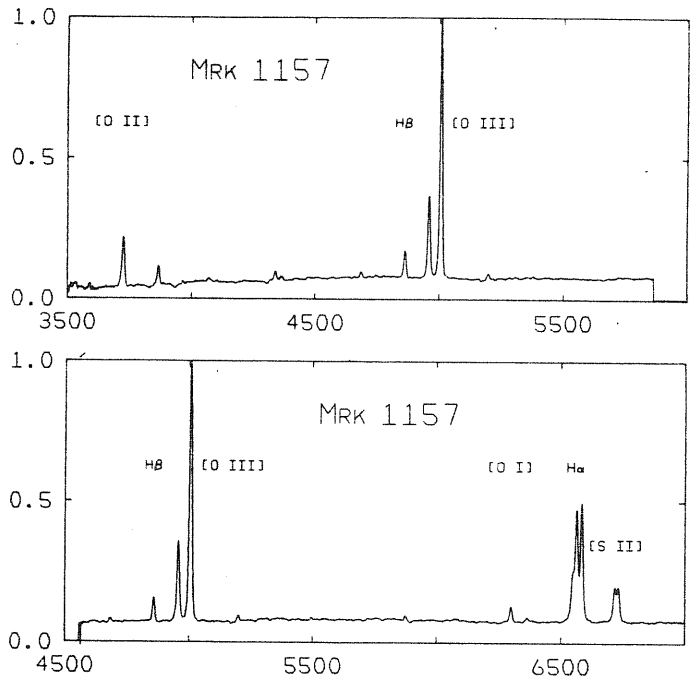

FIG. 3 Spectrum of Seyfert 2 galaxy Mrk 1157, scales and units as in Fig. 1.

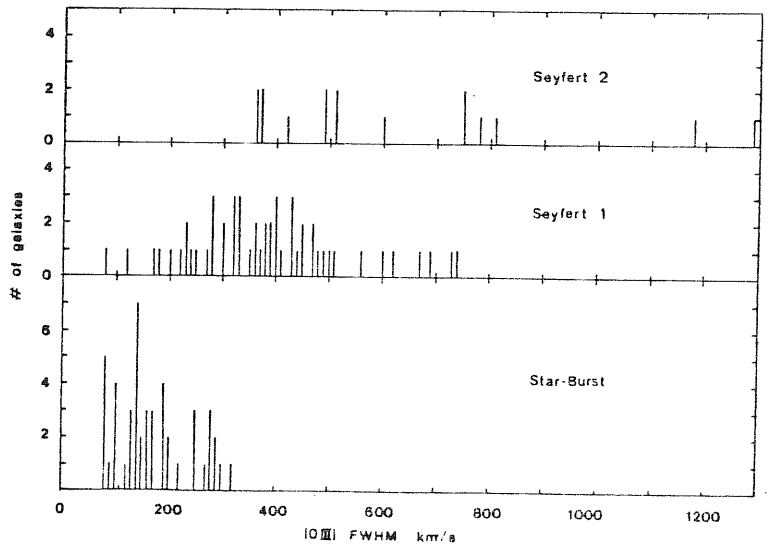

FIG. 4 – Histogram showing distribution of [O III] line widths for galaxies

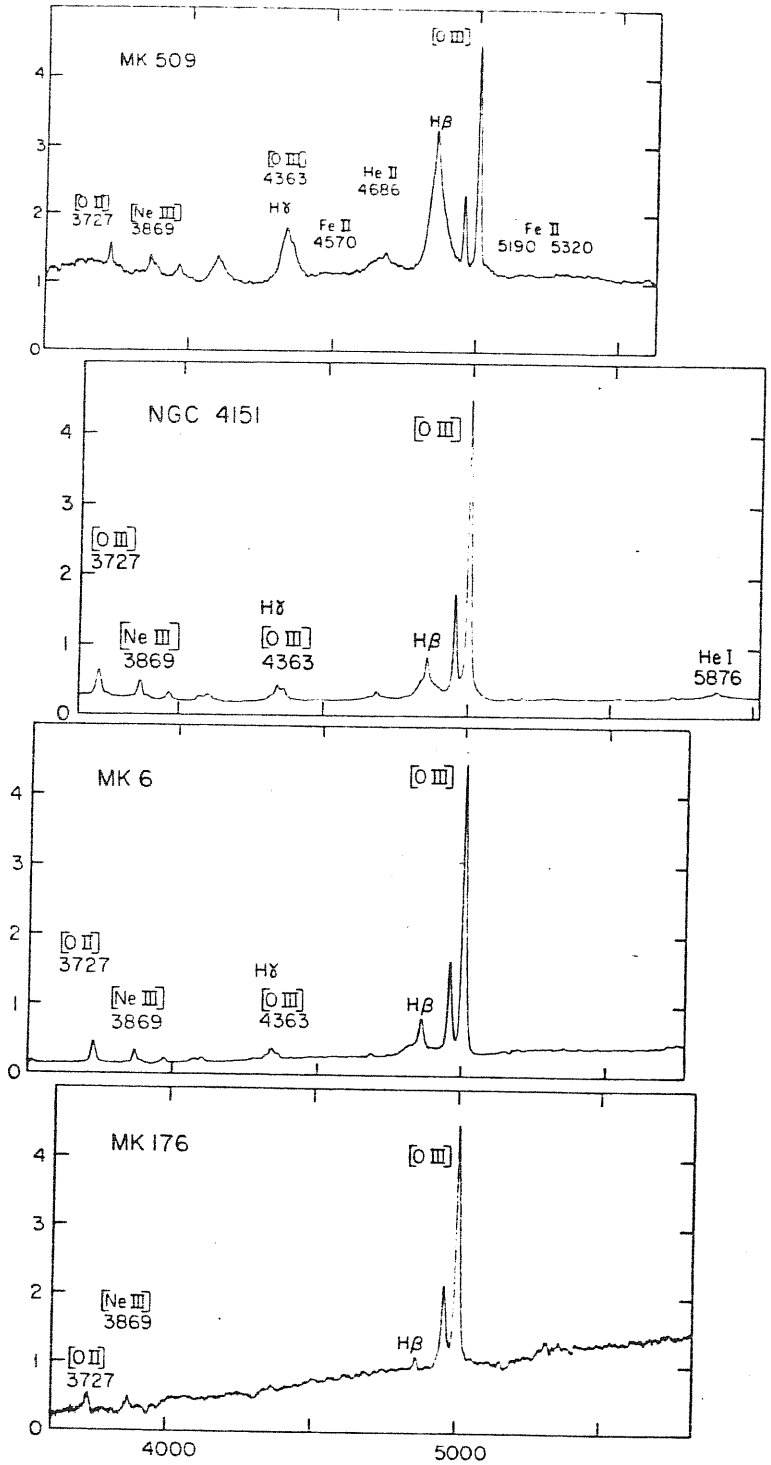

FIG. 5 *Spectra of four Seyfert galaxies, from Mk 509, typical Seyfert 1, with broad Balmer emission lines, to Mk 176, typical Seyfert 2, with narrow Balmer lines. NGC 4151 and Mk 6 have Balmer-line profiles with both narrow and broad components and are intermediate between these two classes.*

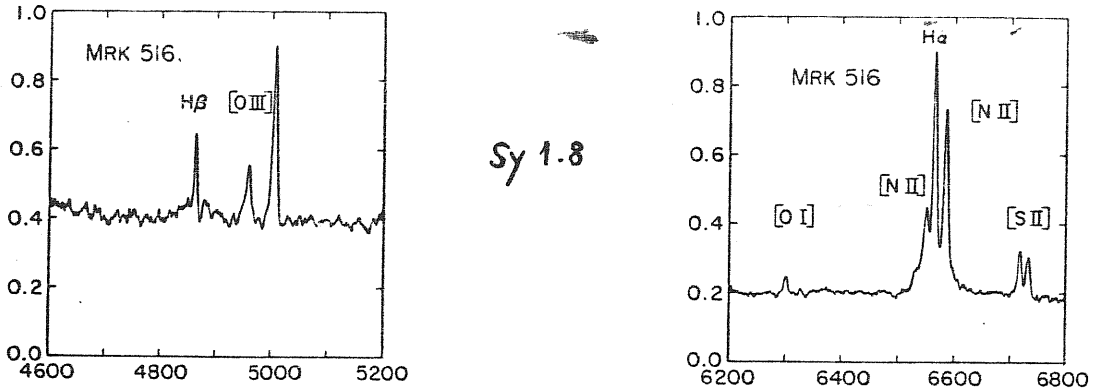

FIG. 6 — High dispersion spectral scans of Mrk 516, plotted in the rest system of the object. Vertical scales are relative energy flux in flux units per unit wavelength interval, horizontal scales are wavelength in Angstrom units. *Left*, λλ4600–5200; *right*, λλ6200–6800.

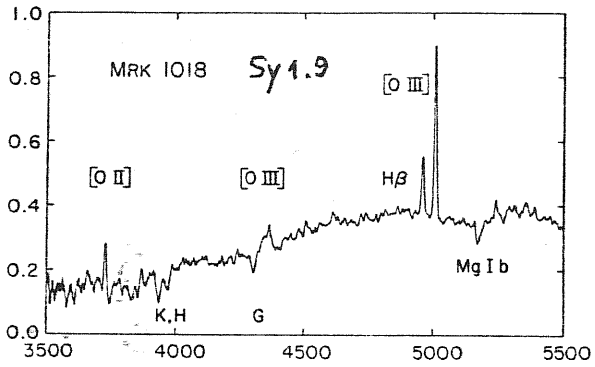

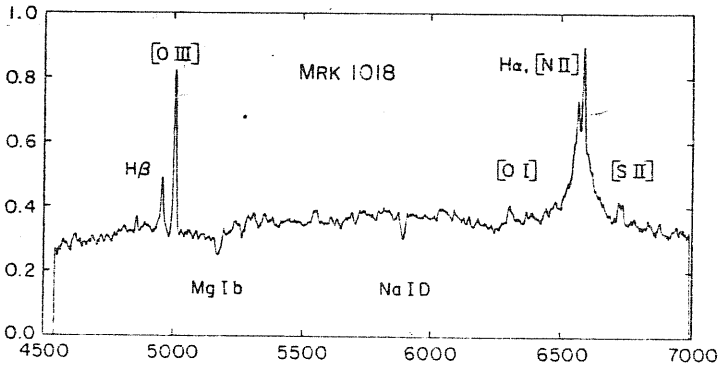

FIG. 7 — Spectral scans of Mrk 1018 plotted in the rest system of the object. Vertical scales are relative energy flux in flux units per unit wavelength interval, horizontal scales are wavelength in Angstrom units. *Upper*, λλ3500–5500; *lower*, λλ4500–7000.

Fig. 11

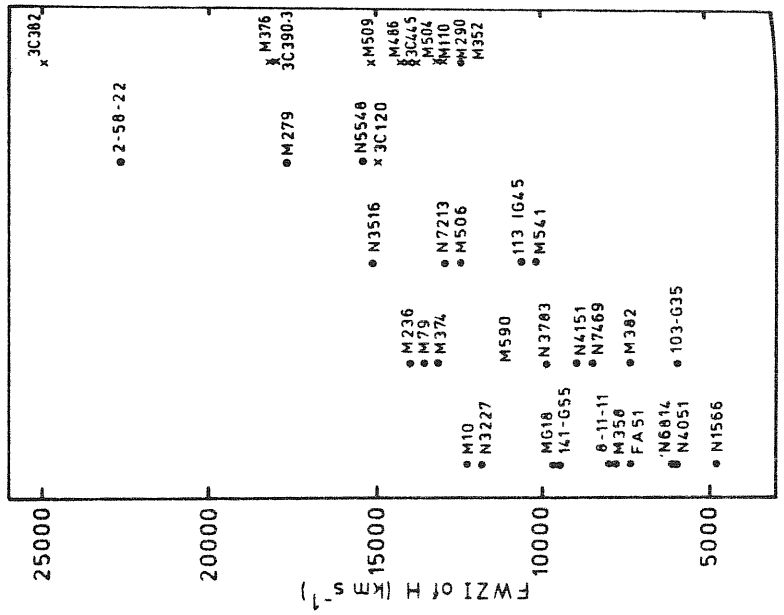

FIG. 11—FWZI vs. morphological class for Seyfert 1 galaxies.

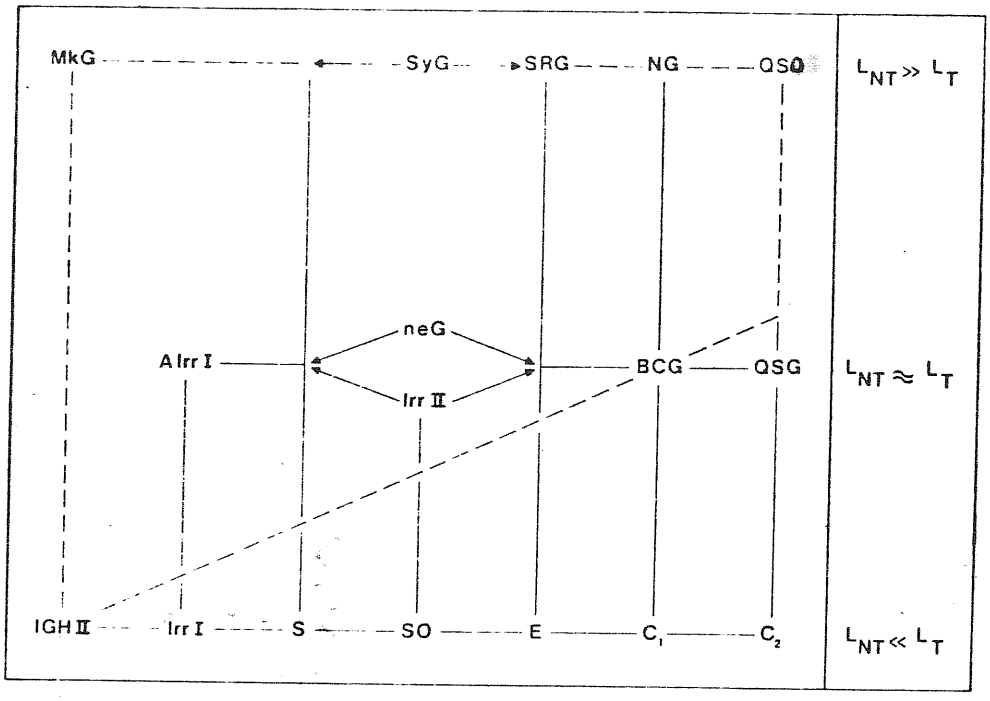

Fig. 8.—Classification of active galaxies. (*Adapted from Ozernoy*, 1970.)

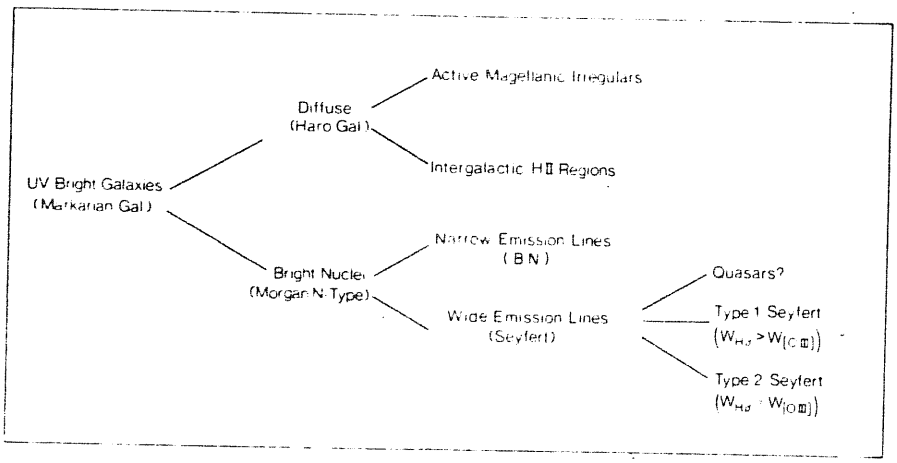

FIG. 9—Classification scheme for UV bright galaxies.

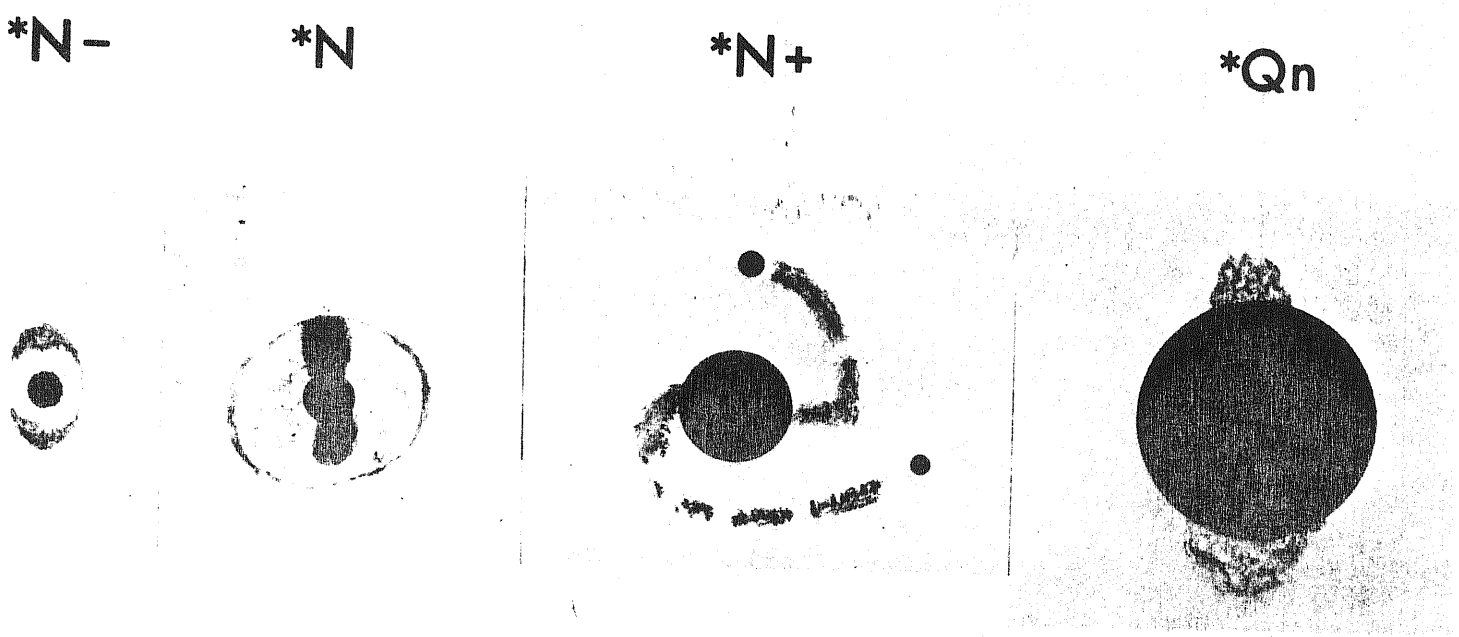

FIG 10.—Sketches of the brighter parts of the four galaxies defining the boxes *N−, *N, *N+, and *Qn. The scales of the galaxies shown are roughly comparable for the first three; the scale for 3C 48 is approximately half that of the others. The starlike nucleus increases in luminosity by the order of 6 mag on passing from NGC 4151 to 3C 48. The starlike nucleus in NGC 4151 is immersed in the bright, inner part of the galaxy. These sketches are intended only to show gross shapes—not details.

MORGAN AND DREISER (*see* page 438)

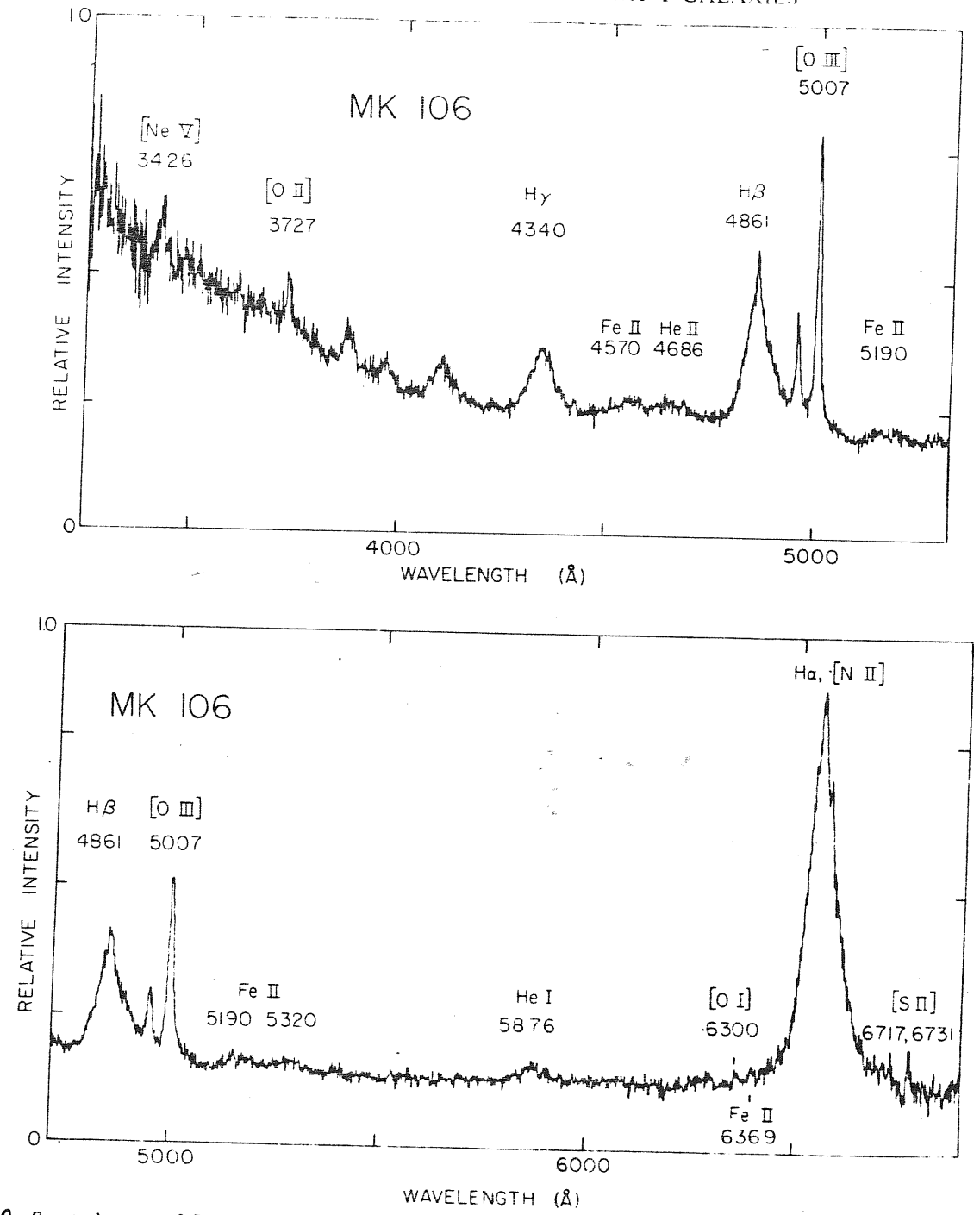

FIG. 12.—Spectral scans of Seyfert 1 galaxy Markarian 106, in relative energy units (ergs $cm^{-2} s^{-1} Å^{-1}$) versus wavelength units (Å). Upper scan shows "blue" spectral region, lower shows "red" region; wavelengths are indicated in the rest system of Mrk 106.

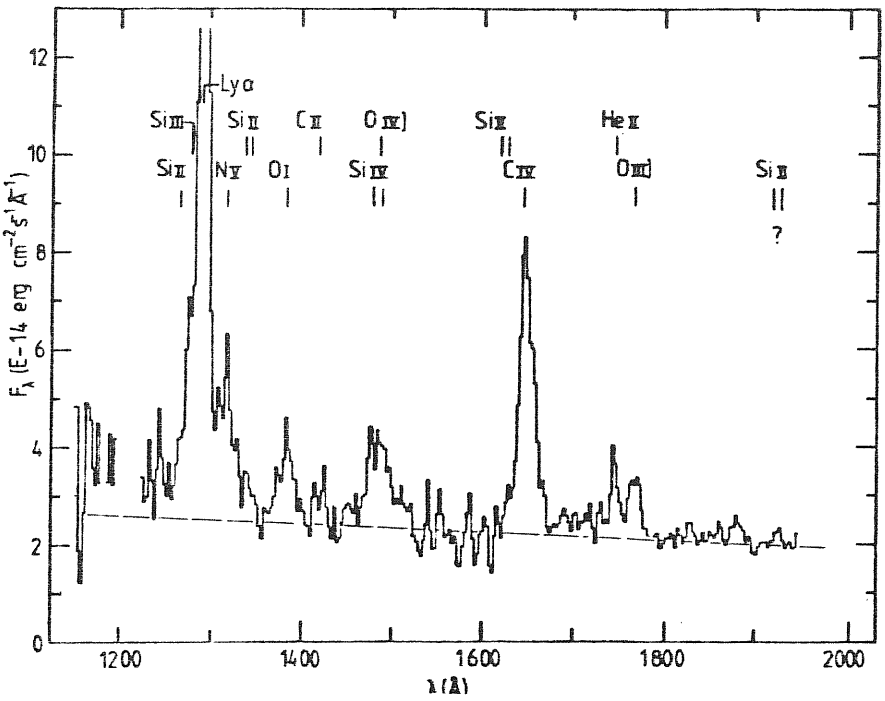

Fig. 13a One of the two short wavelength spectra for II ZW 136.

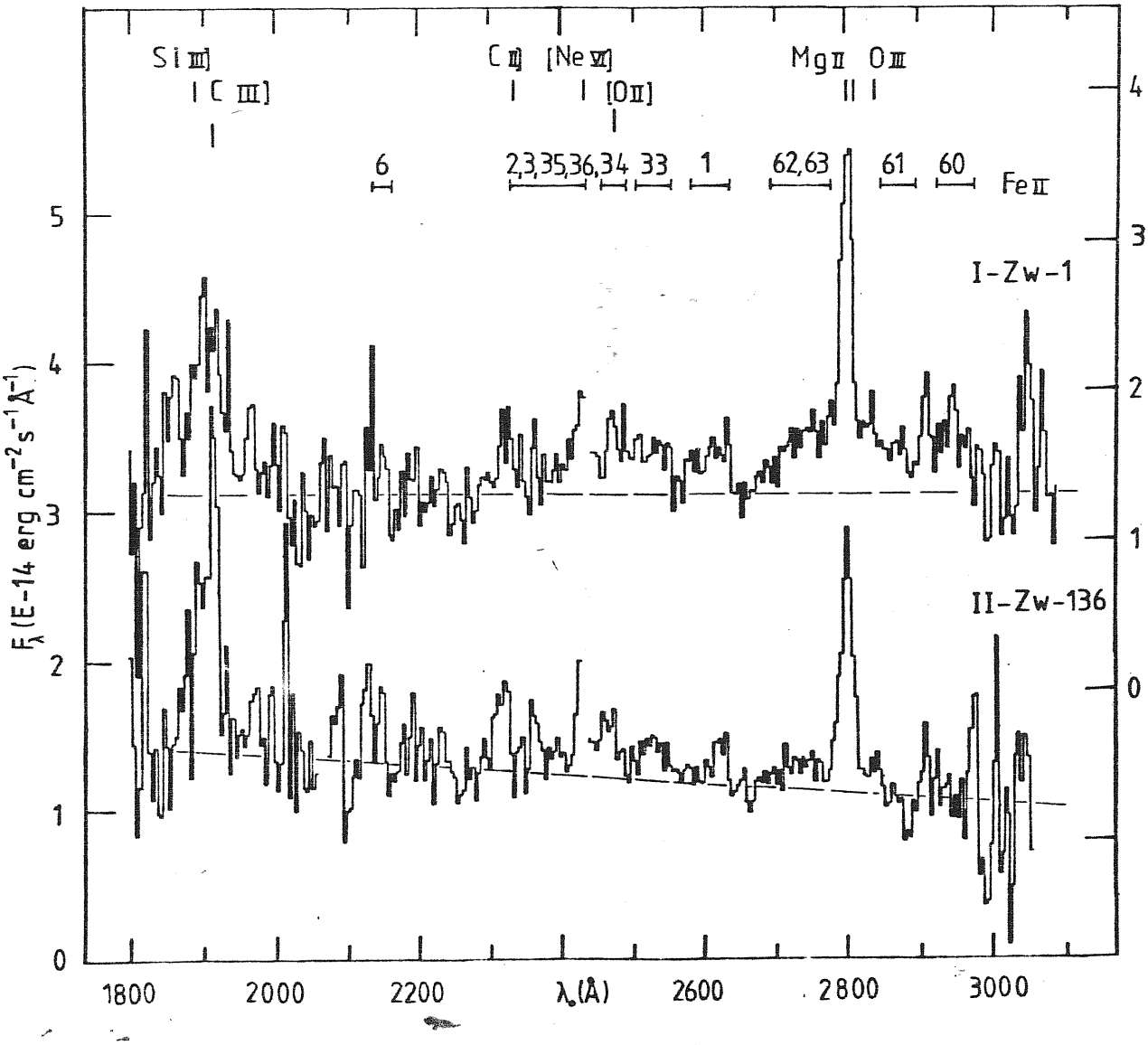

Fig. 13b Mean long wavelength spectra for I ZW 1 and II ZW 136.

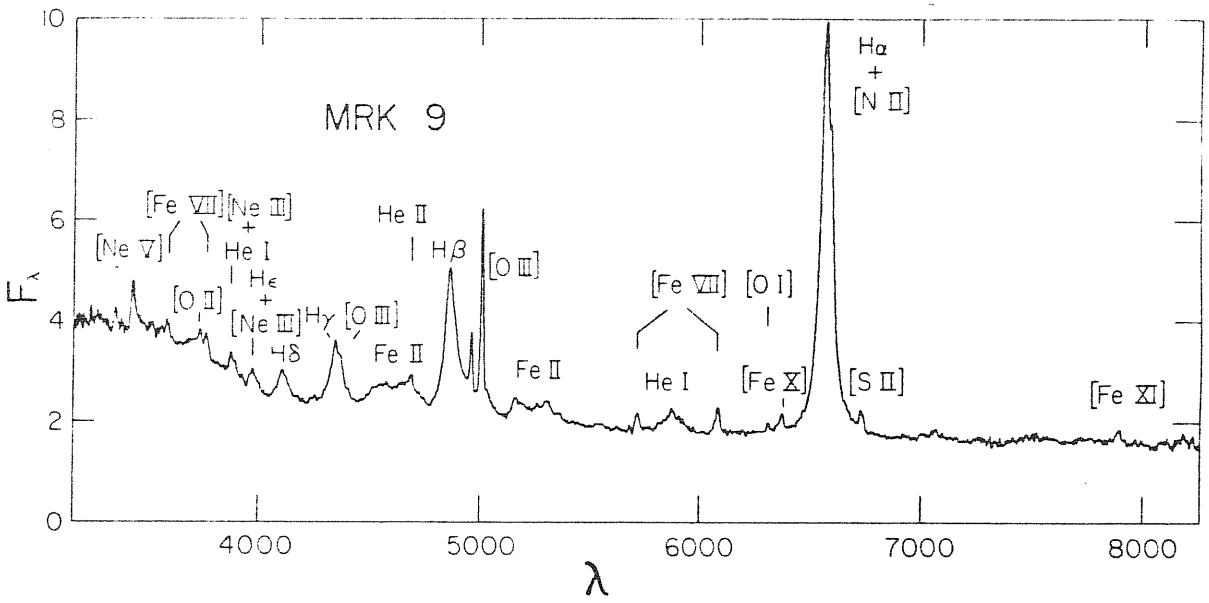

FIG. 14—Composite scan of the Seyfert 1 galaxy Mrk 9. Relative F_λ is plotted against λ in the galaxy's rest frame.

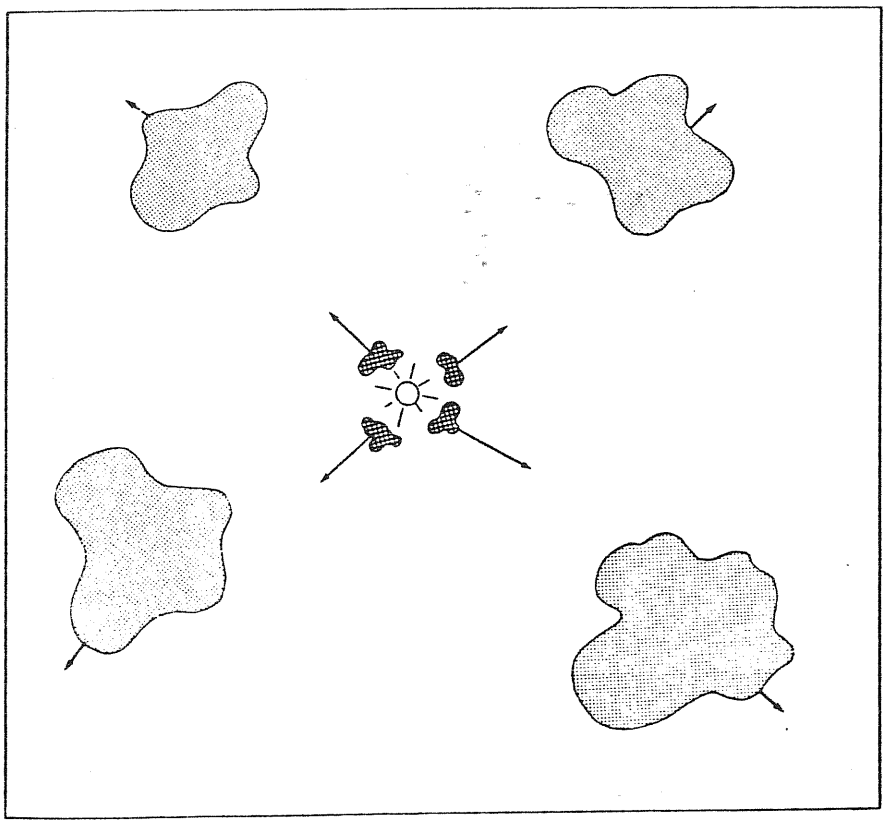

FIG. 15—Schematic model for Seyfert nuclei. The model contains three components: (1) a small central source of non-thermal radiation, (2) a region of radius ~ 0.1 pc containing fast moving (V ~ 3000 km sec^{-1}) dense (n_e ~ 10^8cm^{-3}) clouds that emit permitted line radiation and (3) a region of radius ~ 400 pc containing more slowly moving (V ~ 300 km sec^{-1}) and less dense (n_e ~ 10^5cm^{-3}) clouds which radiate forbidden lines.

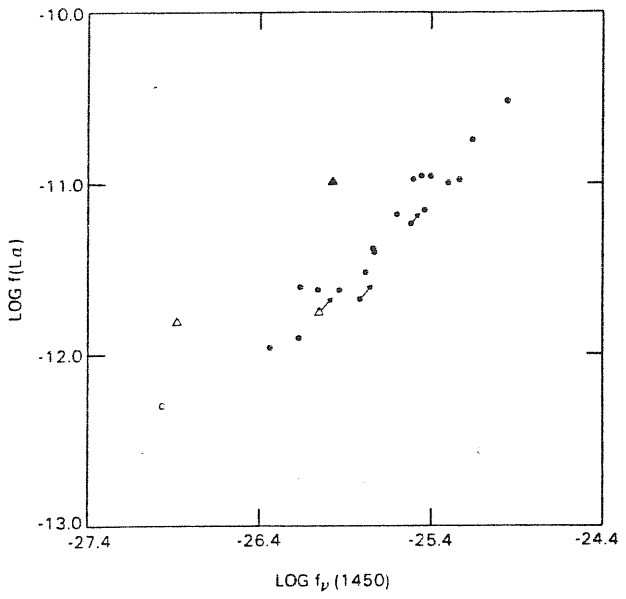

FIG. 2*a*

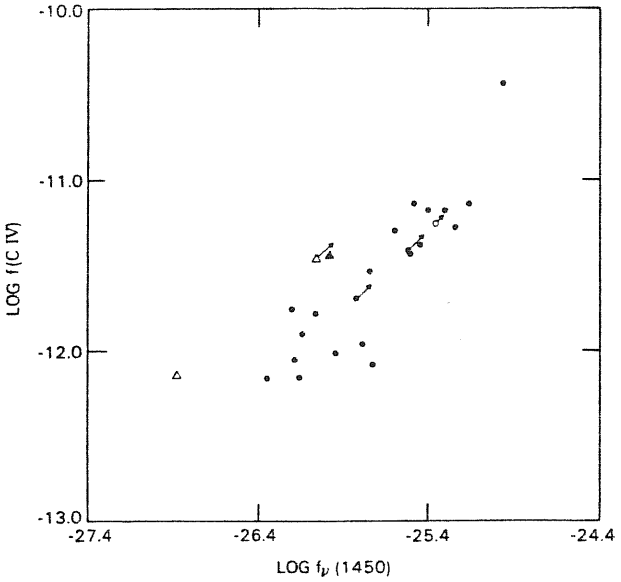

FIG. 2*b*

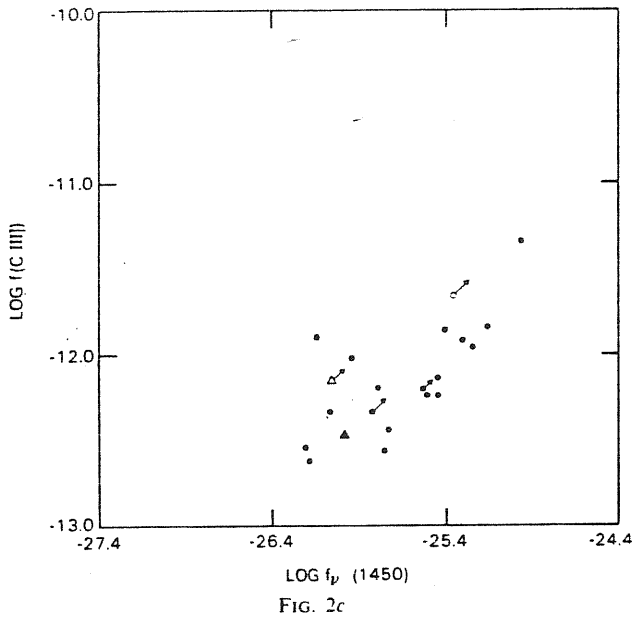

FIG. 2*c*

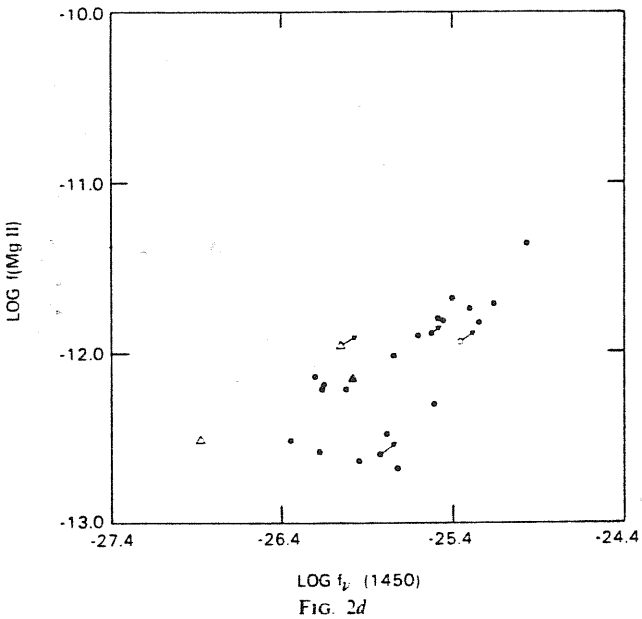

FIG. 2*d*

FIG. 16—The correlation between the observed monochromatic continuum flux at 1450 Å and the observed flux for (*a*) H I Lyα. (*b*) C IV λ1550, (*c*) C III] λ1909, and (*d*) Mg II λ2800. *Filled circles:* type 1 Seyferts; *open circle:* type 2 Seyferts. Mrk 78 for Lyα and NGC 1068 for the other three lines; *filled triangle:* quasar—in this plot it is MR 2251−178; *open triangles:* broad line radio galaxies 3C 120 and 3C 390.3. The arrows indicate the direction of reddening correction. The length of the arrows is arbitrary.

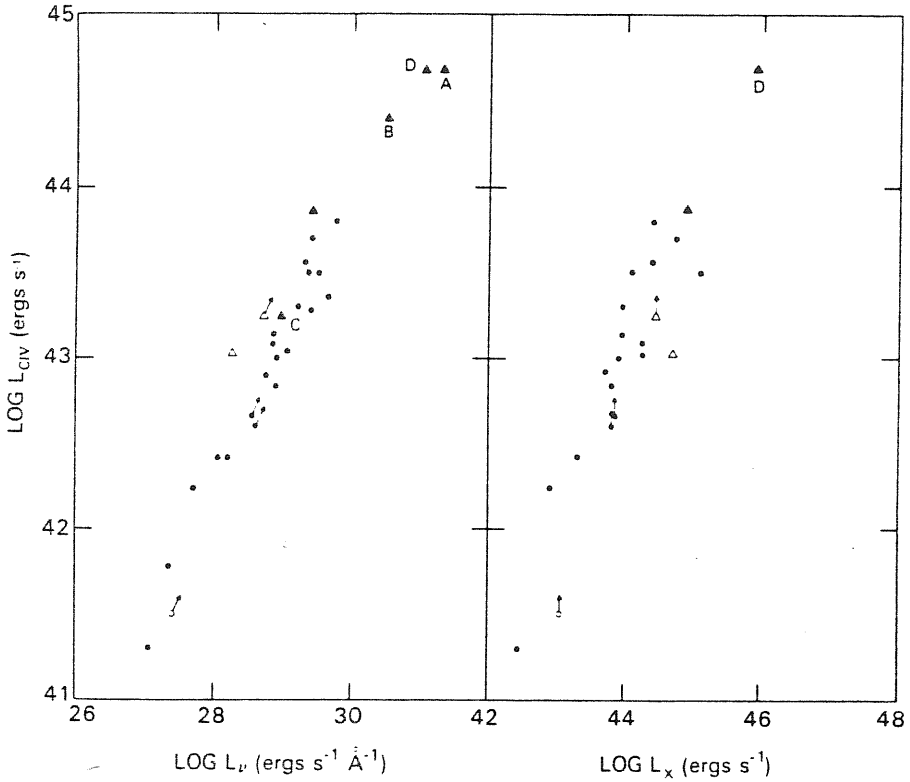

FIG. 17 The correlation between the C IV λ1550 luminosity and the luminosity at 1450 Å and 2–10 keV. The symbols have the same meaning as in Fig. 2. The four other quasars observed by the *IUE* are A: PKS 0405 − 123; B: PG 0953 + 415; C: Mrk 205; and D: 3C 273.

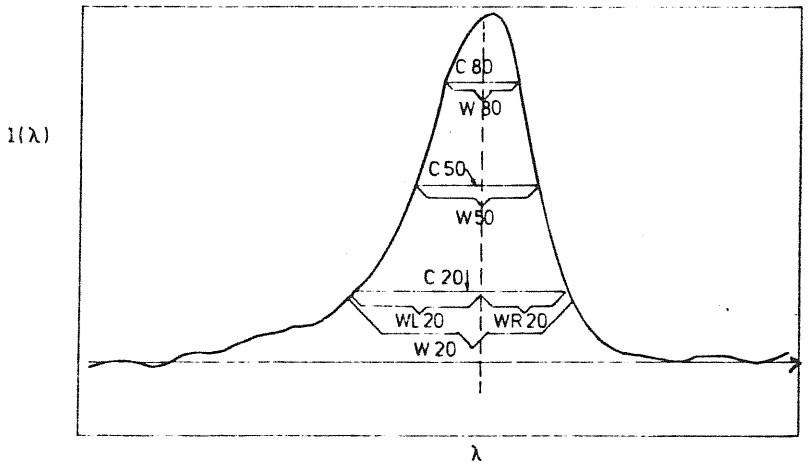

FIG. 18.— Schematic representation of the various line parameters defined in the text (C80, C50, C20, W80, W50, W20, AI_{20}). The vertical line indicates the position of C80, and the relative shifts of C50 and C20 are indicated by tick marks.

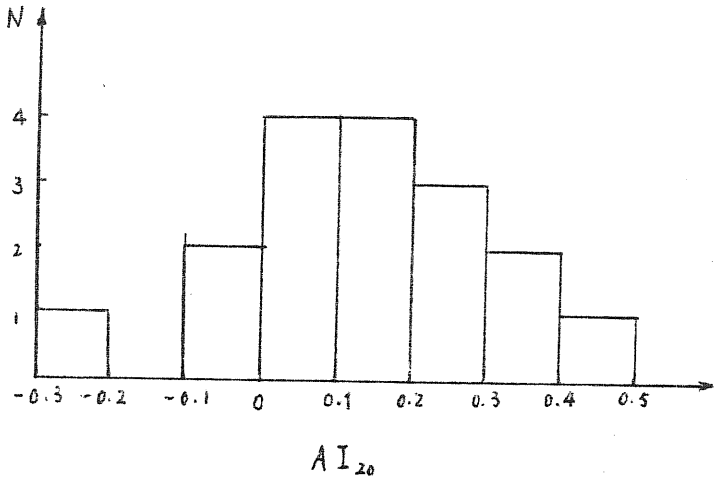

FIG. 19. Histogram of the asymmetry index (AI_{20}) for Sy 1 in Heckman ET AL Sample

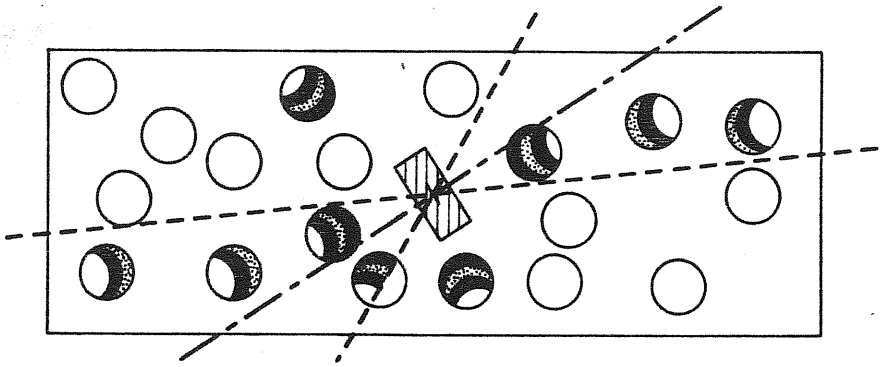

FIG 20. Schematic drawing of side view of narrow line gas, distributed in 'clouds' or condensations in a cylindrically symmetric disc, with the broad-line gas in a *tipped* disc at its centre. The photoionization source is the smaller disc at the centre of the broad-line region. The latter is optically thick to ionizing radiation along most, but not all rays near its equator, but not along rays near its axis. The more remote clouds are not as highly ionized on their faces as the clouds closer to the photoionizing source.

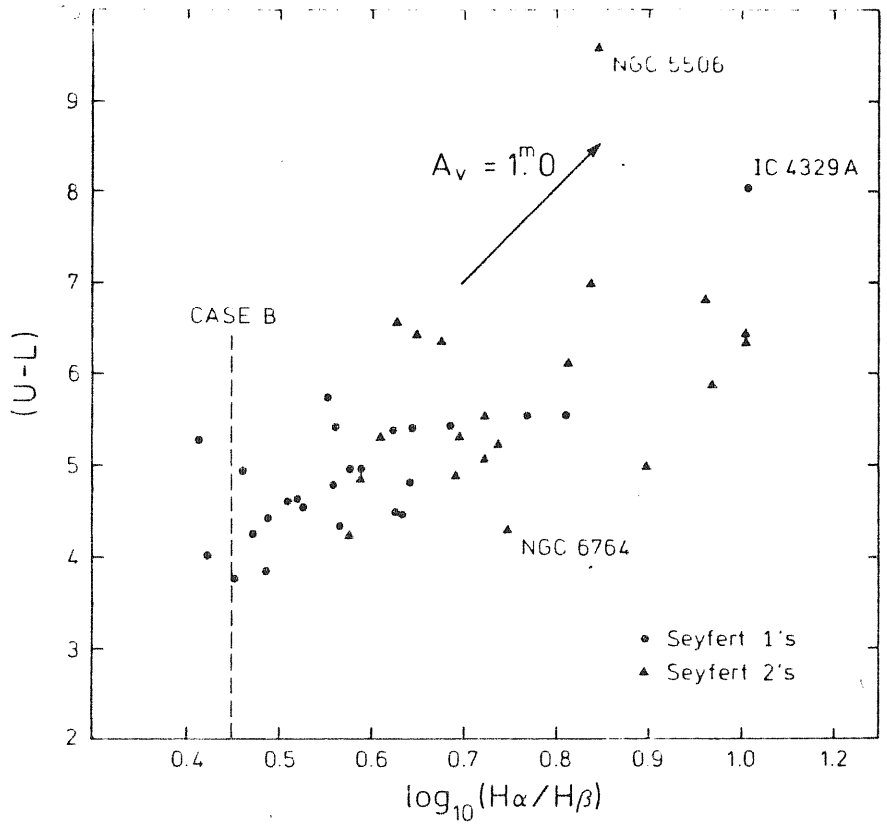

Figure 22 The plot of continuum index versus Balmer decrement. For Seyfert 2's and galaxies with a weak broad component to Hα, the narrow line decrement is used. For Seyfert 1's, in which the narrow lines are weak or unresolved, the broad line decrement is plotted.

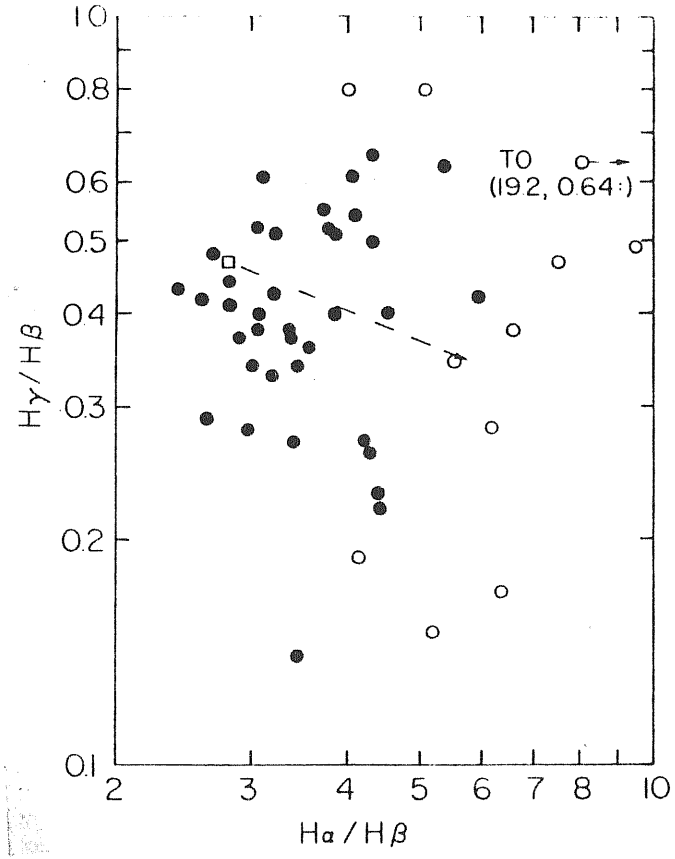

Fig. 21 Observed Hα/Hβ/Hγ ratios for Seyfert 1 galaxies (solid dots) and broad-line radio galaxies (open circles) compared with the calculated recombination decrement (square) as affected by normal interstellar extinction (dashed line).

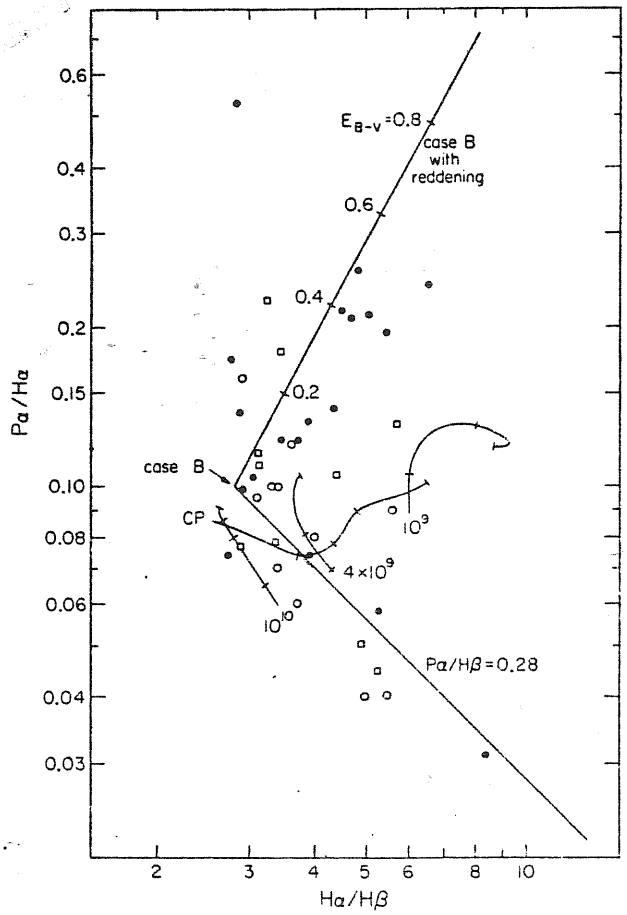

FIG. 2

FIG. 2.—Line flux ratios in Seyfert galaxies and quasars. Solid circles represent Seyfert galaxies, open circles are quasars from Soifer *et al.* (1981), and open squares are quasars from Puetter *et al.* (1981). The two diagonal lines which meet at the case B point show the expected ratios for a case B spectrum reddened by varying amounts of dust external to the line-emitting region (*upper line*), and for $P\alpha/H\beta = 0.28$, the case B ratio, with $H\alpha/H\beta > 2.8$ (*lower line*). The curves show the dependence of the line ratios on optical depth as calculated by Kwan and Krolik (1981), labeled at the high optical depth end by the gas densities, N_0, and as calculated by Canfield and Puetter (1981) for $N_0 = 10^{10}$ cm^{-3}, labeled CP. Each curve starts at a Lyman edge optical depth of $\tau_L = 10^3$ and has tick marks at $\tau_L = 10^3$, 10^4, 10^5, and in some cases 10^6.

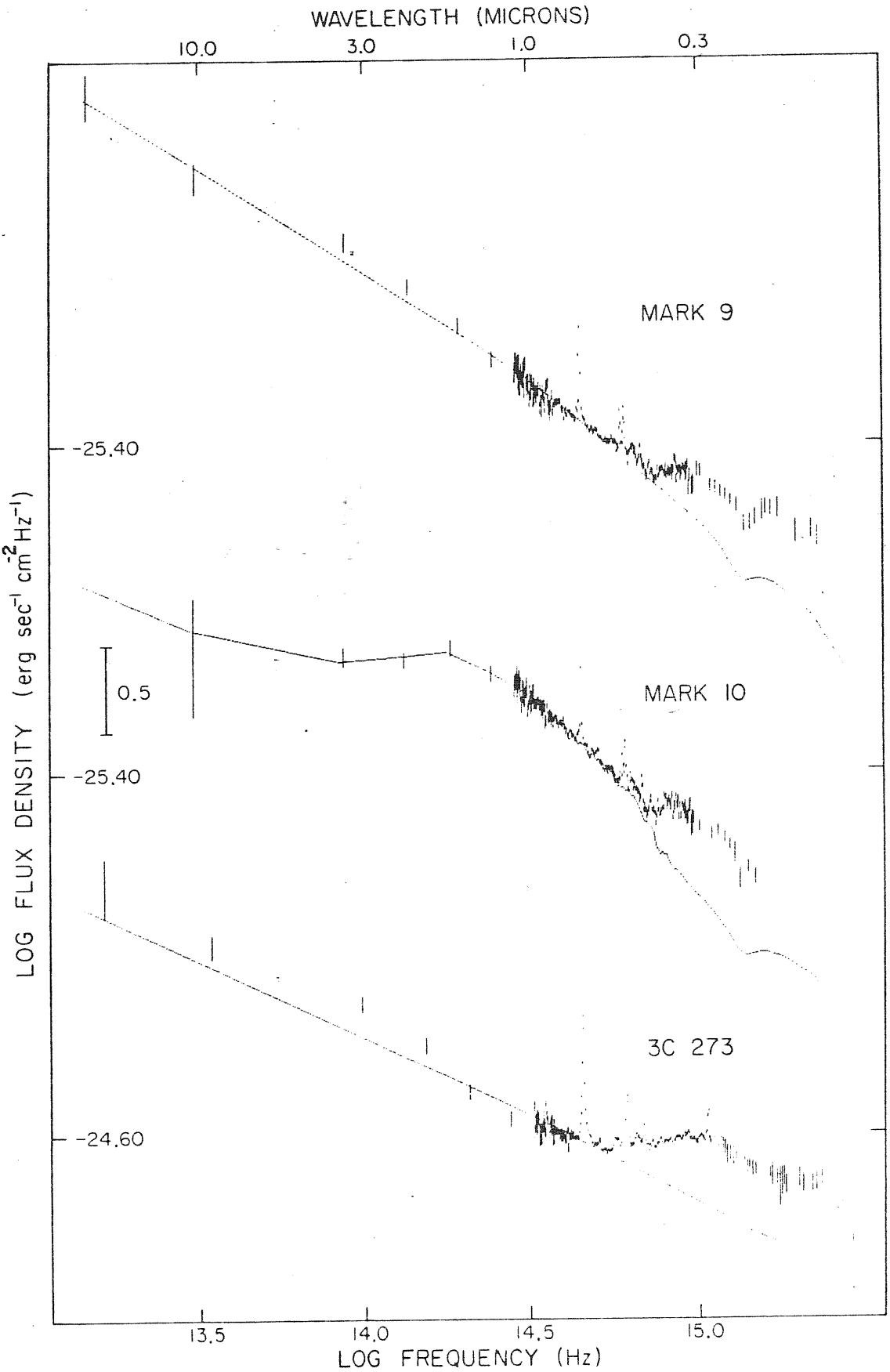

FIG 24.- Power-law subtraction to measure the excess ultraviolet flux. The vertical bars represent observed flux densities, on a logarithmic scale, and their uncertainties. The lines are power laws with slopes $\alpha = -1.2$, -0.90, and -1.0 for Mrk 9, 10, and 3C 273, respectively. In Mrk 10, starlight, which contributes 55% of the visual flux (log $\nu = 14.74$) produces a hump around 1.6 μm

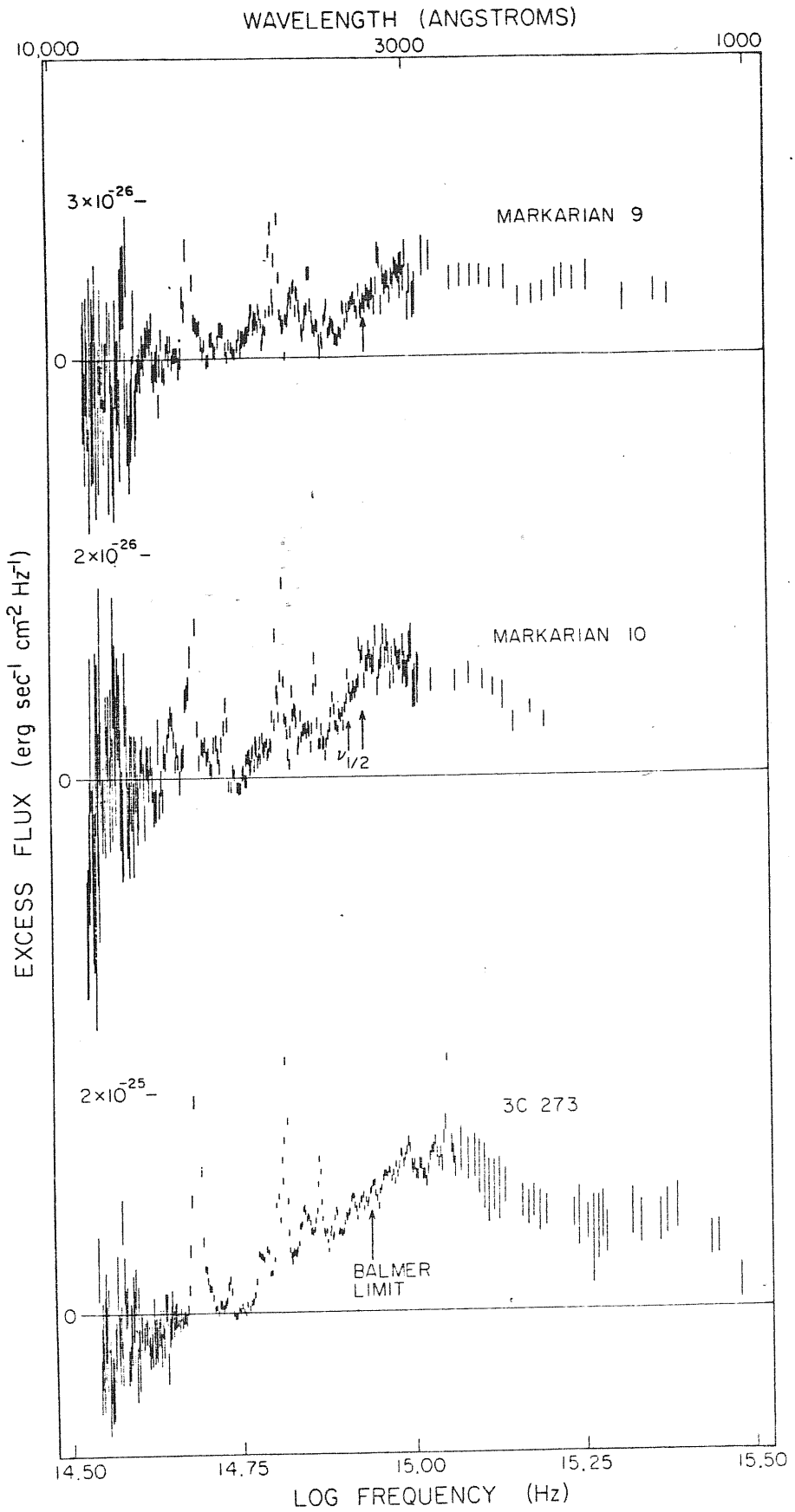

FIG 25 –The excess flux, obtained by subtracting the power laws in Fig. 1 from the data, and converting to a linear flux scale. The points have been corrected for reddening. The ordinate is still log frequency, but the infrared points are not plotted. Arrows indicate the frequency of the Balmer limit (3646 Å) for the three objects and $\nu_{1/2}$ for Mrk 10.

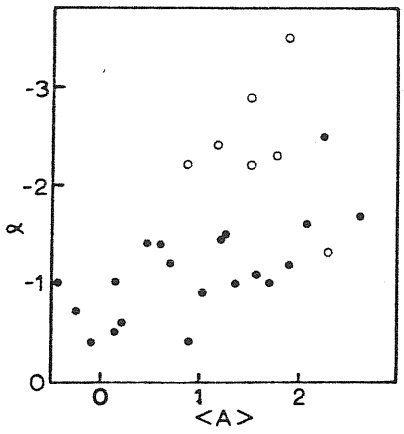

FIG 26.—Comparison of reddening, $\langle A \rangle$, estimated from Balmer decrement, with infrared spectral index, α. Filled dots are type 1 Seyfert galaxies, open dots are type 2.

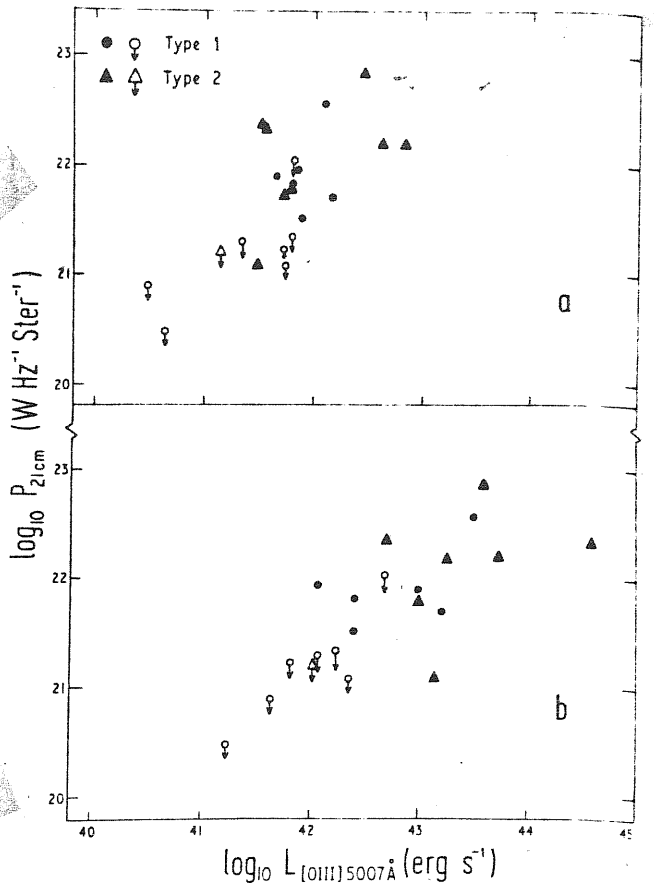

Fig. 27.—Relation between the continuum luminosity at λ 21 cm and the luminosity in the λ 5007 Å line of [O III] for galaxies in the sample of 41 defined in §1. **a** No reddening correction applied to $L_{[OIII]\lambda 5007Å}$. The 22 galaxies in the sample with measured fluxes in the [O III] λ 5007 Å line are plotted. **b** Reddening correction applied to $L_{[OIII]\lambda 5007Å}$ by assuming the Balmer decrement is intrinsically as expected under Case B radiative recombination theory (see text). The 21 galaxies in the sample with measured [O III] λ 5007 Å fluxes and Balmer decrements are plotted

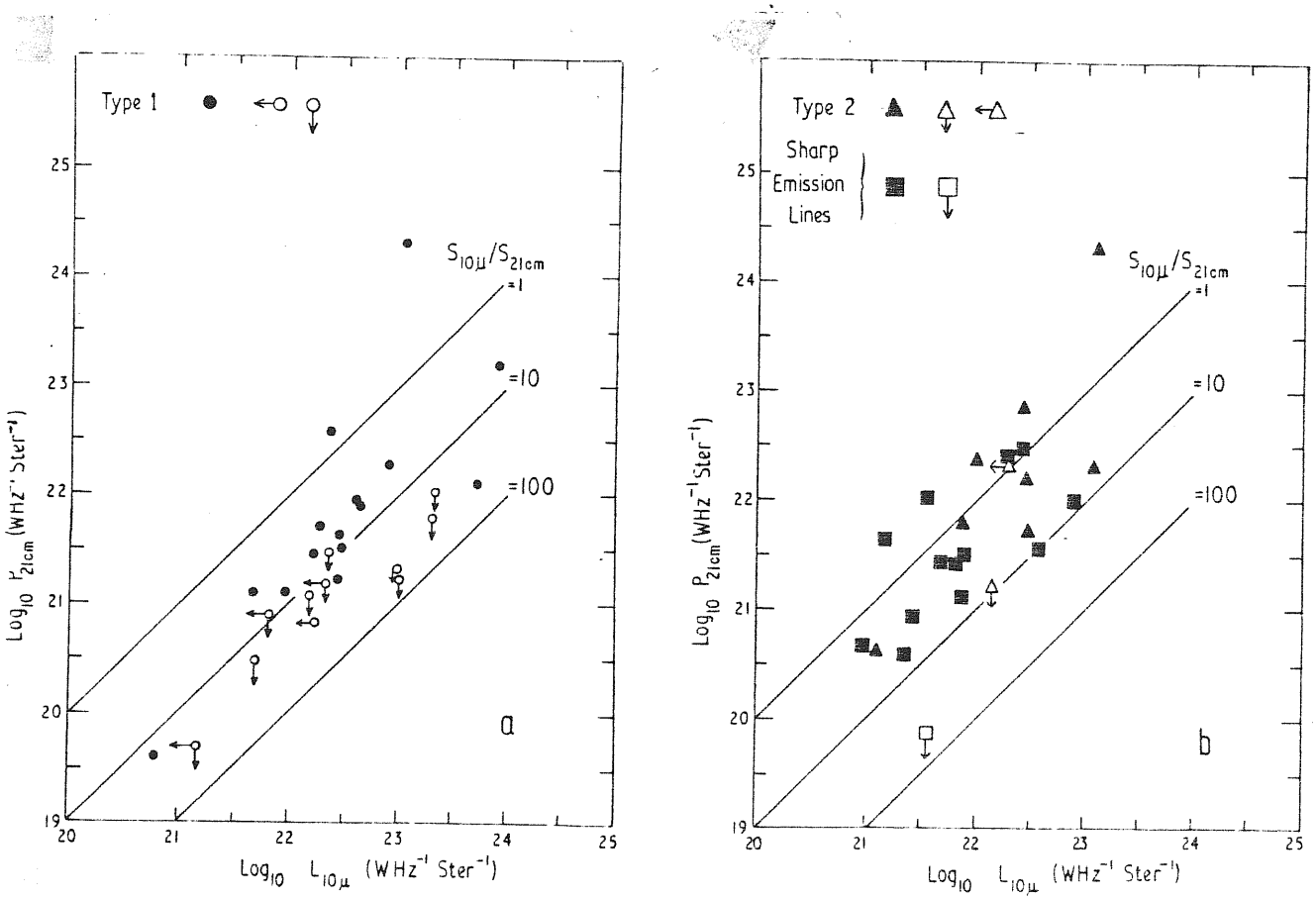

Fig. 28.—Relation between the continuum luminosities at λ 21 cm and λ 10 μ for Seyfert and sharp emission line galaxies. **a** Type 1 Seyfert galaxies. **b** Type 2 Seyfert galaxies and sharp emission line galaxies. Lines of constant flux ratio $S_{10\mu}/S_{21cm}$ are shown. The sample plotted is described in the text

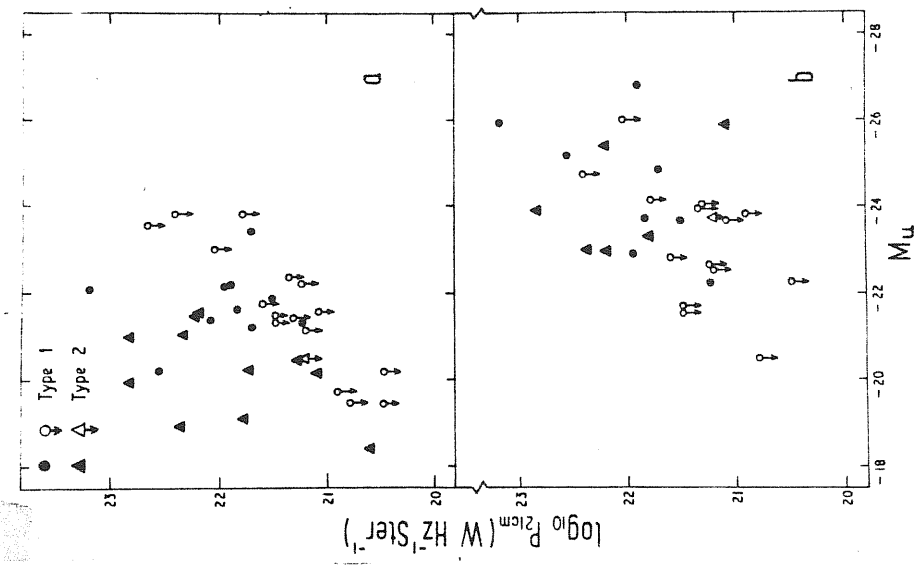

Fig. 29 Relation between the continuum luminosity at 21 cm and the absolute magnitude in the U band for galaxies in the sample of 41 defined in §1. **a** No reddening correction applied to M_U. The 38 galaxies in the sample with measured m_U are plotted. **b** Reddening correction applied to M_U by assuming the Balmer decrement is intrinsically as expected under case B radiative recombination theory (see text). The 29 galaxies in the sample with measured m_U and Balmer decrements are plotted. Note that, for the sake of clarity, detections and upper limits are plotted with different symbols in Figures 3-6

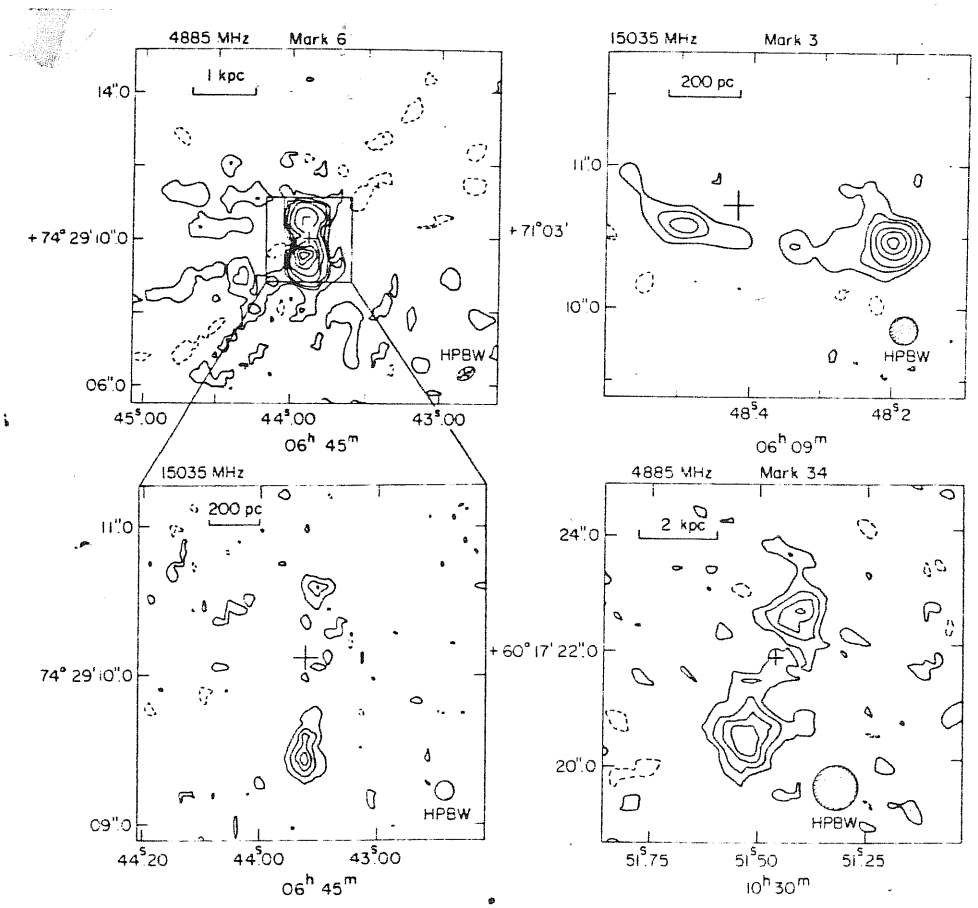

Figure 30 VLA maps of double radio sources in Markarian Seyfert galaxies. The cross marks the optical position (Clements 1981); the r.m.s. errors are typically ≈ 0".1 and are represented by the arms of the cross (except in the top left diagram). Left hand panel: Markarian 6 at 4885 (top) and 15035 MHz (bottom). In the top left diagram, contours are at -2 (dotted),2,4,6,10,20,40,60,80% of the peak brightness of 24.1 mJy (beam area)$^{-1}$. In the bottom left diagram, contours are at -20,20,40,60,80% of the peak brightness of 5.2 mJy (beam area)$^{-1}$. Top right is Markarian 3 at 15035 MHz; contours are at -10,10,20,30,50,70, 90% of the peak brightness of 24.8 mJy (beam area)$^{-1}$. Bottom right is Markarian 34 at 4885 MHz; contours are at -20,20,40,60,80% of the peak brightness of 1.2 mJy (beam area^{-1}).

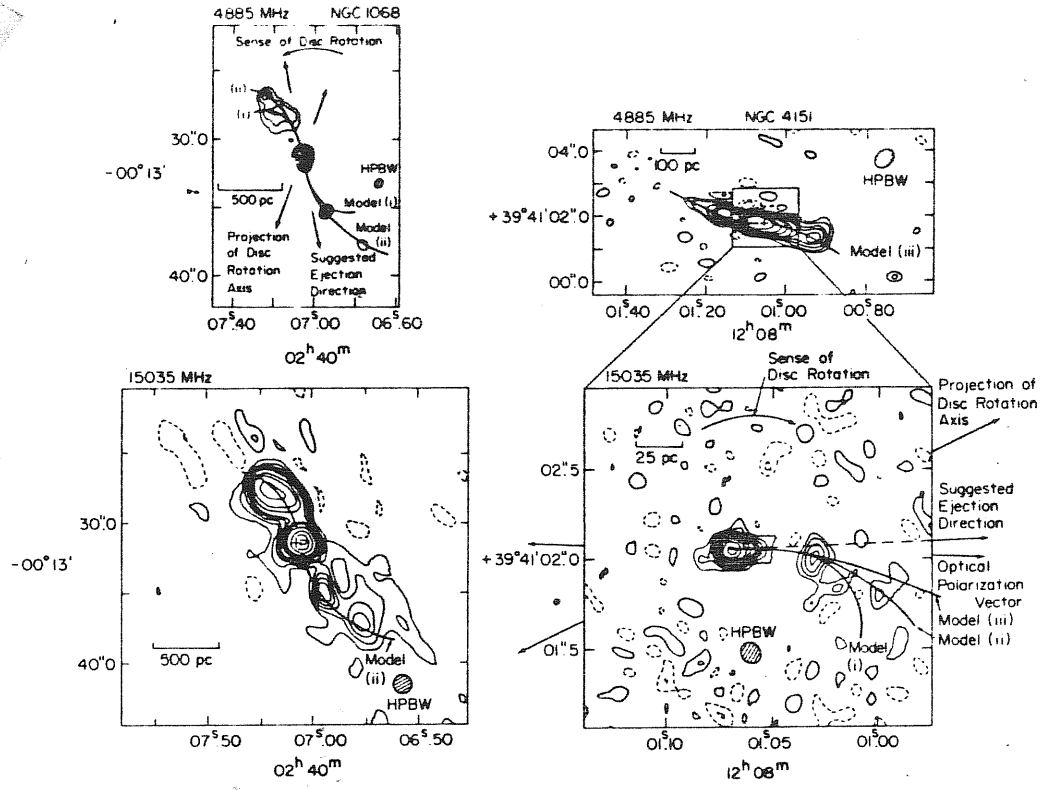

Figure 31 VLA maps of NGC 1068 and NGC 4151. The cross represents the optical nucleus in each case. The lines represent the "bent beam" models of Section 5.1. Left-hand panel is NGC 1068. Top left at 4885 MHz; contours at -2,2,4,6,10,15,20,25,30,35,40,45 times 6.83 mJy (beam area)$^{-1}$ (= 1000K). Bottom left at 15035 MHz; contours at -2,2,4,6,8,10,15,20,30,50,70,90% of the peak brightness of 161 mJy (beam area)$^{-1}$. Right hand panel is NGC 4151. Top right at 4885 MHz; contours at -5,5,10,15,20,30,40,50,60% of the peak brightness of 35 mJy (beam area)$^{-1}$. Bottom right at 15035 MHz; contours at -12,-6,6,12,18,24,30,40,50,70,90% of the peak brightness of 12.2 mJy (beam area)$^{-1}$.

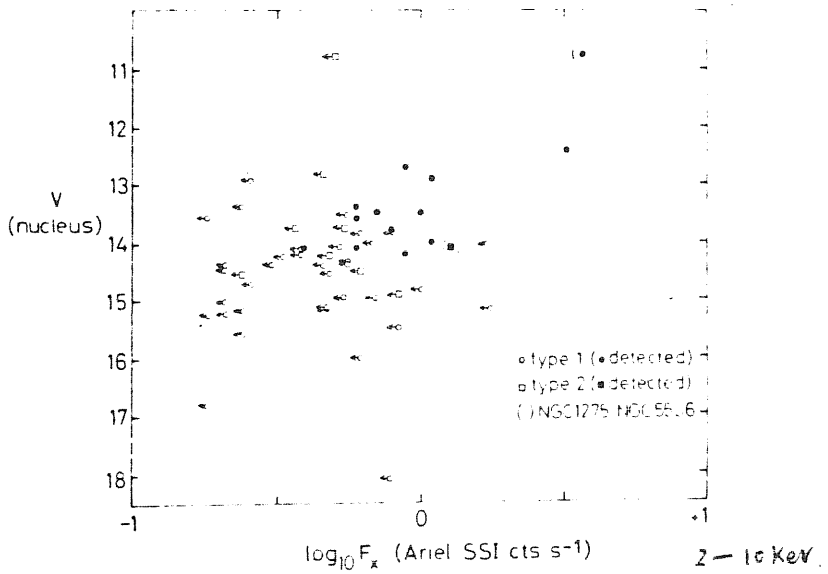

Figure 33 A plot of apparent nuclear magnitude V (corrected for absorption within our own Galaxy using $A_V = 0.18 \operatorname{cosec} b$ mag) against X-ray flux density F_X. The values of V for NGC 1275 and NGC 5506 have also been corrected for internal absorptions $A_V = 2.0$ and 1.9 mag respectively (*cf.* Table 5).

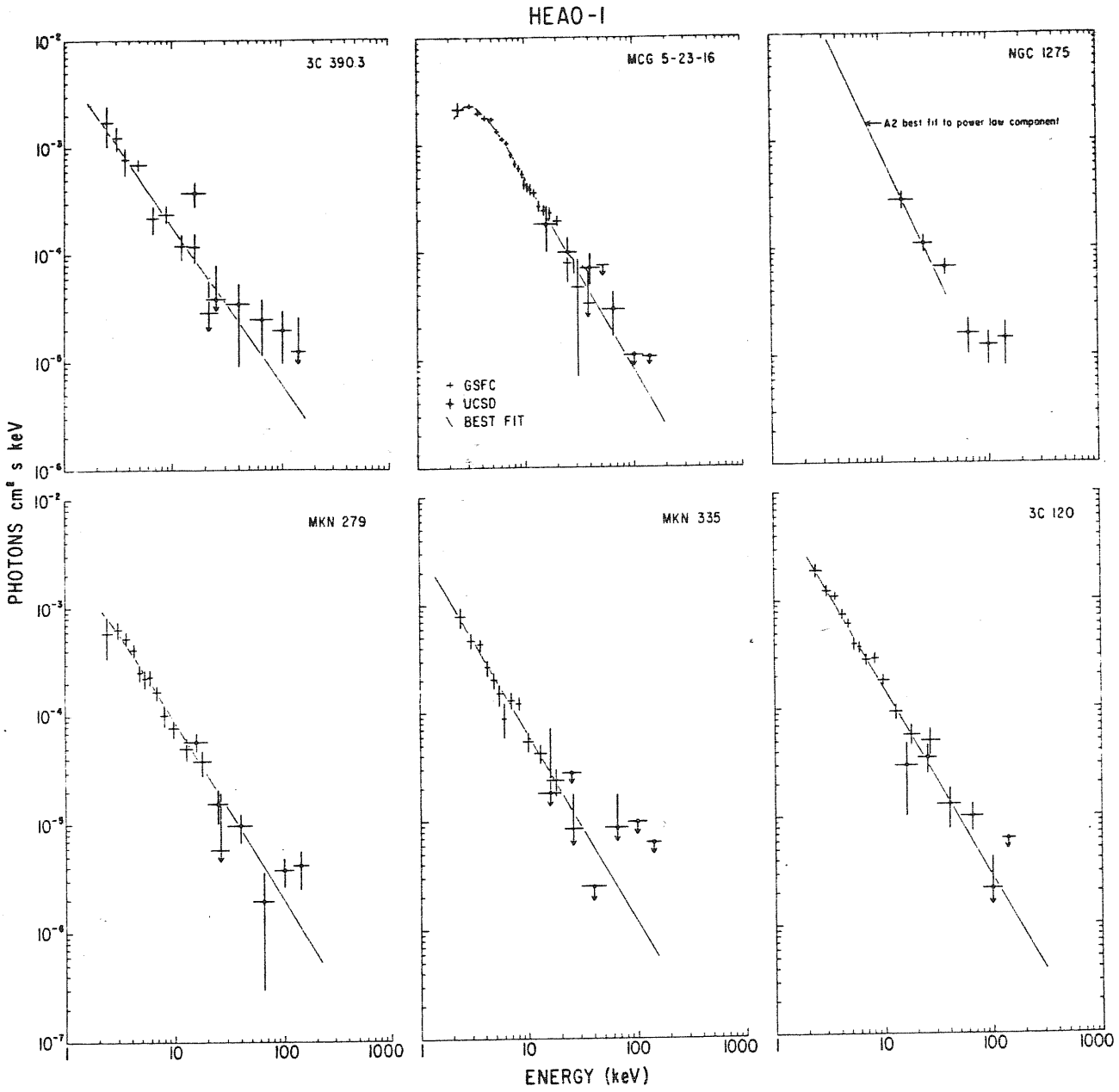

FIG. 1*a*

FIG. 32—(*a*, *b*) The inferred incident X-ray spectrum (2–165 keV) of 12 active galaxies. All error bars are one sigma, and upper limits are two sigma. In the case of NGC 1275, the GSFC measurement is represented by the best-fit model to the power law component. Solid lines in all other cases are the best-fit models. Crosses are the GSFC (A2) data and open circles are the UCSD (A4) data.

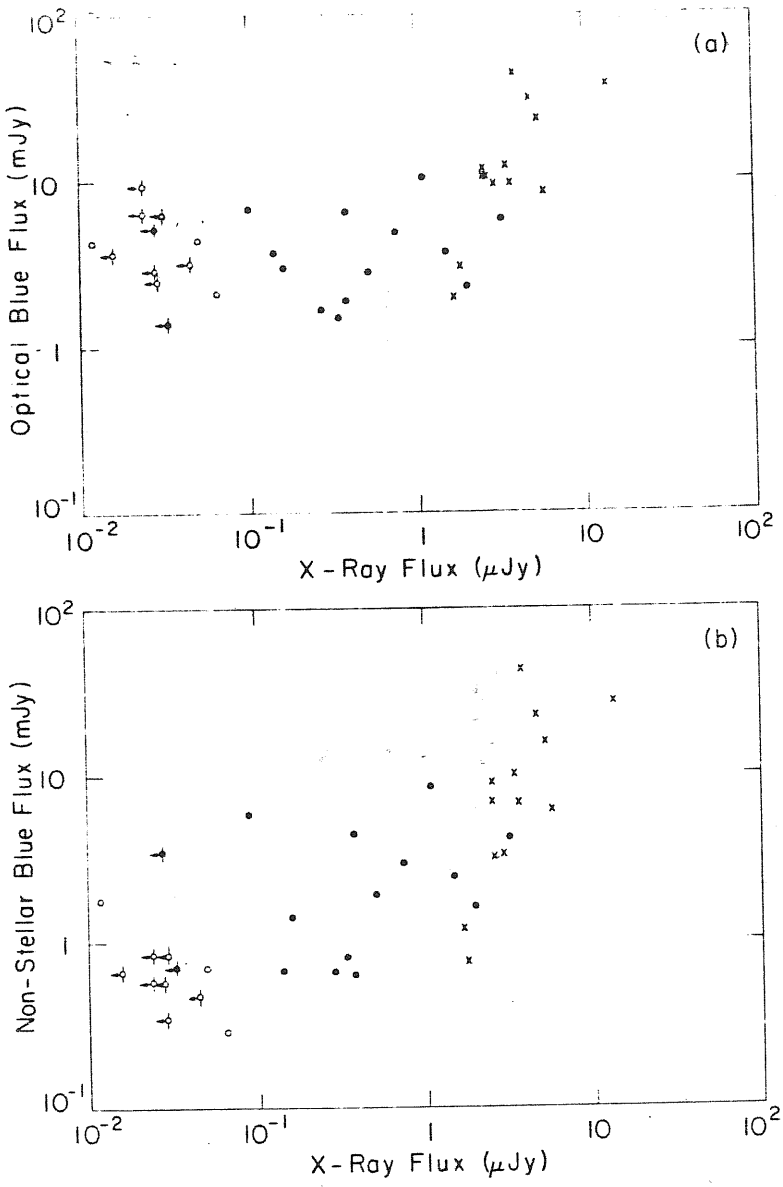

Fig. 34

(a) Blue band optical flux versus X-ray flux at 2 kev

(x) Seyferts detected in x-ray prior to the present observation

(•) Sy1 observed by the Einstein Observatory.

(o) Sy2 observed by the Einstein Observatory.

(b) Non stellar blue flux versus X-ray flux at 2 kev

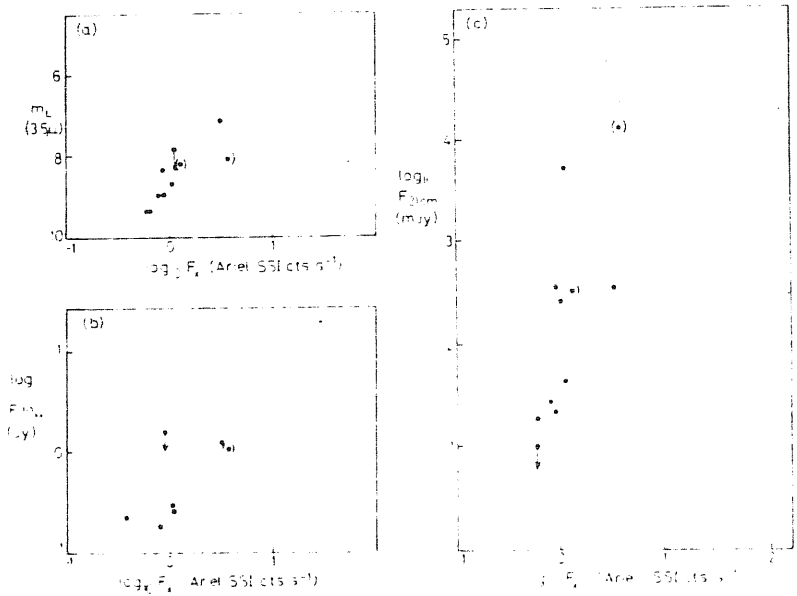

Figure 35 a-c Correlations between various observed parameters and X-ray flux density. Apparent intensities, rather than absolute, have been used for Figs (a)–(c) for reasons explained in the text. NGC 1275 and NGC 5506 are shown in brackets. (a) Apparent magnitude at λ 3.5 μm, (b) flux density at λ 10 μm, (c) flux density at λ 21 cm.

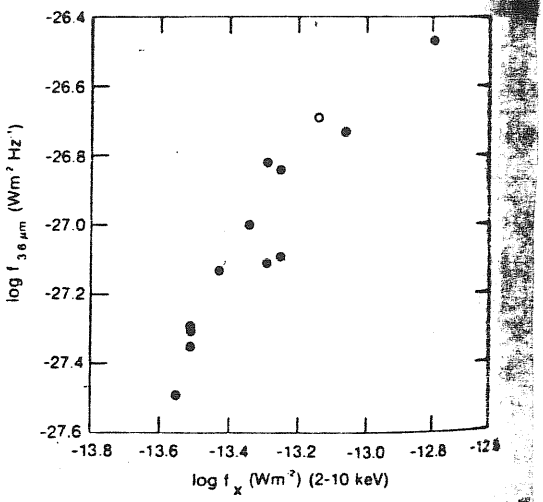

FIG. 36—Observed 3.6 μm flux density versus the 2-10 keV flux for 12 Seyfert galaxies and the quasar 3C 273 (*open circle*).

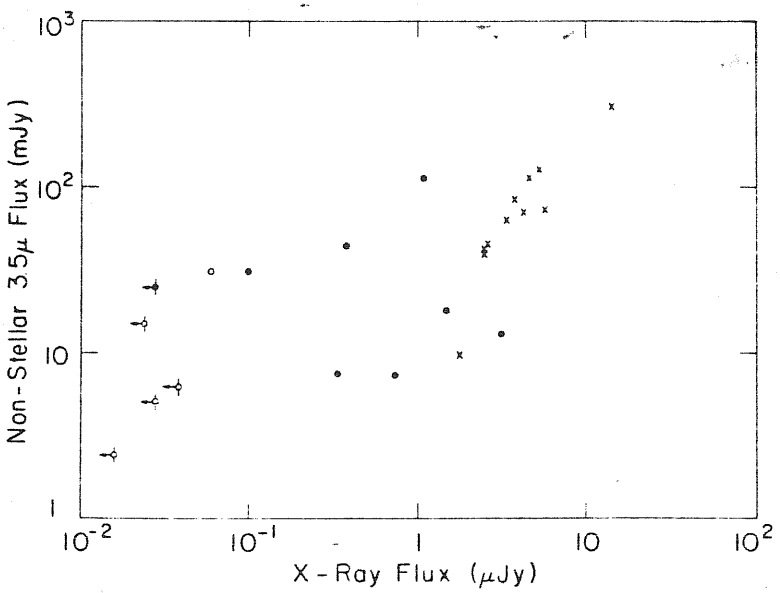

Fig 37 A plot of nonstellar flux near 3.5 μm versus X-ray flux at 2 keV. Symbols are as in Fig 34.

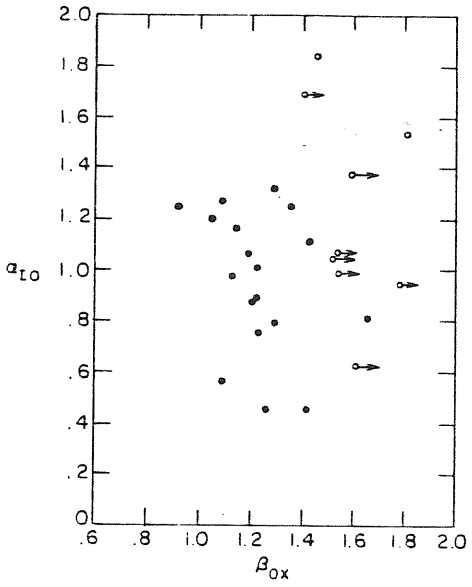

FIG. 38—The 3.5 μm to 4400 Å spectral index α_{IO} versus the optical to X-ray spectral index β_{OX}. Filled circles represent Seyfert 1's; open circles, Seyfert 2's.

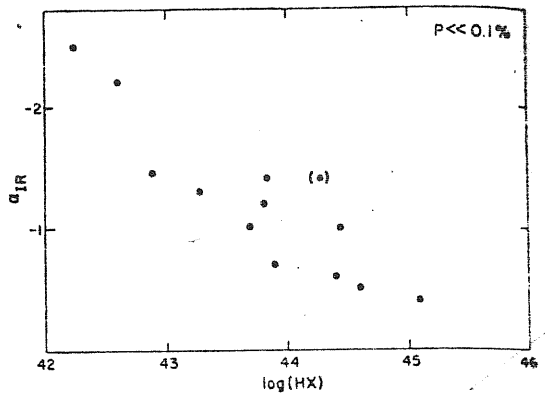

Fig. 39. Infrared spectral index, α_{IR}, as a function of HX.

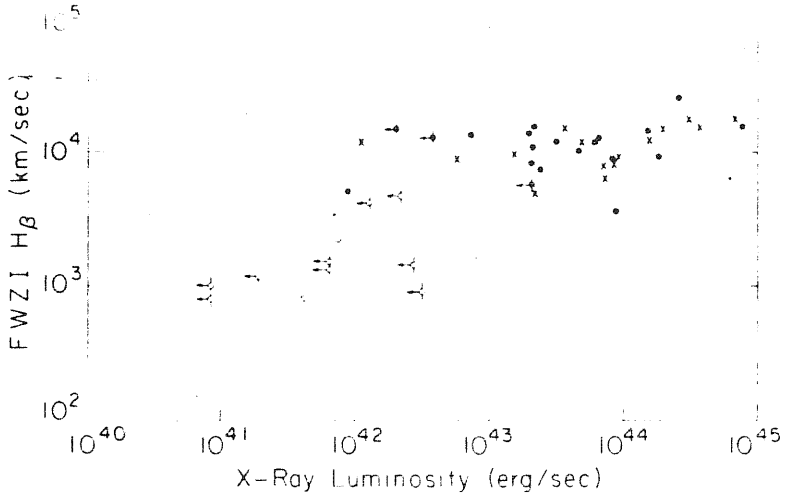

Fig. 40. FWZI H_β versus the X-ray luminosity of range of 0.5 kev – 4.5 kev.

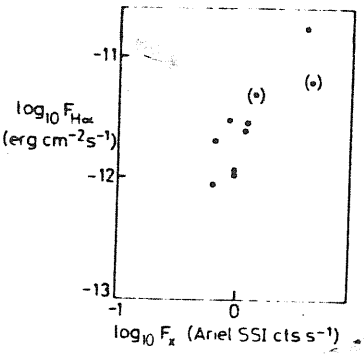

(a) X-ray flux versus H_α emission line flux

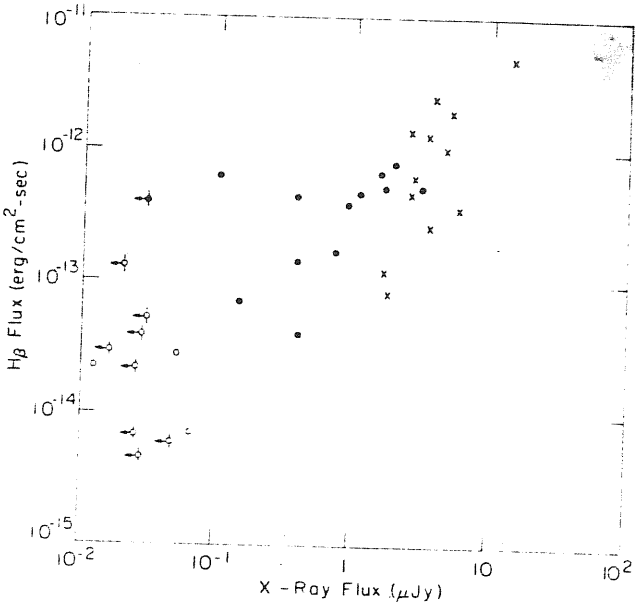

(b) The flux in the H_β emission line versus the X-ray flux at 2 kev.

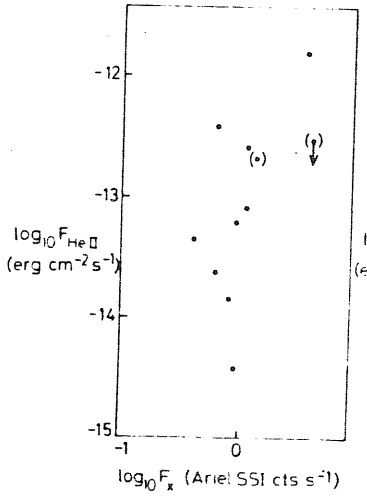

(c) X-ray flux versus intensity of He II λ 4686 Å

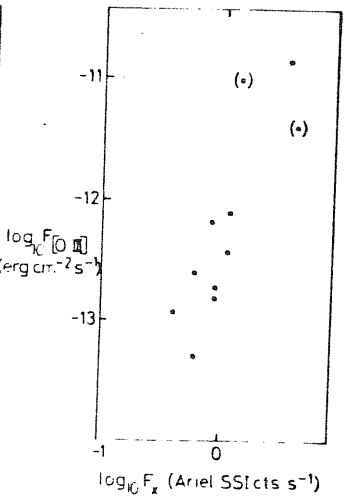

(d) X-ray flux versus intensity of [O III] λ 5007 Å

FIG. 41 a-d

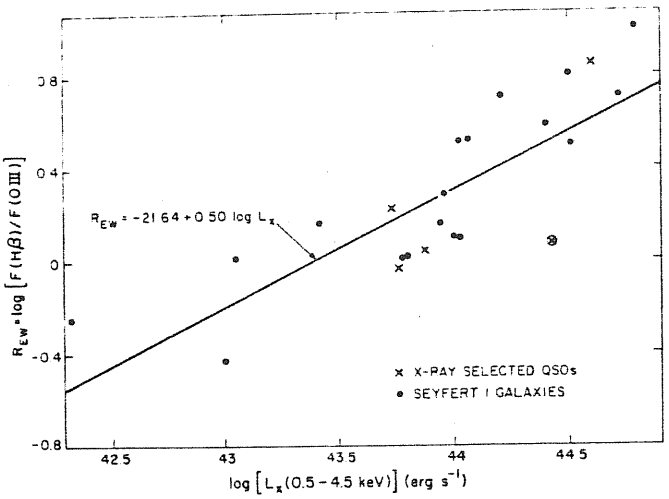

FIG. 42 Correlation between ratio R_{EW} of equivalent widths of Hβ to [O III] λλ4959+5007 vs. L_x for X-ray selected QSOs and Seyfert 1 alaxies (cf. Fig. 3), with least-squares fit line shown. The implied relation $R_{EW} \sim L_x^{0.5}$ may provide a new X-ray luminosity indicator for eyfert 1's and RQ QSOs which, in future studies, could possibly restrict values of q_0.

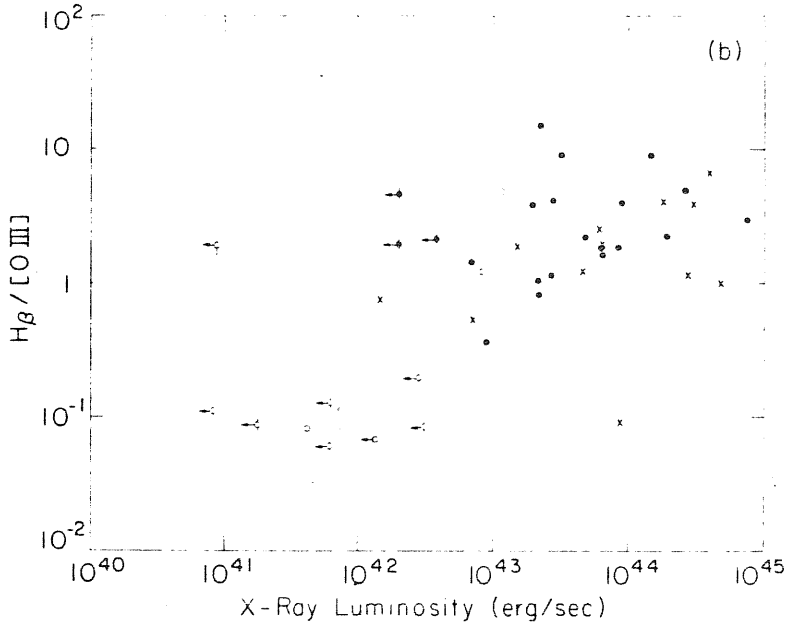

Fig. 43. The Hβ/[OIII]λ5007Å ratio versus the 0.5 keV – 4.5 keV X-ray luminosity.

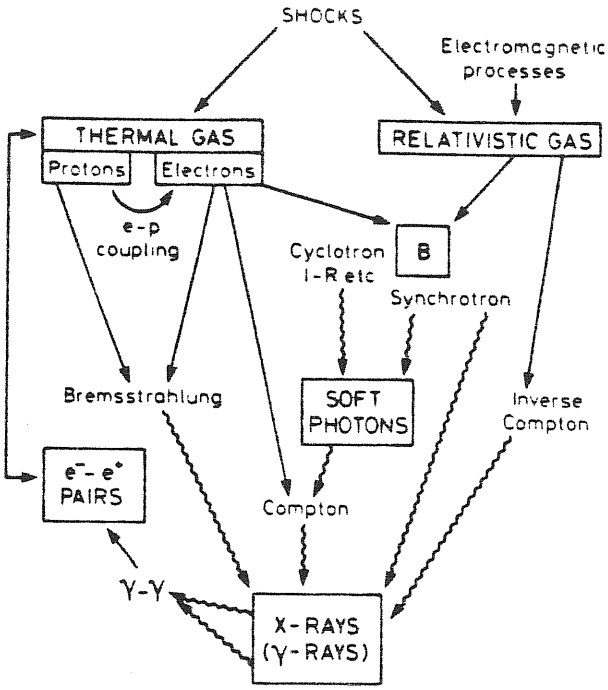

Figure 44. X-radiation processes.

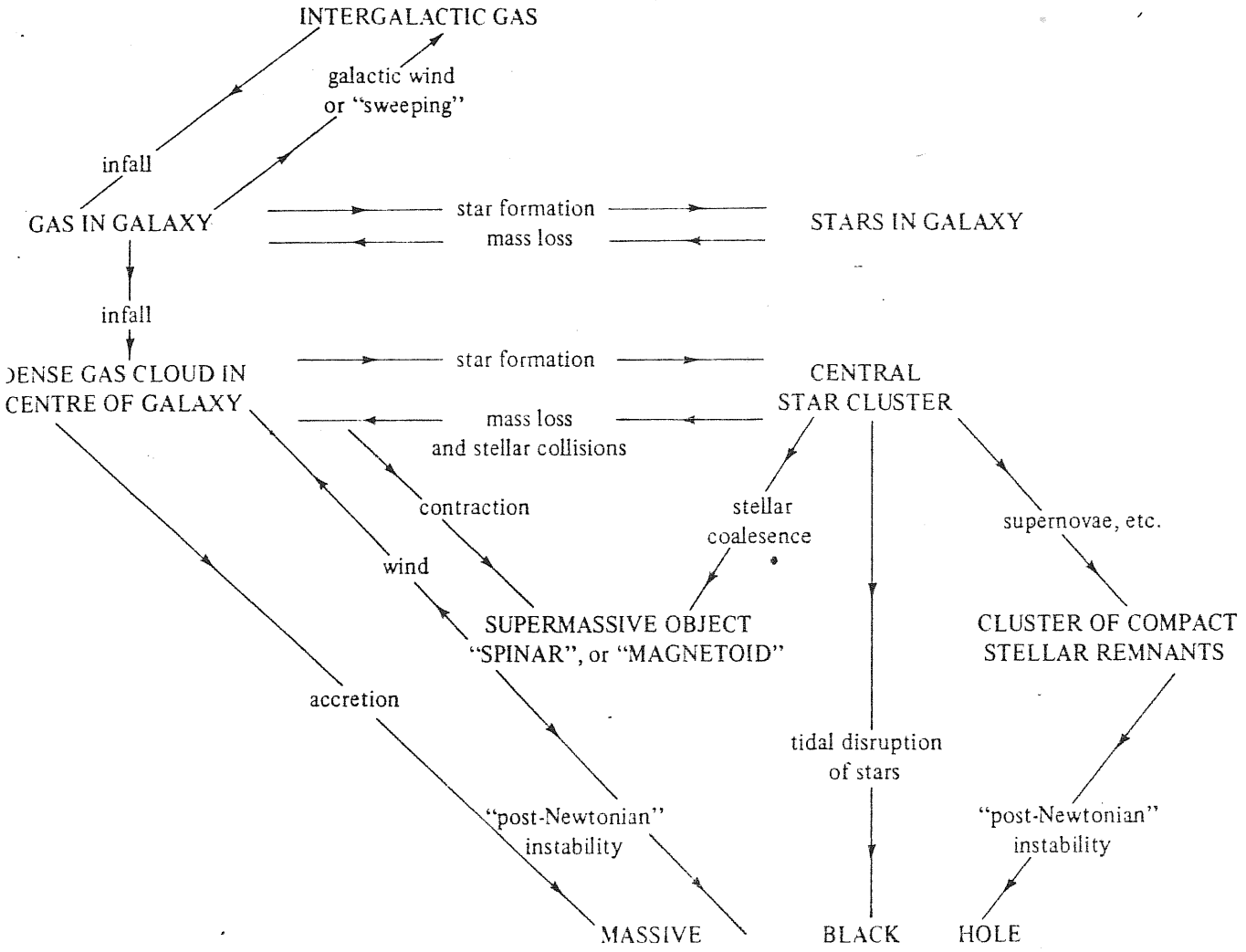

Fig. 45 "Flow diagram" indicating the processes whereby a massive black hole could form in a galactic nucleus. Quasars can be interpreted in terms of accretion of gas (or even entire stars) onto a black hole of 10^7–$10^8\ M_\odot$; and some of the less violent phenomena observed in the nuclei of galaxies may represent "precursor" stages.

Fig. 46. HX (2–10 kev) Luminosity distributions of Sy 1, Sy 1.5, Sy 2.

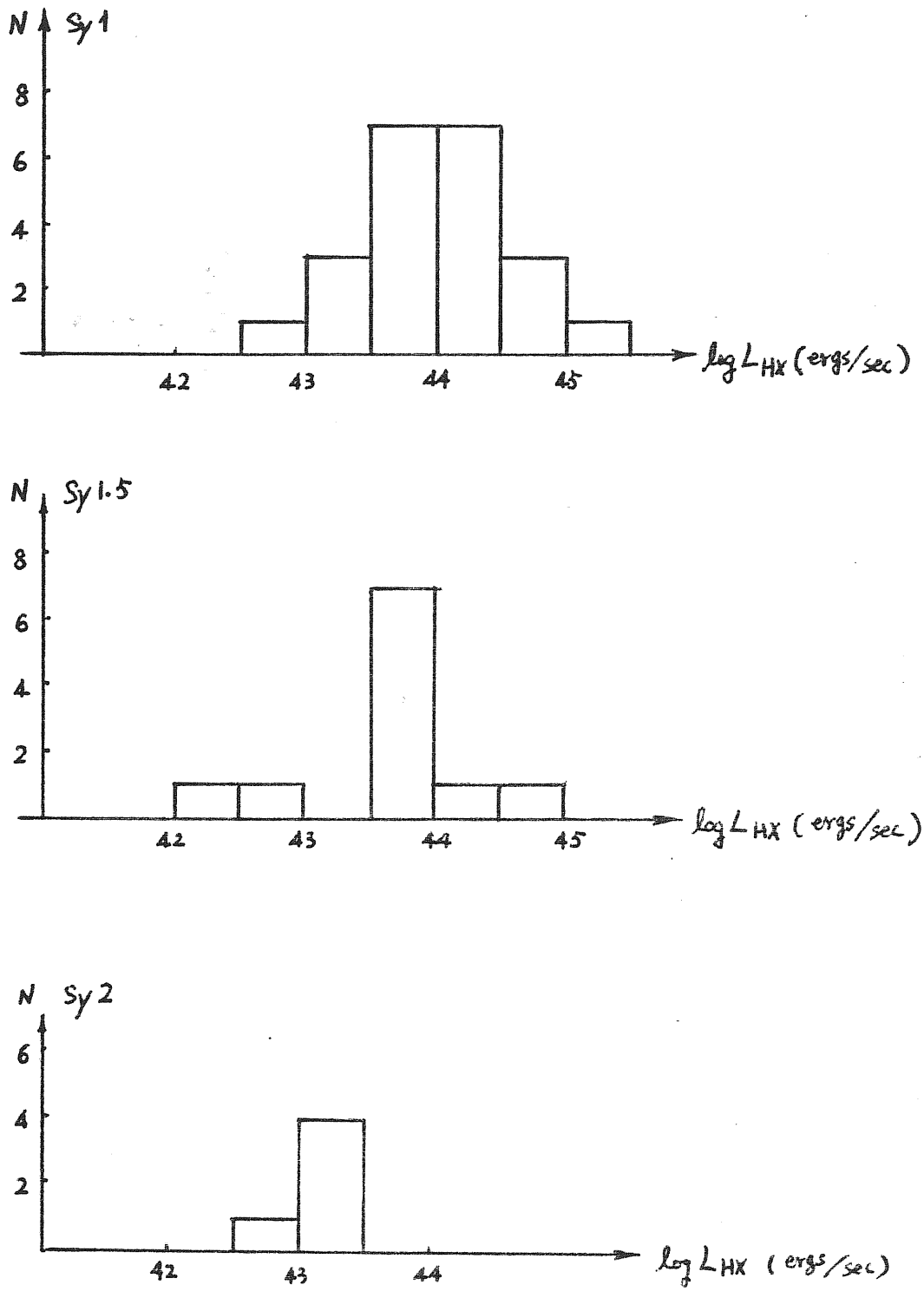

Fig. 47. SX (0.5 - 4.5 Kev) luminosity distributions of Sy 1, Sy 1.5 and Sy 2.

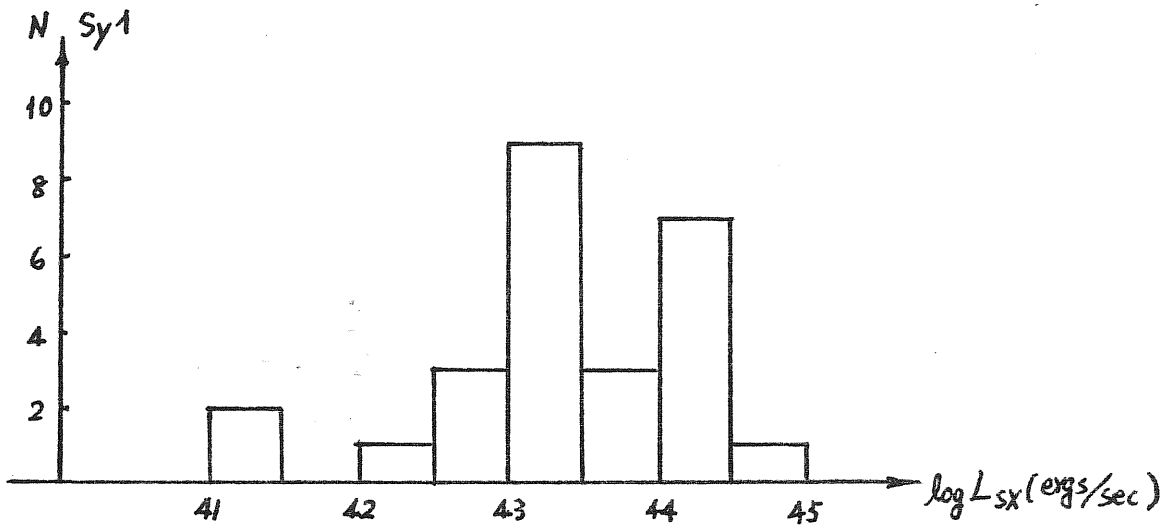

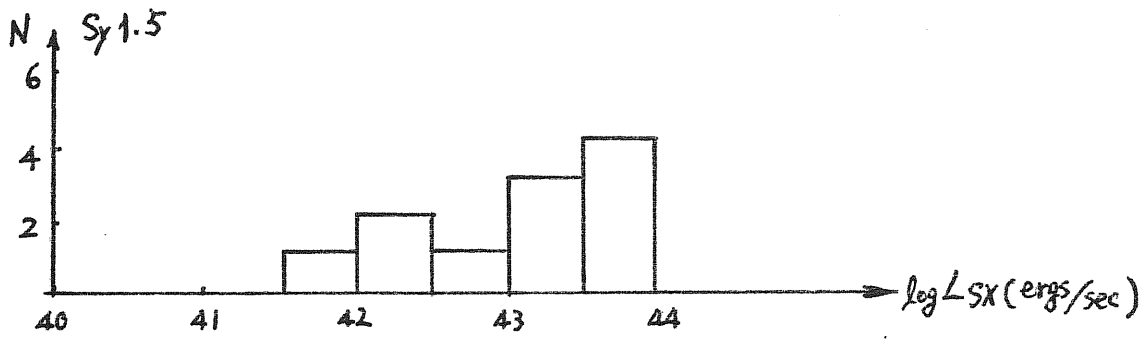

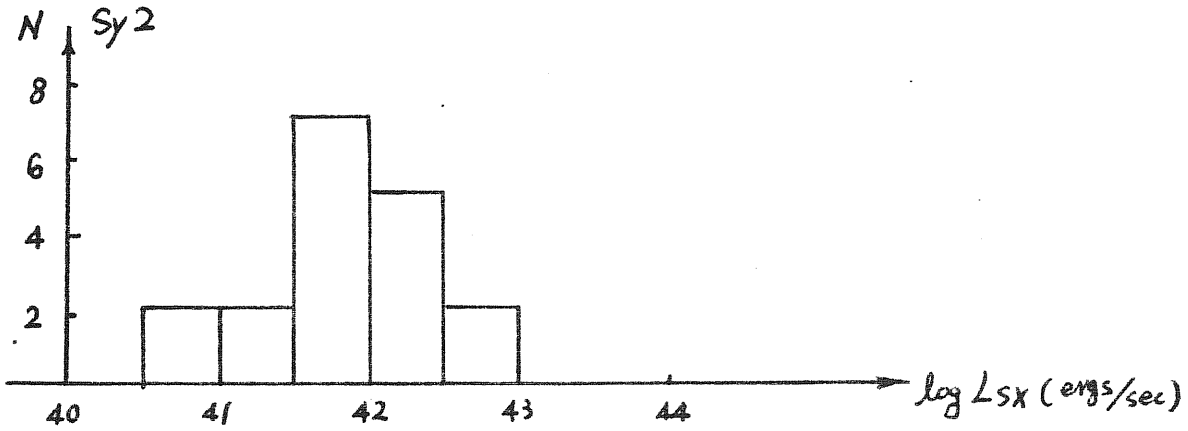

Fig 48. α_{ox} distribution

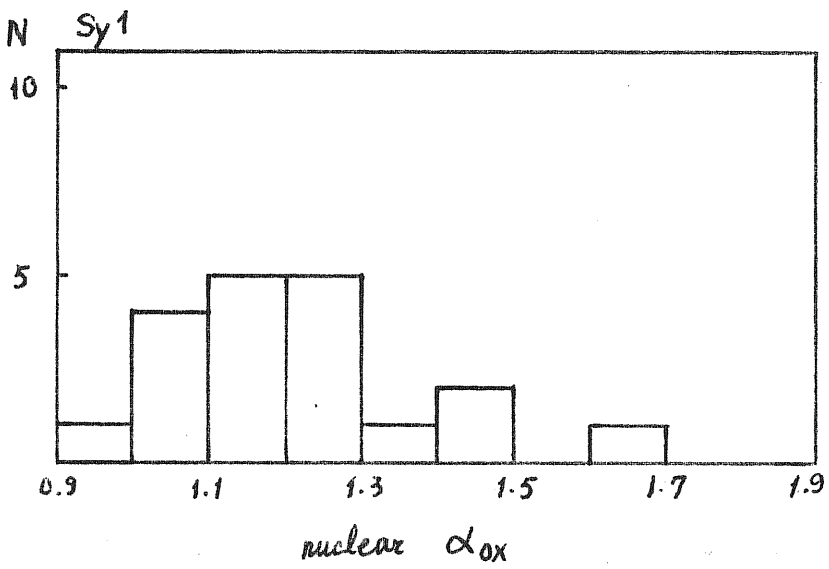

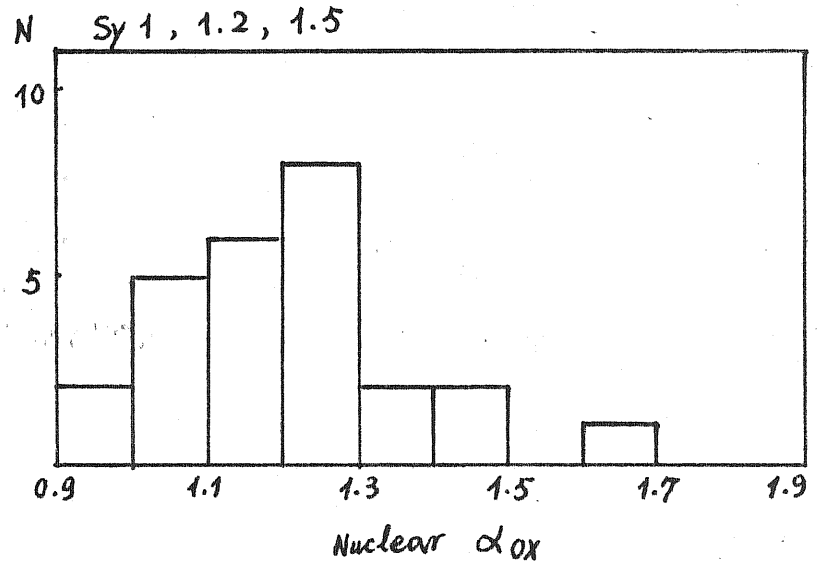

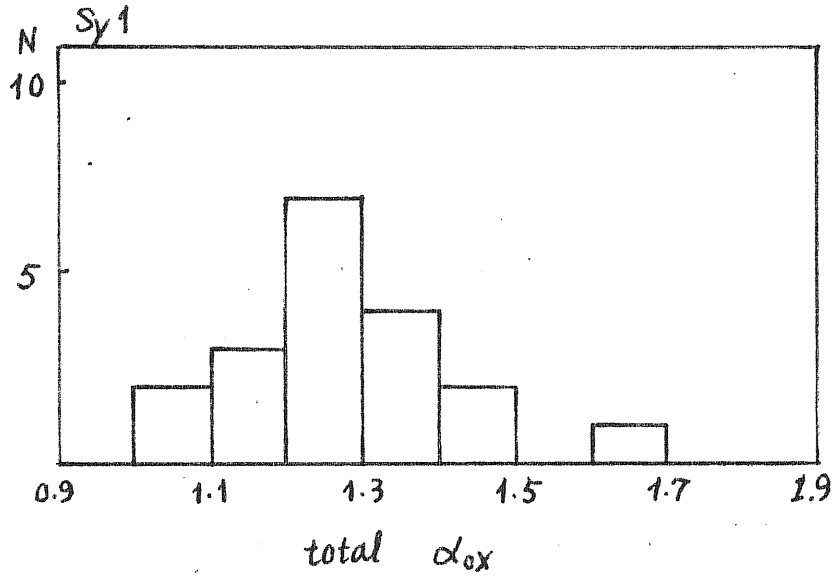

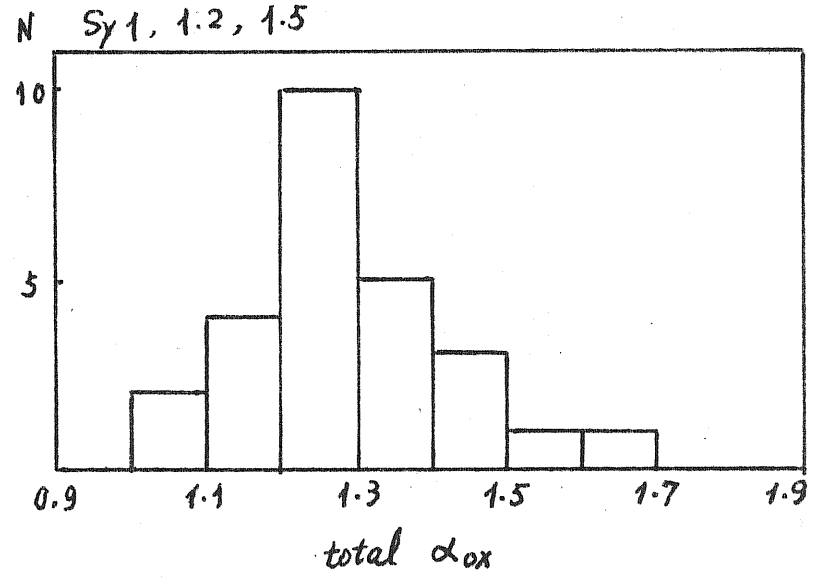

Fig 49.

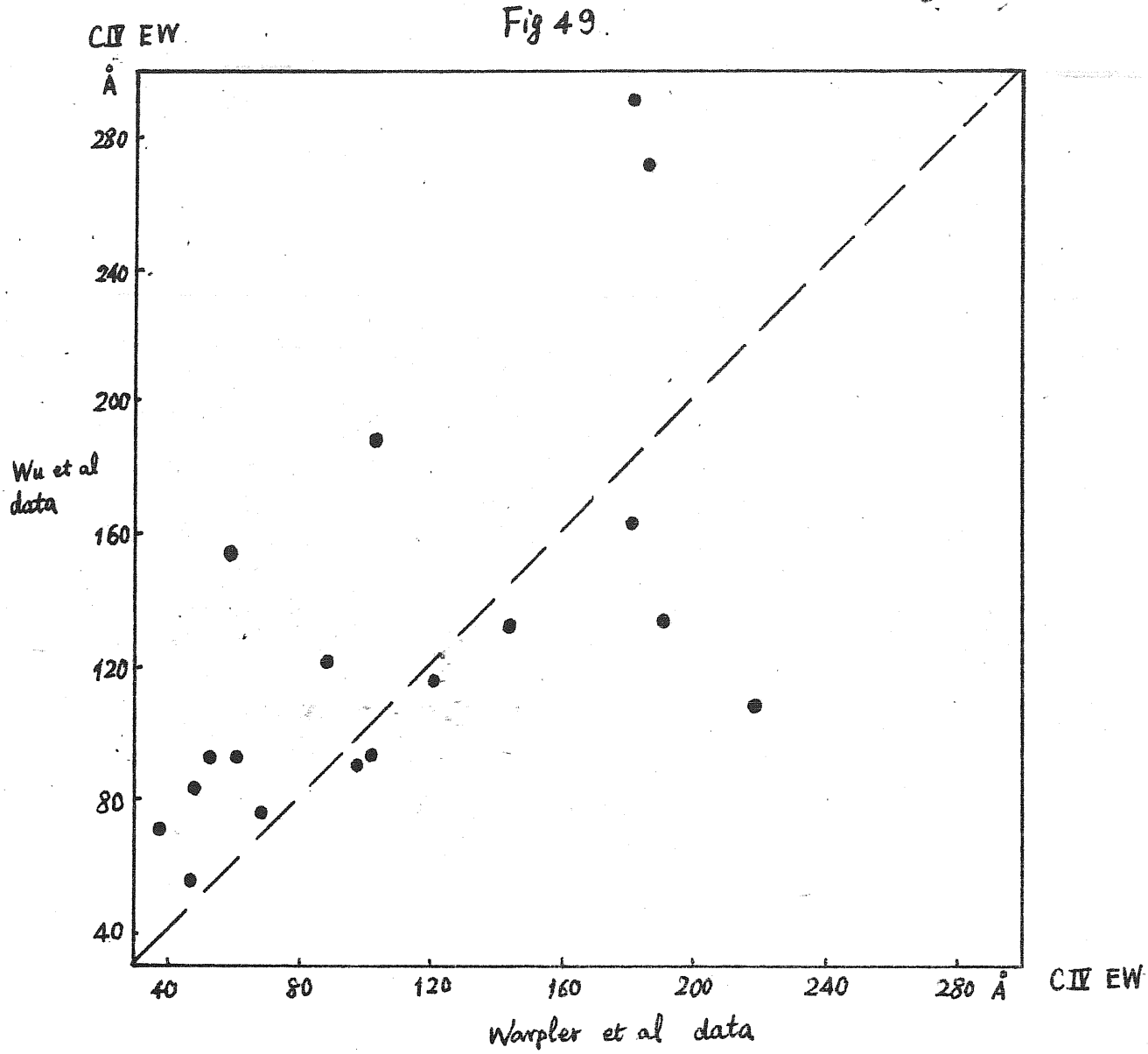

Fig 50 a

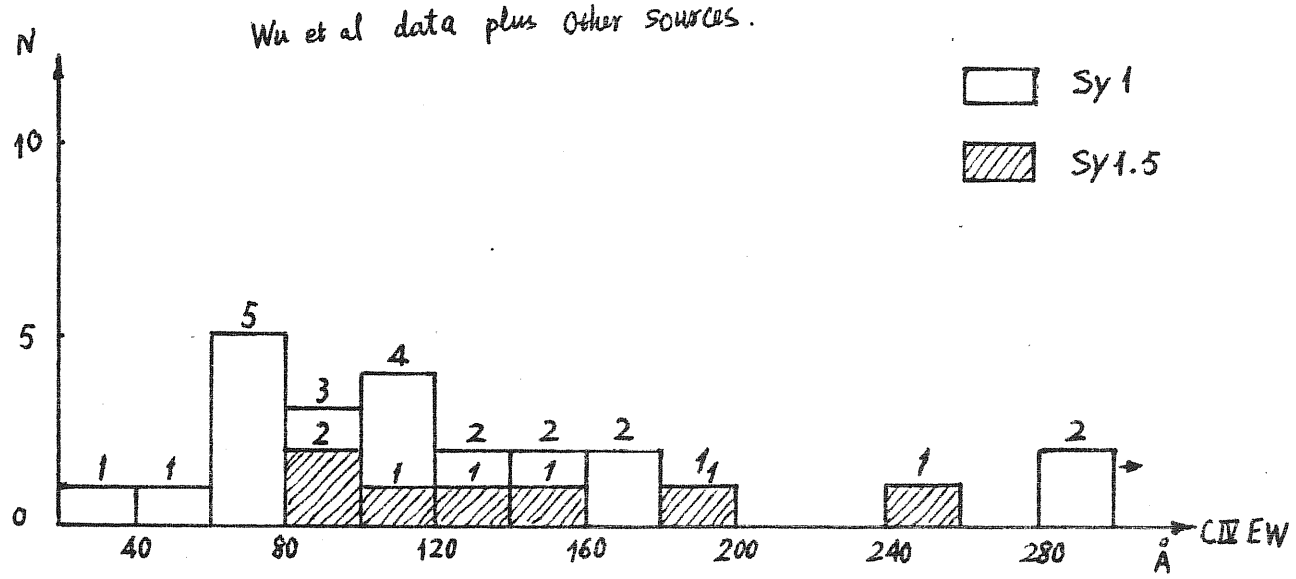

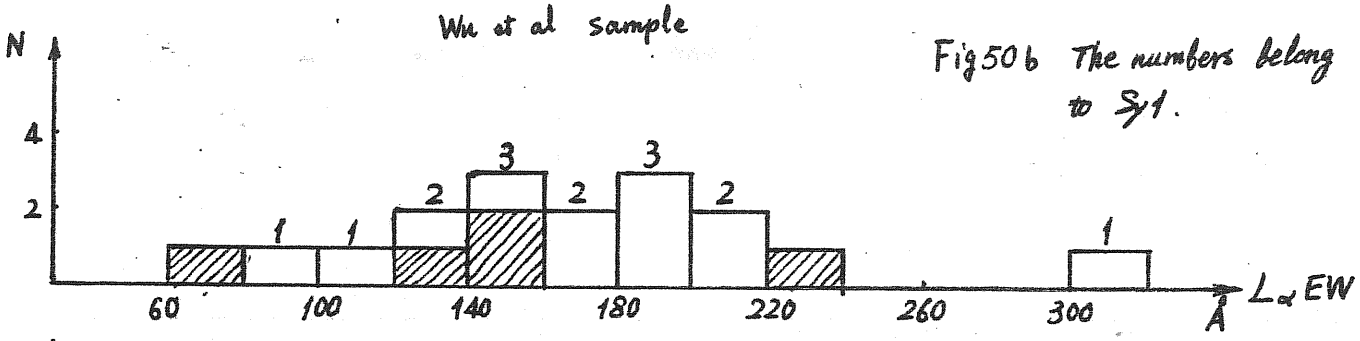

Fig 50 b The numbers belong to Sy1.

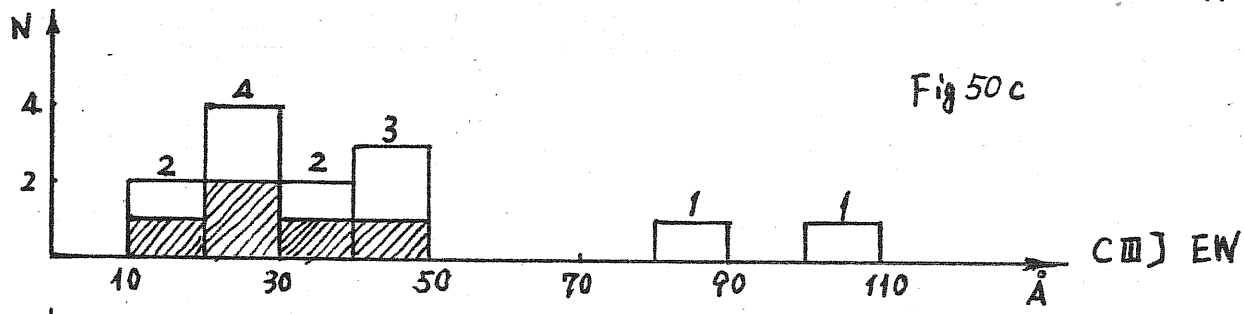

Fig 50 c

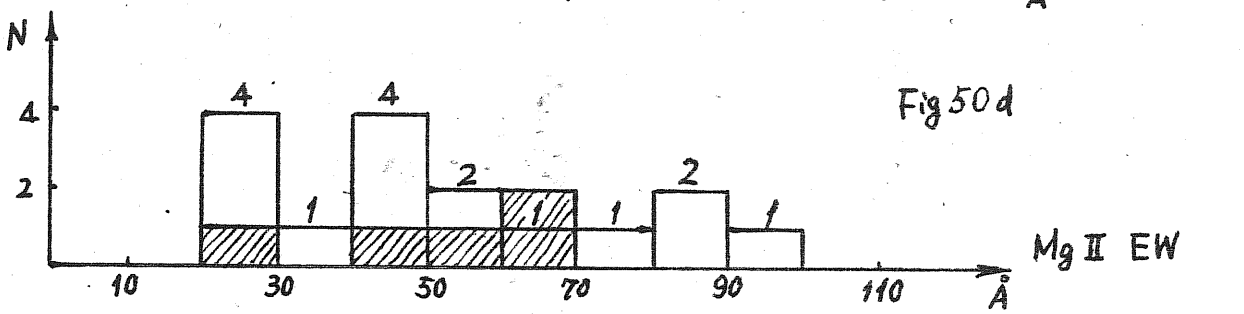

Fig 50 d

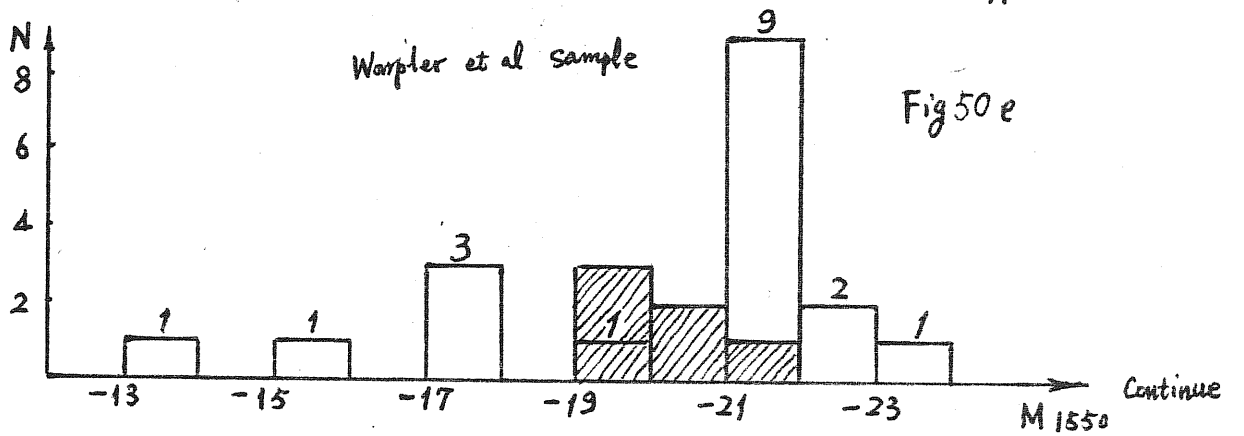

Fig 50 e

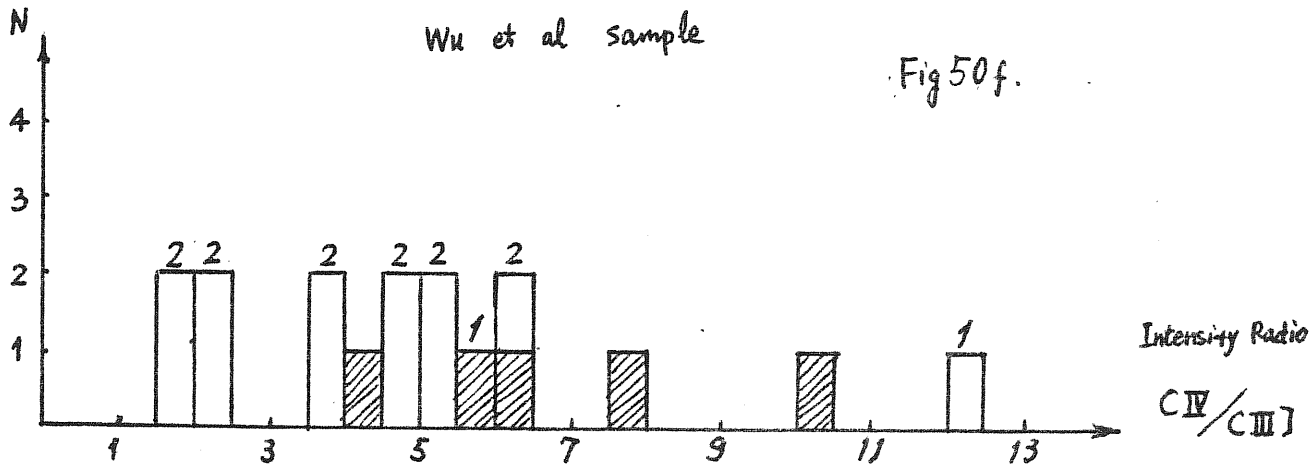

Fig 50 f.

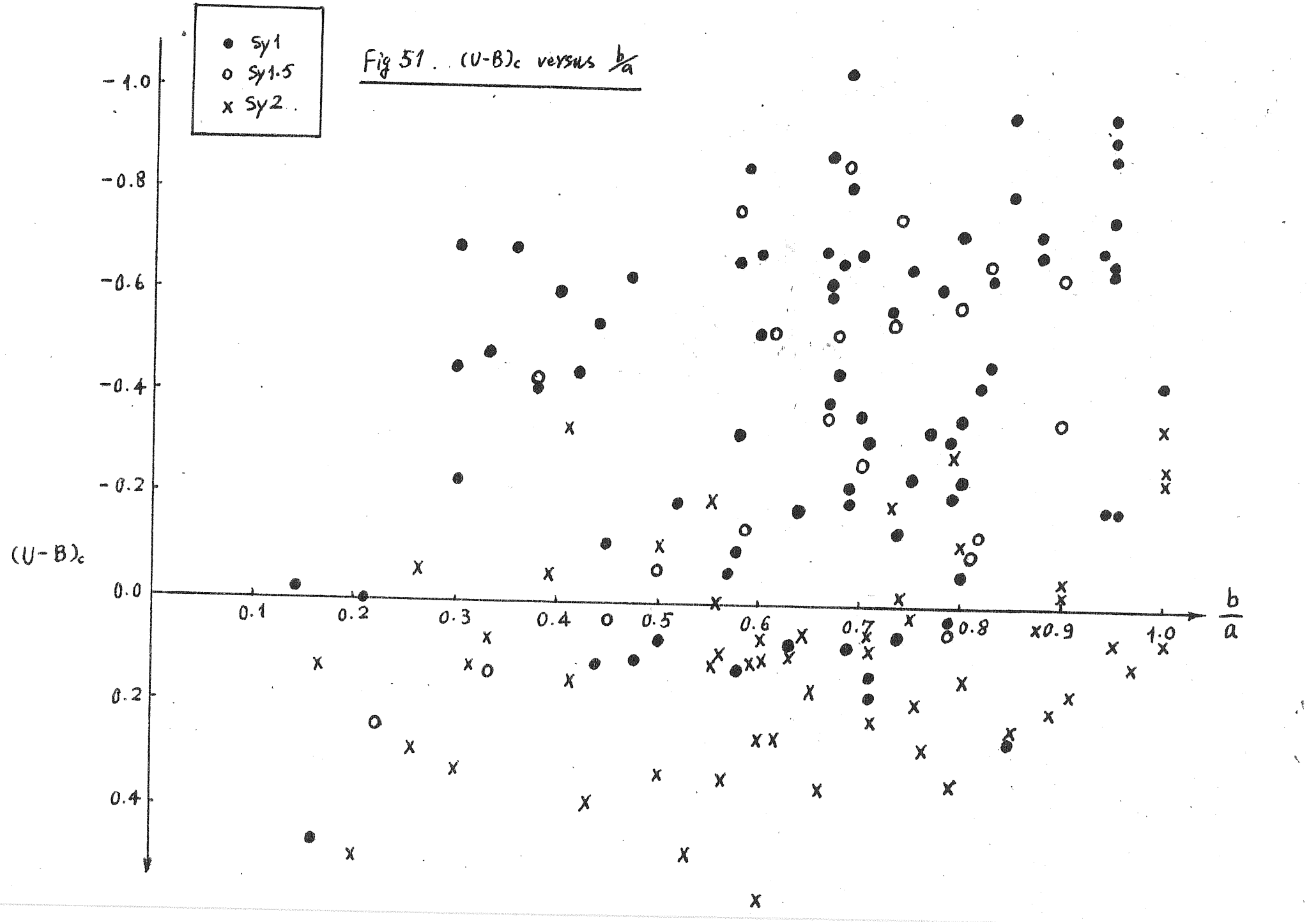
Sy1
Sy1.5
Sy2
Fig 51. (U-B)c versus b/a
-1.0
-0.8
-0.6
-0.4
-0.2
0.0
0.2
0.4
(U-B)c
0.1
0.2
0.3
0.4
0.5
0.6
0.7
0.8
0.9
1.0
b/a

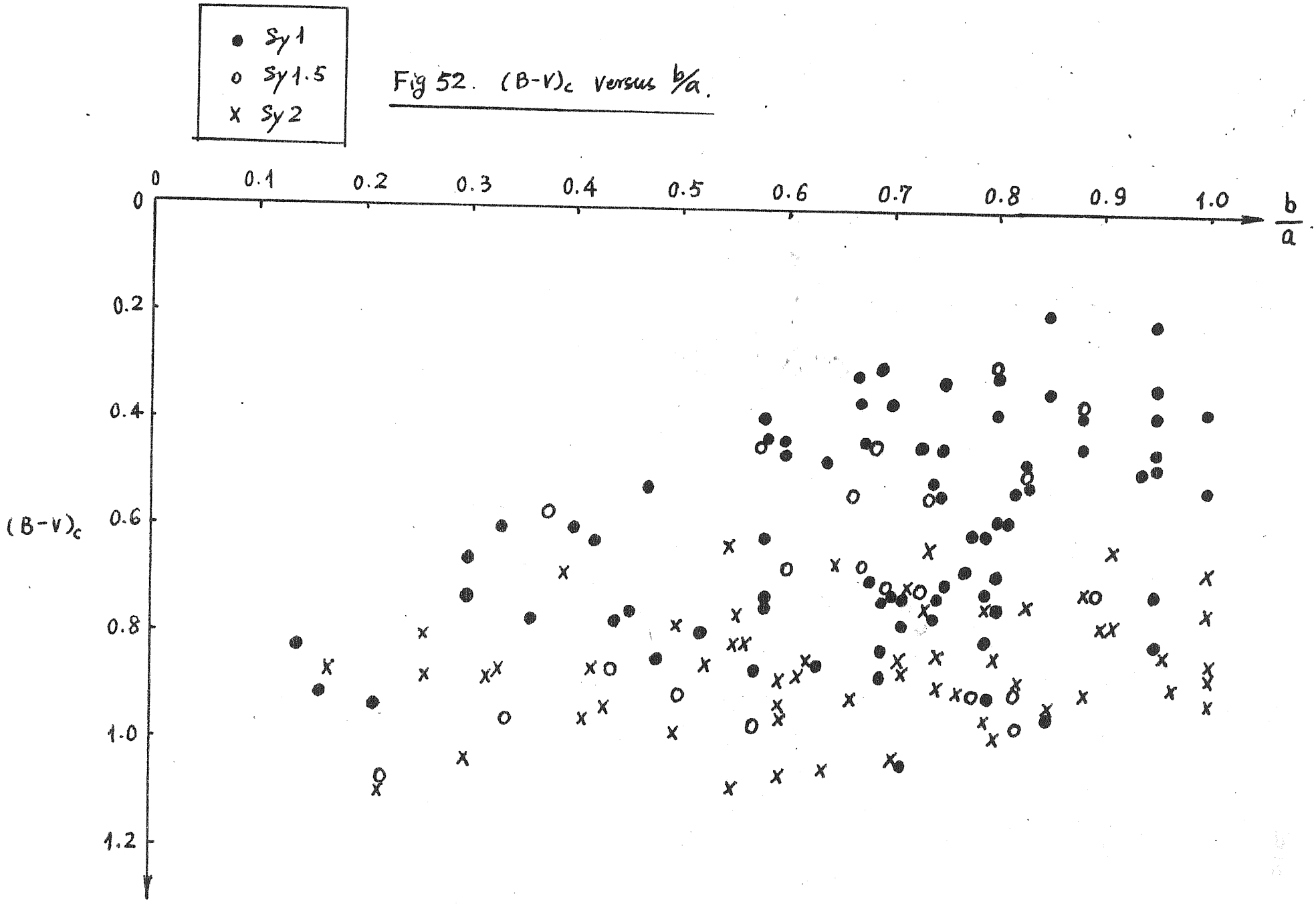

Fig 52. $(B-V)_c$ versus b/a.

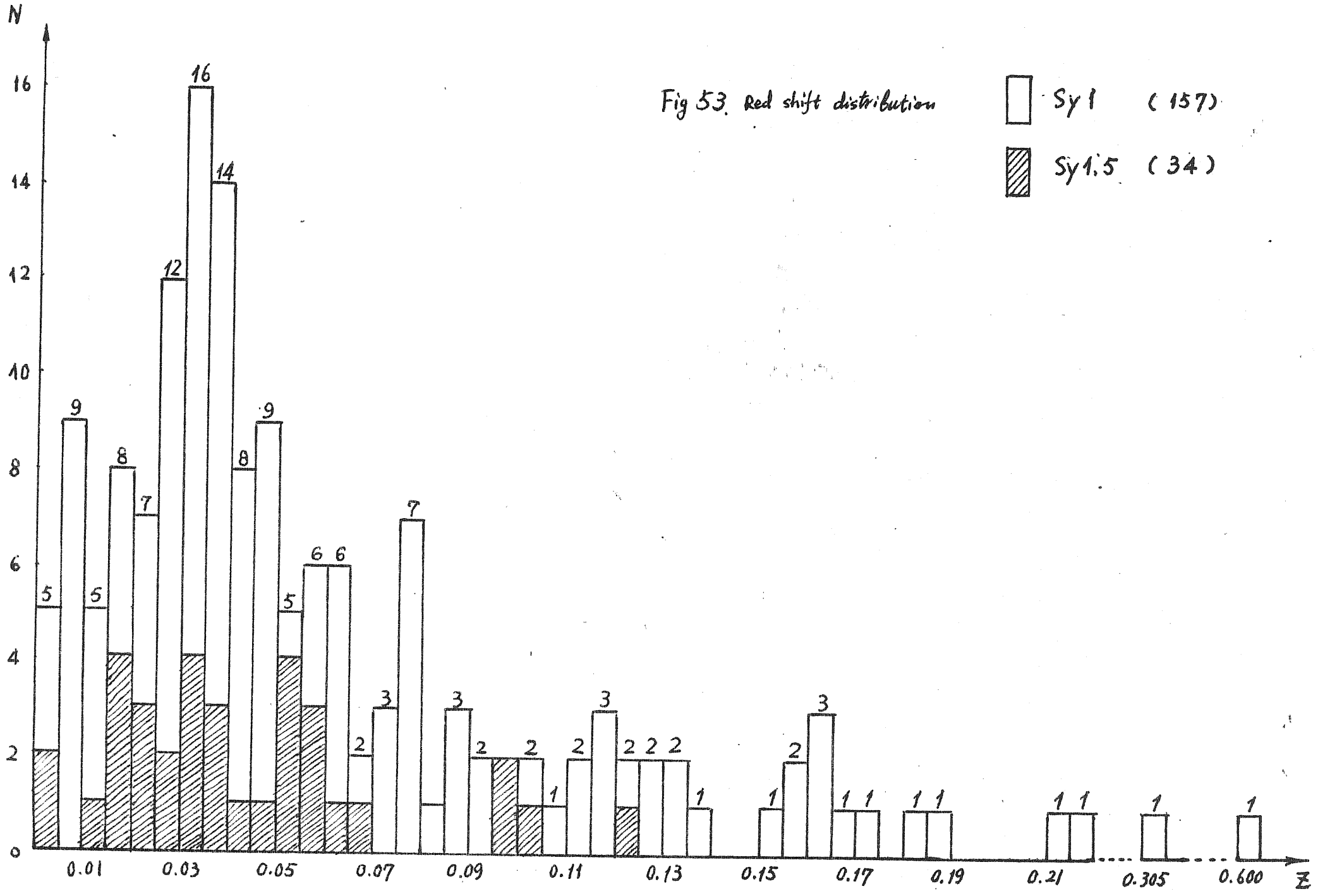

Fig 53. Red shift distribution

Fig 54. Red shift distribution for Sy 2.

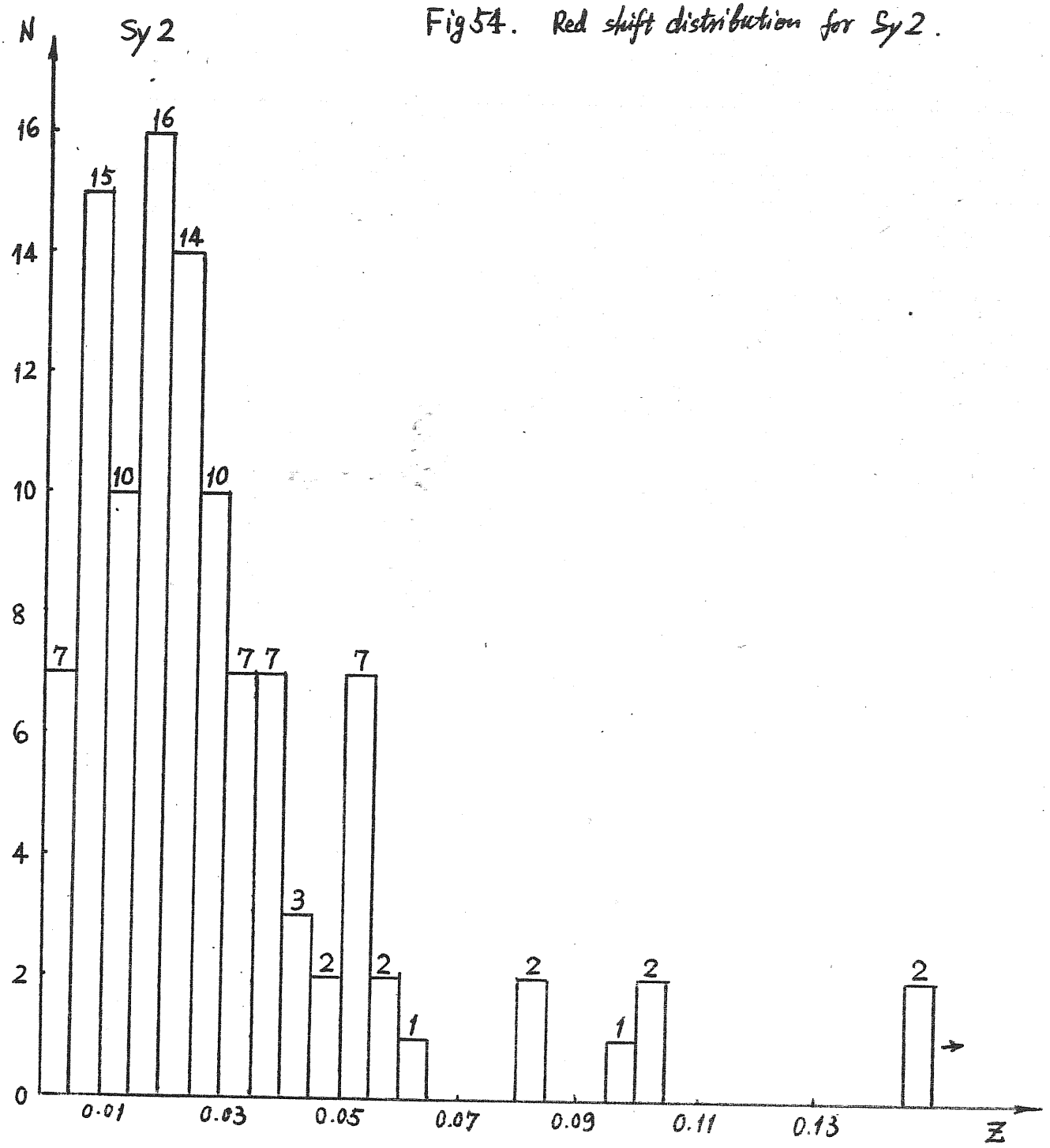

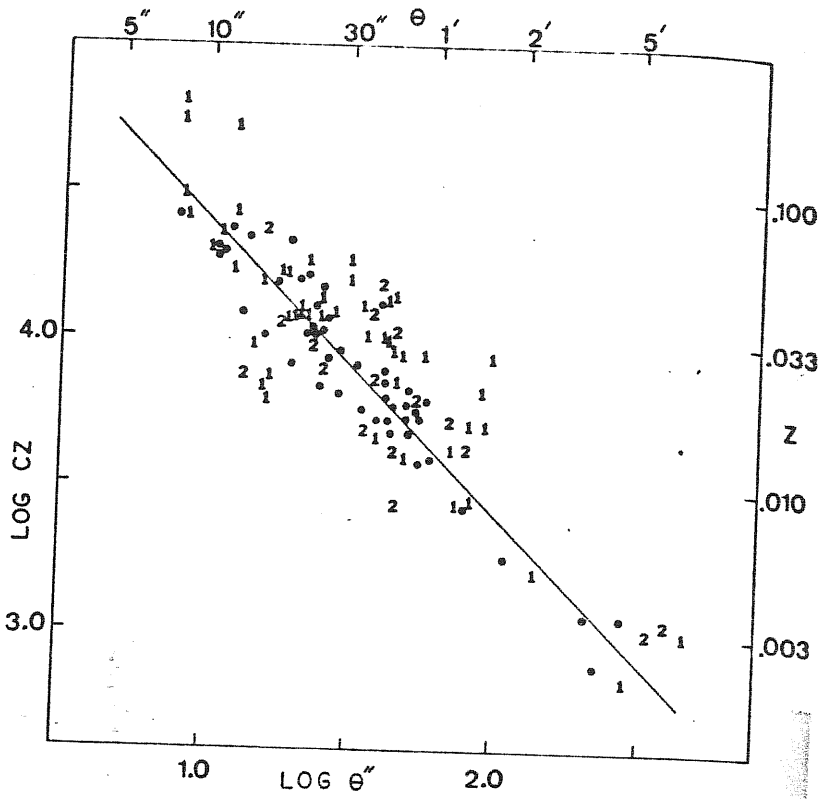

FIG. 55.—Angular-diameter–redshift diagram for Seyfert galaxies and elliptical galaxies. *Filled circles*, (1972*a*); *numbers 1*, class 1 Seyfert galaxies from table 1; *numbers 2*, class 2 Seyfert galaxies from table 1.

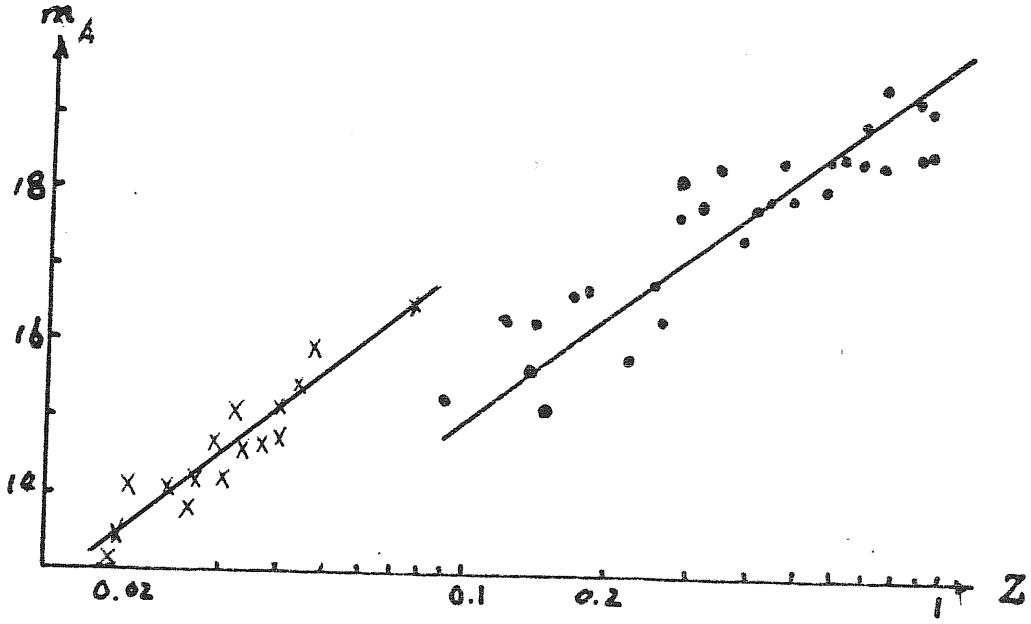

$m_A \equiv m_v - k_v - A_v$

• Low-redshift QSOs with weak radio

× non-violently variable Type I Seyfert galaxies

Fig. 56. Apparent magnitude – redshift diagram

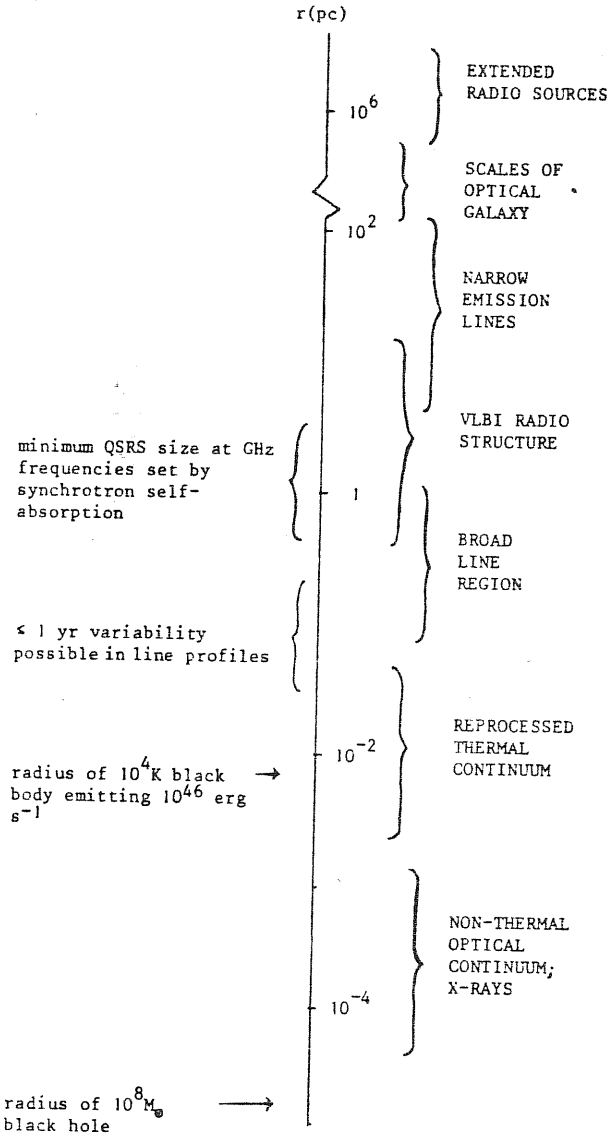

Figure 57 This diagram indicates, very roughly, the dimensions (measured in parsecs) of the regions which give rise to the various forms of emission in quasars and powerful galactic nuclei.

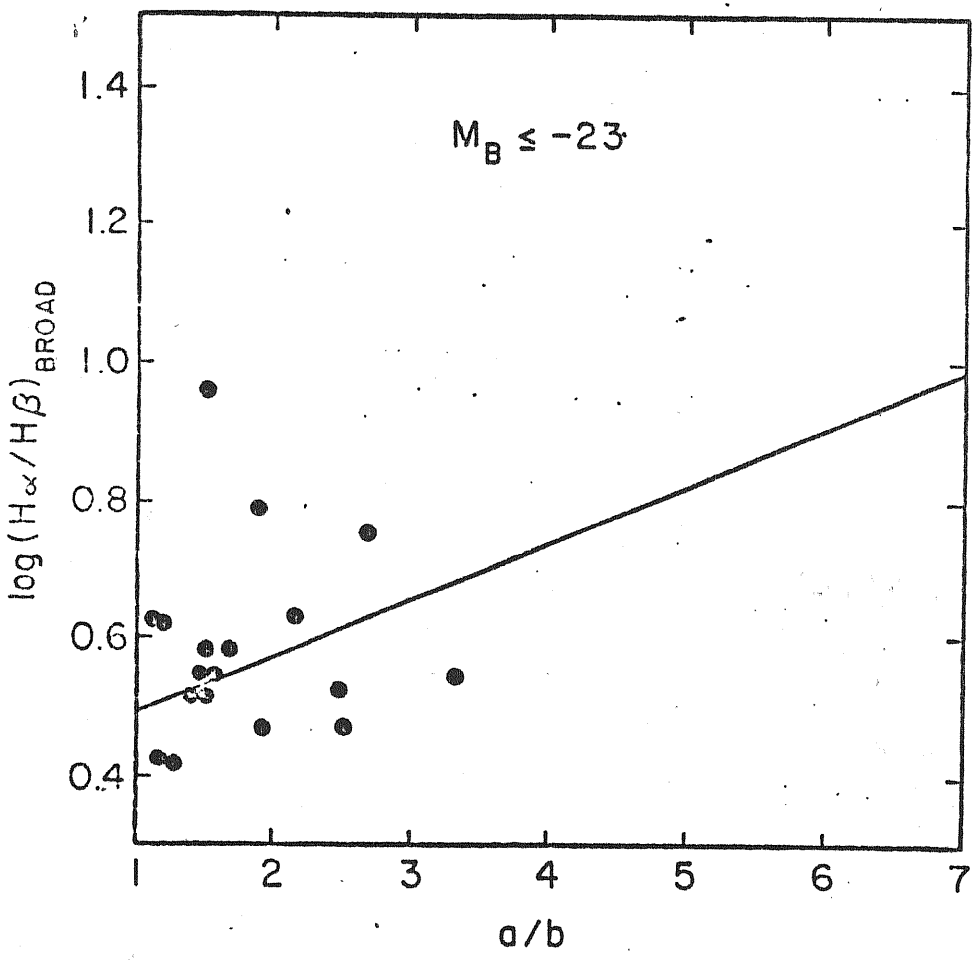

Fig. 58a

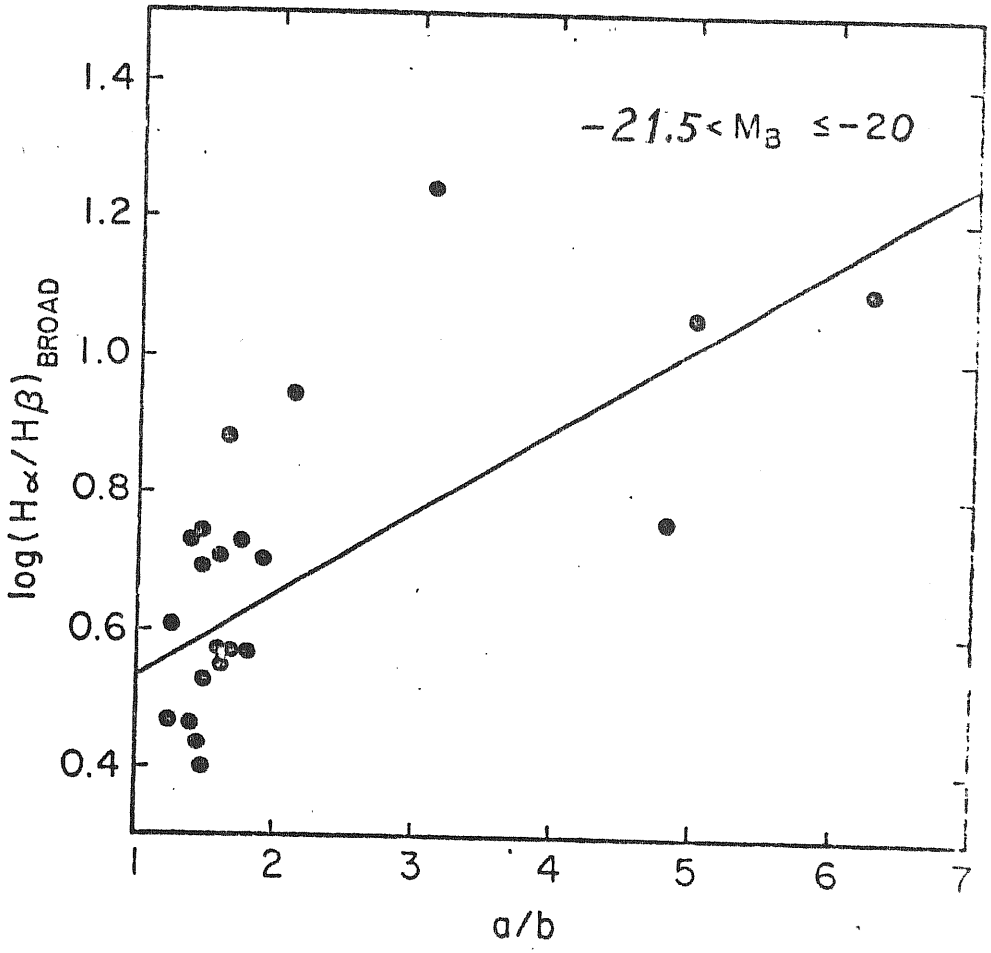

Fig. 58c

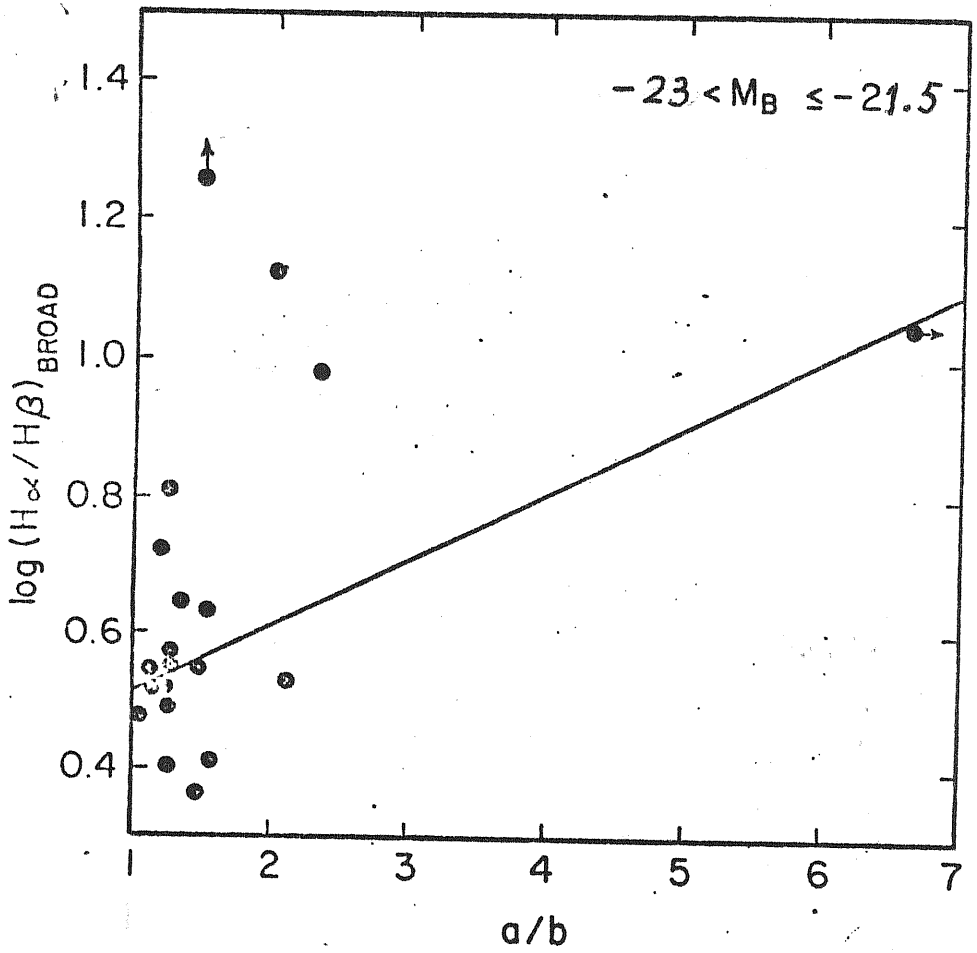

Fig. 58b

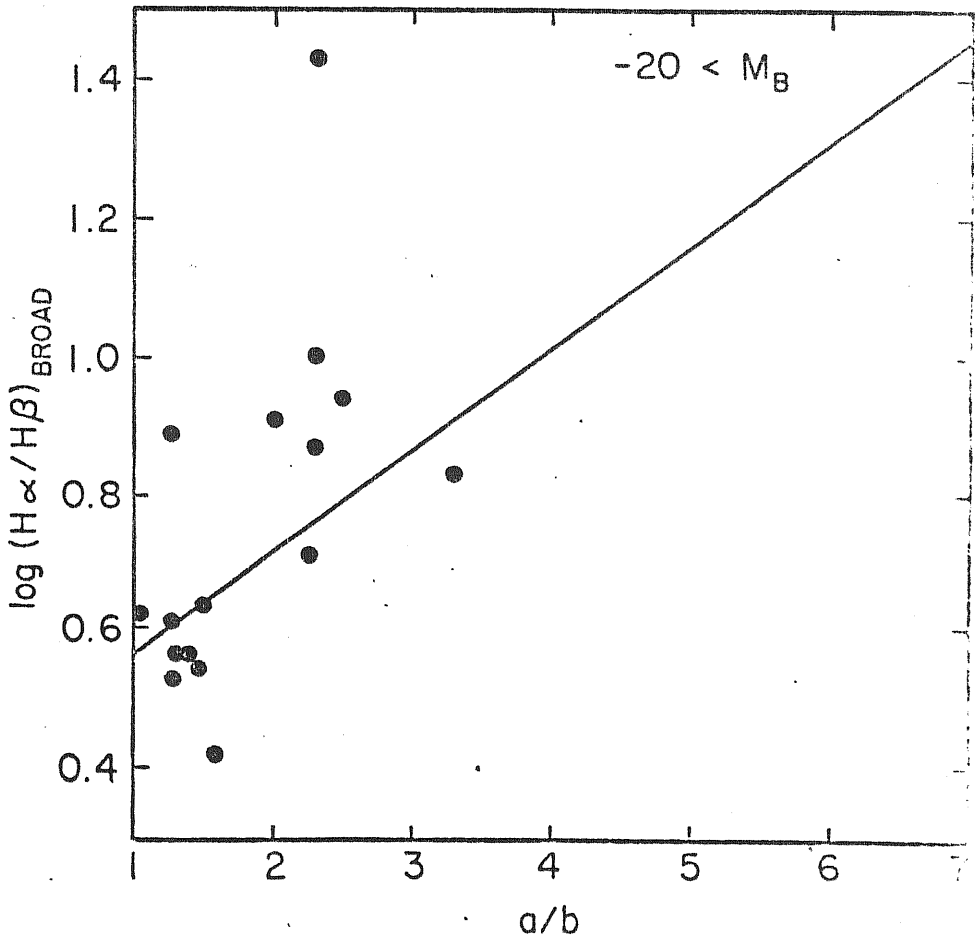

Fig. 58d

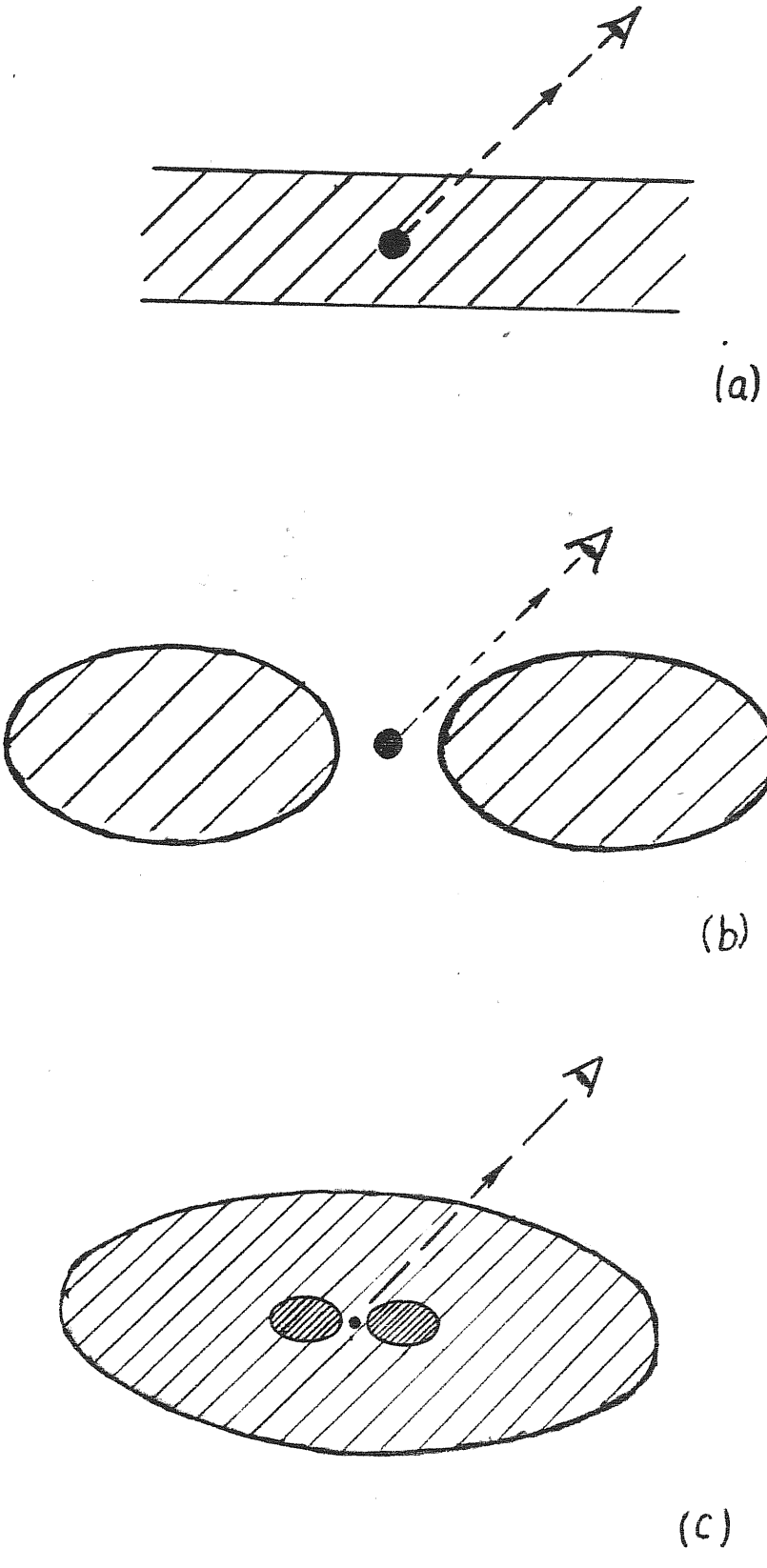

Fig. 59. Possible models for the distribution of the dust

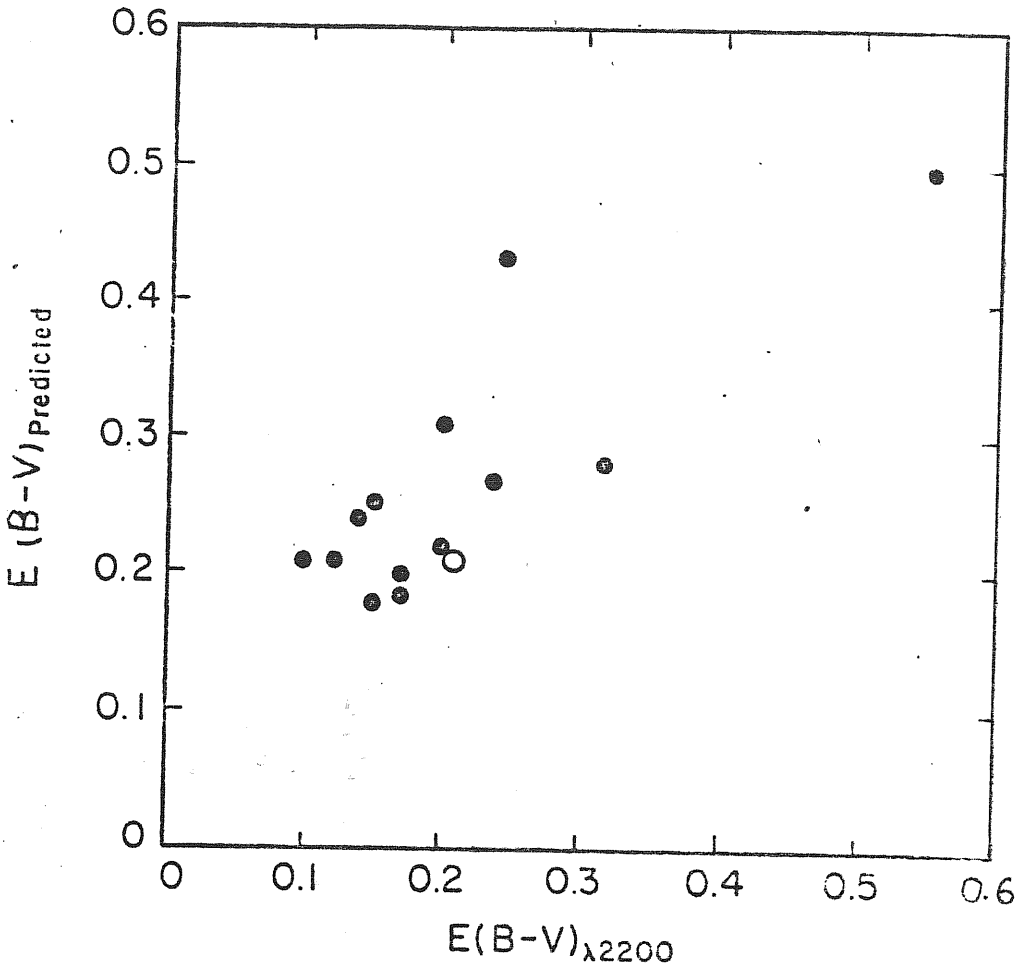

Fig. 60

Table 3

$E(B-V)_{\lambda 2200} = E(B-V)_{Rep} + 0.10$

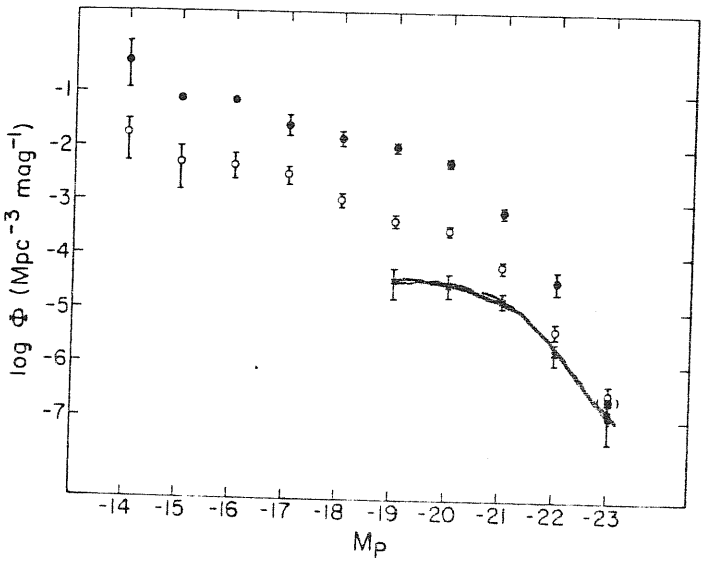

Fig. 61 Log space density versus absolute magnitude for field galaxies (*filled circles*), Markarian galaxies (*open circles*), and Markarian Seyferts (*crosses*), as discussed in the text. Error bars represent the square root of the number of galaxies in each interval. The point representing the space density of field galaxies at $M_p = -23$ (placed in parentheses) has no error bars.

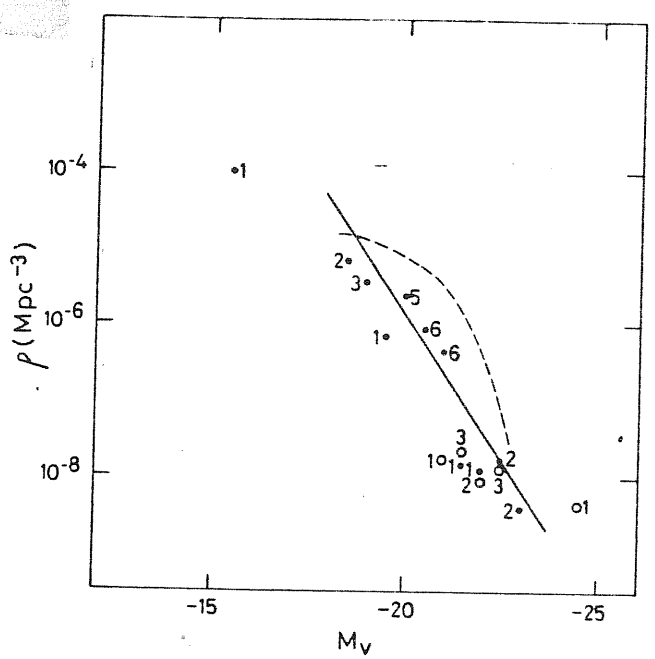

Fig. 62 Log space density versus absolute magnitude for Seyfert 1 nuclei (filled circles) and BL Lac nuclei (open circles) in half-magnitude intervals. The heavy line is the luminosity function for the Seyfert 1 nuclei; the dashed line is the luminosity function for the Seyfert 1 galaxies from Huchra and Sargent (1973) after correction to $H = 50$ km s^{-1} Mpc^{-1}. The numbers give the number of objects contributing to each point

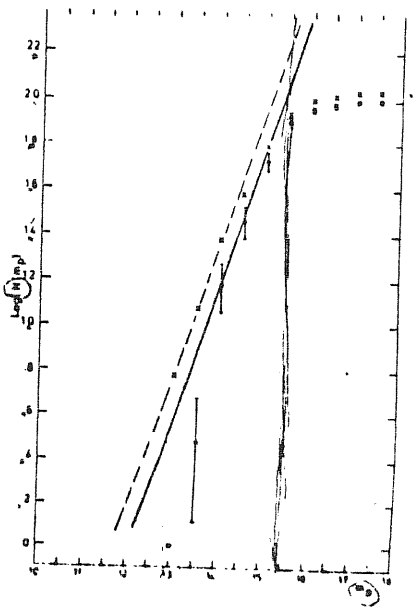

Figure 63
Plot of log $N(m_{p_{Seyfert}})$ versus m_p for all the galaxies in table 1 (dots). The error bars are calculated according to formula 3 in Terebizh (1980). The full line has slope 0.6 (see text). The values of log $N(m_{p_{bright}})$ corrected for missing objects (see § 3.2) are also shown (crosses). The dashed line with slope 0.6 corresponds to these corrected values.

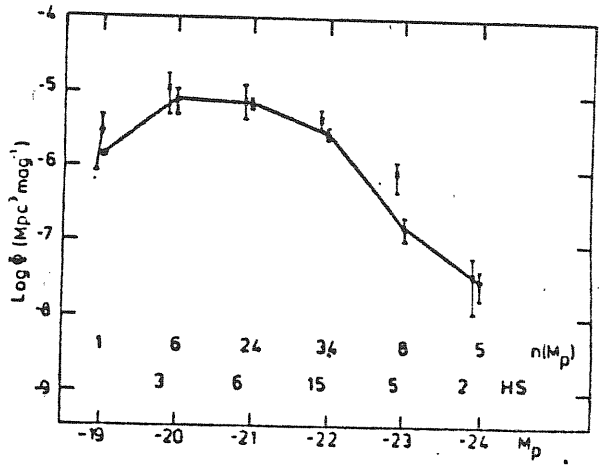

Figure 64 The optical LF derived in § 3.4 (dots). The error bars represent the square root of the number of galaxies in M_p interval. This number, $n(M_p)$, is given in the figure for reference. The dot at $M_p = -19$ is based on only one galaxy and has no error bar. The error bars that are shown at $M_p = -19$ apply to the open circle that represents the NGC addition to the sample at this absolute magnitude (see text). The values of HS are plotted for comparison (crosses), also with error bars; the number of galaxies they used in each M_p interval is again given for reference (indicated by HS).

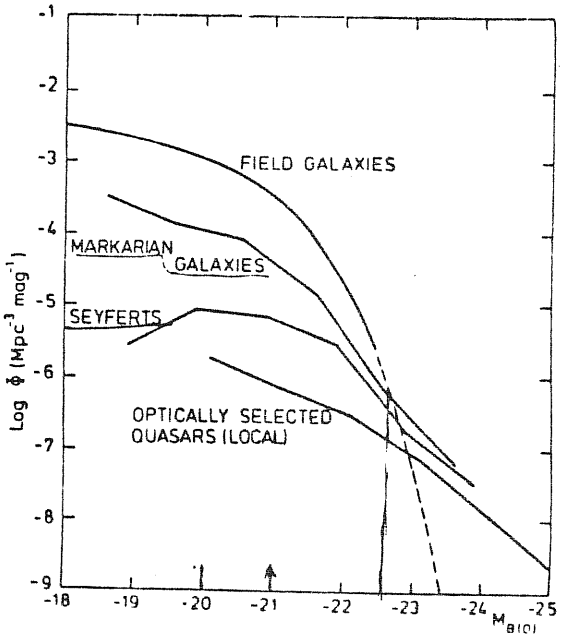

Figure 65
Comparison of the LF's for field galaxies, Markarian galaxies in general, Markarian Seyfert galaxies and optically selected quasars (local). The figure is constructed for integrated blue magnitudes B(0), Sandage galactic absorption and $H_0 = 50$ km s^{-1} Mpc^{-1}, as described in § 3.5.1. Histogrammatic points are simply connected with straight lines. The LF for field galaxies is represented by a Schechter form, and is dashed over the range where no data points were present in Schechter's curve fitting. The excess of active galaxies over the formal extrapolation of the field galaxy LF is discussed in § 3.5.2.